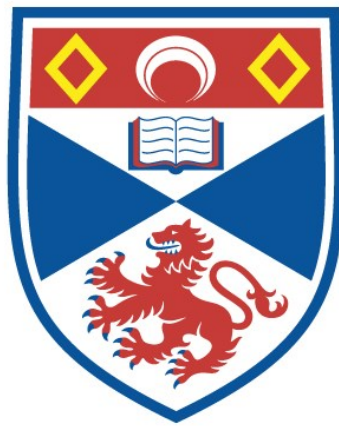


THE EVOLUTION OF LAYERED, BASIC PLUTONS -
EVIDENCE FROM SMALL-SCALE STRUCTURES

Iain McKenzie Young

A Thesis Submitted for the Degree of PhD
at the
University of St Andrews



1984

Full metadata for this item is available in
St Andrews Research Repository
at:
<http://research-repository.st-andrews.ac.uk/>

Please use this identifier to cite or link to this item:
<http://hdl.handle.net/10023/15274>

This item is protected by original copyright

The evolution of layered, basic plutons -
evidence from small-scale structures.

A dissertation submitted for the degree of Ph.D.
at the University of St. Andrews, April 1984.

Iain M. Young

ProQuest Number: 10171082

All rights reserved

INFORMATION TO ALL USERS

The quality of this reproduction is dependent upon the quality of the copy submitted.

In the unlikely event that the author did not send a complete manuscript and there are missing pages, these will be noted. Also, if material had to be removed, a note will indicate the deletion.



ProQuest 10171082

Published by ProQuest LLC (2017). Copyright of the Dissertation is held by the Author.

All rights reserved.

This work is protected against unauthorized copying under Title 17, United States Code
Microform Edition © ProQuest LLC.

ProQuest LLC.
789 East Eisenhower Parkway
P.O. Box 1346
Ann Arbor, MI 48106 – 1346

Frontispiece

Top Cyclic layering on Hallival, Eastern Layered Series, Rum. The snowy slopes are of peridotite, the crags are of allivalite; all the layering dips to the left (westwards). Snow-covered Skye Cuillin complex in the background.

Bottom Lenticular mafic layers and normally graded layers in troctolites of the Lower Zone of the Kiglapait intrusion, Labrador.



ACKNOWLEDGEMENTS.

This work was carried out while in receipt of a NERC studentship for which I am grateful.

I would like to thank my supervisors, C.H. Donaldson and E.K. Walton, for their support and much discussion during the course of this project. Many others have contributed by their readiness to enter into discussion; particular thanks are due to Alan Butcher, Steve Tait, John Faithful, Johannes Volker, Phil Leighton, Ed Stephens, Rob Cowieson and Drew Carey.

I owe my trip to Labrador to Tony Morse and I would also like to thank the following members of the Nain Anorthosite Project; Bob Wiebe, for introducing me to the Kolotulik outcrops, and John Berg, George Marshall, Kathleen Nolan, Suzanne and the crew of the M.V. Pitsiulak for help in the field and for making my stay so enjoyable.

The Nature Conservancy Council kindly allowed me access to Rum and many members of staff helped in making my time there as rewarding as possible.

Pete Hill and Dougie Russell gave invaluable instruction and help on the probe at Edinburgh. I would also like to thank; the technical staff at St. Andrews, particularly Andy Mackie and Jim Allen, for their efforts over the last three years, Kit Finlay, for

typing the tables and part of the ms., and all the other members of the department at St. Andrews for their assistance.

Finally I would like to express my gratitude to my wife, Sheila, and my parents for their support and encouragement over the course of the project.

CERTIFICATE.

We hereby certify that IAIN YOUNG has been engaged in research for nine terms at the University of St. Andrews, that he has fulfilled the conditions of Ordinance No. 12 and resolution of the University Court, 1967, No. 1, and that he is qualified to submit the accompanying thesis in application for the degree of Doctor of Philosophy.

I certify that the following thesis is of my own composition, that it is based on the results of research carried out by me, and that it has not previously been presented in application for a higher degree.

ABSTRACT.

Many basic and ultrabasic plutons are commonly lithologically, texturally and compositionally layered on several scales. Associated with, and defined by, the layering are a variety of small-scale structures, considered analogous to structures found in sedimentary rocks, and capable of interpretation using similar techniques. Observations on these small-scale structures are used to infer the "depositional" and "diagenetic" processes that operated during the solidification of a number of plutons.

Erosion structures and structures associated with lithic fragments indicate that physical redistribution of solids, crystals and rock fragments, was an important process in the evolution of these bodies and that plagioclase was deposited at the floor even where it was less dense than the contemporary magma. From their relationships with lithic fragments normally graded layers are demonstrated to be the solidified remnants of crystal-laden density currents flowing across the transient floor of the magma chamber and are inferred to be the best approximation to truly chronostratigraphic horizons in layered plutons identified to date.

The proposition that crystal- and rock-laden density currents can transport material vertically through the magma body is investigated experimentally by examining the nature of such flows in a small tank. Experiments and calculations indicate that such density currents straddle the range of conditions from laminar to

fully turbulent. Laminar flows do not mix with the contemporary magma and will transport crystals to the transient chamber floor. It is suggested that such a process may have given rise to lensoid mafic layers of limited areal extent in the Kiglapait intrusion.

Structures inferred to have formed during the "diagenetic" stage of the formation of the layered rocks include deformation structures, layers and replacement bodies. Examples of the latter two sets of structures are shown to have textures identical to those in rocks interpreted as cumulates and it is concluded that those textures alone are not sufficient basis on which to infer crystal growth from the contemporary magma. Many of the structures testify to the former presence of mobile pore liquids and the contemporaneity of pore liquids of different compositions. Movement of pore liquid is considered to have been driven by density differences due to variations in pore magma composition and thus the structures can be considered as evidence for interstitial compositional convection.

Under certain circumstances pore liquids may be expelled from the crystal mush and mix with the contemporary magma. The chemical consequences of such mixing events are discussed and it is proposed that chromitite layers in the Eastern Layered Series of the Rum intrusion record the operation of the process.

Several features of the Rum intrusion suggest that the magma chamber was thermally and compositionally zoned at times during its active history and this leads to the formulation of a new scheme for the formation of cyclic stratigraphy in the Rum layered intrusion, based on the progradation and regression of a liquid/liquid interface and two environments of accumulation.

CONTENTS

ACKNOWLEDGEMENTS.....	i
CERTIFICATE.....	iii
ABSTRACT.....	iv
CONTENTS.....	vii
1 INTRODUCTION.....	1
1.1 Development of ideas about the origin of igneous layering and aims of the study.....	1
1.2 Methods.....	6
1.3 Terminology.....	8
2 BASIC PLUTONS - CONDITIONS OF SOLIDIFICATION.....	10
2.1 Introduction - analogy of magma chamber and sedimentary basin.....	10
2.2 Magma chamber geometry.....	12
2.3 Magma convection.....	12
2.3.1 Thermal convection.....	13
2.3.2 Compositional convection.....	15
2.3.3 Double-diffusive convection.....	16
2.4 Direction of infill.....	17
2.5 Discussion.....	20
2.6 Conclusions.....	22

3	TRANSPORT OF SOLIDS - EVIDENCE FROM SMALL-SCALE STRUCTURES.....	24
3.1	Introduction.....	24
3.2	Layer truncation structures.....	25
3.2.1	Description.....	25
3.2.2	Discussion.....	26
3.3	Structures associated with lithic fragments.....	28
3.3.1	Introduction.....	28
3.3.2	Relationships of fragments to igneous lamination.....	28
3.3.3	Relationships of layers and laminae to fragments.....	29
3.3.4	Fragmental layers.....	31
3.3.5	Relationship of fragments to deformed layering.....	32
3.3.6	Discussion.....	32
3.4	Imbrication and erosion in trough layering - an example from the Tigalak intrusion.....	36
3.4.1	The Tigalak intrusion - general features.....	36
3.4.2	Trough layering - field relations.....	37
3.4.3	Petrography.....	38
3.4.4	Mineral chemistry.....	39
3.4.5	Origin of the leucotroctolite lenses.....	40
3.4.6	Origin of the trough layering.....	41
3.4.7	Physical properties of the Tigalak magmatic density currents.....	43

3.4.8 Discussion.....	46
3.5 Conclusions.....	48
4 TWO CONTRASTED LAYER TYPES IN THE KIGLAPAIT INTRUSION, N. LABRADOR.....	49
4.1 Introduction.....	49
4.2 Field relations.....	50
4.2.1 Normally graded layers.....	50
4.2.2 Cm-scale layers.....	52
4.3 Petrography.....	52
4.3.1 Textures - graded layer.....	53
4.3.2 Textures - cm-scale layer.....	54
4.4 Mineral compositions.....	57
4.5 Discussion.....	58
4.6 Conclusions.....	62
5 TWO-PHASE CONVECTION IN BASIC PLUTONS.....	63
5.1 Introduction.....	63
5.2 Field evidence for a roof zone sediment source.....	67
5.3 Crystal transport mechanisms.....	68
5.4 Cotectic suspension densities.....	70
5.5 Crystallisation conditions at magma chamber roofs.....	72
5.6 Vertical density currents - experiments and calculations...	73

5.6.1	Experimental methods.....	73
5.6.2	Melting above a horizontal interface.....	74
5.6.3	Plume spacing and velocity.....	79
5.6.4	Internal flow structure.....	84
5.6.5	Suspension currents.....	87
5.6.6	A possible crystal-sorting mechanism.....	88
5.7	Discussion.....	89
5.8	Conclusions.....	91
6	DIAGENETIC PROCESSES IN CRYSTAL MUSHES.....	92
6.1	Introduction.....	92
6.2	Structures defined by deformed layers.....	93
6.2.1	Symmetrical deformation structures.....	93
6.2.1.1	Harris Bay, Harris Bay Series, Western Layered Series.....	93
6.2.1.2	Unit 9, Eastern Layered Series.....	95
6.2.2	Discussion.....	99
6.2.3	Kiglapait Intrusion - Lower Zone - Hare Point dunitic horizon.....	101
6.2.4	Beinn Buie gabbro intrusion, Centre 1 caldera, Mull...	102
6.2.5	Hypersthene gabbro, Centre 2, Ardnamurchan.....	105
6.2.6	Discussion.....	107

6.3 Asymmetrical deformation structures.....	110
6.3.1 Flame structures.....	110
6.3.2 Cumulate "dykes".....	111
6.3.3 Folded layers.....	111
6.3.4 Discussion.....	113
6.4 Finger structures in the Rum intrusion - evidence for plagioclase resorption by migrating interstitial liquid...	114
6.4.1 Description.....	114
6.4.2 Origin of the finger structures.....	117
6.4.3 A possible cause of finger formation.....	118
6.4.4 Replacement structures in other intrusions.....	120
6.5 Implications of dynamic interstitial liquids.....	121
6.6 Conclusions.....	123
7 MUSH/MAGMA INTERACTION - EVIDENCE FROM THE RUM PLUTON.....	124
7.1 Introduction.....	124
7.2 Chromite layers - previous research.....	124
7.3 Chromite in the Rum intrusion.....	125
7.3.1 Stratigraphic setting and previous research.....	125
7.3.2 Structures associated with, or defined by chrome- spinel concentrations.....	127
7.3.3 Petrography.....	128

1 INTRODUCTION.

1.1 Development of ideas about the origin of igneous layering and aims of the study.

The stratigraphic compositional trends of layered intrusions are held to record the evolution of large magma bodies as they differentiate by fractional crystallisation. Until recently it was believed that the separation of early-formed phases from the parent magma occurred principally by their settling to the transient floor of the chamber under the influence of gravity. The efficacy of olivine crystal settling in a haplobasalt was shown experimentally by Bowen (1915) and liquid evolution paths during fractional crystallisation of haplobasalts have subsequently been shown to successfully model the differentiation of a number of basic layered intrusions (eg. Morse, 1980a pp. 217-237).

However, not only do layered intrusions document crystal fractionation but also crystal sorting, first recognised in 1894 when Geikie and Teall observed that adjacent bands in gabbros of the Skye Cuillin complex consisted of the same minerals in different proportions. The origin of this type of banding, igneous layering, and the mechanisms by which fractional crystallisation occurs, are presently the subject of much petrologic interest, eg McBirney and Noyes (1979), Morse (1979a), Irvine (1980a), Wilson and Larsen

(1982), Thy and Esbensen (1982), Cawthorn (1982). Existing interpretations are based on one-dimensional variations in texture and mode through layers. Layers are not, however, simple objects in three dimensions; they exhibit internal and external structures, and groups of layers may define other structures. Any hypothesis for the origin of layering or layers must be capable of explaining the origin of these structures. Alternatively, interpretations of the structures will place constraints on the origins of layering and the mechanisms by which layered plutons evolve.

Small-scale structures have been used by petrologists in the past to aid interpretations of layered igneous rocks. For example, in his description of the Rum intrusion in the "Small Isles Memoir", Harker (1908) recognised that the banded allivalites showed trachytoid textures and used this observation to support his thesis that the banding had its origins in the flow of "heterogeneous magma". He also noted that allivalite/peridotite contacts are generally wavy rather than straight and used this as evidence to suggest that the peridotite was still soft on intrusion of the allivalite, believing that the complex was built up of repetitive sill-like injections of peridotite and allivalite magmas. In another instance the association of "fluxion structure" and "a roughly gravitative arrangement of the bands" was used by Grout (1918) to argue for convection during the cooling and differentiation of the Duluth gabbro.

Petrologists had to wait, however, for the publication of Wager and Deer's 1939 memoir on the Skaergaard intrusion for an all-embracing interpretation of the layering and associated small-scale structures in one intrusion. Wager and Deer chose to interpret the layering and textures of these rocks principally in terms of nucleation and growth of crystals at, or near, the roof and walls of the intrusion, followed by the sorting of phases due to their differing physical attributes; size, density and shape during settling and current transport to the transient chamber floor. Central to their model was the recognition of small-scale structures within the layered series of the Skaergaard intrusion which bear a remarkable resemblance to structures found within clastic sediments, eg grading, cross bedding, lamination, and which they chose to interpret accordingly.

These ideas were to dominate petrologists' views of layered intrusions for several decades. They continued to be developed by Wager and his co-workers, notably G.M. Brown who introduced the concept of the open-system magma chamber (Brown, 1956), and culminated in the publication of Layered Igneous Rocks in 1968. Other petrologists, notably Jackson (1961), favoured a nucleation zone much closer to the transient chamber floor, though the emphasis was still on the settling of crystals to their eventual resting place on the cumulus pile.

The widespread recognition of the so-called "plagioclase flotation problem" in the 1970s (Bottinga & Weill, 1970; Morse, 1973; Campbell, 1978; Campbell et al, 1978) led to the gradual rejection by most petrologists of explanations of layering based on crystal sorting and deposition. In their place mechanisms involving predominantly rhythmic, diffusion-controlled nucleation events at the mush/magma interface have come to dominate the literature (notable recent exceptions being Irvine (1980a) and Parsons and Butterfield (1981), an idea made more attractive by the suggestion that double-diffusive convection may occur in cooling magma bodies (Elder, 1968; Turner & Gustafson, 1978; McBirney & Noyes, 1979). It is ironic that the most strident rejection of Wager's ideas came in a paper reconsidering the crystallisation of the Skaergaard intrusion, in which McBirney and Noyes (1979) conclude "most crystals probably nucleate and grow in situ".

This shift of opinion left at least one major gap in interpretation, namely the small-scale structures so elegantly accounted for by the clastic sediment analogy. A major part of this thesis is concerned with describing and interpreting these and similar structures from several intrusions in order to determine whether they are compatible with an origin by in situ crystallisation or whether they dictate that some other way round the plagioclase flotation problem must be found such as the depositional mechanism proposed by Irvine (1978a, 1980a).

The initial accumulation of the granular phases (cumulus crystals, rock fragments and immiscible liquids) is of course only part of the transformation of magma to rock. Petrologists have tended to stress the importance of this stage and the solidification of the interstitial phases has been largely ignored since Wager, Brown and Wadsworth's (1960) paper on cumulus textures and the modifications proposed by Jackson (1967) and Wager and Brown (1968). Briefly, their ideas, which have been gathered under the heading of "adcumulus growth theory" by Morse (1980a, p241) and described as "a modern triumph of observational petrology", hold that the final texture of the rock is controlled by the amount of diffusional exchange achieved between the pore spaces in the original textural framework and the overlying magma, which in turn was largely controlled by the rate of accumulation of solid phases at the top of the crystal pile. The pore fluid was held to be essentially stationary and one of Wager et al's textural "end-members", the adcumulates, were held to complete their solidification isothermally at the top of the crystal pile.

Like the ideas on crystal settling and sorting, the adcumulus growth theory did not survive the 1970s unmodified. In 1972 G.B. Hess calculated that for reasonable accumulation rates diffusion was too slow to allow solidification of any rock at the mush/magma interface in the Stillwater intrusion. More recently Irvine (1978b; 1980b) proposed that pore liquid in the Muskox intrusion was driven upwards through the crystal mush, by compaction, for distances of the order of hundreds of metres. On the other hand Morse (1981a) suggested that

successively more iron-rich, and therefore denser, differentiates in the Kiglapait intrusion may have filtered downwards from the overlying magma to depths of kilometres in the mush, though he later rejected the idea (Morse & Nolan, 1980; Morse, 1982). Field evidence for mobile pore liquids was illustrated in the Bushveld intrusion by C.A. Lee (1981) who compared small-scale structures found in layered rocks to fluid-escape and soft-sediment deformation structures in clastic sediments. These studies indicate that post-cumulus processes are much more dynamic and may be more important in the evolution of layered plutons than hitherto suspected. Thus the second major aim of this work is to explore the physical aspects of these essentially diagenetic processes through an examination of the small-scale structures which record their operation.

1.2 Methods.

To these ends work has concentrated on examining as great a variety as possible of small-scale structures in a number of layered intrusions of widely varying size, geometry, composition and complexity. Fieldwork has been carried out on the following bodies; the Kiglapait and Tigalak intrusions (two of many layered intrusions within the Precambrian Nain anorthosite terrain in Labrador), and a

number of examples from the Scottish Tertiary igneous province, including the hypersthene gabbro of centre 2 in Ardnamurchan, the Beinn Buie, Corra Bheinn and Loch a' Chroisg gabbros on Mull and the Rum layered intrusion. In addition, brief visits have been paid to the Belhelvie and Inch intrusions (two of the "Younger basic masses" in N. E. Scotland) and an extensive review of the literature has been undertaken. In order to allow as large an amount of ground as possible to be covered, description is generally qualitative. Though it has not been possible to examine in detail all the structures identified, an attempt has been made to use the whole spectrum of field observations to create a picture of the physical processes operating during the crystallisation of layered plutons. Several structures and layers however have been selected for detailed chemical work with the electron microprobe.

In addition, the proposition that crystal- and rock-laden density currents may redistribute material within large magma bodies has been extended to consider the case where currents may flow vertically through the liquid rather than along a bounding surface, cf. Irvine (1978a, 1980a), by photographing the development of such currents in small tanks (Chapter 5).

It is an a priori assumption that similar structures and layers in different plutons indicate similarity of process, this seems justified in view of the similarity of liquid and solid composition and their physical properties (viscosity, density, thermal and ionic diffusivity etc).

The approach is much more akin to that of the clastic sedimentologist than the igneous petrologist in that observations of structures made at outcrop level guide the interpretation given to the formation of any particular layer (bed), rather than using isolated instances of structures being picked specifically to reinforce a particular hypothesis. The traditional methods of the igneous petrologist (major-, minor- and trace-element and isotope geochemistry, the electron microprobe and experiments with rock melts) are largely ignored since the study is geared to investigating physical processes, (though these of course may have chemical effects). Indeed one of the principal conclusions of the study is that conventional approaches have involved unjustified assumptions about the survival of early-formed compositional relationships.

1.3 Terminology.

A textural terminology was developed by Wager, Brown and Wadsworth (1960) for layered igneous rocks. Recently the subject of criticism, it has been revised by Irvine (1982), together with a systematisation of the stratigraphic nomenclature for layered intrusions. Irvine chose to define cumulus crystals as "the fractionated crystals" which formed a "cumulus framework of touching mineral crystals". Several of the textures and layers described in this thesis fit this definition and yet are not considered to have

cumulus origin since they formed within the crystal pile and not in the main body of magma. Furthermore there is nothing in the mechanics of current deposition to force crystals to form a touching framework (after all lavas transport phenocrysts but these are rarely found to be touching in rocks), but crystals transported in this way would undoubtedly have been considered to be cumulus crystals by Wager et al. Thus several new definitions are developed in Appendix 1 based solely on the classification of cumulus crystals as those crystals interpreted to have grown in contact with the main body of magma, irrespective of their textural relationship with other crystals. Apart from those terms redefined in Appendix 1 Irvine's (1982) terminology is adopted.

2 BASIC PLUTONS - CONDITIONS OF SOLIDIFICATION.

2.1 Introduction - analogy of magma chamber and sedimentary basin.

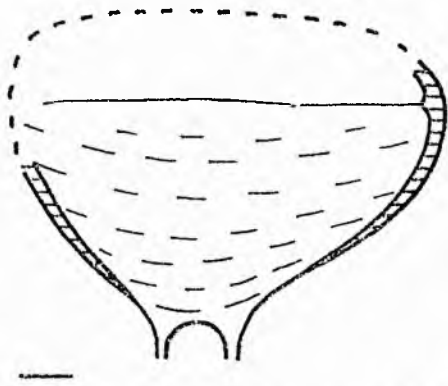
Magma is considered to be the product of partial or total melting events within the crust and mantle. The initial melt composition is probably rarely, if ever, erupted but is modified by a variety of processes on its journey from the source; some of this modification can occur in crustal reservoirs. It is presently impossible to sample contemporary reservoirs directly - indeed only a few have been positively identified. Plutonic rocks, however, testify to the former presence of such magma bodies and compositional heterogeneity in plutons records the operation of certain modification processes. In basic and ultrabasic plutons these heterogeneities often take the form of layers of texturally and/or compositionally distinct rock. Associated with these layers are a variety of small-scale structures considered analogous to structures found in sedimentary rocks (Chp 1) and capable of interpretation in a similar fashion.

The sedimentologist has the advantage of studying modern sedimentary structures in the secure knowledge of their environment of formation. Similar structures in the rock record can then be used to reconstruct the environment in which the structures formed (eg Reading, 1978). The igneous petrologist on the other hand is faced

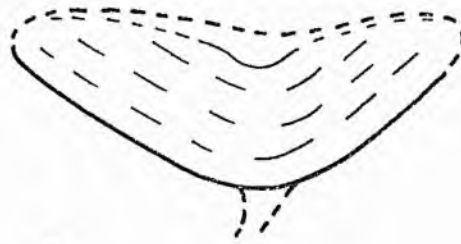
only with the rock record and observations of extrusive magma with which to make interpretations. It ought to be possible, however, to make predictions as to how plutonic magma bodies behave, based on estimates of the relevant boundary conditions. Thus far, an all-embracing model has not been attempted, the most complete probably being G.B. Hess' treatment of heat and mass transport in the Stillwater complex (Hess, 1972). Models of magma chamber convection are more numerous (eg Bartlett, 1969; Huppert & Sparks, 1980; Chen & Turner, 1980; Turner, 1980; Irvine, 1980c; Huppert & Turner, 1981a; Huppert et al., 1981; Hardee, 1983) principally because of recent concentration on the possible role of double-diffusive effects. In this chapter I have used these studies, together with other information in the literature to indicate the conditions under which magmatic sediment accumulates.

The deposition of any set of sediments is a response to a complex interplay of factors including source composition, transport dynamics, basin geometry, tectonics, sea level changes and climate. In the same way the solidification of plutonic bodies is governed by a number of extensive and intensive parameters (geometry, heat flow, composition, replenishment, eruption, pressure).

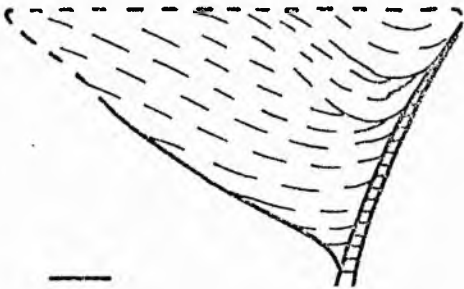
Parent magma compositions are well-established for some plutons though in most they are fairly rough estimates. In a few plutons, intensive parameters are reasonably accurately known (eg Morse et al., 1980) and in many others the case for replenishment and/or eruption is well-established (eg Brown, 1956; Berg, 1980; Browning & Smewing, 1981).



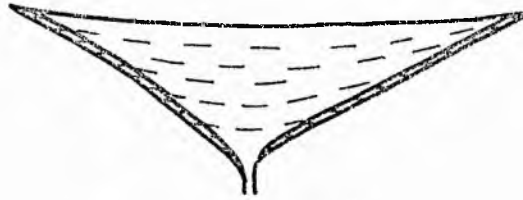
SKAERGAARD (Naslund, 1976)



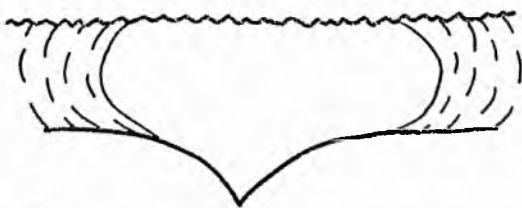
KIGLAPAIT (Morse, 1979a)





IMILIK (Myers, 1980)



MUSKOX (Irvine & Smith, 1967)



N. ARM Mt., BAY OF ISLANDS
(Casey & Karson, 1981)

 Border groups
 Trace of rhythmic layering

Scale bars - 1km

Figure 2.1 Cross-sections of several well-known plutons showing development of rhythmic layering on dipping and overhanging surfaces. In some intrusions, Skaergaard, Muskox, this may be due to preferential compaction in the centre but in others, Kiglapait, Bay of Islands, it is certainly a primary feature.

2.2 Magma chamber geometry.

The bearing that the geometry and direction of infill of basic plutons have on layer-forming processes has been curiously neglected. Very few plutons are exposed in complete cross-sections, and for even fewer is the three-dimensional geometry known. However the attitude of layering is known in many intrusions and in others it can be reconstructed. Cross-sections of several well-known plutons are presented in figure 2.1.

Two features of fig 2.1 are particularly important. Layering is developed on surfaces ranging in attitude from horizontal to overhanging, a point previously stressed by Campbell (1978) and Casey and Karson (1982). In most intrusions however, it displays moderate dips.

In many intrusions the layered rocks are separated from the country rocks by a border series, generally interpreted as being in part due to chilling and in part to crystallisation on the chamber walls (eg Hoover, 1978). In some plutons (eg Skaergaard, Muskox) the layering exhibits a marked angular discordance with the marginal border series whereas in others (eg Kiglapait) border series are succeeded conformably by rocks of the layered series.

2.3 Magma convection.

2.3.1 Thermal convection.

The idea that convection occurs in magmatic bodies and thus allows fractional crystallisation to take place is attributable to Becker (1897a,b), according to Wager & Brown (1968). Early workers considered that convection was driven by variations in liquid density associated with changes in magma temperature and crystal content (eg Grout, 1918; Wager & Deer, 1939; Hess, 1960). Thermal convection was discussed by Bartlett (1969) who calculated crystal distributions on the basis of the competing effects of settling and convective fluxes. Shaw (1965) dealt with thermal convection in granite magmas.

A continuing aspect of interpretations based on mapping and mineral variation has been the repeated application of the concept of the Benard cell (eg Maaloe, 1976; Morse, 1979b). However it is now known that Benard's original experiments were driven by variations in surface tension brought about by local variations in temperature on the free surface (Tritton, 1977). In this way a much more regular flow pattern than that due to gravitational instability is established (ibid). Convection patterns during thermal convection depend on values of the Rayleigh number, Ra , defined as

$$Ra = g\alpha(T_2 - T_1)d^3/\nu k \quad (2.1)$$

and the Prandtl number, Pr, defined as

$$Pr = \nu/k \quad (2.2)$$

where d is the depth of the fluid layer, $(T_2 - T_1)$ is the temperature difference across it, g is the acceleration due to gravity, α is the coefficient of thermal expansion of the fluid, ν is the kinematic of the fluid and k is the thermal diffusivity of the fluid (Krishnamurti, 1970; Tritton, 1977). From the onset of convection until full turbulence is developed, transitions to more complex and time-dependent modes occur at higher values of Ra with constant Pr and each particular transition occurs at higher values of Ra with increasing values of Pr . Magmas have extremely high values of Pr and it has been shown that the transition to turbulence does not occur till $Ra = 4.5 \times 10^{12}$ (cf 10^9 for water, Rohsenow & Choi, 1961), however since d is very large in most magma chambers convection can be expected to be fully turbulent (Hardee, 1983). During turbulent thermal convection between horizontal bounding surfaces strong thermal gradients are established close to the walls and the interior is kept essentially isothermal (Tritton, 1977). Flow is established by the periodic breakoff of packets of fluid from the bounding surfaces known as "thermals" (Howard, 1966; Sparrow et al 1970). In more complex geometries a general circulation can be established, which may be uni-, bi- or multi-cellular and in which flow may be directed up or down at the walls or be oscillatory (Hardee, 1983).

2.3.2 Compositional convection.

It has recently been suggested that convection in magma bodies is not only driven by thermally induced density variations but also by compositional variations. In general, compositional effects will have a much greater effect on melt density than thermal ones due to the low values of the coefficient of thermal expansion for basic magmas (see Murase & McBirney, 1973). The density changes associated with fractionation can be calculated (Sparks et al, 1983; Grove & Baker, 1983; Sparks & Huppert, 1984) and have led to the introduction of the parameter, "fractionation density" (Sparks et al, 1983; Sparks & Huppert, 1984) which is defined as the density of the liquid components being removed by crystallisation. Depending on the chemistry of the system under consideration, fractionation at a bounding surface may lead to either a local reduction or increase in liquid density (McBirney, 1980; Sparks et al, 1983; Sparks & Huppert, 1984) and lead to compositional convection.

The continued production of denser or lighter fluid at the boundaries of fractionating liquid can lead to the build of stably stratified fluid at either the top or bottom of the fluid-filled chamber by the so-called "filling-box mechanism" (Turner & Gustafson, 1978). In this way it has been proposed that quite extreme differentiation of magmatic liquids can occur in the liquid state (McBirney, 1980; Turner, 1980; Turner & Gustafson, 1981). Indications of the existence of zoned acid to intermediate magma chambers comes from their compositionally-zoned eruptive products

(see examples given in Hildreth, 1981). Evidence for the existence of zoned chambers involving basaltic liquids comes from bimodal basalt-rhyolite eruptions (eg Sigurdsson & Sparks, 1981) and interpretations of the origin of mixed-magma minor intrusions (eg Bell, 1983; Marshall & Sparks, 1984).

2.3.3 Double-diffusive convection.

The combination of both thermal and chemical diffusive fluxes at the boundaries of liquid bodies can lead to the development of double-diffusive convection. This phenomenon arises when two (or more) diffusive fluxes in a liquid have opposing effects on its density and has been of particular interest to oceanographers (see Huppert & Turner, 1981b for a review) where heat and salt are the diffusive fluxes concerned. In magmatic systems heat and iron are commonly proposed as having a similar effect (Elder, 1968; McBirney & Noyes, 1979), though fluxes of other chemical components may have an effect also (see Irvine, 1980b).

Double-diffusive convection leads to the formation of stratified liquid bodies. These liquid layers form horizontally except adjacent to cooled side walls where they may display slight dips (eg Huppert & Turner, 1981b; Turner & Gustafson, 1981). As the system loses heat and crystallises the bottom-most layer thins and eventually disappears and in this way the whole liquid column gradually subsides. In crystallising aqueous systems this

phenomenon can have a pronounced effect on the proportions, compositions and textures of the phases crystallising at the base of the liquid column (Chen & Turner, 1980; Turner, 1980; Kerr & Turner, 1982) Liquid stratification may also arise following entry of some new magma to a chamber (Sparks et al, 1980). The exact nature of the stratification (if it occurs at all) is dependent on the new magmas input rate and density contrast and whether any stratification is developed in the magma already in the chamber (Sparks et al, 1980; Huppert et al 1981; Campbell et al, 1983). At present dynamic modelling of chamber replenishment has been confined to inputs of relatively large volume. There is however abundant field evidence to suggest that inputs of small volume occur (Berg, 1980; Wiebe, 1980) and there can be little doubt that replenishments occur on all scales and periodicities from a steady trickle to large periodic influxes, as proposed by O'Hara (1977) and O'Hara and Mathews (1981).

2.4 Direction of infill.

In this section I examine the basis on which the well-developed stratigraphies in layered intrusions are interpreted in terms of the solidification directions of the original magma bodies. Recent work has shown that the nature of succeeding time planes is not well established (Wilson & Larsen, 1982). True chronostratigraphic horizons are rare even in sedimentary successions and are confined to deposits produced by steady fallout from a fluid, such as

volcanic ash and pelagic ooze (Reading, 1978; Conybeare, 1979; Leeder, 1982). It is possible, however, to use some strictly diachronous units as time markers, if they are deposited in times much less than the that of the whole stratigraphic interval being considered. Thus turbidite units may be considered to be "instantaneously" deposited and it would be useful to identify some criteria whereby chronostratigraphic horizons could be identified in layered intrusions.

The rates of accumulation of igneous sediments are generally estimated as being on the order of centimetres per year (Irvine, 1970; Hess, 1972) or tens of centimetres per year in replenished chambers where the replenishing magma mixes with the resident magma (Usselman & Hodge, 1978), though up to an order of magnitude greater if the replenishing magma ponds at the base of the chamber (Huppert & Sparks, 1980). In chapters 3 and 4 it is demonstrated that normally graded layers are the solidified remnants of magmatic density currents. The velocities of such currents (see Irvine 1980a) indicate that they will produce layers in times several orders of magnitude shorter than similar thicknesses of crystal accumulate could be produced by steady crystallisation. Normally graded layers are thus considered to be the best approximation to chronostratigraphic units yet identified within layered plutons. Other forms of rhythmic layering are generally developed parallel to normally graded layers, though the law of superposition does not necessarily apply (Chp 6).

Discordance between cryptic layering, phase layering and rhythmic layering has been documented in the Skaergaard intrusion (Naslund, 1976) and Fongen-Hyllingen intrusion (Wilson & Larsen, 1982). This observation has been used to argue that these bodies were compositionally heterogeneous in the liquid state and that crystallisation occurred in situ (Naslund, 1976; McBirney & Noyes, 1979; Wilson & Larsen, 1982). However variations in olivine and orthopyroxene composition may only reflect the rate of crystallisation through variations in the amount of liquid trapped (Hess, 1960; Cawthorn, 1982) or postcumulus reaction with migrating liquid (Irvine, 1980b; Chps 6,7). Plagioclase is more likely to retain its original composition however (Chp 6), and thus the case for magma heterogeneity is particularly well-established for the upper portions of the Skaergaard intrusion where plagioclase compositions have been used to infer magma chamber inhomogeneity.

Phase entries and exits identified on the basis of texture alone must also be considered suspect due to the recognition that "cumulus textures" can be formed within the crystal mush on the chamber floor (Chp 6) and that poikilitic phases may have cumulus status (Brooks & Nielsen, 1978).

Magma heterogeneity cannot however be considered evidence for in situ crystallisation any more than constant crystal compositions could be considered evidence for crystal settling.

The development of compositional inhomogeneity in crystallising plutons has been assigned to diffusion and/or convection (eg Turner & Gustafson, 1978; Turner, 1980; Hildreth, 1981; Irvine et al, 1983). Walker and DeLong (1983) have demonstrated the Soret effect experimentally and invoked it to explain anomalies in the compositions of MOR basalts and gabbros, though they suggest that in basic systems its effect is limited to boundary layers with high thermal gradients.

2.5 Discussion.

It is generally agreed that major magma bodies convect for most of their crystallisation histories but that convection need not act to homogenise the fluid and, indeed, may act to unmix it. In the case of replenished chambers, zonation can occur by input of fresh magma into the chamber. The presence of liquid layers in magma bodies may have an influence on the phase proportions and compositions crystallising at any point in space and time (Chen & Turner, 1980; Kerr & Turner, 1982).

Horizontal igneous layers are very rarely found and it is important to consider whether this is a primary feature or not. It has been proposed by Petraske et al (1978) that the synformal structure of layered intrusions can be explained by plastic deformation of the lithosphere in response to stress produced by the

magma body. Their model has been adopted by Loney and Himmelberg (1983) to explain the synformal structure of the La Perouse gabbro in Southeast Alaska. There is little doubt that the mechanism does not apply to intrusions where the country rock is undeformed (Skaergaard, Imilik), where the dips of the layering do not decrease upwards and inwards (Kiglapait, Bay of Islands), or where an angular discordance between the layered series and the border series is developed (Skaergaard, Muskox). In these cases the layering must have formed in a dipping attitude though it may have been accentuated by differential postcumulus compaction (cf Irvine, 1980b).

The recognition that some forms of rhythmic layering are essentially isochronous allows younging directions to be established. This aspect of the stratigraphy of layered intrusions has only previously been addressed by Casey and Karson (1982) though they offered no justification for their choice of the trace of rhythmic layering as time horizons.

It is clear that many chambers can be considered to fill inwards from the sides as much as upwards from the base. It may then be possible to test and/or quantify chamber zonation, if cumulus mineral compositions could be established along single time planes.

The recognition that layering forms on dipping surfaces in most intrusions, allied to the possibility that magma chambers are compositionally zoned allows interpretations of layered sequences in terms of prograding and regressing "environments of deposition" (cf

discussion on Walther's law in Reading, 1978) and thus cryptic reversals and discontinuities and phase exits and entrances may only be evidence for relative movement of zoned magma and the transient chamber floor. Relative movement of chamber floor and contemporary magma could occur by replenishment, eruption, emplacement of minor intrusions, displacement by solids (eg stoped blocks) or changing chamber geometry. On the basis of this and other observations (Chp 6) a tentative reinterpretation of some features of the Eastern Layered Series of the Rum intrusion is attempted in chapter 8.

2.6 Conclusions.

- 1) Layering surfaces are generally observed to be inclined and most probably formed in inclined orientations.
- 2) Magmas convect vigorously. Convection may be driven by thermal or compositional effects or by some combination of the two. Convection need not act to homogenise magma bodies but may cause them to become compositionally and thermally stratified.
- 3) Chamber stratification may also occur by replenishment. Replenishment need not be abrupt or large-scale, but is likely to occur on all periodicities and scales from a steady trickle to major periodic influxes.
- 4) Normally graded layers in basic and ultrabasic rocks trace

isochronous surfaces and thus most rhythmic layers in such intrusions are also likely to trace isochronous surfaces, though the layers themselves need not form isochronously. Phase and cryptic layering is often diachronous, though to what extent this is a cumulus feature is not known.

5) The concepts of transgression and regression of different environments of deposition, developed further in chapter 8, may usefully be applied to layered igneous rocks and can explain many features of one-dimensional compositional profiles through such rocks.

3 TRANSPORT OF SOLIDS - EVIDENCE FROM SMALL-SCALE STRUCTURES.

3.1 Introduction.

The question of whether nucleation and growth of crystals occurs wholly in situ or at some remote site followed by transport to their final resting place is not presently resolvable on either theoretical or textural grounds. In this chapter I set out my observations of small-scale structures from which I infer that physical redistribution of solids is a real and significant feature of crystallising basic plutons of a variety of compositions.

The first section deals with structures which record the erosion, and therefore redistribution, of magmatic sediment, and the second with structures related to lithic fragments, themselves unambiguous results of solid transport and deposition. The third section describes an outcrop where examples of both types of structure are displayed and shows how the structures may be used to define the physical properties of magmatic density currents.

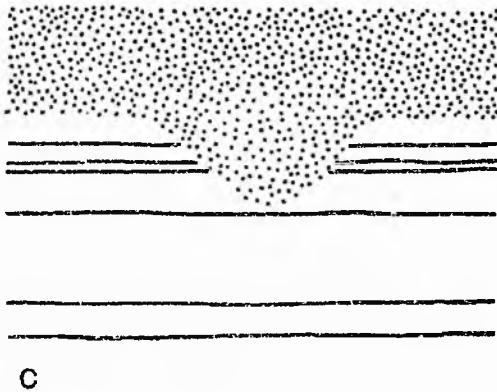
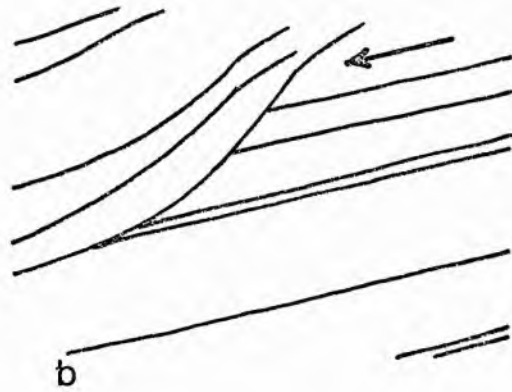
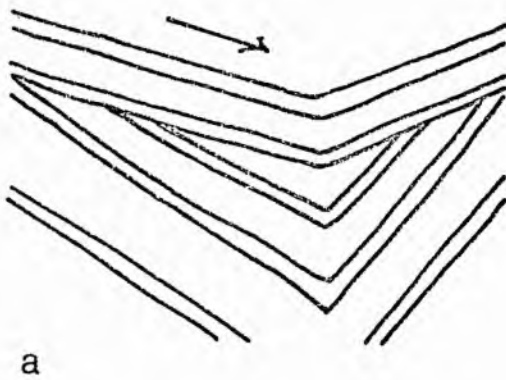


Figure 3.1 Schematic sketches of types of erosion structures observed in several intrusions. Arrows show the direction of regional dip.

(a) Erosion of previously deformed layers.

(b) Asymmetric erosion surface in undeformed layers - possibly due to slumping.

(c) Symmetrical erosion surface in undeformed layers - possibly due to the scouring action of currents. Note that in all cases the erosion surface is coincident with the succeeding depositional surface.

3.2 Layer truncation structures.

3.2.1 Description.

The truncation of one layer, part of a layer or group of layers by another layer or group of layers is a common type of structure. This set of structures can be subdivided into those in which the truncation surface is coincident with the succeeding depositional surface and those in which it is not. This latter group is interpreted as being due to postcumulus faulting and not discussed further here.

The first group can be further split into two sub-groups; one in which the older layered rock is conformable with the regional dip and one in which the younger is (see fig 3.1). Examples of the former have been noted in the Kiglapait intrusion where they take the form of shallow, arcuate, concave-up surfaces in both strike and dip sections. In dip sections the down-dip portion of this surface is more nearly conformable with the regional dip. In strike sections they tend to be symmetrical. They rarely penetrate more than a few layer thicknesses into the underlying cumulates. Exposure does not allow a determination of whether these structures are equant or elongated along strike or down dip. Geometrically similar structures can be found in rhythmically layered peridotites in the Western Layered Series of the Rum intrusion, where they tend

Plate 3.1 Minor unconformity in olivine cumulates, Western Layered Series, Rum. Layering is defined by variations in olivine grain-size and shape. Some olivines, up to 1cm long, are orientated perpendicular to layering planes while others lie in the layering plane. The presence of perpendicular olivines on erosion surfaces is consistent with a crescumulate growth model of olivine crystallisation (cf Donaldson, 1982).

Plate 3.2 Scour structure in gabbroic cumulates of the Beinn Buie intrusion, Mull. Layering is defined by variations in the proportions of plagioclase, clinopyroxene and olivine. The laminae in the lower quadrant are cut off along a line on which the pen sits. This erosion surface is chute-like in three dimensions and the structure is filled with concave-up laminae.



to have shallow, chute-like forms arranged with their axes pointing down-dip. In gabbroic rocks of the Beinn Buie intrusion several small, chute-like structures are developed in microrhythmically layered rocks (see plate 3.2)

Examples of the second type of structure are rarer. Several good examples have been noted in Rum (see plate 3.1) and in other intrusions by other authors (eg Irvine, 1980c; Parsons & Butterfield, 1981).

3.2.2 Discussion.

The first type of structure is interpreted as recording erosional events at the mush/magma interface and the second as recording deformation followed by erosion. In clastic sediments erosion occurs by two mechanisms; by the abrading action of currents and by the slumping of unstable accumulations of sediment. The former process produces structures which are aligned downcurrent and the latter produces structures which are elongate along strike (Collinson & Thompson, 1982). In plutonic environments a third possibility must be added, that of resorption by magma with which the cumulate is not in equilibrium.

The possibility of resorption is probably limited in well-mixed magma bodies undergoing steady differentiation, since the magma will generally be in equilibrium with all of the cumulates, though complex, embayed zoning patterns in Skaergaard plagioclases have been interpreted as being due, at least in part, to partial resorption (Maaloe, 1976). Erosion surfaces produced by resorption may be expected in replenished chambers (Huppert & Sparks, 1980) or in stratified chambers where liquid/liquid interfaces have undergone rapid vertical motion (Chp 8) in which case magma may come into contact with cumulate with which it is not in equilibrium. Structures interpreted as being due to resorption have been recognised in the Rum intrusion (Chp 7) and the Bushveld intrusion (Irvine et al., 1983). The structures described above are interpreted to have formed by either the slumping of unstable masses of cumulate or by the abrading action of currents. The best candidates for an origin by the latter process are those which have chute-like forms. Better exposed examples of erosion channels and slump scars have been documented in the Kolotulik troctolite (see section 3.4), the Nunarssuit syenite (Parsons & Butterfield, 1981) and the Skaergaard intrusion (Irvine, 1980c).

Slump scars and erosion channels testify to the presence of both mass instability and currents within magma chambers. The eroded material is conventionally assumed to be crystals (eg Irvine, 1980a; 1980c), however some authors postulate a gradation from scattered nuclei through increasing grain size and decreasing porosity to rock (Grout, 1918; McBirney & Noyes, 1979). If so, many erosion

structures may only be evidence of the redistribution of microlite- to crystallite-sized material which can be readily mixed with, or assimilated by the contemporary magma.

3.3 Structures associated with lithic fragments.

3.3.1 Introduction.

Lithic fragments provide the only unambiguous evidence for solid transport and deposition in magma chambers, whether they are autolithic or xenolithic. This section describes structures associated with, and defined by, rock fragments; it then assesses the implications for mechanisms of crystal accumulation and for the nature of the transition from crystal mush to contemporary magma at the top of the crystal pile.

3.3.2 Relationship of fragments to igneous lamination.

Tabular, lithic fragments generally lie in the plane of the lamination developed in cumulates (fig 3.2a). They range in size from cm-scale fragments (section 3.4) to fragments on the order of 10^2 m in their longest dimension (Kangerdlugssuaq intrusion, Wager &

Plate 3.3 Fragment of leucotroctolite in troctolitic cumulates, Lower Zone. Kiglapait intrusion. Fragment lies in the layering plane, note thinning and disappearance of laminae over the fragment and unusual concentration of olivine at its right hand side.

Plate 3.4 Allivalite fragment in allivalite, Central Series, Rum. Olivine-rich laminae are deflected around the fragment, though a rapid return to flat layers takes place above it.



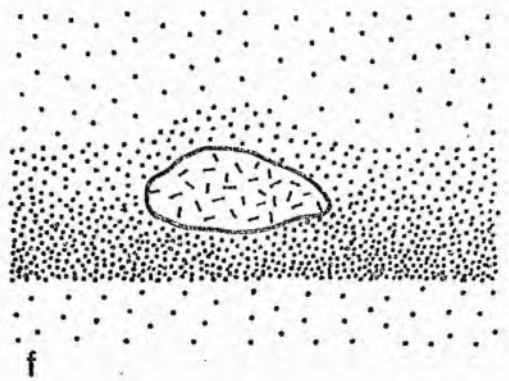
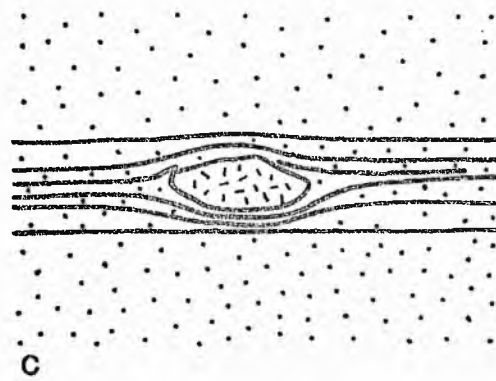
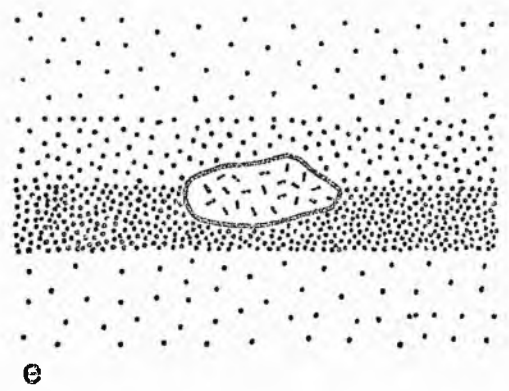
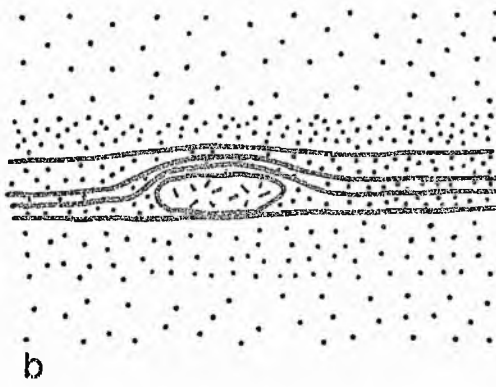
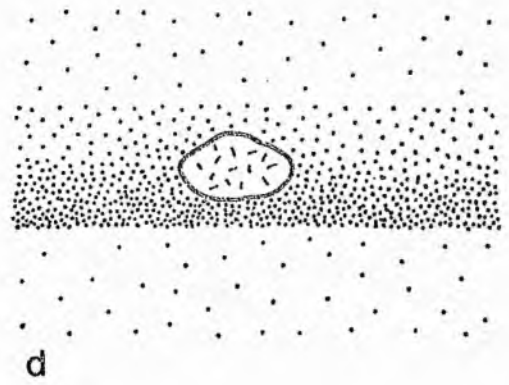
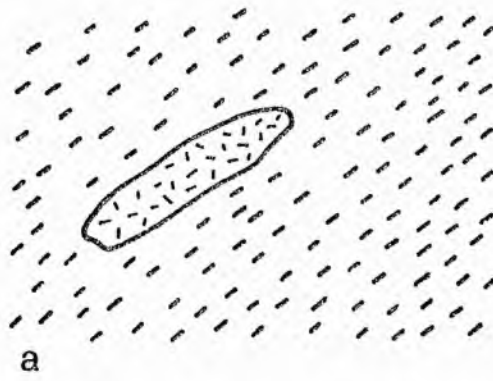
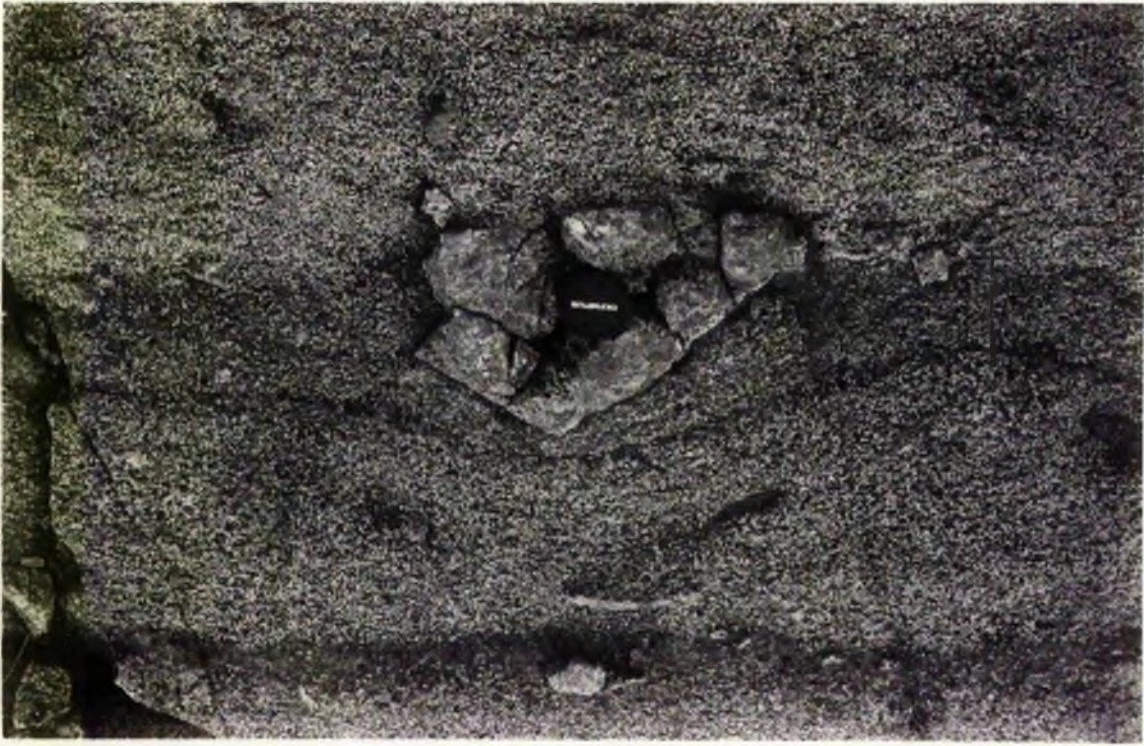


Plate 3.5 Anorthosite fragment in paired layer, Central Series, Rum, showing draping and deflection of layer over and under fragment.

Plate 3.6 Asymmetric draping of unimodal layer over anorthosite fragment, Central Series, Rum. Note flat layer base, and small leucocratic fragment set above mafic portion in overlying layer.



(plate 3.7) but are most often found wholly within layers (figs 3.2d,e,f and plates 3.5 & 3.8). Leucocratic fragments within layers most commonly occur above the most mafic portion of the layer (figs 3.2d,3.2f) and, if elongate, are oriented in the plane of the layering, unless imbricated. Graded layers often pass laterally into paired mafic/leucocratic layers and are therefore considered co-genetic (see also App 2). In these cases leucocratic fragments are generally located straddling the transition plane (fig 3.2e, plates 3.5 & 3.8).

The tops of layers above fragments may be planar (fig 3.2e) or deflected (fig 3.2f, plate 3.5) and similarly with layer bases. Overlying layers may also be deflected over these structures (fig 3.2h). In layers locally thickened in this way, and in layers with planar bounding surfaces, the mafic portion is often thickened and asymmetrically distributed around the fragment. In the Kiglapait intrusion this asymmetry is most commonly in the form of greater accumulations down dip (fig 3.2h, plate 3.9). McBirney and Noyes (1979) make a point of stating that this structure does not occur in the Skaergaard intrusion, though it is clearly illustrated by plate 2b of Irvine (1980a).

The foregoing observations apply to isolated fragments; however some layers contain numerous fragments. In such layers they are commonly distributed on one plane within the layer, though they may be randomly distributed (fig 3.2k, plate 3.11). Layers showing lateral variation from a fragment-rich facies to a fragment-poor facies have been described in the Skaergaard intrusion by Irvine

(g) Graded layer draped over fragment set in the underlying cumulate.

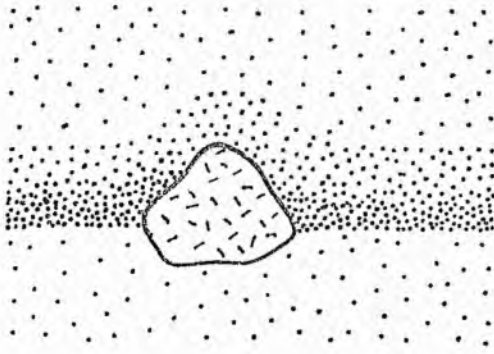
(h) Graded layers draped asymmetrically over fragment set in the underlying cumulate, note greater accumulation of mafic material on the down-dip side of the fragment.

(i) Comb layer draped over fragment.

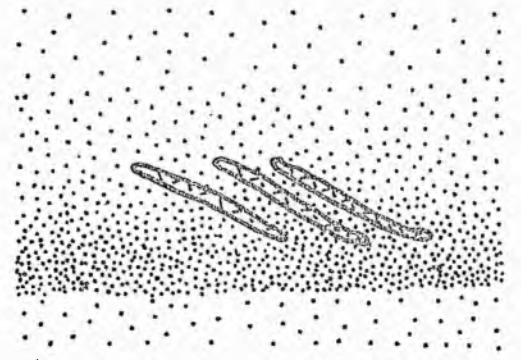
(j) Imbrication of tabular fragments, note that they do not sit on the base of the layer.

(k) Fragment-rich graded layer, fragments set within the layer.

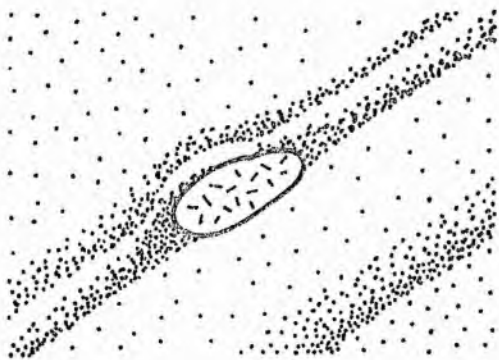
(l) Layer of normally-graded, rounded fragments.



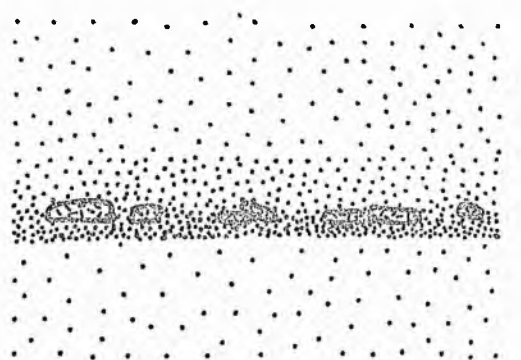
g



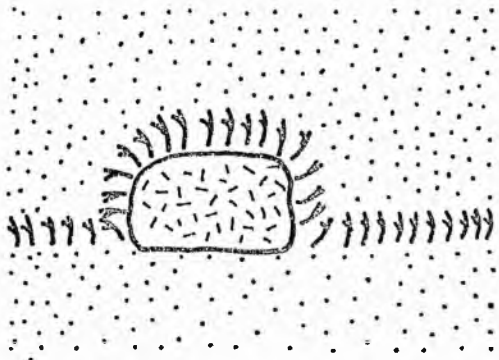
j



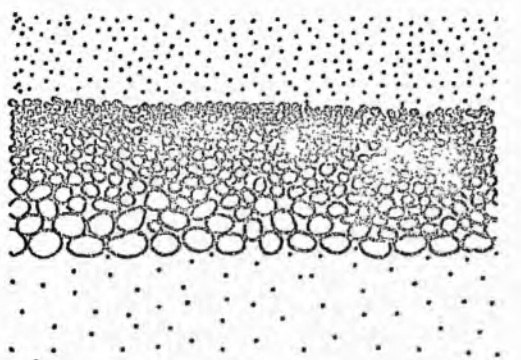
h



k



i



l

Plate 3.7 Anorthosite fragment in the uppermost portion of a normally graded layer, Central Series, Rum. The most leucocratic rock is apparently eroded at the right hand side of the fragment and thickened at the left hand side.

Plate 3.8 Anorthosite fragment sitting astride the junction in a paired (mafic/leucocratic) layer. Layer base and top are unaffected by the presence of the fragment, Central Series, Rum.

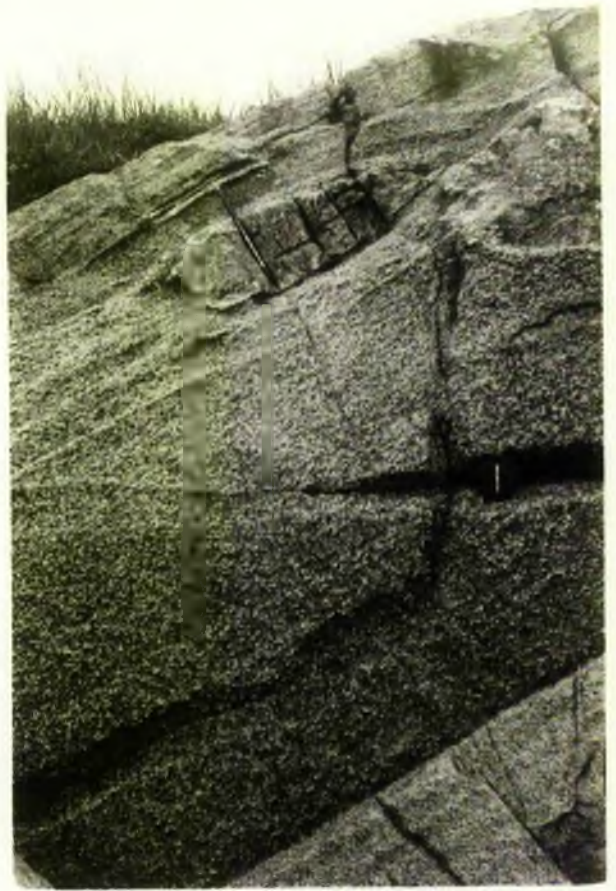


Plate 3.9 Asymmetric distribution of mafic layers around leucotroctolite fragment (approximately 20cm in diameter), Lower Zone, Kigaplait intrusion.

Plate 3.10 Plagioclase comb layer draped around troctolite fragment, Kolotulik troctolite, Tigalak intrusion, Labrador.



(1980c). Imbrication of fragments (fig 3.2j) is rare but has been noted in the Tigalak intrusion (see section 3.4) by this author and reported in the Skaergaard intrusion (Irvine, 1980c) and the Rum intrusion (McLurg, 1982).

3.3.4 Fragmental layers.

Only one layer composed mostly of fragments has been noted during the course of this study, situated in the Central Series of the Rum intrusion. In this outcrop rounded dunite fragments have accumulated on a base of layered allivalite. The base of the fragmental layer is undulatory, a feature associated with thickening and thinning of the underlying allivalite, and is intruded by flames of allivalite (plate 3.12 & 6.24). Basal fragments penetrate down into the allivalite. The fragments show a rapid reduction in size through the lower 0.5m of the layer from 2-3cm to 0.2-0.3cm in diameter (fig 3.21, plate 3.12) until they are indistinguishable from equant olivine crystals. The remainder of the outcrop is composed of this finer material, though in some parts rare, abrupt reversals occur followed by graded material. Through the whole layer, blocky allivalite fragments are randomly distributed but lie within the plane of the layering.

Plate 3.11 Anorthosite fragments associated with irregular mafic layer, Central Series, Rum.

Plate 3.12 Rounded dunite fragments set in feldspathic matrix, Central Series, Rum. The fragments decrease in size in the direction indicated by the pencil point (up stratigraphy). The protrusion of allivalite into the fragmental layer on the left of the photograph is interpreted as being due to postcumulus deformation.



3.3.5 Relationship of fragments to deformed layering.

Deformation of layering occurs under fragments, where layers are attenuated and punctured by the fragment (fig 3.2m, plates 3.13 & 3.14), though overlying layering generally shows a rapid return to planar surfaces. In more complexly deformed cumulates, fragments often occupy the cores of synclines in rocks whose structures are reminiscent of liquefaction structures in clastic sediments (fig 3.2n, plate 3.15, see also Chp 6) and layering is generally attenuated around them (figs 3.2n & 3.2o, plates 3.15 & 3.16).

3.3.6 Discussion.

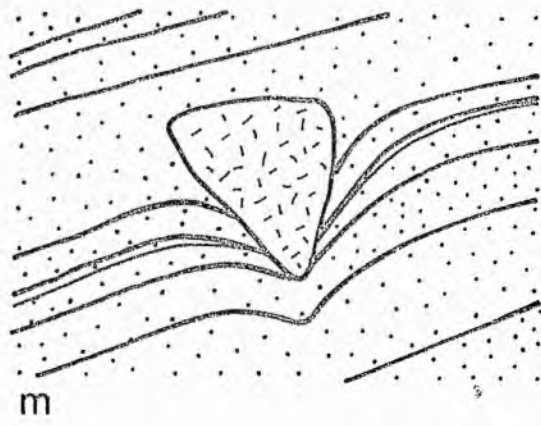
The common orientation of fragments in individual outcrops cannot be fortuitous and is interpreted as indicating the depositional surface. The orientation of lamination and layering surfaces parallel to fragments in most cumulates thus indicates that layering and lamination generally forms parallel to the depositional surface though not necessarily at it.

The deflection and puncturing of layers underneath fragments is interpreted as being due to the deformation of flat, though not necessarily horizontal, layers under the weight and/or momentum of the dropping fragment and thus confirms the existence of a mush zone. Similar interpretations have been given to similar structures

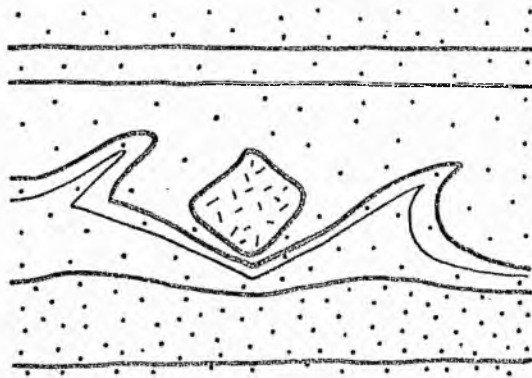
(m) Deformation with attenuation and puncturing of layers under fragment, note planar layering above fragment.

(n) Fragment sitting in deformed (?liquefied, see chp 6) layering.

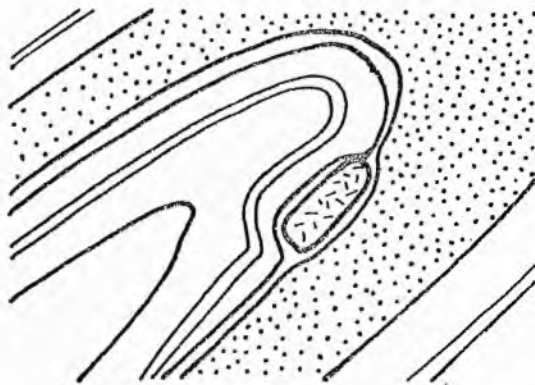
(o) Fragment within highly deformed cumulates, note extreme attenuation of layers around fragment.



m



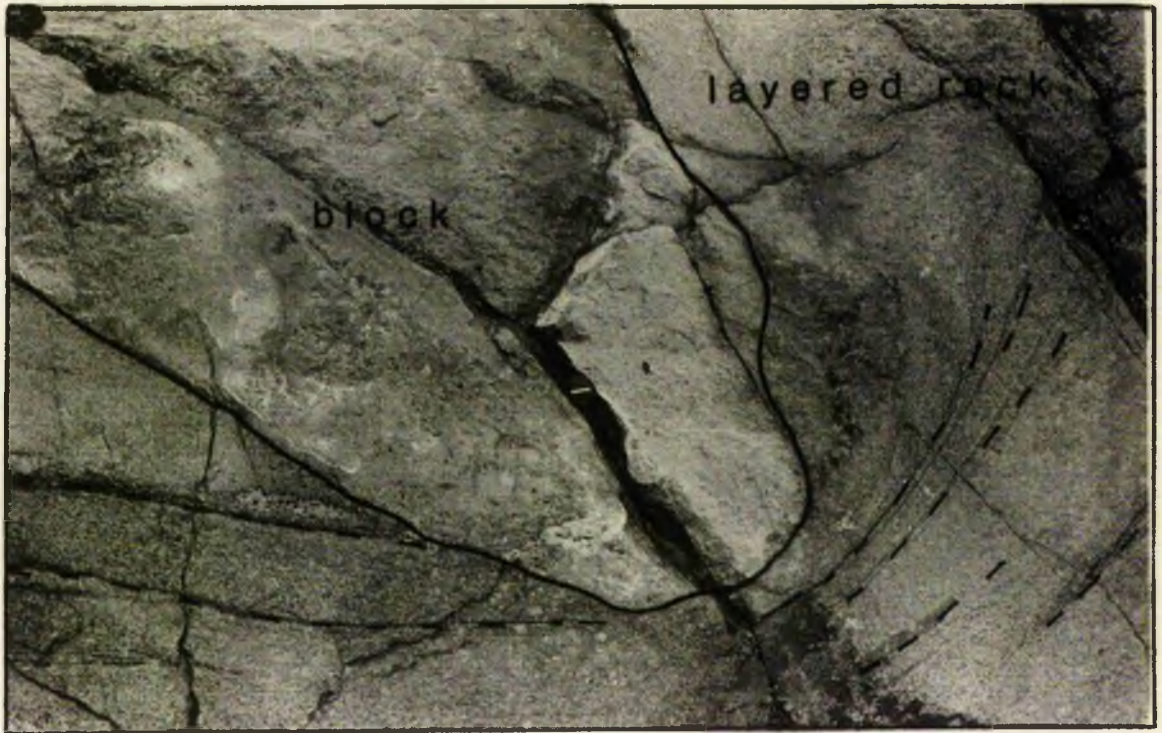
n



o

Plate 3.13 Deformation, attenuation and puncturing of layering underneath a leucotroctolite block, Lower Zone, Kiglapait intrusion.

Plate 3.14 Deformation and attenuation of layering underneath an anorthosite xenolith, Lower Zone, Kiglapait intrusion.



by Thompson & Patrick (1968). Where depression of layering is accompanied by deflection of layering over the top of the fragment, the structure can equally well be interpreted as being due to compaction of the cumulate around the fragment, or to deformation followed by accumulation, or to both. Some fragments, however, lie on layering planes without any associated deformation, thus suggesting that this surface has a degree of rigidity, in agreement with the Bingham liquid rheological models of magmatic porous media proposed by Shaw et al (1968), Shaw (1969) and Marsh (1981).

In most structures a rapid return to planar layering is noted, even above large blocks. This suggests that the effect of post-depositional compaction is limited. It also suggests that any zone of incipient layering formed by microlites/crystallites (eg McBirney & Noyes, 1979) postulated to exist above the depositional surface is either very thin, or rapidly reorders after the disrupting passage of the rock fragment.

The arrangement of banks of crystals around and over lithic fragments is a distinctive structure. In the case of plagioclase comb layers draping lithic fragments the structure requires that nucleation and growth of plagioclase occurred on and around the block. There is thus no reason to doubt equant crystals could also nucleate and grow around lithic fragments producing blocks draped with "normal" cumulate. Asymmetric distributions could be produced by differential shear affecting nucleation rate and/or the supply of components to growing crystals.

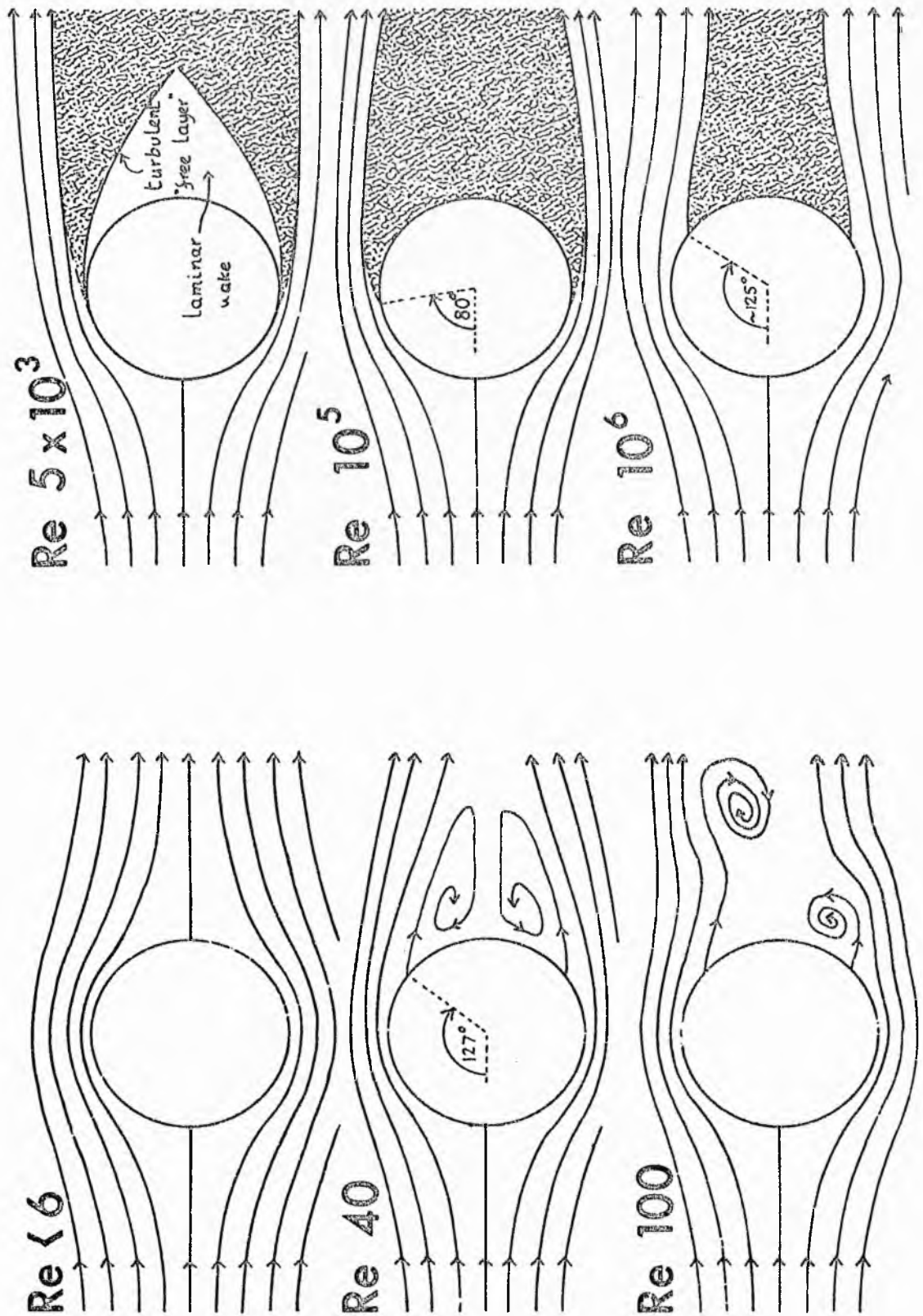
Plate 3.15 Peridotite blocks in deformed allivalite, Central Series, Rum. Layering in the allivalite is deflected and attenuated underneath the blocks, and often defines flame structures between them. Layering at the top of the outcrop is undisturbed.

Plate 3.16 Allivalite and anorthosite fragments set in isoclinally folded allivalite and feldspathic peridotite, Central Series, Rum. Layering is attenuated around the blocks.



An alternative explanation is that blocks are draped by crystals carried by magmatic currents. McBirney and Noyes (1979) have rejected this hypothesis because no scour at the base of blocks has been noted and deposition has apparently occurred symmetrically in contrast with deposits formed in the lee of obstacles in aqueous sediments. On the other hand this lack of structure may be expected when the fluid dynamics of flow and deposition around obstacles in the path of currents are considered. Sedimentary structures formed around obstacles in the path of currents in aqueous environments can be subdivided into (a) current crescents, arcuate troughs scoured upstream of obstacles and (b) obstacle shadows, flow aligned features originating by scour and/or deposition in the lee of obstacles (Karcz, 1968). By approximating the shape of such obstacles to that of a vertical cylinder resting on the bed, an analysis of the flow patterns leading to the generation of obstacle marks can be carried out (Richardson, 1968; Karcz, 1968). These studies conclude that obstacle scours can be explained in terms of stretching and accumulation of vorticity in the flow approaching an obstacle and that scour-deposit and scour-remnant ridges owe their existence to flow separation and the formation of a von Karman vortex sheet in the lee of obstacles. Accepting this as an approximation to the physical situation described (and note that the following analysis ignores the formation of a velocity gradient close to the bed), then the dynamics of flow around the obstacle can be described by the Reynolds number for steady flow past a circular cylinder. The Reynolds number is defined as

Figure 3.3 Flow patterns around circular cylinders normal to the flow, for Reynolds numbers from less than 6 to about 10^6 . (From Middleton & Southard, 1978)



$$Re = \rho U d / \mu \quad (3.1)$$

where ρ is the density of the fluid, U is the velocity of the current, d is the diameter of the cylinder and μ is the dynamic viscosity of the current. Flow patterns in the lee of circular cylinders orientated perpendicular to the flow for a range of Reynolds numbers are shown in figure 3.3. Flow separation first occurs at a value for the Reynolds number of about 40 (Middleton & Southard, 1978) and a fully turbulent wake at a value of about 1.5×10^4 . The Reynolds number for a fluid whose viscosity is 10^3 poises and density is 2.8 g cm^{-3} (Skaergaard liquid at approximately 50% solidified, McBirney & Noyes, 1979) flowing past a cylinder 10cm in diameter at 7 km hr^{-1} (194.4 cm s^{-1}) (experimentally determined by Irvine, 1980a) is 5.4. In magmas with viscosities about an order of magnitude lower (eg Duke Island, Rum, Kiglapait during Lower Zone time) the value of Re will be an order of magnitude higher and flow separation can be expected to occur (see fig 3.3). For comparison the value of Re for water flowing past a similar cylinder at 0.2 cm s^{-1} is greater than 10^4 . Thus for examples with no asymmetry flow separation has not occurred and Re must be very low. For those examples with asymmetry flow separation occurred and Re was greater than 40.

Models of magmatic density currents together with consideration of the likely density contrasts and settling velocities of crystals have led Irvine to suggest that such density currents do not deposit crystals, but that they stop and become layers (Irvine, 1980a). Symmetrical and asymmetrical accumulations of crystals around blocks

may then be a reflection of asymmetry during flow of a particular magmatic density current. These observations are consistent with an origin for the structures in the flow of crystal-laden currents.

3.4 Imbrication and erosion in trough layering - an example from the Tigalak intrusion.

3.4.1 The Tigalak intrusion - general features.

The Tigalak intrusion is one of a number of layered intrusions associated with the Precambrian Nain anorthosite (Morse, 1980b). At present the subject of detailed study by R.A. Wiebe, it has a horizontal sheet-like form, measures approximately 10 x 6 km in areal extent and ranges in composition from norite to ferrodiorite. The intrusion rests on a floor of leuconorite and is roofed by leucotroctolite and strongly layered troctolite (Wiebe, 1980). Layered troctolite similar to that forming the roof of the pluton also occurs as rotated inclusions within the Tigalak ferrodiorite and has been named the Kolotulik troctolite (Berg, 1980). These inclusions have dimensions of the order of tens to hundreds of metres and the ferrodiorite is chilled against them. The following observations were made during the summer of 1981 following work on layering styles in the Kiglapait intrusion.

3.4.2 Trough layering -- field relations.

In one inclusion the rocks display spectacular trough layering, bounded by massive troctolite, which consists of repeated modally graded layers, 2 - 20 cm. thick, with generally sharp lower contacts and either sharp or gradational upper contacts. Individual troughs are shallow and apparently on the order of ten metres wide. Exposure does not, however, allow an assessment of their true width and thus the possibility exists that the outcrop is an oblique section through much narrower troughs. The layers themselves grade from relatively mafic bases to feldspathic tops. Individual graded layers may be separated vertically by uniform troctolite or lie one on top of the other. Several examples of a lower layer being truncated by an upper one are present (plate 3.17). Individual layers thin and lose definition laterally (plate 3.17), eventually merging with the bounding massive troctolite.

Within many of the graded layers fine-grained, lens-shaped bodies of leucotroctolite occur (plates 3.17 & 3.18), which will henceforth be referred to as lenses. They are apparently discoidal, measuring approximately 2 - 8cm. in diameter by 0.2 - 0.5cm. thick. They are sharply defined and do not cut across layer boundaries. Their long dimension is arranged either parallel or obliquely to the plane of the layering. Typically they occur above the most mafic portion of the enclosing layer. Where isolated from one another they tend to lie parallel to the plane of the layering but where they are grouped they exhibit a marked tendency to stack

Plate 3.17 Margins of Kolotulik trough structures. Note thinning of layers towards the margins, erosion surfaces and the presence of leucotroctolite lenses in the layers.

Plate 3.18 Detail of the graded layers and imbricated leucotroctolite lenses. The lenses do not cut layer boundaries, tend to be found above the most mafic portion of each layer and are only oriented at an angle to the layering where lenses overlap.



obliquely to it, en echelon (plates 3.17 & 3.18).

3.4.3 Petrography.

a) Layered rocks.

Olivine occurs as small (0.5 - 1.0 mm.), rounded grains which are commonly clustered in groups of crystals exhibiting mutual interference boundaries with 120° triple junctions. Plagioclase is subhedral and occasionally encloses olivine. The grains are typically elongate, with a length to breadth ratio of 3:1, and the long dimension is typically around 1mm. All the rocks described have a lamination defined by plagioclase feldspar (plate 3.19) parallel to the layer contacts. Fe-Ti oxide crystals occur as small grains enclosed in olivine or between olivine and/or plagioclase crystals. Commonly they are rimmed with a red-brown biotite, probably fluorine oxy-biotite, a feature common in troctolites of the Nain province and ascribed to reaction with late-stage melt and whose presence is considered to be an indicator of dry magmas (Morse, 1979b). Clinopyroxene occurs as colourless or pale-brown rims on olivine and, less commonly, between plagioclase crystals. In sections containing lenses the mode is restricted (olivine 59.3% - 67.1%, plagioclase 30.3% - 38.7%, augite 0.9% - 2.6%, Fe-Ti oxides 0.4% - 0.7%, biotite 0.3% - 0.6%), though these extend to more olivine-rich and feldspar-rich values towards the tops and bases of layers respectively.

Plate 3.19 Photomicrograph of a section through three leucotroctolite lenses. (x7, partially crossed polars)



b) Leucotroctolite lenses.

Olivine occurs as small (0.1 - 0.2 mm), sub-spherical to spherical grains. Plagioclase is less elongate than in the enclosing layered rocks and often poikilitically encloses olivine (plate 3.19). Opaque phases occur as inclusions in olivine and between plagioclase tablets. Biotite rims some oxide crystals. The mode is very restricted, the mean of six lenses being: plagioclase 70.7%, olivine 29.0%, Fe-Ti oxide 0.2%, biotite 0.1%. Six thin sections of lenses were examined and only two small crystals of clinopyroxene were identified (less than 0.01% mode).

3.4.4 Mineral chemistry.

Analyses of all the main phases were obtained using standard wavelength-dispersion spectrometry microprobe techniques (see footnotes to table 3.1 for microprobe operating conditions). Core-rim pairs were analysed in each crystal to gain some insight into the extent and direction of marginal zoning. Olivine and Fe-Ti oxide compositions within the lenses and the enclosing layered rocks are essentially identical (table 3.1). Plagioclase analyses reveal differences between lenses and layered rocks in both core composition and extent and direction of zoning. Examination of table 3.1 and figs 3.4 and 3.5 reveals that rim compositions in both sets of feldspars are similar, with the exception of two extremely

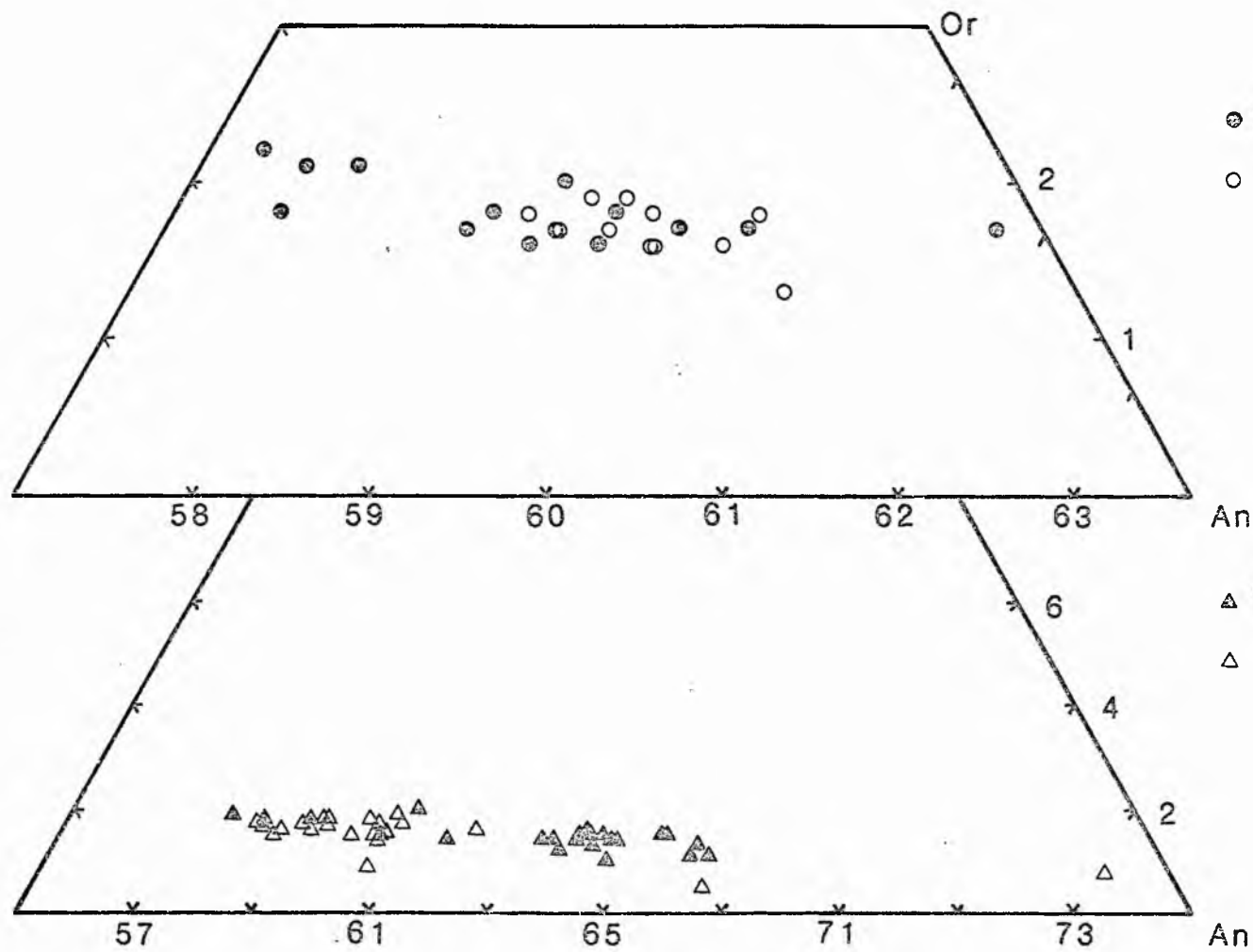
Table 3.1 Mineral compositions in the Kolotulik trough layers and leucotroctolite lenses. All analyses made using an accelerating potential of 20kV and a probe current (as measured in a Faraday cage) of 30 nanoamps, 4 x 10 second counts made on peak and 2 x 10 second counts on background. Note the similarity of olivine and plagioclase rim compositions in the layered rocks and the lenses, and the more calcic compositions of layer plagioclase cores and less calcic compositions of lens plagioclase cores.

Phase Olivine (layer) Olivine (lens) Plagioclase (layer/core) Plagioclase (layer/rim) Plagioclase (lens/core) Plagioclase (lens/rim)

No of analyses	10	9	22	20	13	12
Wt% SiO ₂	36.84	36.84	51.32	52.17	52.48	51.93
TiO ₂	-	-	0.06	0.04	0.07	0.05
Al ₂ O ₃	0.03	0.04	30.24	29.61	29.56	29.71
Cr ₂ O ₃	0.00	0.01	-	-	-	-
FeO	29.56	29.76	0.19	0.46	0.21	0.30
MnO	0.38	0.39	-	-	-	-
MgO	33.19	33.02	0.04	0.07	0.04	0.06
NiO	0.12	0.13	-	-	-	-
CoO	0.09	0.08	-	-	-	-
CaO	0.05	0.04	13.12	12.33	12.21	12.36
Na ₂ O	-	-	4.03	4.40	4.48	4.42
K ₂ O	-	-	0.26	0.28	0.32	0.30
TOTAL	100.36	100.31	99.26	99.36	99.37	99.13

Atoms	Si ⁴⁺	Ti ⁴⁺	Al ³⁺	Cr ³⁺	Fe ²⁺	Mn ²⁺	Mg ²⁺	Ni ²⁺	Co ²⁺	Ca ²⁺	Na ⁺	K ⁺	O ²⁻	FO	FA
Si ⁴⁺	0.993	-	0.002	0.000	0.671	0.005	1.327	0.003	0.003	0.002	-	-	4.000	66.6	33.4
Ti ⁴⁺	-	-	-	-	-	-	-	-	-	-	-	-	-	-	-
Al ³⁺	-	-	-	-	-	-	-	-	-	-	-	-	-	-	-
Cr ³⁺	-	-	-	-	-	-	-	-	-	-	-	-	-	-	-
Fe ²⁺	-	-	-	-	-	-	-	-	-	-	-	-	-	-	-
Mn ²⁺	-	-	-	-	-	-	-	-	-	-	-	-	-	-	-
Mg ²⁺	-	-	-	-	-	-	-	-	-	-	-	-	-	-	-
Ni ²⁺	-	-	-	-	-	-	-	-	-	-	-	-	-	-	-
Co ²⁺	-	-	-	-	-	-	-	-	-	-	-	-	-	-	-
Ca ²⁺	-	-	-	-	-	-	-	-	-	-	-	-	-	-	-
Na ⁺	-	-	-	-	-	-	-	-	-	-	-	-	-	-	-
K ⁺	-	-	-	-	-	-	-	-	-	-	-	-	-	-	-
O ²⁻	-	-	-	-	-	-	-	-	-	-	-	-	-	-	-
TOTAL	9.408	0.010	6.536	-	0.030	-	0.013	-	-	2.418	1.432	0.061	32.000	59.8	38.6
FO	9.544	0.007	6.386	-	0.071	-	0.024	-	-	2.391	1.560	0.075	32.000	59.0	38.6
FA	9.521	0.011	6.423	-	0.033	-	0.010	-	-	2.430	1.572	0.070	32.000	59.7	38.6
														1.8	1.7

Figure 3.4 Individual plagioclase analyses from the Kolotulik leucotroctolite lenses and enclosing layers plotted in a segment of the An - Ab - Or triangle. Note that the lens feldspars tend to be reversely zoned whereas those from the layers tend to be normally zoned.



● lens plag. cores
○ lens plag. rims

▲ layer plag. cores
△ layer plag. rims

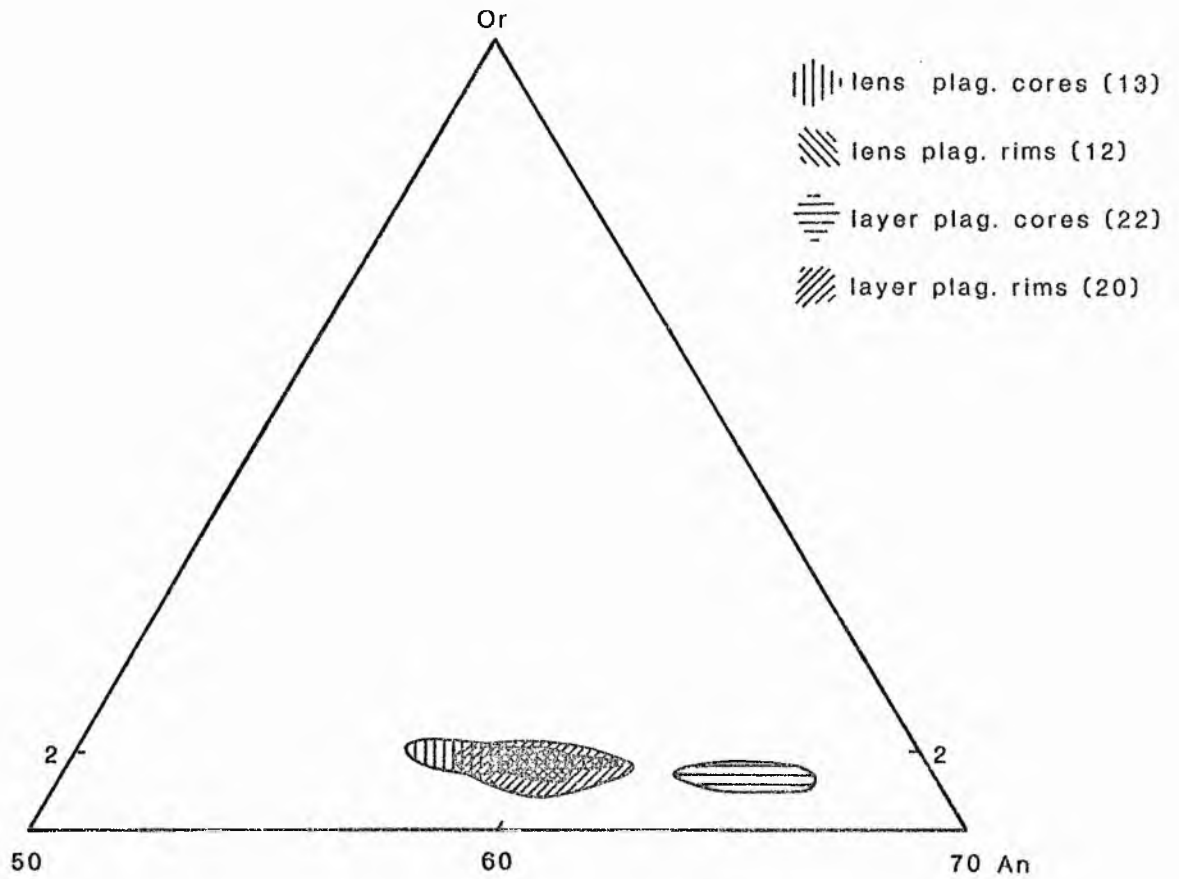


Figure 3.5 Summary of the data in figure 3.4 showing the similarity of rim compositions from lens and layer plagioclases. Number of analyses in each field in brackets.

calcic analyses in feldspars from the layers. Similar localised zoning to extremely calcic values has been noted in feldspars of the nearby Kiglapait intrusion and ascribed to enhanced partitioning of anorthite components into feldspars in residual liquids enriched in clinopyroxene components by growing olivine and plagioclase crystals, the "augite effect" (Morse, 1982). The core compositions of lens feldspars tend to be more sodic than this common rim value, whereas the feldspar cores from the layers tend to be more calcic.

3.4.5 Origin of the leucotroctolite lenses.

The undoubted resemblance of the stacked lenses to imbricate structure in clastic sediments is potentially significant, but the lenses are not obviously rock fragments. Thus the other two possibilities, namely that the lenses formed contiguously with, or after, the layered rocks must be examined.

Bodies of rock which have formed within crystal piles have been ascribed to replacement (Chp 6; Irvine, 1980b), or segregation of interstitial liquid (Chp 6; Morse, 1969; Donaldson, 1982). Such bodies have been recognised by their transgressive nature and/or their evolved composition. The lenses meet neither criterion, since they do not cut layer boundaries and they are pyroxene depleted, not enriched as might be predicted by the petrography of the layered troctolite, phase relations in the system Forsterite - Diopside - Anorthite and comparison with liquid segregations in the troctolitic

Lower Zone of the nearby Kiglapait intrusion which are invariably gabbroic (Morse, 1969).

Textural and modal variations are common in vertical sections of layered intrusions. Abrupt changes to very fine grain sizes have been described by Parsons (1979) and Thy and Esbensen (1982) and ascribed to chilling and fluctuations in volatile pressure, respectively. Neither mechanism can apply on the very local scale demanded here, nor can they explain the apparent diachronism of the enclosing layers.

The simplest and most satisfying explanation is that in which the lenses represent fragments of previously crystallised material which have been transported to their present position. Such a hypothesis accounts for the modal and textural differences and the similarity of feldspar rim compositions by equilibration with, or crystallisation from, interstitial liquid in the layered troctolites.

3.4.6 The origin of the trough layering.

Present debate on the formation of trough and normally graded layering centres on the possible role of crystal-laden density currents (Irvine & Stoesser, 1978; Taylor & Forester, 1979; McBirney & Noyes, 1979; Irvine, 1980a). Two features of the Tigalak troughs suggest that they were the loci of current activity.

i) The cutting off of layers by overlying layers is interpreted as being due to physical erosion rather than to resorption or faulting. Similar interpretations have been proposed of similar structures in other intrusions (eg Section 3.2; Irvine & Stoesser, 1978; McBirney & Noyes, 1979; Parsons & Butterfield, 1981).

ii) The presence of lithic fragments within the troughs alone points to the existence of a transporting agent rather than the random settling of fragments from above; once again current flow along the axes of individual troughs is the most likely explanation. Thus the evidence suggests that these troughs were the sites of active currents, able to erode their substrate and transport and deposit lithic fragments and crystals, even though, as shown later, the feldspar was most likely less dense than the contemporary magma.

Trough formation may have proceeded in the manner suggested by Irvine and Stoesser (1978) and individual graded layers may be the solidified remnants of individual density currents as suggested by Irvine (1980a). The above conclusions support Irvine's proposition that normally graded layers in "gabbroic" plutons can be formed from crystal-laden density currents, in spite of feldspar being less dense than the ambient fluid.

The en echelon stacking of the lenses remains to be explained. This structure can be legitimately termed imbricate structure. Imbricate structure in clastic, water-lain sediments can occur in two ways; by rolling of clasts during bedload transport,

each clast being arrested by that in front, or by intergranular collisions forcing clasts into positions of least resistance to the flow (Collinson & Thompson, 1982). Models of magmatic density currents suggest that deposition from currents does not take place, but rather that currents stop and become layers (Irvine, 1980a). The lenses cannot then have been a part of any bedload since they are most commonly found within layers (currents). A mechanism analogous to the second outlined above may have brought about their imbrication by shearing in the vertical velocity gradient of the current tail.

3.4.7 Physical properties of the Tigalak magmatic density currents.

Further discussion of crystal and rock fragment transport and sorting mechanisms within magmatic density currents is hindered by a lack of empirically or theoretically derived values of their physical characteristics. Irvine's experimental work is applicable to a large range of natural currents depending on the scaling chosen. The viscosities and densities of naturally occurring silicate liquids are well known or can be calculated (Bottinga & Weill, 1970; 1972). The major unknown in defining the parameters which describe density currents is then the proportions and amounts of suspended solid. The Tigalak structures can be used to obtain this information at a point within a current as outlined below.

	<u>Wt%</u>
SiO ₂	47.55
TiO ₂	1.10
Al ₂ O ₃	18.57
Fe ₂ O ₃	1.91
FeO	10.08
MnO	0.16
MgO	8.08
CaO	8.97
Na ₂ O	3.20
K ₂ O	0.23
P ₂ O ₅	0.14
TOTAL	<u>99.99</u>

Table 3.2 Kiglapait liquid at 40 PCS
(from Morse. 1981h)

Leucocratic lithic fragments can be found within normally graded layers in a number of intrusions and are commonly situated above the most mafic portion of the layer (see section 3.3.3). This feature suggests that these fragments have found their own density level within any particular current (layer) and thus the bulk density of the current at that point was equal to that of the rock fragment. Accepting this, the physical properties can be quantified as follows.

The physical parameters of interest are the density and viscosity of the current. To define these the densities and amounts of the suspended solids must be known together with the density and viscosity of the liquid. The density and viscosity the liquid can be calculated from its composition and temperature. This liquid is considered to have been in equilibrium with olivine, Fo 66.5, and plagioclase, An 63.0, (from table 3.1). Olivine and plagioclase of these compositions in petrographically similar troctolites of the Lower Zone of the nearby Kiglapait intrusion were in equilibrium with the Kiglapait liquid at 40 PCS (compositions and conventions from Morse, 1979a). The composition of this liquid is given by Morse (1981b) and presented in table 3.2 and its cotectic temperature can be calculated using the relation

$$10^3/T(^{\circ}\text{K}) = -0.273 X_{\text{An}} + 0.838 \quad (3.2)$$

from Morse (1979a) which gives a value of 1228^oC. The density and viscosity have been calculated as 2.685 g cm⁻³ and 1.23 x 10² poises

by the methods of Bottinga and Weill (1970 & 1972) using the revised estimates of the partial molar volumes of the oxide components given by Nelson and Carmichael (1979).

Solids now have to be added to this liquid until its bulk density equals that of the lenses. The density of the lenses has been calculated from their mode and the compositions of their included phases. Considering Fe-Ti oxides, biotite and clinopyroxene with olivine (together they only make up 0.3% of the mode) the lenses are made up of 29% olivine, Fo 66.5, and 71% plagioclase, An 59. Using the density versus composition curves in Deer et al. (1966) and estimating the volume increase due to thermal expansion to be 4% and 2% for olivine and plagioclase respectively, from the data given in Clark (1966) the lens density at the magmatic temperature is 2.88 g.cm.⁻³ Adding olivine, Fo 66.5, and plagioclase, An 63, in the proportions 2:1 (estimated from their modal proportions) and calculating their densities as outlined above until the bulk density equals 2.88 g.cm.⁻³ gives a value of 39.5% for the proportion of solids.

The viscosity of the current can now be calculated using the relationship

$$\mu_C = \mu_L(1 - RX)^{-2.5} \quad (3.3) \quad (\text{Roscoe, 1953})$$

where μ_C is the dynamic viscosity of the current in poises, μ_L is the dynamic viscosity of the liquid, X is the proportion of solids (0.395) and R is a numerical constant. Using a value for R of 1.35

(approximating the particle shapes to that of solid spheres) gives a value of 8.26×10^2 poises.

The foregoing assumes that the lenses were wholly solid during transport. There is nothing in the petrography to suggest that this was necessarily so, indeed the presence of some clinopyroxene suggests that they may have contained some liquid. An upper limit can be placed on the possible amount of liquid since at porosities of about 20% silicates disaggregate (D.P. McKenzie, pers. comm. 1983). Repeating the above calculations assuming the lenses were 20% liquid, of a similar composition to that of the ambient fluid gives a value of 2.84 g cm^{-3} for the lens density. The proportion of solids is then calculated at 32% and the current viscosity at 7.43×10^2 poises.

3.4.8 Discussion.

These estimates are strictly only applicable to one point within a current. Gradients of density and/or viscosity may be expected across it, though are presently inestimable. The estimated proportion of solids is much greater than most previous intuitive estimates (eg Wager & Brown, 1968) which are typically around 10%.

Magmatic density currents are thought to be initiated by slumping of loosely packed cumulate (Irvine, 1980a). They therefore must maintain their initial proportion of solids unless the current is diluted by entrainment of the ambient fluid. In aqueous turbidity currents entrainment occurs by ambient fluid passing into clefts in the current head (Allen, 1971) and by turbulent mixing across the upper interface of the current (Middleton & Hampton, 1973). Both processes only occur during turbulent flow. The degree of turbulence in a gravity flow can be described by its Reynolds number which is defined as

$$Re = \rho Ud/\mu \quad (3.4)$$

Using values for viscosity and density as calculated earlier and estimating the flow depth as 10 cm and the current velocity at 30 cm s⁻¹ from Irvine (1980a) gives values of just over 1 for Re. Thus magmatic density currents of these dimensions and flowing at velocities of this order will be laminar in character, will not entrain ambient fluid and the current will reflect the porosity of the source cumulates. Initial porosities of cumulates are commonly estimated at 30 - 60% on textural and experimental grounds (Jackson, 1961; Campbell *et al.*, 1978; Irvine, 1980b).

3.5 Conclusions.

1) Erosion structures record the physical redistribution of solids in layered intrusions.

2) Lithic fragments are the products of physical deposition. Structures associated with lithic fragments indicate that they locally affect the depositional process. These structures have forms which are consistent with the physical deposition of magmatic sediment.

3) Deformation of layers underneath fragments implies that the transition from magma to rock is not an abrupt one, ie it implies the presence of a crystal mush. Symmetrical deformation above and below fragments may be physical evidence for compaction of cumulates.

4) Calculated values of the crystal content of density currents are high, but they are consistent with the flow characteristics of viscous density currents with low Reynolds numbers.

4 TWO CONTRASTED LAYER TYPES IN THE KIGLAPAIT INTRUSION, N. LABRADOR.

4.1 Introduction.

The conclusions on the origin of graded layers in chapter 3 are based on structures which affect the layers only locally. Presumably the mode of formation of any layer type is reflected in its variations in texture, mode and composition in three dimensions. An attempt was made to test this belief in the Kiglapait intrusion but unfortunately failed due to insufficient exposure and post-cumulus deformation (see App 4). Attention was thus focussed on the whole spectrum of Kiglapait layering and the structures and textures which defined each particular layering style, or facies, were catalogued. These descriptions and a short discussion are appended (App 4) and were submitted for inclusion in the 1983 field report of the Nain Anorthosite Project.

As proponents of a rhythmic, diffusion-controlled mechanism of layer formation, McBirney and Noyes (1979) have suggested that its operation will be recorded by cryptic variation on the scale of the layering, in support of which they present compositional profiles of a graded layer from the Upper Zone of the Skaergaard Layered series. Their evidence is inconclusive, however, since (a) it is based partly on whole-rock and mineral separate analyses, in which it is impossible to distinguish between the cumulus and postcumulus

components of any cryptic variation, (b) the mineral assemblage studied is likely to have undergone extensive postcumulus reaction and (c) textural information is lacking. The possibility that primary cryptic variation is a feature of graded layers cannot be discounted on the basis of these objections alone, however. Therefore a drill core section through a graded layer from the Lower Zone of the Kiglapait intrusion (see plate 4.1) was selected for detailed mineralogical and textural study. For comparison a sample of the layer type considered, on the basis of its field relations, most likely to have formed by in situ crystallisation was also selected. The results of these studies are described below.

4.2 Field relations.

4.2.1 Normally graded layers.

These are layers which grade from a relatively mafic base to a more feldspathic top (plate 4.1). The lower contact is always sharp, the upper generally so, but may be gradational into "average rock". These layers are the "gravity stratified layers" of Wager and Brown (1968) or "graded layers" of Morse (1979a). They exhibit a marked tendency to occur in groups in the intrusion (Morse, 1979a) though they interdigitate, unlike the cm-scale layers (see 4.2.2). Layers of this type range in thickness from 5cm to 1m and the portion rich

Plate 4.1 Group of normally graded layers in troctolite, Lower Zone, Kiglapait intrusion. The layer under the pencil was selected for detailed study.

Plate 4.2 Plastic deformation structure in graded layers in troctolite, Lower Zone, Kiglapait Intrusion.



in mafic minerals generally represents between 20% and 80% of this amount. The internal modal gradation can occur through the whole layer or be confined to a narrow zone. Some graded layers can be observed to pass down dip into sharply-defined, paired, leucocratic/melanocratic layers as the grading zone thins to a plane. This feature suggests that other similarly paired layers may also be related to normally graded layers. No individual layer could be traced along strike for more than 70m, though groups of layers could be traced for much longer distances (100s of m). Since most extensive outcrops are strike sections, no accurate assessment of the down-dip dimension of these layers can be made, though layer terminations are rarer in dip sections than strike sections, suggesting some elongation down dip. Layer terminations occur by gradual thinning and loss of definition or more rarely by truncation by overlying layers.

Normally graded layers contain or define more small-scale structures than any other layer type in the intrusion. These include erosional bases (eg fig. 3.1b), asymmetric draping over, or distribution around autoliths fragments (fig 3.2g,h, plate 3.9) and post-cumulus deformation structures in the form of shear zones in which individual layers are attenuated or lose their identity altogether (plate 4.2).

4.2.2 Cm-scale layers.

This style of layering is characterised by 1-2cm of mafic material in otherwise modally "average" (at least in its field appearance) rock. In the Lower Zone these mafic layers are olivine concentrations (plate 4.3) while in the Upper Zone they are of pyroxene or pyroxene and oxide (plate 4.4). In the field they appear to have a slightly sharper base than top. They commonly occur in groups (plate 4.3), though isolated examples exist, and they are remarkably persistent along strike (one such layer in the Lower Zone was traced for over 200m before being lost due to lack of exposure. Where they occur in groups they are remarkably parallel. Traced along strike, groups of layers tend to become less clearly defined as a group, though retaining a constant thickness and separation, until they become indistinguishable from the enclosing average rock. No layer of this type was observed cutting across another layer, though they do occur within large scale macrorhythmic layers.

4.3 Petrography.

One drill core section for one example of each layer type described above was selected for detailed study in the laboratory. They were sampled at approximately the 10 PCS level, near the base of the Lower Zone, and within approximately 10 m stratigraphically

Plate 4.3 Group of cm-scale layers (under the hammer) selected for detailed study, Lower Zone, Kiglapait Intrusion. The appearance in places of thickened mafic laminae is purely a function of weathering being initiated along olivine-rich laminae.

Plate 4.4 Cm-scale layers defined by concentrations of clinopyroxene in ferrodiorite, Upper Zone, Kiglapait intrusion.



and 100m along strike of one another. According to the systematics and liquid compositions in Morse (1979a, 1981b), contemporary magma compositions can be considered identical through this stratigraphic interval at this level in the intrusion. Composite photomicrograph sections through each layer type are presented in plates 4.5 and 4.6.

4.3.1 Textures - graded layer.

Olivine is equant and anhedral. At the base of the layer the diameter of most olivines is 1-2 mm, upwards in the layer these values decrease steadily to 0.5-1 mm. At the base of the layer olivine exhibits well-developed mutual boundaries with 120° triple junctions; upwards, as the olivine becomes smaller and the olivine/plagioclase ratio decreases, the development of these triple junctions becomes less common.

Plagioclase is tabular to equant, anhedral or rarely subhedral. At the base of the layer the feldspar is present as small grains (approx. 0.1-0.25 mm across) in the interstices of olivine crystals and becomes larger upwards. The feldspar defines a very marked trachytoid texture, or lamination, developed parallel to the margins of the layer. Both olivine and plagioclase are slightly deformed. Several finer-grained domains of olivine and plagioclase are present and typically have the dimensions of the larger crystals.

Plate 4.5 Composite photomicrograph of sections through the graded layer (left) and cm-scale layer (right) described in the text. Virtually all of the sections are of plagioclase (low relief) and olivine (high relief). Opaques and clinopyroxene rich in exsolved opaques show up as dark spots. (x1.2, plane polarised light)



Clinopyroxene occurs as pale-brown to colourless rims on olivine and plagioclase, or rarely as small interstitial grains. Fe-Ti oxide occurs interstitially and is often rimmed by a red biotite, probably fluorine oxybiotite formed by reaction with late-stage melt (Morse, 1979b).

4.3.2 Textures - cm-scale layer.

Olivine is granular, equant and anhedral and 0.5-1 mm in diameter. Olivines show poorly developed mutual boundaries with 120° triple junctions in the mafic layers, whereas in the intervening leucocratic rock triple junctions are very rare. Short chains of a few olivines are often found adjacent to plagioclase crystals.

Plagioclase is tabular, subhedral to anhedral and measures up to 1cm in its longest dimension. A lamination is developed in the mafic laminae and only very weakly developed in the intervening leucocratic rock. Fine platelets of Fe-Ti oxide are present in these plagioclases, though an inclusion-free zone is developed around the margins of each crystal.

Clinopyroxene occurs as thin rims on olivine, rarely as small interstitial grains in the olivine-rich laminae, and also as discrete, anhedral crystals in the interlayer leucocratic rock. Fe-Ti oxide crystals occur interstitially between the major silicate

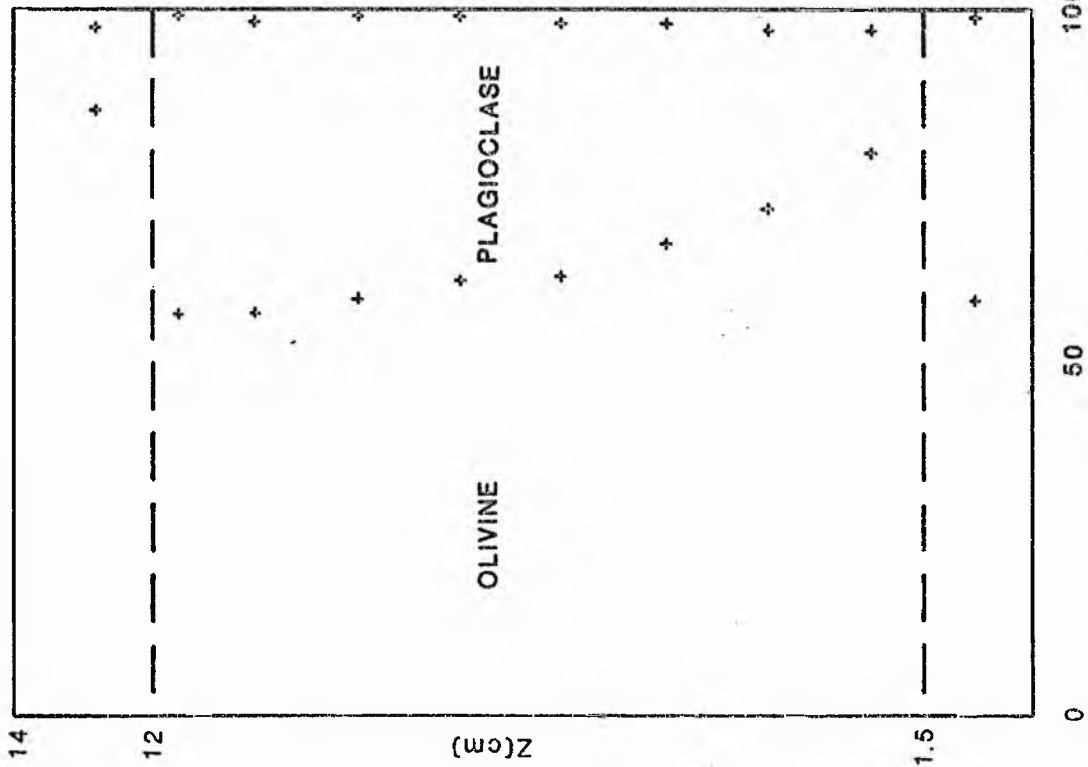
phases.

4.3.3 Modal variation.

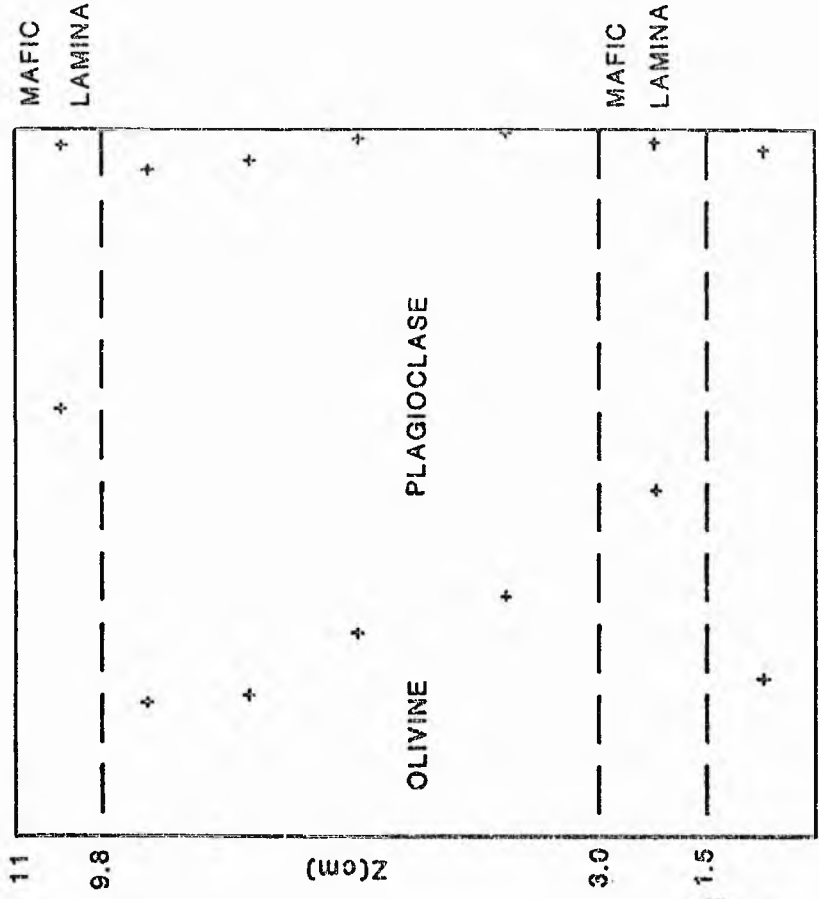
Modal data were collected with the objectives of defining (a) the relationship between the mafic/felsic oscillations in each layer and the cotectic ratio of olivine to olivine and plagioclase and (b) to determine variations in the amount of trapped liquid in each layer. Each drill core section was split into 2 cm segments, some segments being split between two thin sections, and 1500 points counted in each segment. Data for olivine, plagioclase, and clinopyroxene + opaques + biotite are plotted at the mid-point of each segment against position in each layer in fig 4.1.

Modal data have been used to calculate the ratio of olivine to olivine + plagioclase in each segment, which has been plotted against z (stratigraphic height within the layer measured relative to some arbitrary point in the underlying rock) in fig 4.2. This ratio is virtually identical to the colour index of each segment. The mean colour index for the Lower Zone is approximately 22 which is considered equal to the cotectic ratio (olivine/olivine + plagioclase) (Morse, 1979a,b). Figure 4.2 shows that oscillation in the olivine/ olivine + plagioclase ratio brackets the cotectic ratio in the case of the cm-scale layers but that the graded layer is always more mafic than cotectic rock. It is my impression that this is true of graded layers throughout the intrusion, and possibly in

Figure 4.1 Modal variation through graded and cm-scale layers. Fields of olivine and plagioclase marked, the rest is made up of clinopyroxene (dominant), opaques and biotite. Examination of the thin sections indicates the mode is constant within each cm-scale mafic lamina. Note the decrease upwards in the graded layer and the increase upwards in the cm-scale layered rock of modal clinopyroxene + opaques + biotite.



LAYER TOP



LAYER BASE

MAFIC LAMINA

MAFIC LAMINA

MODE %

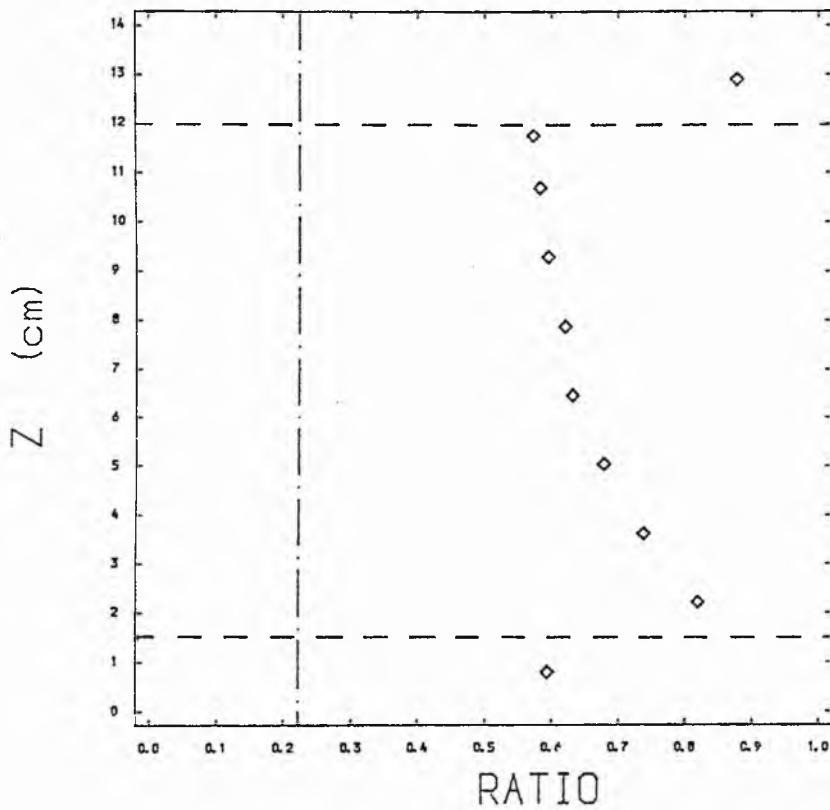
MODE %

Z(cm)

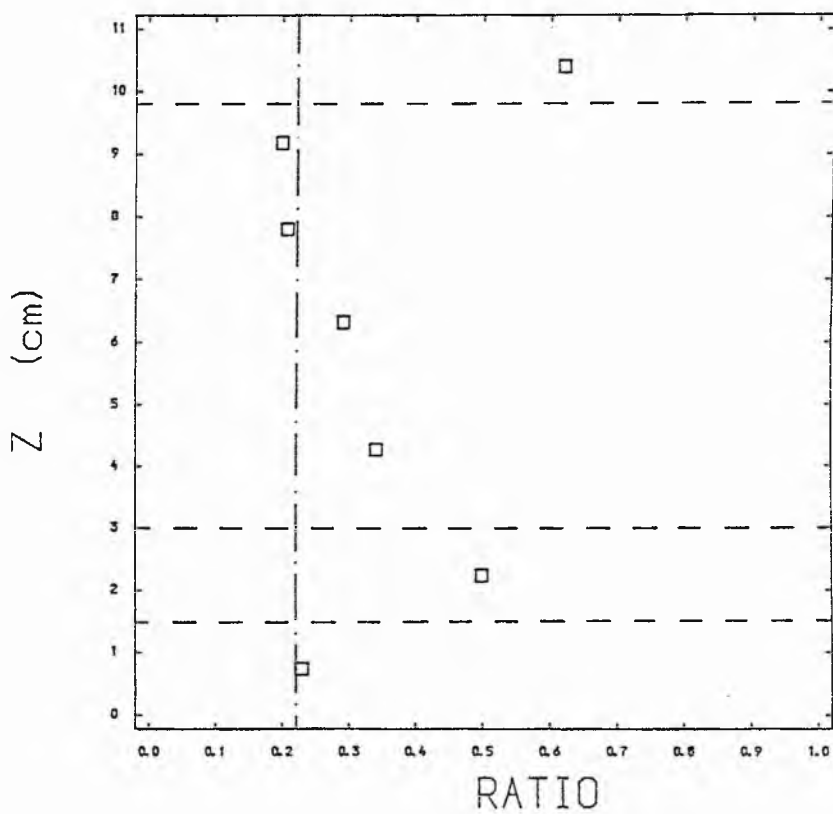
Z(cm)

Figure 4.2 Ratio of mode % olivine to olivine + plagioclase for the data in fig 4.1. The cotectic ratio (0.22 - indicated by vertical dashed line) is bracketed by the cm-scale layer data but not by the graded layer data.

Graded layer



Cm-scale layer



the other intrusions studied, the leucocratic portion of the layer only appearing so in contrast to the mafic layer base.

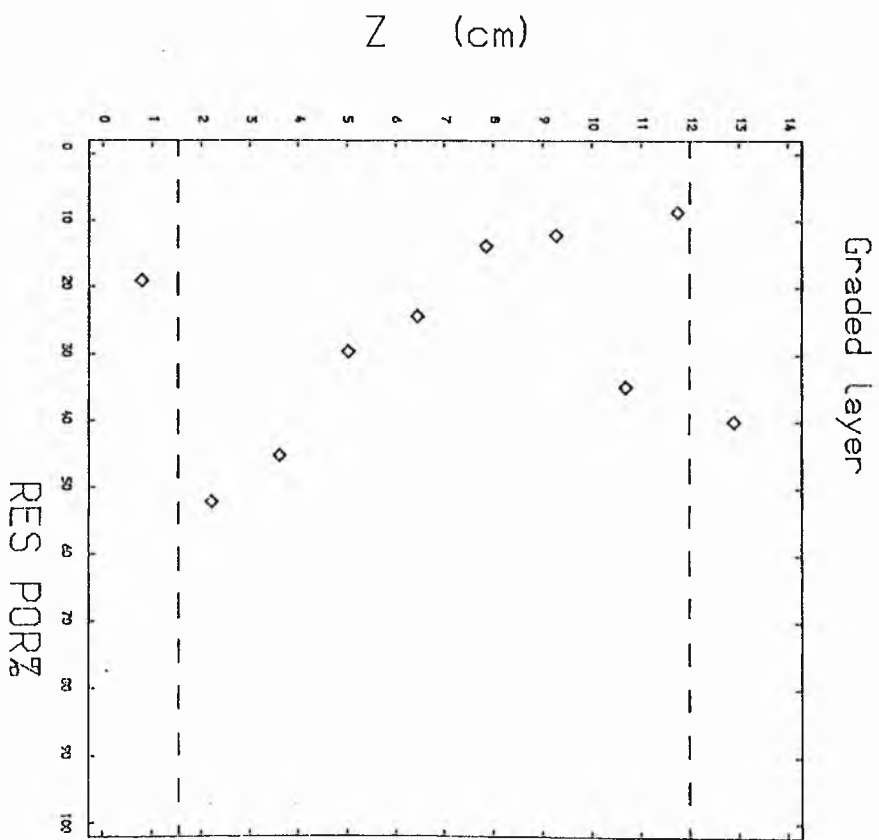
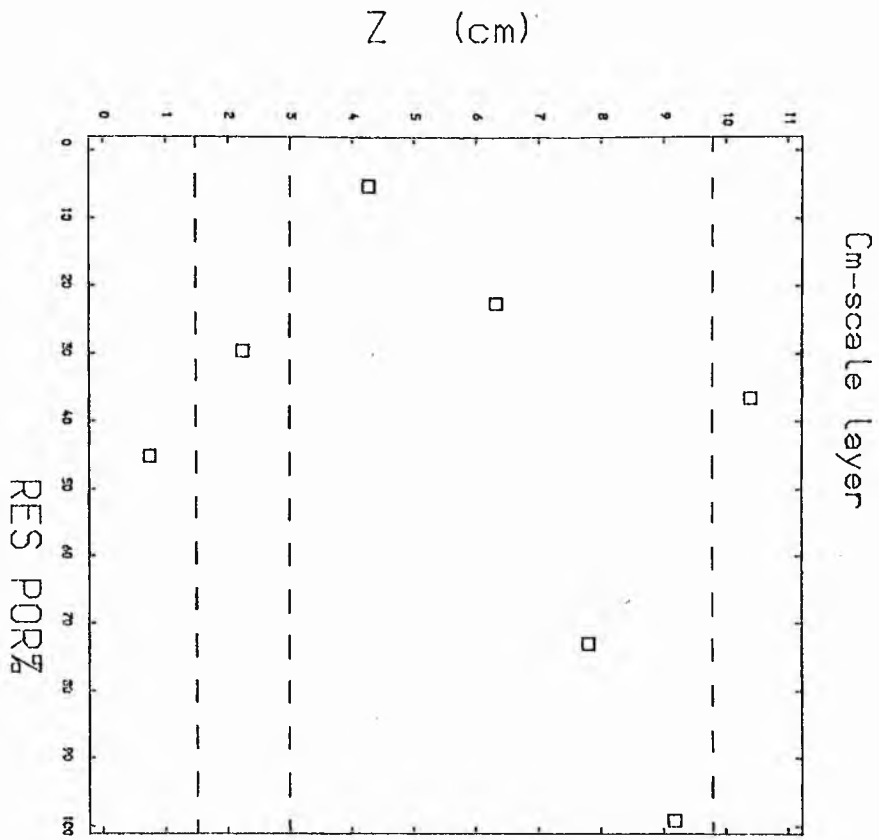
The data for clinopyroxene have also been used to calculate the residual porosity for each segment. The term "residual porosity" implies the amount of liquid trapped on closure of the rock, "closure" being used in the sense of Morse (1979b) to mean cessation of "accumulus growth". Residual porosities are calculated using the relation

$$F_{L(tr)} = C_S / C_L \quad (\text{Morse, 1979b}) \quad (4.1)$$

where $F_{L(tr)}$ is the amount of trapped liquid (residual porosity) and is defined as the amount of a postcumulus phase in the rock (C_S) over the amount of the potential phase in the contemporary magma (C_L). From fig 12 of Morse (1979b) C_L is approximately 5.75 at 10 PCS and this value has been used in the construction of fig 4.3. Figure 4.3 shows that, with the exception of one value, residual porosity decreases upwards within the graded layer to a minimum at the top (below the olivine-rich portion of the overlying layer). In the cm-scale layered rock however, the residual porosity increases upwards to a maximum below the overlying olivine-rich lamina.

Note that this assumes that the liquid trapped has the composition of the calculated contemporary magma. In the light of the suggestion by Irvine (1978b; 1980b) that interstitial liquid may be driven upwards by compaction, and the suggestion by Morse (1981a) that it may have percolated downwards (though later retracted, Morse

Figure 4.3 Residual porosity data calculated on the basis of mode % clinopyroxene (see text) for both layer types. Residual porosity decreases upwards in the graded layer but increases upwards in the case of the cm-scale layers.



& Nolan, 1980; Morse, 1982), together with the conclusions of chapters 6 and 7 this assumption needs justification. In the Kiglapait Lower Zone the value of C_L rises to only 10% at about 55PCS (a stratigraphic thickness of the order of 2000m). Downward percolation of liquids through this stratigraphic thickness is unlikely if the thermal models of Irvine (1970) and Hess (1972) are applicable to the Kiglapait intrusion. Thus the absolute values are considered accurate within a factor of two. The relative values will not be affected in any case, subject to the assumption that any infiltration has been pervasive.

4.4 Mineral compositions.

The possibility that compositional variations existed within and between layers was investigated using the electron microprobe. All analyses were made using an accelerating potential of 20kV and a probe current (as measured in a Faraday cage) of 30 nanoamps. All elements except Ba and Sr in plagioclase were analysed by making 4 x 10 second counts on peak and 2 x 10 second counts on background. Plagioclase spots were then re-analysed for Ba and Sr by making 10 x 10 second counts on peak and 10 x 10 second counts on background.

Feldspar analyses plotted in the An - Ab - Or triangle (fig 4.4) reveal little variation in core composition, either within, or between, layers. The data reveal the presence of reverse zoning in most crystals. Plots of An against z, position in the layer,

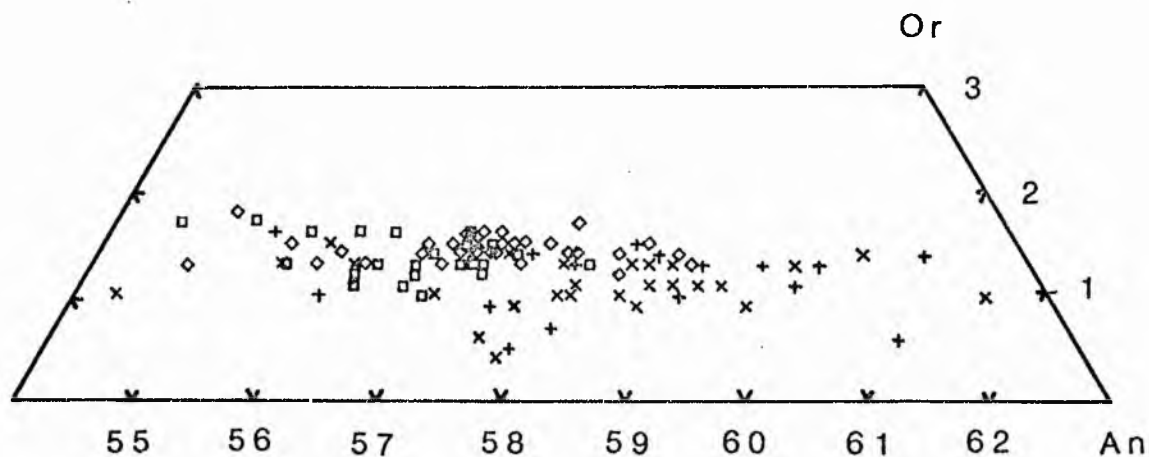
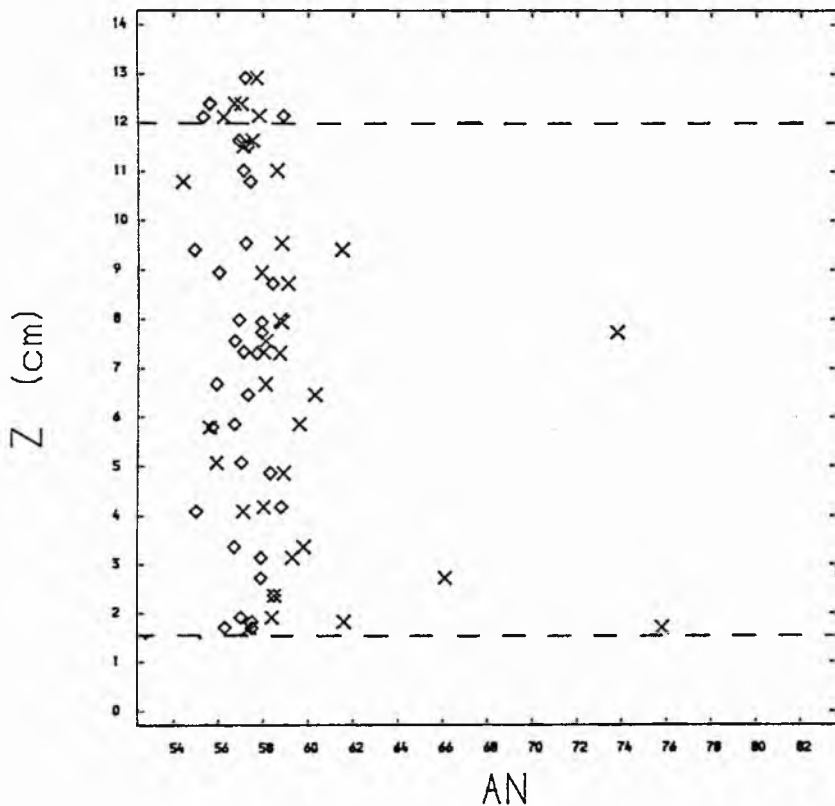


Figure 4.4 Plagioclase compositions from both layer types plotted in a segment of the An - Ab - Or triangle. Graded layer analyses are represented by diamonds (cores) and inclined crosses (rims), cm-scale layer analyses by squares (cores) and vertical crosses (rims). Rim compositions extend off the diagram to a maximum of approximately An 83 for both layer types. The figure illustrates the similarity of plagioclase compositions in both layers and the reverse-zoned character of most feldspars.

Figure 4.5 Plagioclase composition plotted against z (position within the layer) for both layer types. No significant variation in An, or any element analysed, was found in either layer type.

Graded layer - plagioclase



Cm-scale layer - plagioclase

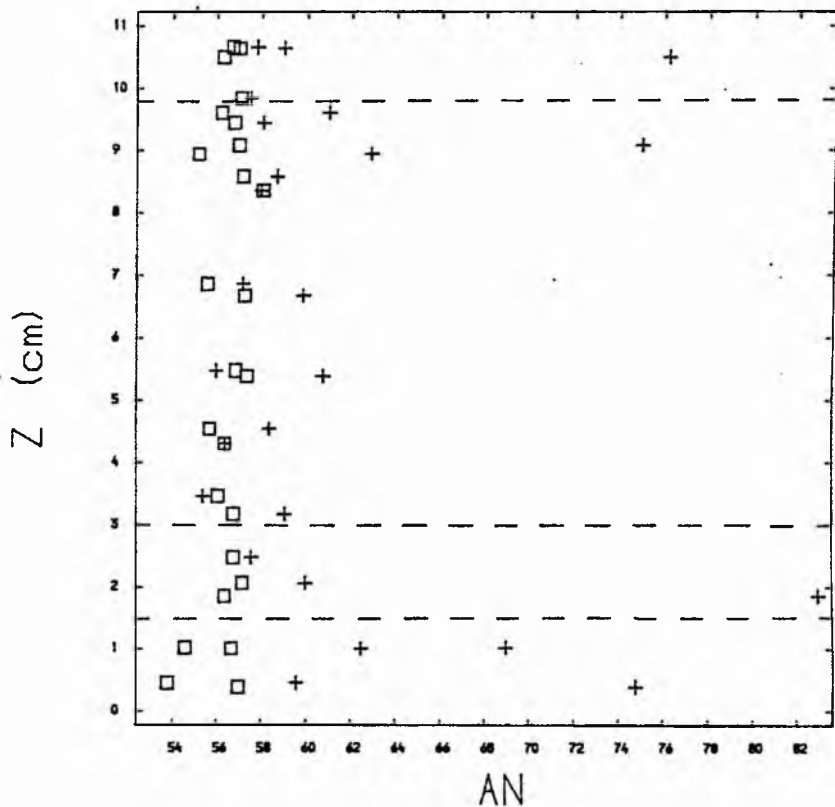
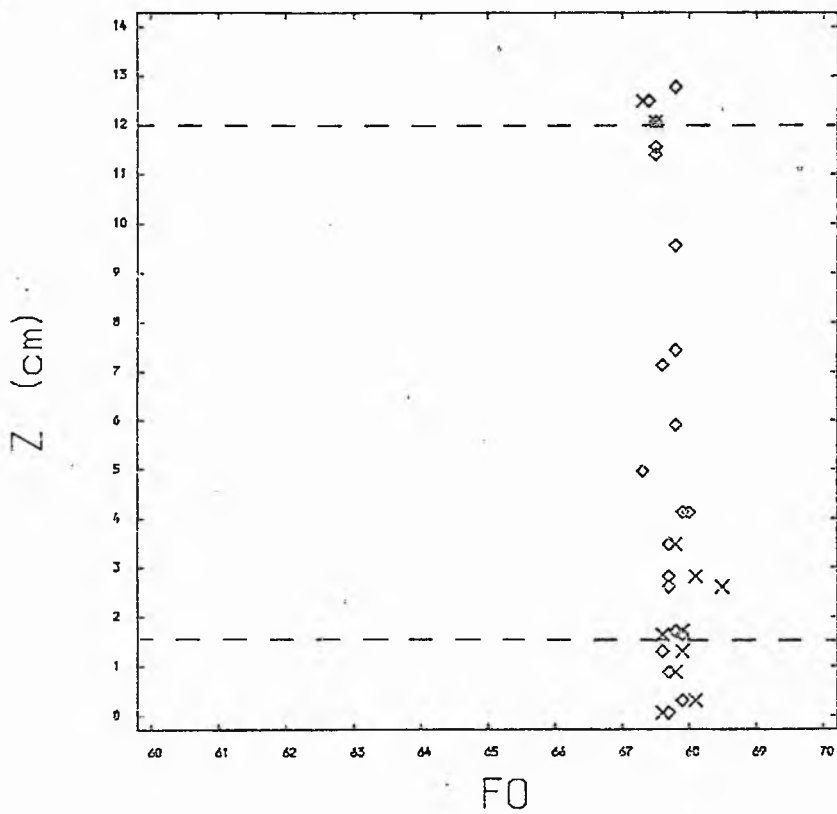


Figure 4.6 Olivine composition plotted against z (position within the layer) for both layer types. No significant variation in Fo or any element analysed was found in either layer type.

Graded layer - olivine



Cm-scale layer - olivine

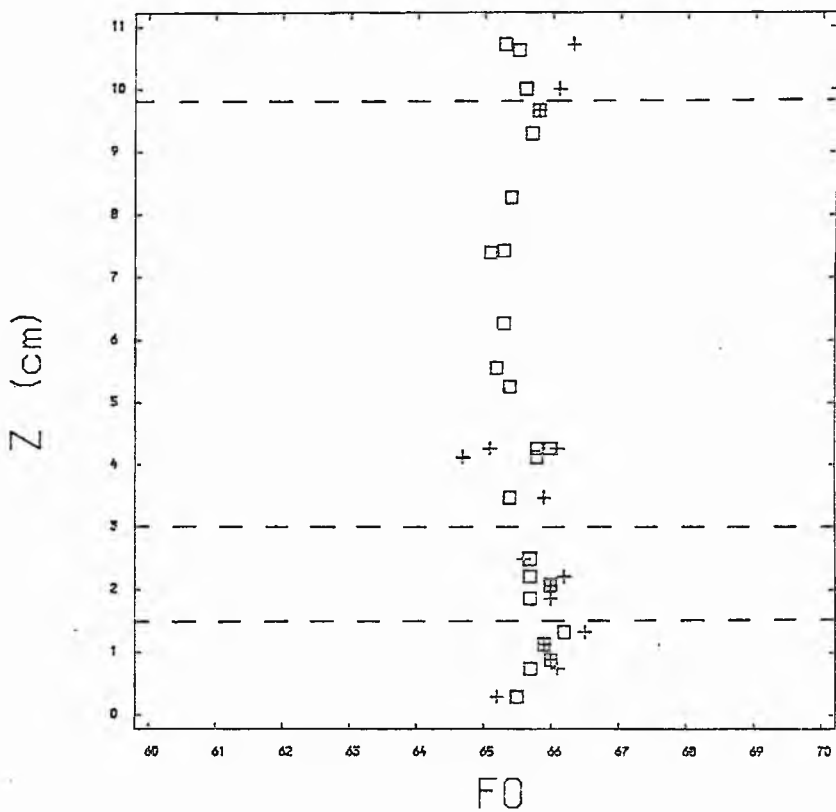
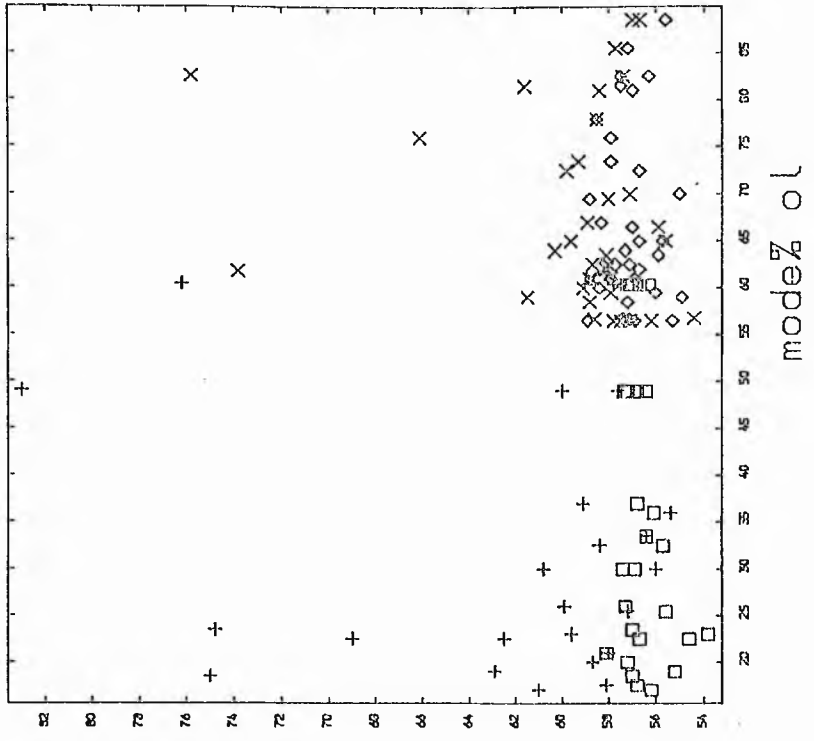
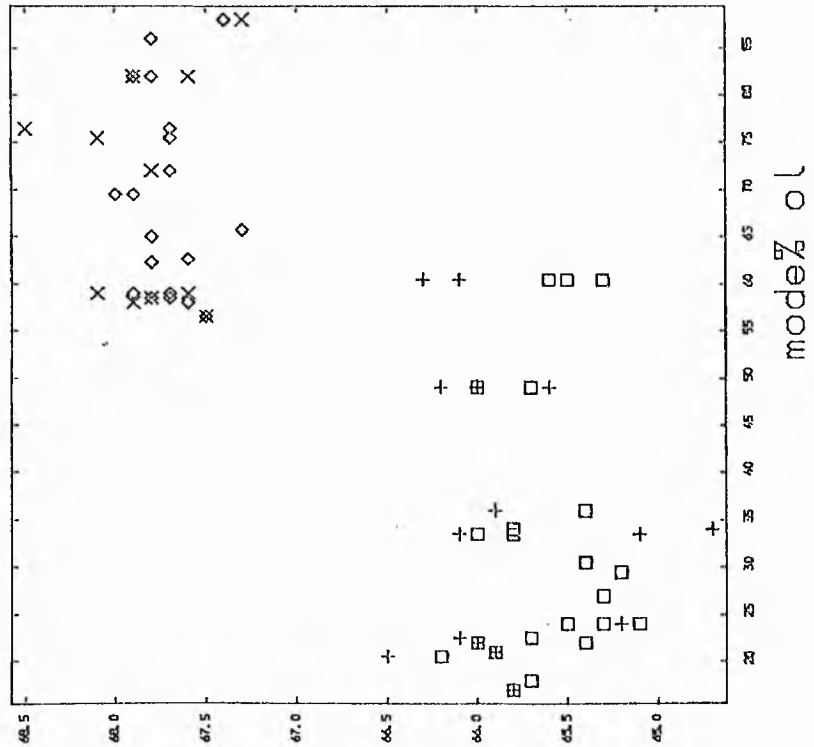


Figure 4.7 Plots of An and Fo against mode % olivine for both layer types. Graded layer analyses are represented by diamonds (cores) and inclined crosses (rims), cm-scale layer analyses by squares (cores) and vertical crosses (rims). Note the similarity of plagioclase compositions and more iron-rich nature of the olivines in the cm-scale layered rock.



AN



FO

indicate that there is no systematic variation (see fig 4.5) in either layer type. Likewise no systematic variation can be discerned for any other element analysed. Plots of olivine composition similarly show no systematic variation with stratigraphic height (eg Fo in fig 4.6). When mineral compositions are plotted against mode % olivine however (fig 4.7), systematic differences in olivine composition between layers are revealed, the olivine in the cm-scale layered rock being more iron-rich than in the graded layer. The lack of correlation of rim composition with (z) indicates that there is likewise no correlation with residual porosity.

4.5 Discussion.

Since the cotectic ratio is not bracketed by the modal variation in the graded layer it cannot represent oscillation about the cotectic (as was suggested by Maaloe, 1978; Morse, 1979a; McBirney & Noyes, 1979). Rather, the geometry, structures, textures, modes and compositions of the normally-graded layer are consistent with formation by current action. The exact mechanism whereby the sorting of phases takes place is presently obscure. Irvine (1980a) has suggested that sorting occurs in the the head of the density current; however analogy with aqueous turbidity currents makes it equally likely that sorting occurs in the current tail (see Middleton, 1966) and may be particularly influenced by the effect of shear on the rheology of the fluid (see Grunfest, 1963; Shaw, 1969;

Naylor, 1981) Better models of crystal sorting mechanisms must await the development of techniques to determine the dimensions of the clasts being transported. One feature noted above, the presence within the layer of finer-grained domains with the dimensions of the larger crystals, suggests that fragmental material may be more common than hitherto suspected. Glomeroporphyritic clusters of one or more phases are, after all, a common feature of extrusive rocks. In addition, since there is nothing implicit in the crystal-sorting model which dictates that individual clasts end up touching one another, final grain size variation may only reflect the spacing of the transported and sorted crystals.

The upward decrease in residual porosity (fig 4.3a) is spectacular and was completely unsuspected prior to point counting. This observation is consistent with the Wager et al (1960) model of adcumulus growth in which crystals near to the top of the crystal pile grow by diffusion of components from the contemporary magma. The postcumulus deformation structures indicate however that these layers were capable of plastic deformation along with those immediately above and below and thus lithification must have occurred at some depth in the crystal mush. This point will be returned to later in the discussion.

The coincident lateral extent of the cm-scale layers argues strongly that they are genetically related to one another and, together with the lack of any associated structures and identical appearance in dip and strike sections, suggests that currents were not important in their formation. Thus they are inferred to have

crystallised in situ. Mechanisms whereby periodic chemical reactions may give rise to igneous layering have been reviewed by McBirney and Noyes (1979). All the mechanisms postulated so far depend on static boundary layers in which relative depletion and enrichment in included and excluded components respectively takes place by diffusion towards or away from the growing crystals. Compositional boundary layers have been reported adjacent to growing crystals by Donaldson (1975b) and others. It is known, however, that fractionation of selected components has a large effect on liquid density (Sparks et al, 1983; Grove & Baker, 1983; Loomis, 1983; Sparks & Huppert, 1984), such that these boundary layers must convect away quickly by comparison with crystal growth rates (see Loomis, 1983 and discussions by Hurle, 1972 and Carruthers, 1976). Furthermore in the case of inclined surfaces (the Kiglapait cm-scale layers have dips of about 30°) it is known that thermal boundary layers are more unstable than on horizontal surfaces (Tritton, 1977). Convection rapidly destroys structures produced by periodic chemical reactions in fluids (eg Welsh et al, 1983). Thus it must be concluded that unless good physical reasons for the development of static boundary layers can be produced such models must be rejected.

It is demonstrated elsewhere (Chp 6) that "normally" textured (ie non poikilitic) layers and laminae can form within crystal mushes. The tortuosity of porous media has the effect of damping convection (thereby increasing, for example, the temperature difference need for the onset of convection, all other things being equal) and therefore the likelihood of static compositional boundary

layers being produced is much greater than in the free magma. Thus it is proposed that these layers and others like them, for example the Stillwater inch-scale layers, may be produced by rhythmic crystallisation events within a previously existing porous medium (crystal mush), in which the liquid through which diffusion occurs is essentially stationary. Some support for this hypothesis comes from the observation that olivines in the cm-scale layers are more Fe-rich than in the nearby graded layer, which formed in contact with the contemporary magma, though this may in part be due to the greater amount of trapped liquid in the cm-scale layered rock (see Cawthorn, 1982).

The residual porosity data for the cm-scale layered rock are more complex than those for the graded layer. Residual porosity minima are coincident with the mafic laminae and in the interlaminae regions are inversely related to mode % olivine (cf graded layer). If the above proposal of porous media layer formation is correct, then the development of residual, or sustained, porosity postdates the formation of the laminae and may reflect local ponding of liquid below relatively impermeable mafic laminae (cf Donaldson, 1982). Such a process can also explain the graded layer observations, if significant porosity reduction, though not enough to give rigidity, occurred prior to burial.

4.6 Conclusions.

1) The textures, modes and mineral compositions in sections through the two layers are consistent with the interpretations based on field evidence alone.

2) Significant variations in residual porosity are present and are interpreted as reflecting permeability variations in the crystal pile.

5 TWO-PHASE CONVECTION IN BASIC PLUTONS.

5.1 Introduction.

It has been concluded in the previous two chapters that transport of solids is a significant feature of cooling plutons. Till now the source of this magmatic sediment has not been considered. Evidence from erosion structures suggests that some may be derived from the dipping floors of magma chambers and the region proximal to the walls may be especially important (eg Irvine, 1978a; 1980a,c). Local instability in the mush may be produced by liquefaction (see chapter 6) or more simply by the growth of an unstable layer of crystal-charged fluid (cf Jaupart & Brandeis, 1982). However, such sources must be less important in gently-dipping or flat-lying cumulates. Three possible alternative sources of magmatic sediment exist in such cases.

i) Partially crystalline magma input.

The possibility that magma influxes are numerous, intermittent, of small volume and crystal-rich has apparently been neglected in discussions of the origin of layering. There are, however, several good reasons to suppose that this may be so. For example, in the British Tertiary Volcanic Province:

a) porphyritic minor intrusions are widespread (eg Simkin, 1967;

Gibb, 1968; Donaldson, 1977);

b) a recent interpretation of the geochemistry of part of the Rum complex suggests that major inputs became more crystal-rich with time (McLurg, 1982) and Hutchison and Bevan (1977) have suggested that the parent magma of a portion of the Skye Cuillin intrusion was crystal-rich (and note that layered plutons elsewhere in the world have been shown to have porphyritic chilled margins, eg Sharpe, 1981).

Input of crystal-charged magma of small volume could give rise to layers on the scale of rhythmic layers by spreading out across the intrusion floor due to density differences (Huppert et al, 1981) and irrupted magma has been identified in the Hettasch intrusion (Berg, 1980).

ii) Crystallisation within the main body of liquid.

The possible role of crystallisation wholly within major magma bodies has been discounted by Campbell (1978) in favour of heterogeneous crystallisation at chamber-margins. Support for this view comes from the realisation that homogeneous nucleation of silicates requires large amounts of supercooling and/or inordinately long incubation times (Berkebile & Dowty, 1982). Yet there are, circumstances in which nucleation could occur within a body of magma at low supercooling and others in which large supercooling may develop:

a) Nucleation sites may be present throughout the liquid. Lofgren has

shown (1983) that heterogenous nucleation commonly occurs on refractory residues present in most basalts and refractory inclusions have been identified within olivines in MORB (Fisk & Bence, 1980). Phenocrysts held in suspension by turbulent convection (Bartlett, 1969; Huppert & Sparks, 1980) may also serve as heterogeneous nucleation sites.

b) Diffusive interfaces formed after chamber replenishment are regions of large thermal and compositional gradients (Huppert & Sparks, 1980; Huppert & Turner, 1981; Huppert et al, 1981) and may be sites where nucleation rates are high.

c) Crystallisation at large supercooling may occur after magma mixing events where the liquids lie on a convex-up liquidus surface, or after rapid devolatilisation following pressure release, perhaps associated with eruption.

iii) Crystallisation at the upper bounding surfaces of magma chambers.

The roof of the Skaergaard intrusion was considered by Wager and Deer (1939) to be the major source of magmatic sediment for the layered series, since it was assumed that most heat was removed there. Later authors (eg Jackson, 1961; Irvine, 1970; Campbell, 1978) proposed that crystallisation occurred at, or near to, the transient chamber floor because the liquidus temperature of basalt increases with increasing pressure and does so more rapidly than the magma is adiabatically heated. G.B. Hess pointed out (1972) that convection is able to supply all the heat which can be removed at the roof by conduction, and thereby inferred that the roof zone of

the Stillwater intrusion was not a site of significant crystallisation.

One problem with this interpretation is that solidification continues to occur preferentially upwards, even when the thickness of the liquid body is of the order of 100m, either in sills or in the final stages of the solidification of major intrusions. If the liquidus temperature gradient interpretation is correct then this would be occurring because of a 0.3°C temperature difference in the case of a body 100m thick and 0.03°C in one 10m thick. It is unlikely that such small temperature differences could be consistently maintained. Secondly, it has been shown (Chp 2) that synformal intrusions can be considered to have filled inwards just as much as upwards (eg Kiglapait, Jimberlana) and there is little evidence in these cases for more rapid accumulation at greater depths. Finally, Hess ignored the effect of hydrothermal cooling (Taylor & Forester, 1979; Parmentier, 1982) which is known to accelerate the solidification of plutons (Norton & Knight, 1977; Cathles, 1977; Elder, 1982). Furthermore, Ahern *et al* (1981) point out, in a paper concerned with the upward migration of intrusions due to melting at the roof and crystallisation on the floor, that where high-level intrusions are cooled by hydrothermal convection heat removal is faster than heat can be supplied by magma convection (the Rayleigh number of the former process is much larger than the latter). Though they make no further comment, it is evident that this implies that crystallisation at the roof does occur.

This chapter is concerned with this last possibility, that the roof zones of basic intrusions are significant sources of magmatic sediment for their layered series.

5.2 Field evidence for a roof zone sediment source.

It is presently impossible to recognise crystals which have been roof-derived, though roof-derived rock has evidently been transported and deposited on the floor of several intrusions. For example, in the Kiglapait intrusion xenoliths of metasediment and anorthosite are found within the layered series (app 4) which must have been derived from the roof. Fragments of the Skaergaard Upper Border Series are found within the layered series (Wager & Brown, 1968; Naslund, 1984). In the Klokken intrusion there are layers of syenite interpreted as spalled portions of material crystallised on the roof (Parsons, 1979). This rock must have been overlain (in a chronostratigraphic sense) by crystal mush (the Upper Border Series of the Kiglapait and Skaergaard intrusions are typified by normally zoned feldspar and large modal proportions of poikilitic and interstitial phases; Wager & Brown, 1968; Morse, 1969; Naslund, 1984). Thus, in order for rock to be eroded from the roof, crystal mush must also have been redistributed within the magma chamber.

5.3 Crystal transport mechanisms.

Most proponents of crystal transport stress the role of settling at low Reynolds numbers (within the range described by Stokes law) (eg Wager & Brown, 1968; Wadsworth, 1973; Parsons & Butterfield, 1981). Likewise, those authors critical of crystal transport concentrate on the problems associated with the settling of individual crystals (eg Jackson, 1961; Campbell, 1978; McBirney & Noyes, 1979).

All discussions of Stokes Law settling assume that if there is more than one grain in the fluid, then they are sufficiently far apart such that they do not interact (less than 1% by volume), though this may be true in some cases, it is likely that this proportion is often exceeded. Therefore interaction between crystals must be considered.

According to Middleton and Southard (1978) two opposite bulk effects are possible:

i) hindered settling due to interaction between the grains and an overall reduction in the cross section available for the upward movement of the fluid that is displaced by the downward movement of the grains. This effect may be especially important at or near to the transient chamber floor and will not be considered further here.

ii) group settling due to local concentrations of grains. High concentrations of grains locally raise (or lower) the bulk density of the suspension and cause it to move through the surrounding fluid as a density current.

This idea was first suggested in the context of crystal transport in crystallising plutons by Grout (1918) and has been adopted by several authors since (eg Wager & Deer, 1939; Hess, 1960; Irvine, 1980a) Hess is particularly explicit in how he envisages the process might work, "a layer of liquid might develop below the roof which by loss of heat and impregnation by crystals became denser than the underlying liquid. Although mechanically unstable it might develop and remain in this position for a time, just as in winter a layer of colder water sometimes exists metastably for a short time at the surface of the sea. Such a condition would be more readily imaginable in a viscous liquid than in water. Eventually overturn of the unstable mass of liquid will occur. One might expect that some inhomogeneity in the layer would cause it to get started at one point first. A downward bulge would form, the nose of which would accelerate rapidly. The velocity would be enormously greater than the settling of crystals. A single descending column of denser liquid might draw off the whole of the layer from below the roof. It would spread rapidly over the floor and come to rest. Alternatively one might postulate tear-droplike masses starting downward from many points, and at different times, from the lower surface of the denser liquid." Before describing experiments investigating this process, the effect of crystal content on magma density is quantified and compared to the effects on density of cooling and fractionation.

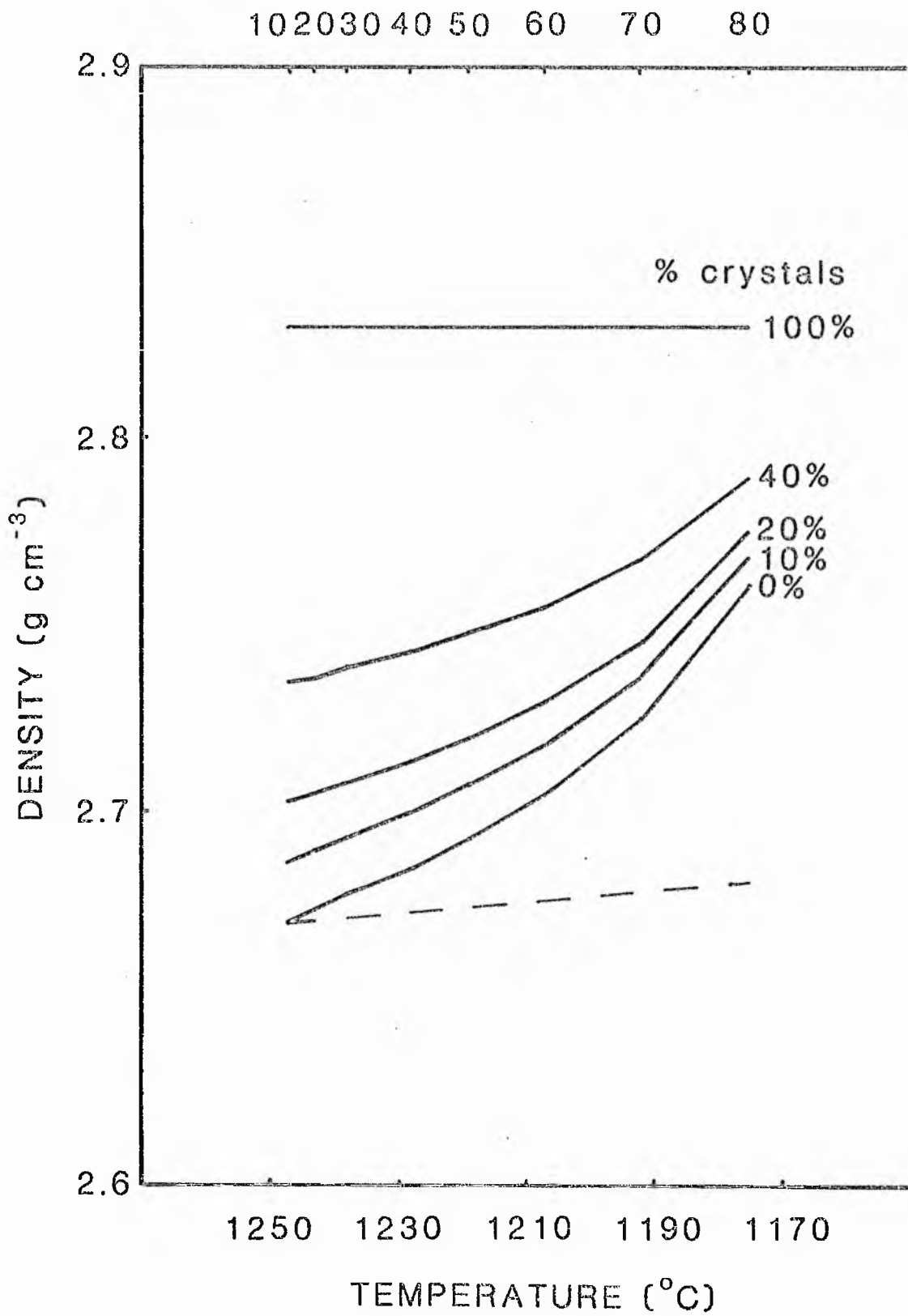
5.4 Cotectic suspension densities.

Much attention has been given to the density changes arising in magmatic liquids due to cooling (eg Bottinga & Weill, 1970; Murase & McBirney, 1973) and to changes in composition (Turner & Gustafson, 1978; McBirney & Noyes, 1979; Sparks et al., 1983; Grove & Baker, 1983; Sparks & Huppert, 1984). Huppert and Sparks (1982) have also shown that nucleation of a new phase (vesiculation) can have a spectacular effect on the bulk density of the fluid. Crystallisation can similarly have a spectacular effect on fluid density. The relative effects of cooling, fractionation and crystallisation have been quantified for two liquid lines of descent and are presented in figures 5.1 and 5.2.

In figure 5.1 the densities of successive liquids in the Lower Zone of the Kiglapait intrusion (from 10 - 80 PCS) have been calculated by the method of Bottinga and Weill (1970), using revised estimates of the partial molar volumes of the oxide components given by Nelson and Carmichael (1979) - the compositions of successive liquids are given by Morse (1981b) and their temperatures are estimated from the relation between T and X_{An} given by Morse (1979a). For comparison the effect of cooling the 10 PCS liquid to the cotectic temperature of the 80 PCS liquid is indicated by the dashed line. Plagioclase and olivine were added to each of these liquids in cotectic proportions (78/22) given by Morse (1979b) and their densities were estimated from data in Deer et al. (1966) adjusted to the cotectic temperature by estimating the thermal

Figure 5.1 Densities of Kiglapait liquids from 10 to 80 PCS and of suspensions of olivine and plagioclase in the ratio 22:78 (cotectic proportions, Morse, 1979b) in those liquids. The dashed line shows the effect on density of cooling a 10 PCS liquid to the cotectic temperature at 80 PCS. See text for method of construction of the diagram.

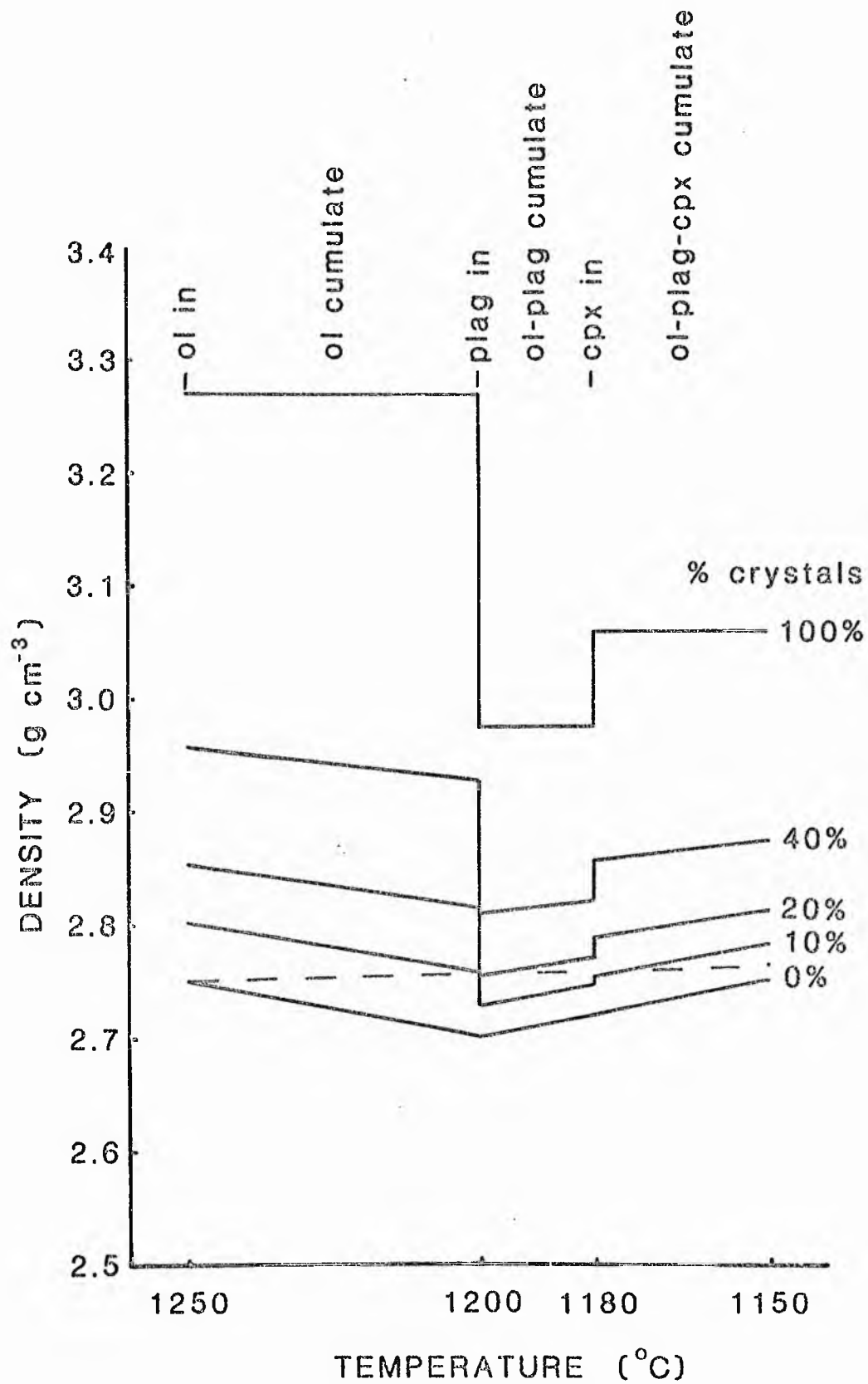
PCS



expansion using data given by Clark (1966). The figure illustrates that the effect on bulk fluid density of fractionation is much greater than that of cooling, due to the extreme iron-enrichment trend of the Kiglapait liquid-line of descent, and that the effect of adding modest proportions of crystals is greater still.

Figure 5.2 shows the results of a similar exercise carried out on a MORB-like liquid-line of descent. The shape of the density versus fractionation curve (see Sparks *et al*, 1980 and Stolper & Walker, 1980) is approximated to two straight-line segments, and liquid densities were taken from Sparks *et al* (1980) for the most primitive, most evolved and least dense compositions. The effect of cooling the most primitive liquid is indicated by the dashed line as in figure 5.1. The arrival of the liquid at the two- and three-phase cotectics is indicated by plagioclase in and clinopyroxene in, these arrivals are assumed to be abrupt and phase proportions crystallising from the magma are assumed constant throughout each interval. Crystals were added in the following proportions in each segment of the liquid line-of-descent; olivine 100%; olivine 50%, plagioclase 50%; olivine 50%, plagioclase 25%, clinopyroxene 25%. Temperatures are rough estimates and crystal densities are obtained as for the Kiglapait Lower Zone example. The diagram clearly illustrates again that fractionation has a greater effect on magma density than cooling and that the addition of crystals has a still greater effect.

Figure 5.2 Densities of liquids on a MORB-like liquid line of descent and of suspensions of olivine, plagioclase and clinopyroxene (see text for proportions and method of construction of the diagram) in those liquids. Saturation of the liquid with olivine, plagioclase and clinopyroxene indicated by olivine in, plagioclase in and clinopyroxene in. The dashed line shows the effect of cooling on density of cooling the most primitive liquid through 100° C.



5.5 Crystallisation conditions at magma chamber roofs.

Concepts of the transition from magma to rock on intrusion floors range from discontinuous ("classical adcumulates", Wager, 1963; McBirney & Noyes, 1979) to gradual reductions in porosity through 10s or even 100s of metres (Hess, 1972; Irvine, 1980b). Many small-scale structures testify to the presence of a mush zone (Chps 3,4,6,7). Mush zones on chamber floors are capable of plastic deformation in response to gravitational stresses (Chp 6). Upper Border Series rocks, by their very nature, tend to be less well exposed than chamber floor deposits and are apparently poor in structures (Wager & Brown, 1968), though Smith has reported (1975) complex structures in the roof zone of the Chebucto Head granitic intrusion which he attributes to plastic deformation. Petrographic descriptions of upper border series rocks indicate that they are generally polythermal rocks, ie they are classically interpreted as orthocumulates (eg Wager & Brown, 1968; Morse, 1969; Naslund, 1984).

It is concluded that roof zones of basic magma chambers are regions where crystallisation occurs which increases the bulk fluid density. This bulk fluid is therefore unstable and will be released into the underlying magma (see fig 5.3). This physical situation has been modelled and the results of these experiments are described in the following sections.

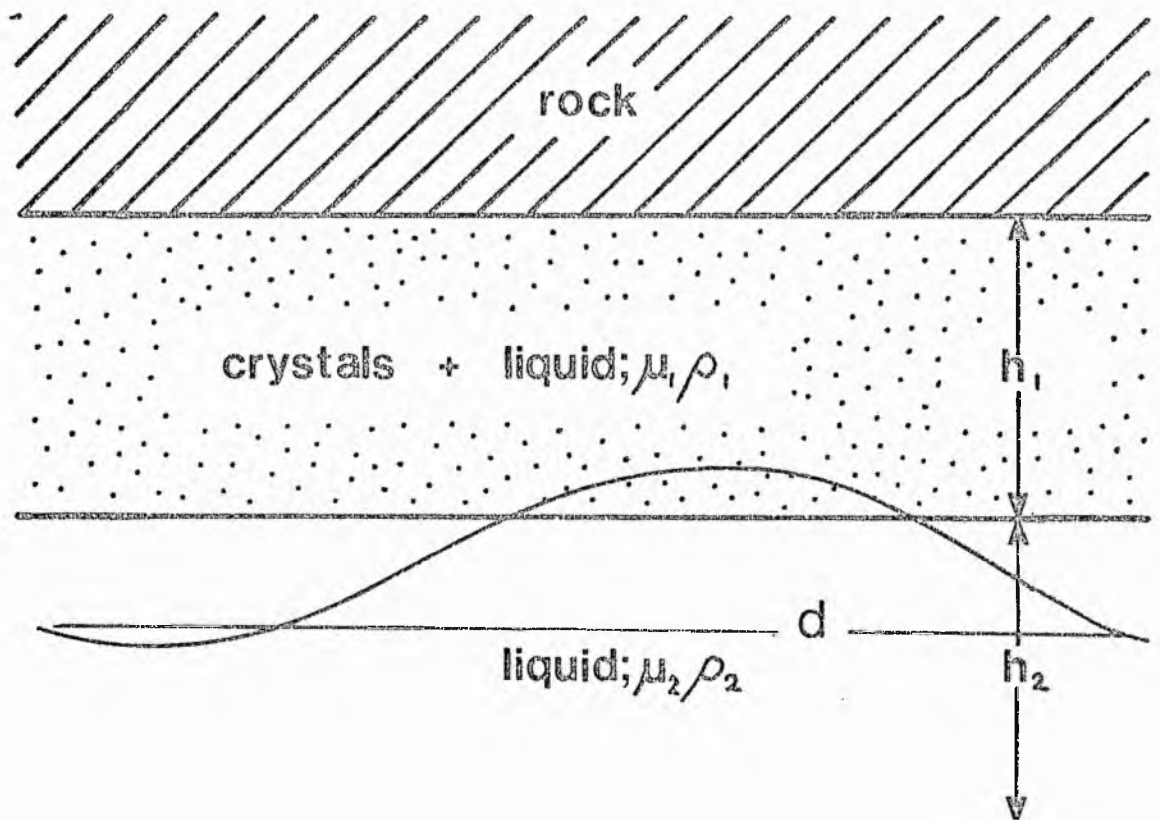


Figure 5.3 Sketch illustrating the conventions used in the modelling and calculations throughout chapter 5. A layer of crystal-charged liquid with dynamic viscosity μ_1 , density ρ_1 and thickness h_1 lies below a solid rock roof and above a layer of liquid with dynamic viscosity μ_2 , density ρ_2 and thickness h_2 . $\mu_1 \gg \mu_2$, $\rho_1 > \rho_2$, $h_1 \ll h_2$. In reality region 1 would have gradients of viscosity, density and probably rheological behaviour across it and the transition to "rock" would be represented by a zone in which the proportion of solids in the suspension would cause it to "lock" (see Marsh, 1981 and the text). The spacing between instabilities is represented by d .

5.6 Vertical density currents - experiments and calculations.

5.6.1 Experimental Methods.

Experiments were carried out in a glass tank whose internal dimensions are 6cm x 9.5cm x 20cm high with an open top. Several types of experiment were run involving immiscible liquids, miscible liquids and suspensions. The principle objective was to delineate the internal flow structure of vertical density currents to determine the possibility and nature of crystal sorting within such currents and whether they could accomplish transport of particles less dense than the ambient fluid to the transient chamber floor.

There have been many experiments performed designed to investigate the geometry of the fluid flows considered to lead to diapir formation (eg Whitehead and Luther, 1975; Marsh, 1979). None, to my knowledge, has specifically delineated the internal structure (flow pattern) of the rising diapir. A major problem in experiments of this nature is that of producing the initial instability. Whitehead and Luther (1975) solved the problem by upending a much smaller tank containing an initially stable arrangement of fluids, but this proved impracticable with a larger tank. Marsh (1979) used two coaxial cylinders equipped with slots which could be aligned. Three approaches were used in this study; melting a solid which gave off a dense fluid, sieving solids gently

onto the free surface of fluid, and introduction of plumes of fluid through spouts or by pouring directly from another container.

The development of the currents was recorded using a camera equipped with an autowinder which operated at 1.5 frames per second. Timing was accomplished by treating the times between frames as being constant, though it is known that the first few frames tend to be 'slow' as the autowind accelerates to working speed. Much effort was devoted to experimenting with lighting angle, flash intensity, film speed and aperture setting. The arrangement used side lighting with a flash gun (flash duration $1/10\ 000 - 1/30\ 000$ sec controlled by a thyristor), 400 ASA black and white film with an aperture setting of f4 and a shutter speed of $1/60$ sec. The fluids used were glycerol (density $1.26\ \text{g cm}^{-3}$, dynamic viscosity 15.0 poises at $20\ ^\circ\text{C}$) and a silicone oil (density $0.97\ \text{g cm}^{-3}$, dynamic viscosity 3.4 poises at $23\ ^\circ\text{C}$). Plastic shards sieved to between 16 and 30 phi mesh size were used as tracers and glass shards of a similar size as the driving force in suspension currents.

5.6.2 Melting above a horizontal interface.

Many experiments have been carried out to investigate the instability of two fluids with constant fluid properties. This series of experiments were used to investigate the situation where the unstable fluid was produced by melting, a dynamically similar

process to roof crystallisation, and in which there was large viscosity gradient.

Scaling.

The experiments described below are not well-scaled to magmatic conditions (see Hubbert, 1937 for a review of scaling geological phenomena), indeed, as pointed out by Irvine (1980d) one would need to use a tank the size of a swimming pool filled with water to properly model a basaltic magma chamber. However the flows are all laminar in character (they have low Reynolds numbers), as is calculated for similar flows under magmatic conditions (see section 5.4.3) The qualitative observations on flow structure are therefore considered directly applicable to the magma chamber situation.

Method

A semicircular dish, 1cm deep and with a radius of 5cm was constructed on a plate which covered the top of the experimental tank. This dish was filled with glycerol which was then solidified by immersion in liquid nitrogen. The dish was then upended and placed on top of the tank filled with silicone oil so that the lower (originally free) surface of the glycerol was in contact with the silicone oil and the resulting fluid flows observed. Ideally a perfectly horizontal surface is desired (see also Whitehead and Luther, 1975) and an absence of air bubbles at the interface. In practice neither of these conditions could be ideally achieved since it proved impossible to freeze a perfectly flat glycerol surface,

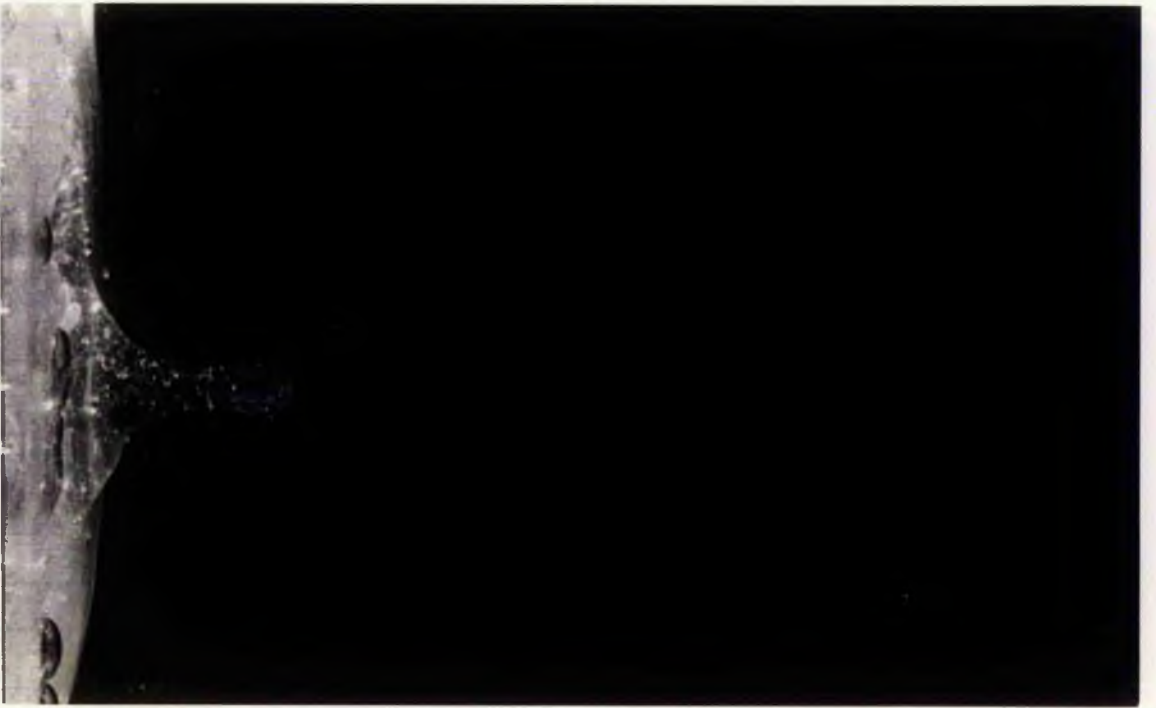
which also tended to trap air in fine cracks in its surface. Indeed the presence of small air bubbles turned out to be an asset, as it allowed thermal convection in the tank to be identified.

Observations.

As soon as the cold glycerol comes into contact with the warm silicone oil, the silicone oil loses heat to the glycerol and begins to convect. Convection in the silicone oil is initiated by the build up of an unstable, cold layer at the top of the tank which eventually breaks away and forms a cold descending plume in the central portion of the tank and which spreads out across the floor, warmer fluid rises up the sides and moves inward across the roof to replace the descending cool fluid. This thermal convection in the silicone oil can be traced by the presence of small air bubbles introduced into the fluid at the glycerol/silicone oil interface and which are carried along by the flow in spite of their tendency to rise.

As the glycerol warms up its viscosity decreases (the viscosity of glycerol is an exponentially decreasing function of temperature,) and since it is denser than the silicone oil, one or more downward bulges begins to form at its lower surface. This bulge grows into a diapir shape which ultimately breaks off and the fluid drop descends through the silicone oil trailing a thin pipe of glycerol. The growth and descent of one such diapir is illustrated in plate 5.1 and in figure 5.4a.

Plate 5.1 Two views of the development of a vertical density current produced by melting a horizontal slab of glycerol lying on silicone oil. (magnification x1.5)



A plot of distance to the tip of the head against time for one such current is presented in figure 5.4b. The curve can be split roughly into three sections. In (1) the velocity is approximately constant and the surface is deforming by a Rayleigh - Taylor instability, thus the growth of the disturbance is linear and the equations that govern the growing flow are well-established (eg Berner et al., 1972; Whitehead & Luther, 1975). In the second stage the flow is accelerating and the physical processes that govern the growth of the flow and that between adjacent flows are not well understood. In the third stage the fluid drop is descending at a constant velocity which is given by Stokes law for a fluid drop:

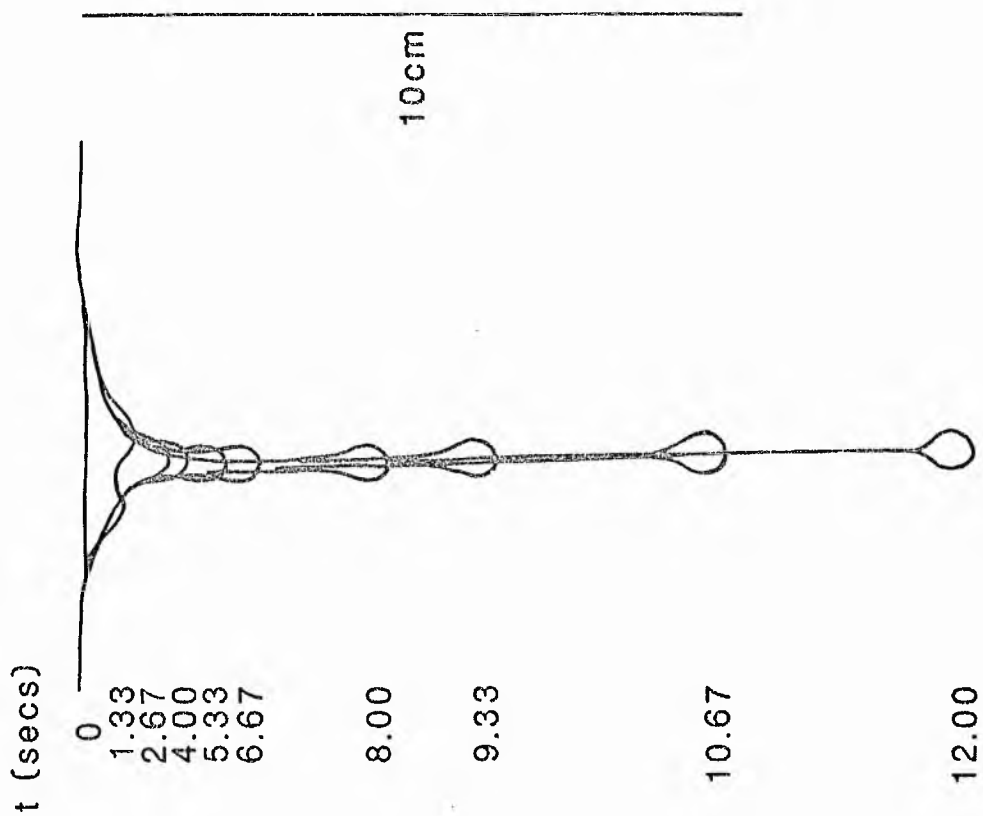
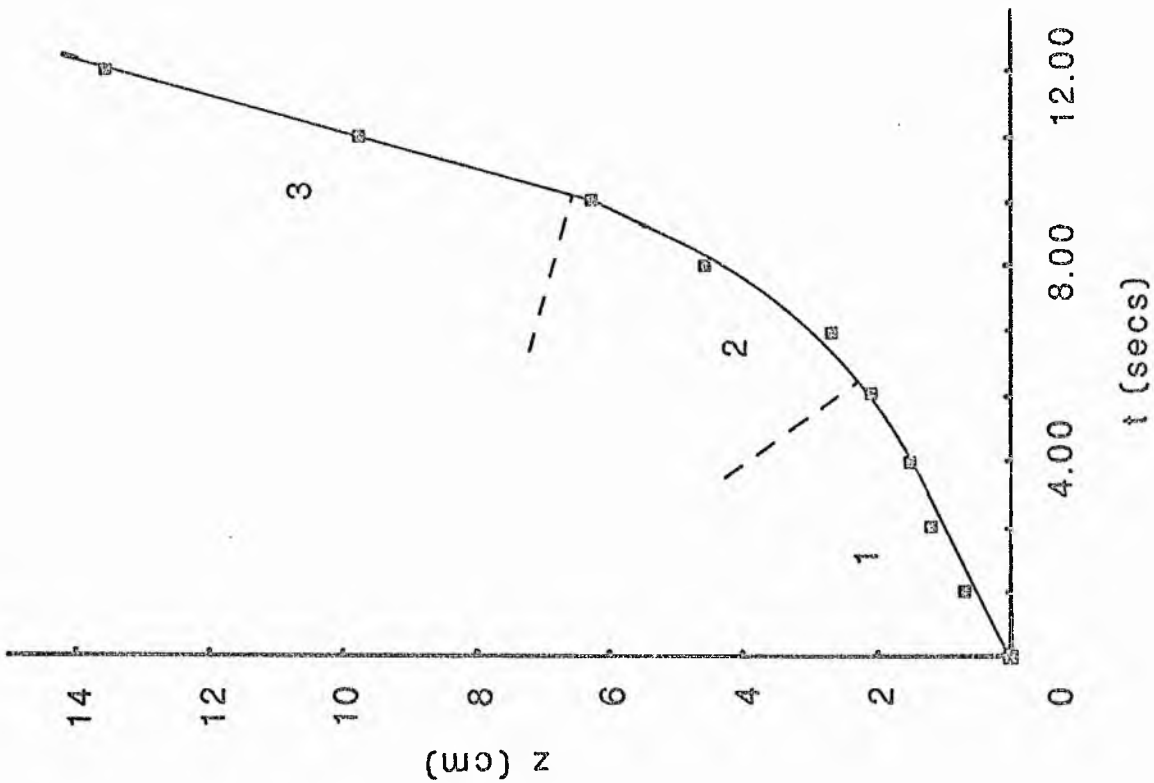
$$v = \frac{a^2 g \Delta \rho}{3 \mu_2} \left(\frac{\mu_2 + \mu_1}{\mu_2 + \frac{3}{2} \mu_1} \right) \quad (5.1)$$

where v is the velocity of the fluid drop, a is its radius, g is gravitational acceleration, $\Delta \rho$ is the density contrast between the two fluids, μ_2 is the viscosity of the host fluid and μ_1 is the viscosity of the drop.

The shape of the curve in figure 5.4b and the interpretations given to each segment are similar to the observations made by Marsh (1979) in which less viscous, less dense fluid rises through denser, more viscous fluid.

Figure 5.4a Outlines of developing vertical density current traced from a series of photographs. $t = 0$ is chosen as the last frame in which no movement can be detected. The diagram illustrates the development of a diapir which eventually forms a bulb of fluid which breaks away from the top layer and drops to the base of the tank trailing a thin pipe of fluid.

Figure 5.4b Plot of the distance (z), moved by the tip of the current illustrated in figure 5.4a, away from the originally horizontal surface of the upper fluid layer, in time (t). The curve has been split into three sections; in 1 and 3 the current has a constant velocity whereas in 2 it is accelerating.



As the glycerol continues to melt more becomes available to form descending plumes. The trailing pipes from these currents continue to transport glycerol to the base of the tank after the head of the current has reached the floor.

When the current impinges on the flat floor of the tank it spreads out radially and appears to exhibit the features of the viscous gravity currents described by Irvine (1978, 1980a). When vertical density currents impinge on dipping floors the current spreads outwards and downwards and effectively turns into a flow similar to those described by Irvine (ibid). Experiments were run with floors dipping at angles of 0° , 15° , 30° and 45° . These showed qualitatively that the angle of spread of the current is inversely related to the angle of dip.

Summary.

These experiments confirm qualitatively that plumes emanating from a planar source with variable viscosity have similar structures to those from isoviscous sources. These plumes flow vertically through the host liquid and when they impinge on dipping floors they spread downwards and outwards, or on flat floors radially outwards, exhibiting the internal structure of the density currents described by Irvine (1980a).

5.6.3 Plume spacing and velocity.

The spacing of plumes across the surface is a function of the viscosity ratio of the two fluids (Whitehead and Luther, 1975). These experiments are not however, well scaled to magmatic conditions and thus no quantitative information can be gained. The theory of plumespacing has however been developed by Selig (1965) for the case where the thin layer is much less viscous than the thick one ($\mu_1 \ll \mu_2$) with a specific application to salt dome dynamics in mind. Whitehead and Luther (1975) rederive Selig's expression and extend it to the cases where $\mu_1 = \mu_2$ and $\mu_1 \gg \mu_2$. Marsh (1979) experimentally confirmed Whitehead and Luther's results and extended them to dipping sources.

The spacing of plumes can be calculated from the relation;

$$d/4\pi h_1 = (180\epsilon)^{-1/5} \quad (5.2)$$

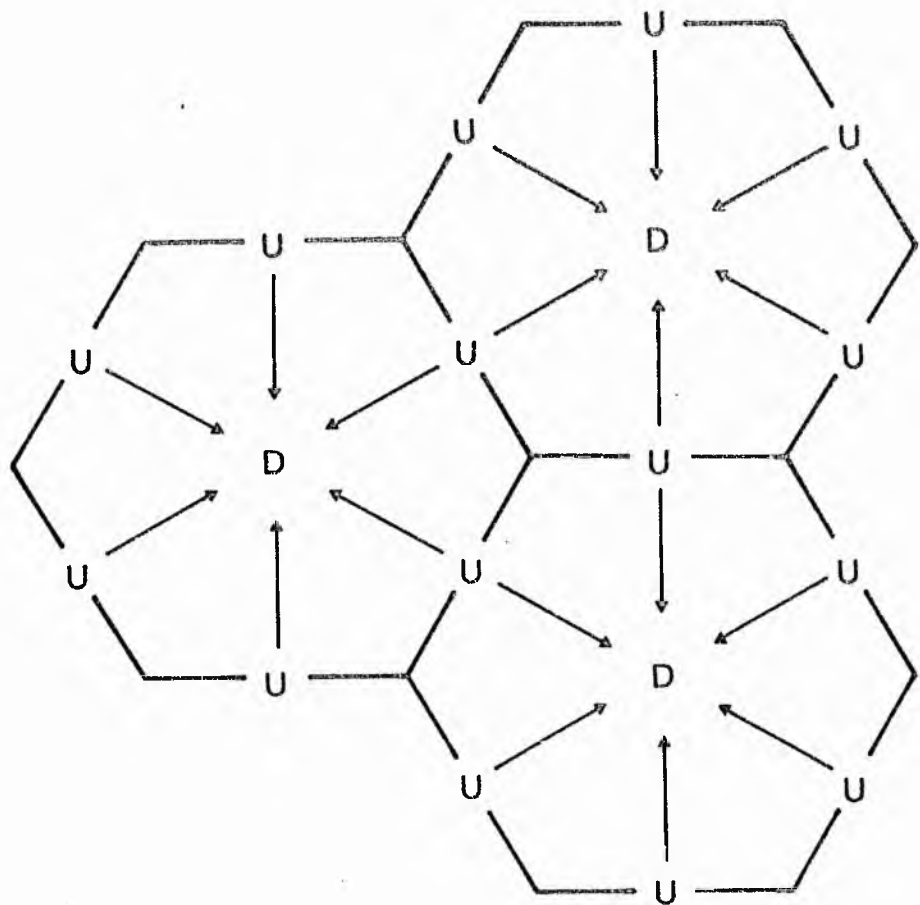
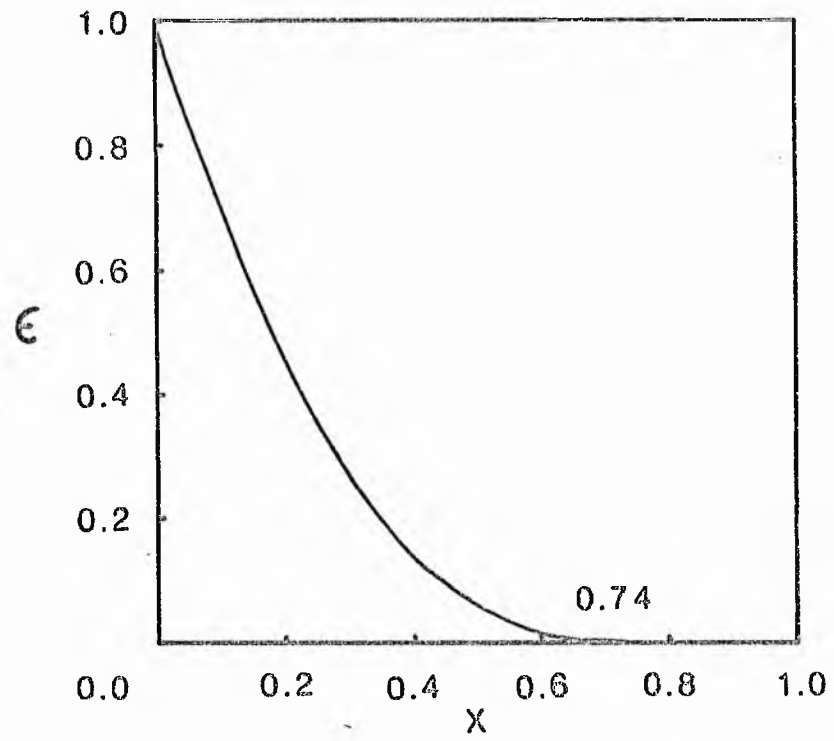
where d is the spacing between plumes, h_1 is the thickness of the thin viscous layer and ϵ is the ratio of the viscosities (μ_2/μ_1). The physical situation envisaged is illustrated in figure 5.3. Thus the spacing of plumes depends on both h_1 and ϵ . The viscosities of basic magmatic liquids range from on the order of 10^1 to 10^3 poises (Shaw, 1969; Bottinga & Weill, 1970; Murase & McBirney, 1973; Huppert & Sparks, 1980). The viscosities of crystal/liquid suspensions can be calculated using equation 3.3, therefore

$$\mu_1 = \mu_2 (1-RX)^{-2.5} \quad (5.3)$$

and from this the relationship between X and ϵ has been calculated and is shown graphically in figure 5.5. Reasonable values of X for magmatic density currents probably lie between 0.30 and 0.45 and almost certainly between 0.2 and 0.55 (see chapter 3) and therefore values of ϵ range from 0.05 for the highest concentration to 0.5 for the lowest concentrations. For these values $d/4\pi h$ lies between 0.41 and 0.64, and thus d has a value between about $8h$ and $5h$.

Figure 5.5 Graph illustrating the relationship between ϵ (the ratio of the viscosity of the host liquid to the viscosity of the current, μ_2/μ_1) and X (the proportion of crystals within the current). As X approaches 0.74, ϵ tends to 0 (μ_1 becomes infinite).

Figure 5.6 Plan view of the developing flow. Each descending plume (marked D) drains a hexagonal area. Along the boundaries of adjacent hexagons the flow is ascending (marked U) and within the hexagons the fluid moves towards each plume (marked by the arrows).



In plan these flows take the form of isolated descending domes surrounded by a hexagonal matrix of ascending material (see fig 5.6) (Whitehead and Luther, 1975). The area of cumulate (A) "drained" by such a flow can be calculated using

$$A = 1.5d^2/\sin 60^\circ \quad \text{where } 5h \leq d \leq 8h \quad (5.4)$$

and therefore the volume, assuming no "replenishment" (crystallisation) of the unstable layer, by multiplying A by h. Taking values of between 10cm and 1m for h and assuming that the resultant suspension spreads out across the floor to form a circular layer 10cm in thickness, then (5.4) predicts that the layers produced will range from about 0.5m to about 20m in radius. These values are of a similar order of magnitude to the strike dimensions of mafic and graded layers in the Kiglapait Lower Zone and the Rum intrusion.

The fluid dynamics of buoyant fluid introduced into the base of a reservoir of denser fluid have previously been described in a geological context by Sparks et al, (1980). The situation envisaged here is opposite to this in the sense that the density difference and flow directions are opposite, but they are dynamically similar. As noted above the descent velocity of the current is approximately that of a drop of fluid which is more simply given by:

$$v = \frac{g a^2 \Delta \rho}{12 \mu_2} \quad \text{Sparks et al, 1980 (5.5)}$$

where v is the velocity of the drop, $\Delta \rho$ is the density difference ($\rho_1 - \rho_2$), a is the diameter of the drop and μ_2 is the viscosity of the host fluid. Whether laminar or turbulent flow occurs can be assessed by estimating the Reynolds number, which for this particular system is:

$$Re = \frac{\rho_2 v a}{\mu_2} \quad (5.6)$$

A value for a can be obtained from Marsh (1979), who shows that the radius of the bulbous head of the current where $\mu_1 \ll \mu_2$ (the opposite to the situation considered here) at the moment it "lifts off" from the source, a , is related to the diameter of a circular source (h^*) and the viscosity ratio between the two fluids, such that:

$$a h^* \approx 1.13 \left(\frac{\mu_2}{\mu_1} \right)^{1/4} \quad (5.7)$$

However Marsh also states that the numerical factor in (5.6) is insensitive to both the angle of dip of the source and the viscosity ratio, thus for the situation described above

$$a = 1.13h \epsilon^{1/4} \quad (5.8)$$

and thus with values of ϵ ranging from 0.05 to 0.5 (section 5.6.3).

$$0.53h = a = 9.95h \quad (5.9)$$

Equations (5.5) and (5.6) can now be combined and Re set equal to a desired value (for example 1 to define conditions when laminar flow is certain). Geologically reasonable values of $\Delta\rho$ are around 0.1 (see figs 5.1 & 5.2) and thus the range of reasonable conditions straddles the whole range of situations from laminar to fully turbulent (see fig 5.7).

These calculations are based on an assumed Newtonian behaviour for both fluids. Crystal-rich magmatic liquids may well be significantly non-Newtonian however (Shaw et al., 1968; Sparks et al., 1977), with significant yield strengths. The effect of this is to raise the Reynolds number threshold for the transition to turbulence, thus extending the range of current diameters and viscosities for which flow will be laminar. The possibility that crystal sorting may take place in such vertical density currents is addressed in the next section.

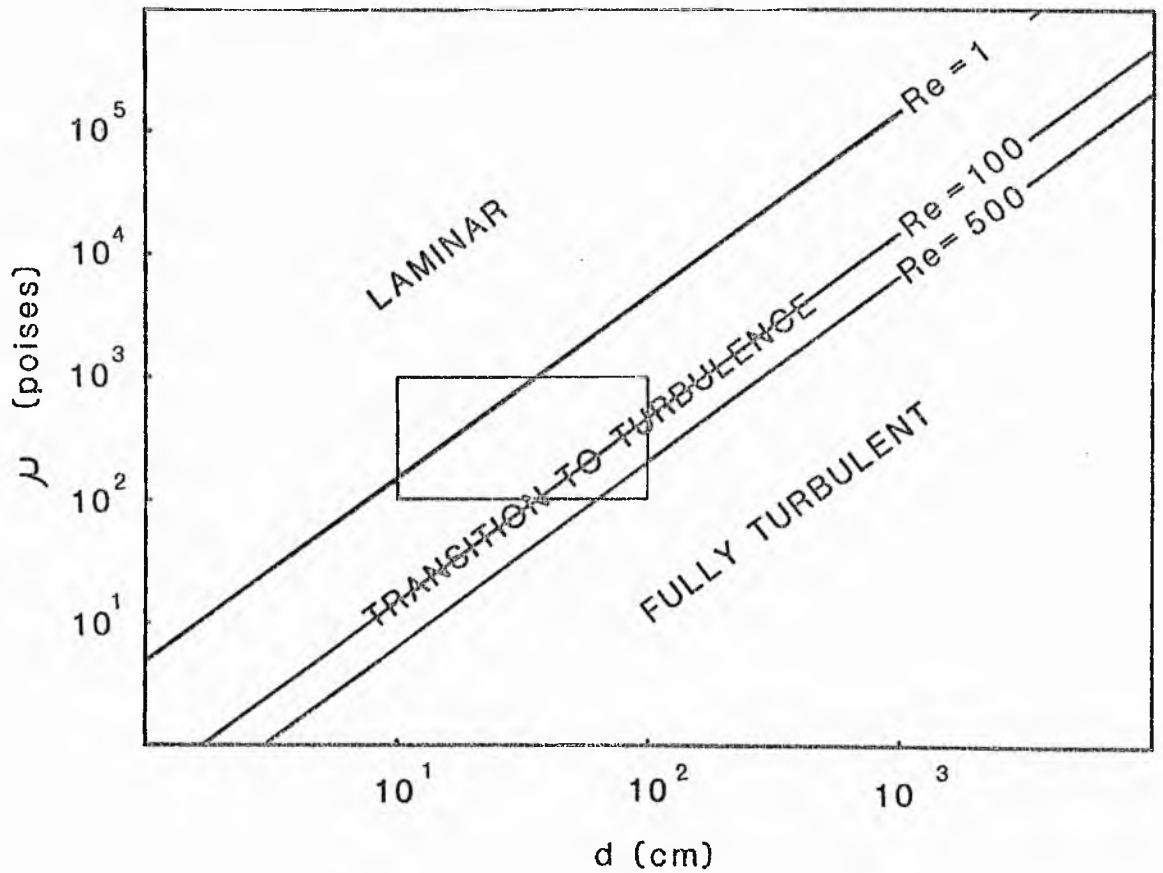


Figure 5.7 Diagram illustrating the fields of laminar, transitional and fully turbulent flow for vertical density currents in basaltic magma chambers. Lines of equal Reynolds number are shown for $Re = 1$, $Re = 100$ and $Re = 500$ at $\Delta\rho = 0.1$. The boxed region shows combinations of viscosity and current diameter probable in basaltic magma chambers. The behaviour is laminar up to $Re = 1$ and probably so for values of Re up to 100.

5.6.4 Internal flow structure.

Any interpretation of crystal sorting within currents is dependent on an understanding of their internal flow structure. Three principal problems were associated with delineating particle path lines in the currents.

i) the flow is three dimensional, unlike the essentially two-dimensional currents described by Irvine (1978a, 1980a), though they exhibit radial symmetry. Thus, though sections through the centre of the current are representative of the whole current they are difficult to identify. This problem was partially overcome by using a wide aperture setting (f2.8 or f4) to limit the depth of field and a narrow, vertically elongated light source. This has the effect of keeping only the portion of the current of interest in focus.

ii) flows consisting of the proportions of solids thought to occur in magmatic density currents (30-40%) are virtually opaque, thus individual particles, particularly in the centre of the current, are difficult to trace. This problem was overcome by using a denser, more viscous liquid as the current and tracing particle paths within it.

iii) the most convenient liquids to use are immiscible ones since the outline of the current is easily traced and the liquids are constantly reusable. Such combinations work well for two-dimensional flows. In this case, however, immiscible liquid

combinations proved impracticable due to internal reflections from the interface between the two fluids.

A workable solution to these problems was found by using cold silicone oil (7 ± 0.5 °C) as the density current and silicone oil at room temperature (22 ± 0.5 °C) as the host liquid. Cooling the silicone oil has the effect of increasing both its density and viscosity. Crushed plastic sieved to between 18 and 30 phi was used as a tracer material in both the current and the host liquid. The plastic shards used were in fact denser than both fluids but their settling velocities are negligible compared to the velocity of the current. In practice no movement can be detected when settling one isolated shard through the oil for the duration of a typical experiment.

The problem of finding a lock and gate system was overcome by introducing the current into the host liquid either by pouring onto the surface or introducing it through a spout. Whitehead and Luther have shown (1975) that the dynamics of plumes produced by instability of a layer and at a spout are identical. The development of the currents was photographed as before. Enlargements of selected portions of the current then allowed tracing of particle movement through time. Plate 5.3 shows an enlargement of the head of one current flowing through a host of silicone oil in which there are no tracers. Particle movement was traced both relative to the flume and relative to the moving front top of the current.

Observations.

Motion vectors of tracer particles plotted relative to the tank walls and to the moving tip of the current are shown in figures 5.8a and 5.8b. Each line represents the distance travelled in a time of 0.67 seconds and thus the length of line is directly proportional to particle velocity. The following aspects of these figures are considered important in the present context.

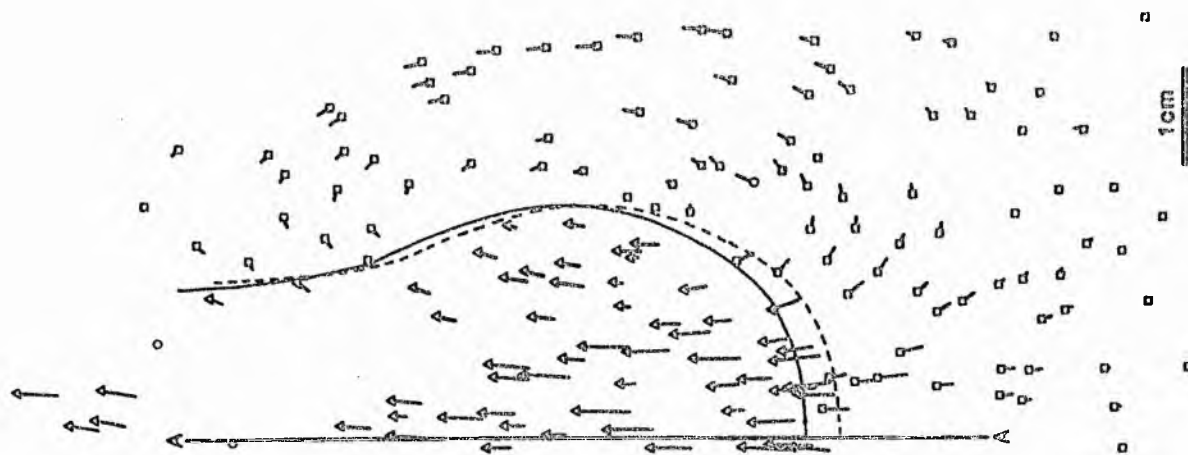
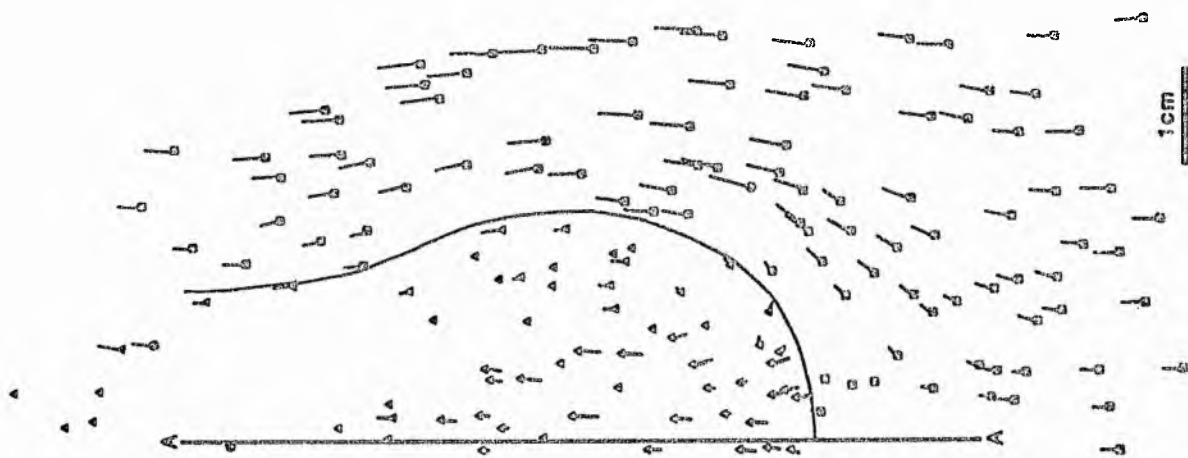
i) the particles (and small air bubbles) within the flow have a large downward component of velocity relative to the tank walls.

ii) relative to the tip of the current however, only those particles in the centre of the flow are gaining on the tip.

iii) all the particles have a radial component of velocity. Plotted relative to the tank walls this is manifest as a radial divergence in the front portion of the current head and a convergence of the particle path vectors immediately behind the head. Plotted relative to the tip of the current the particles indicate an internal circulation in which they are being swept radially outwards at the current tip, and up and back behind the current head.

iv) particles in the host liquid move downwards and outwards at the tip of the current, sweep up around the sides of the current head and then down with the moving tail of the current as shear is imparted to the host fluid. No mixing between current and host liquid occurs however (the flows have low Reynolds numbers).

Figure 5.8 Motion vectors of tracer particles for a 0.67 second interval during flow of cold silicone oil into silicone oil at room temperature. The symbols mark the first position of the tracers; the line extends to their second position. Tracers within the current are indicated by triangular symbols; those within the host liquid by squares. In the left-hand diagram (open symbols) the motion is mapped relative to the walls of the tank; in the right-hand diagram (filled symbols) the motion is mapped relative to the moving tip of the current. Several traces are obviously anomalous and are due to difficulty in distinguishing only those from the central portion of the current.



In summary, all the particles in the current are transported downwards at velocities far in excess of their terminal settling velocities as described by Stokes Law. At the front of the current the central portion of the flow is gaining on the front tip and then being swept outwards, and being left behind by the current tip, ultimately to take its place in the steady flow. The host liquid is shouldered aside by the moving current tip (which is the ultimate cause of the broadening of the current (Whitehead and Luther, 1975) and presumably its internal circulation), sweeps up and around the tip and is transported downwards in the region of the current tail, but is not entrained by the flow.

5.6.5 Suspension currents.

Several simple experiments were carried out to check on whether these observations are applicable to suspension currents. Glass shards were sieved gently onto the free surface of the silicone oil. A layer built up which became unstable after some time and a downward bulge began to form, as in the melting experiments. This bulge grew with time until it broke away from the layer and transported the glass shards to the floor of the tank where the glass-charged fluid spread out in a layer. As the current was flowing through the oil, glass shards were being pushed radially away from the centre of the current tip. The current trailed a pipe, or tube, of glass-charged fluid which continued to transport

Plate 5.2 The head of a vertical density current, defined by tracer particles, produced by introducing cold silicone oil into silicone oil at room temperature. The head of the current is approximately 2cm across.

Plate 5.3 Vertical density current driven by glass shards introduced into the host liquid. The effect whereby material is transferred from the centre of the current to its margins is clearly visible. The head of the current is approximately 2cm across.



glass to the tank floor after the head of the current had reached the floor. These features can be seen in plate 5.4. The observations are consistent with those described above on liquid density-driven currents.

5.6.6 A possible crystal-sorting mechanism.

The most important feature of these currents has already been noted, namely that they transfer particles downwards at velocities far in excess of their terminal settling velocities. In natural currents however, not all the particles have identical physical attributes. The particle paths were delineated using tracers with virtually neutral buoyancy. Particles denser than the liquid would however have an extra component of velocity downwards, whereas those lighter than the liquid will have an upward component of velocity. Consideration of figures 5.8a and 5.8b suggest that the former will be transferred radially outwards in the current less than the latter. Thus plagioclase may be separated from mafic minerals and, if the suggested process were efficient enough, may lead to a return flow driven by the negative buoyancy of plagioclase: in this way feldspar may be returned to the roof zone of the intrusion which in basic layered bodies are often quasi-anorthositic (Wager & Brown, 1968; Morse, 1969;

5.7 Discussion.

The petrologic consequences of density variations amongst magmatic liquids have recently received much attention (Stolper & Walker, 1980; Sparks et al, 1980; Huppert & Sparks, 1980; Huppert & Turner 1981; Grove & Baker, 1983; Sparks & Huppert, 1984; Tait et al, 1984 etc). With the exception of the paper by Huppert et al (1982), the implications of the nucleation of a new phase within magmatic liquids for the bulk density have been ignored, though the principle has been noted (Sparks et al, 1980, p 428). The analysis above indicates that transport of crystals from a roof zone to a intrusion floor is a real possibility. The volumes involved cannot be very large, otherwise turbulent mixing with the contemporary magma will occur (see fig 5.7 and discussion of the behaviour of "thermals" in Sparks et al, 1980). If, however, mixing does occur, this could lead to the development of instability on an even larger scale, and convection could occur in increasing scales of length (cf Foster, 1969), perhaps leading to overturn of the whole chamber. Where a chamber was compositionally and thermally stratified this could lead to complex growth/resorption cycles in the suspended phenocrysts for which there is some petrographic evidence (Maaloe, 1976).

Laminar flows on the other hand will transport their loads to the chamber floor and may undergo some crystal sorting on the way. On impinging on the floor they may form "Irvine-style" density currents or simply spread locally, if of small volume. Layers

formed in this way may be impossible to identify positively. However, local accumulations of autoliths and xenoliths in the Skaergaard and Kiglapait intrusions have been interpreted as the deposits of vertical density currents (McBirney and Noyes, 1979, Appendix 4). Localised, mafic, lensoid layers which occur in the Kiglapait intrusion (Morse, 1969; Appendix 4) may also have originated in this way, since (a) they have features consistent with an origin by physical deposition including rare erosional bases and grading yet are much less elongate down dip than normally graded layers (App 4), and (b) they are more mafic than the surrounding rock but there is no sign locally of the "missing" feldspar. The volumes of suspension which can be removed from roof zones are similar to the volumes of these layers, which are typically on the order of 10 cm thick and 1-30m in their lateral dimensions. In other intrusions layers formed in this way may be identified by being lenticular in cross-section, circular in plan (if the floor was horizontal) and interleaved. It is possible however that such a process may give rise other graded layers indistinguishable from those originating from sources on the walls and floors of intrusions. If the supply of crystals is maintained at the source then they can be continuously supplied to the chamber floor by flow along stream tubes. Such a steady flow may build up unlayered rock.

The analysis above ignores however, the possible effects on vertical density currents of turbulent thermal, or double-diffusive convection. Convection may act to mix fluid from the currents in with the host magma, alternatively fluid transported downwards by

the crystal-rich currents may break up stratification in the chamber. An estimate of the relative importance of these effects will probably have to await a better understanding of the fluid velocities in convecting magma chambers.

5.8 Conclusions.

- 1) The roof zones of layered intrusions have been sites of significant amounts of crystallisation.
- 2) The addition of crystals in cotectic proportions has a larger effect on fluid density than either cooling or fractionation.
- 3) The combination of (1) and (2) suggests that unstable layers of crystal-rich suspensions may build up, perhaps metastably, below the roofs of crystallising plutons. These may be released spontaneously or following seismic activity to form vertical density currents which may either transport crystals to the intrusion floor at low Reynolds numbers (in which case they may undergo some sorting on the way) or cause the suspension to mix with a large volume of magma at high Reynolds number and may ultimately cause large-scale overturn of the magma in the chamber.

6 DIAGENETIC PROCESSES IN CRYSTAL MUSHES.

6.1 Introduction.

The preceding chapters have all been principally concerned with the cumulus stage of the solidification of major basic magma bodies; this can usefully be compared to the depositional stage in the formation of sedimentary rocks. The postcumulus stage of the solidification has largely been ignored by petrologists, though all studies which attempt to trace magma compositions by means of mineral chemistry involve assumptions about the retention of cumulus compositions and stratigraphic relationships. The postcumulus stage of the solidification can usefully be compared to the diagenetic stage of the formation of sedimentary rocks. 'Diagenesis' covers all the chemical and physical processes which act on sediment grains within the sediment (Leeder, 1982). This chapter describes structures which have evidently formed beneath the mush/magma interface and discusses the processes which have formed them. It is concluded that fluid flow within unconsolidated mushes is pervasive and can critically influence mineralogical, textural and bulk chemical characteristics of the rocks.

6.2 Structures defined by deformed layers.

Structures which have evidently formed by deformation of pre-existing layers are common, especially so in the Rum intrusion where the original dips are often very shallow. The development of many of these structures has important implications for interpretations of the textural and compositional evolution of layered rocks in general. The simplest-looking structures will be described first, followed by increasingly geometrically complex structures.

6.2.1 Symmetrical deformation structures.

The structures described in this section are roughly symmetrical in cross-section and occur in two localities in the Rum intrusion.

6.2.1.1 Harris Bay, Harris Bay Series, Western Layered Series.

The Harris Bay Series is thought to be structurally the lowest exposed portion of the layered rocks in southwest Rum and is composed of olivine eucrites, interpreted as olivine-feldspar-pyroxene cumulates, (Wadsworth, 1961).

Plate 6.1 Interlayered plagioclase - olivine - clinopyroxene (relatively resistant) and olivine - plagioclase - clinopyroxene cumulates. The more feldspathic layers have sharp bases and protrusions of feldspathic rock into the mafic layers on their tops.

Plate 6.2 Teardrop-shaped body of feldspathic rock enclosed in mafic layer.



On the south-east margin of the bay (grid reference N1341749) there is an outcrop of interlayered, medium-grained, plagioclase - olivine - clinopyroxene and finer-grained olivine - plagioclase - clinopyroxene cumulates. Both layer types are 10-20 cm thick and flat-lying (plate 6.1). The upper surfaces of the more feldspathic layers are characterised by knobbly protrusions of feldspathic rock into the more mafic rock. These protrusions are generally radially symmetrical about a vertical axis, have bulbous tops and often narrow towards their bases (plate 6.2). In some instances teardrop-shaped masses of feldspathic rock are totally enclosed in the more mafic rock. Where the protrusions can be seen in plan they are circular and are sometimes joined by ridges of feldspathic rock. Rare downward protrusions of feldspathic rock can be found on the bases of feldspathic layers, but, in contrast to those on the upper surfaces, these are generally pointed.

The layered rocks are unlaminated and the feldspars are extensively normally zoned. In contrast, tabular feldspars in the protrusions tend to be orientated parallel to the margins of the structures along their upper surfaces.

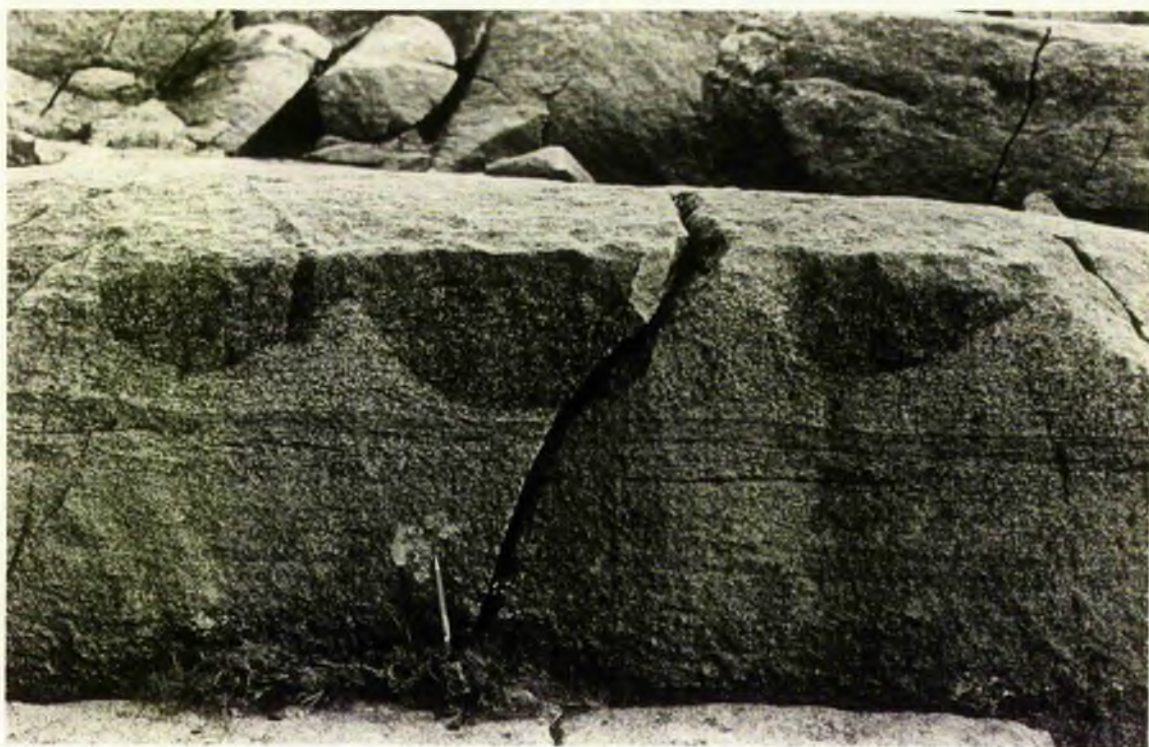
6.2.1.2 Unit 9, Eastern Layered Series

About 6 m below the top of unit 9 there is a distinctive pyroxenic allivalite layer with an undulatory base (Brown, 1956). Similar layer junctions are present in units 3 and 8. The three-dimensional form of the unit 9 example is best examined at grid reference N13967968 on the northern flank of Hallival. The pyroxenic layer is 1-2 m thick and is underlain by an allivalite in which pyroxene is only a minor phase. For convenience, these lithologies will henceforth be referred to as gabbro and troctolite, rocks respectively. The contact is a ratio one, defined by an abrupt increase in the modal ratio of clinopyroxene to plagioclase. The proportions of phases in the gabbroic layer are plagioclase 63%, clinopyroxene 27%, olivine 10% and in the troctolitic layer plagioclase 85%, olivine 10% and clinopyroxene 5%. Chrome-spinel is present in minor amounts in the troctolite but extremely scarce in the gabbro.

The contact is generally sinusoidal in form in both strike and dip sections. Departures from this geometry occur where the troctolitic rock exhibits more pointed crests (plate 6.3) or more rarely forms diapir-like structures with pronounced overhangs below a bulbous top. The culminations in the troctolite are sometimes arranged en echelon (plate 6.4). The wavelength and amplitude are variable, though typically around 1 m and 30 cm, respectively. Figure 6.1 is a composite exploded block diagram of the contact observed in several outcrops.

Plate 6.3 Undulatory contact between clinopyroxene-rich (upper) and clinopyroxene-poor (lower) allivalite, unit 9, Eastern Layered Series, Rum. Note the undeformed, olivine-rich layer immediately below the undulations and the horizontal fabric in the whole outcrop.

Plate 6.4 Horizontal section through unit 9 undulatory contact showing aligned culminations of troctolite and valleys filled with gabbro.

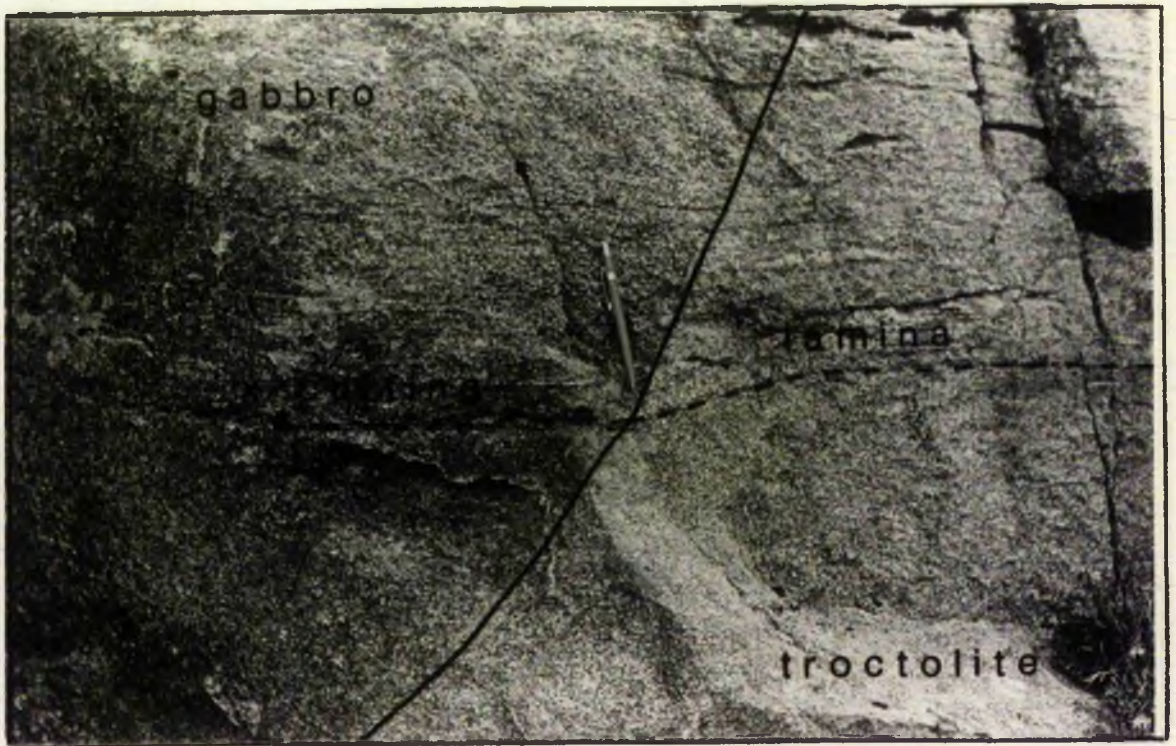


Relationship of ratio contact to rhythmic layers and laminae

Both rock types are layered and laminated on several scales. A prominent thin (3-4 cm) peridotite layer is developed 0.5-1 m below the ratio contact and tends to follow the undulations in that contact, though with much reduced amplitude. Other layers and laminae are defined by variations in the modal proportions of olivine and plagioclase. These are developed through the whole sequence and may follow the form of, though with an amplitude less than the major contact, or they may remain straight, even when very close to the undulatory contact (plate 6.3). Still others cut straight across the undulatory contact or, more usually, exhibit a slight kink at the contact, which is always towards the contact. Examples of cross-cutting layers and laminae are shown in plates 6.5 to 6.8. These cross-cutting features are commonly thin, discontinuous olivine laminae, though rare 2-3 cm thick layers of plagioclase and olivine occur. It is possible that this undulatory contact and the cross-cutting layers and laminae are what Harker compared to concretionary growths in the Durham magnesian limestone "in which concretionary growth has not obscured the original lamination" (Harker, 1908).

Plate 6.5 Sinusoidal contact with clearly cross-cutting laminae. Note the deflection towards the major ratio contact.

Plate 6.6 Isolated olivine-rich laminae (below pencil point) cutting across the undulatory contact.



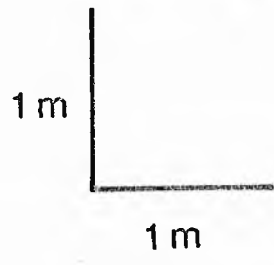
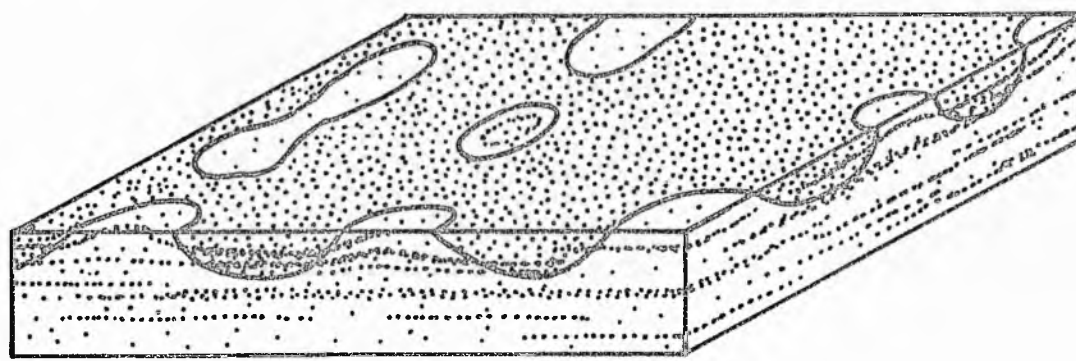
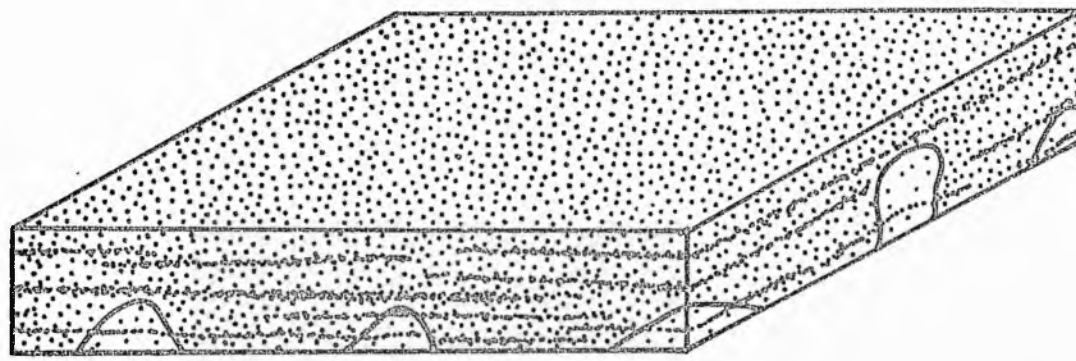
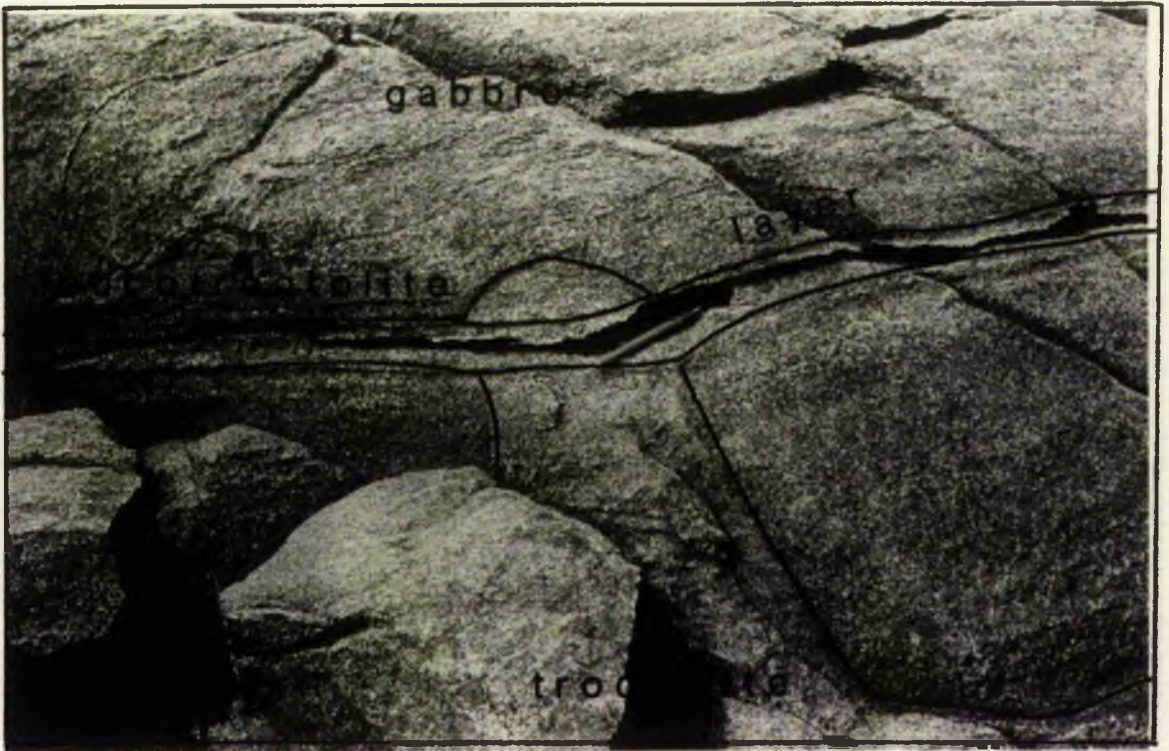
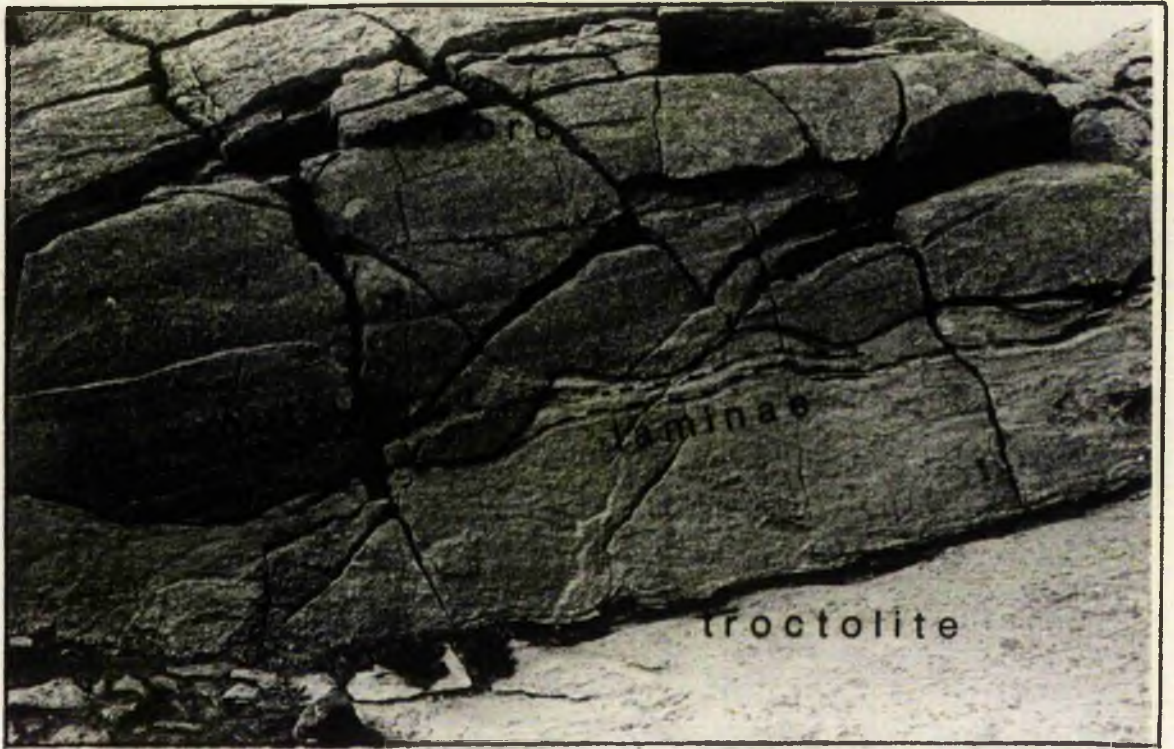


Figure 6.1 Exploded block diagram showing the three-dimensional form of the undulatory contact between gabbro (above) and troctolite (below) and its structural relationship with the olivine laminae and layers.

Plate 6.7 Two thick olivine-rich laminae in allivalite: at the right of the photograph they run parallel to the major ratio contact, whereas at the left the upper lamina cuts across the contact.

Plate 6.8 Leucotroctolite layer cutting across protrusion of troctolite into gabbro. A photomicrograph of a section through this layer is presented in plate 6.10.



Textures and mineral compositions

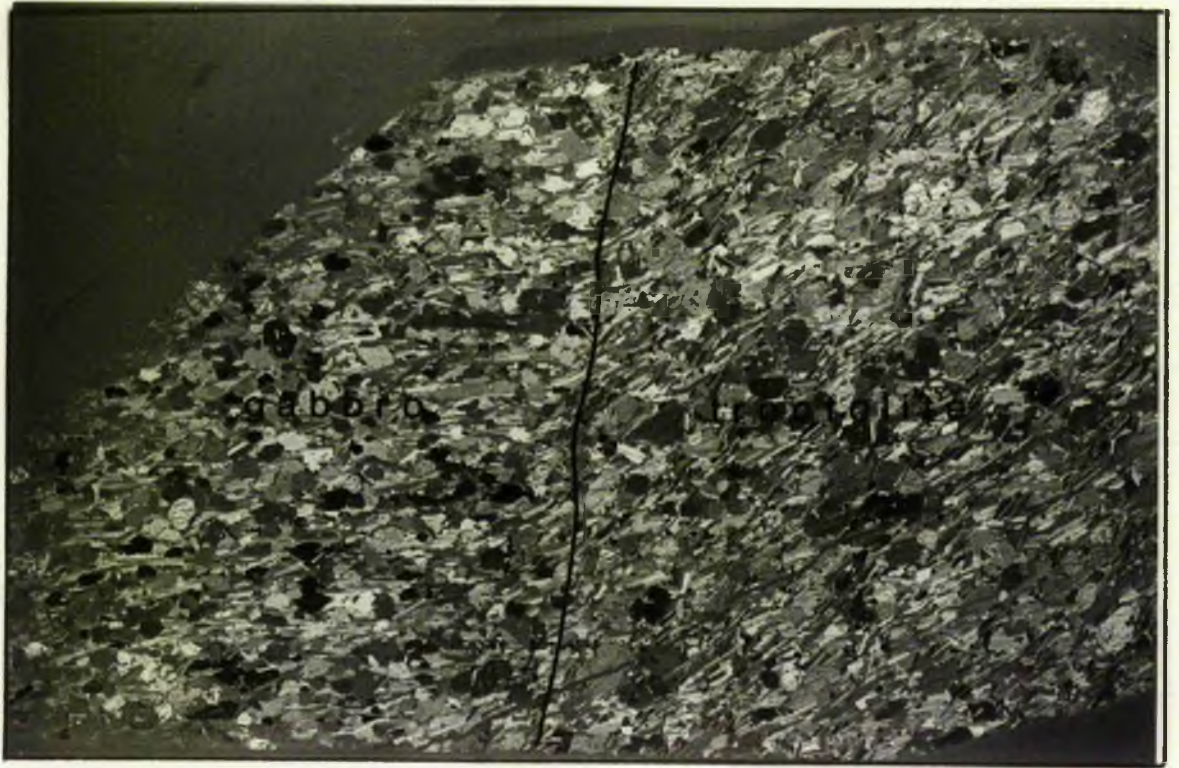
Both the gabbro and troctolite rocks are medium-grained with a pronounced igneous lamination displayed by tabular plagioclase feldspars. Sections cut in the plane of the lamination reveal that the plagioclase tablets are not aligned. Where a mafic phase is encountered the lamination follows the outline of the crystal, individual feldspars being arranged tangentially around the mafic phase. Within domes of the troctolite the lamination displays a similar sinusoidal form to, though of lower amplitude than, the undulatory contact. Right on the contact, at the margins of the structures the feldspar lamination is aligned parallel to the contact (see plate 6.9).

Olivine is generally equant, subhedral and about 2 mm in diameter though rare elongate grains occur. Olivine rarely poikilitically encloses plagioclase grains, where it does so, the feldspars are more commonly found near to the margins of the enclosing phase.

Clinopyroxene in the gabbroic layer is generally equant, subhedral to euhedral and about 1 mm in diameter, though rare elongate grains occur. Only a few clinopyroxenes have been seen to poikilitically enclose plagioclase and, as in the case of olivine, this generally occurs at the margins of the clinopyroxene. In the troctolitic layer clinopyroxene occurs as thin rims on plagioclase and olivine and as oikocrysts up to 3 mm in diameter.

Plate 6.9 Photomicrograph of a section across the unit 9 undulatory contact. Note deflection of the feldspar lamination in the inferred direction of movement (see text) of the load structure and its alignment parallel to the contact at the contact. (x2.5, partially crossed polars)

Plate 6.10 Photomicrograph of a section through the cross-cutting layer in plate 6.8 enclosed in gabbro. (x2, partially crossed polars).



Discontinuous olivine laminae formed of trains of crystals are present in both rock types. Most are only a few millimetres thick, ie one to two grain diameters. Thicker, cross-cutting layers are composed of tabular, laminated plagioclase and equant, subhedral olivine. In contrast to the petrographically similar troctolite these are virtually spinel free.

All phases appear unzoned under optical examination (though see below) and all the rocks described would be termed adcumulates in present textural classification schemes for layered igneous rocks (Wager *et al*, 1960; Irvine, 1982).

The compositions of the major phases in both lithologies have been investigated by electron microprobe (see footnotes to table 6.1 for microprobe operating conditions). Mean values of An mol% (Ca/Ca+Na) for plagioclase, En mol% (Mg/Mg+Fe) for clinopyroxene and Fo mol% (Mg/Mg+Fe) are presented in table 6.2 and complete analyses of selected phases in table 6.1. Data from a traverse across one plagioclase grain from the upper part of the troctolite are presented in figure 6.2. The mineral data indicate the following:-

i) Olivine is of constant and similar composition (maximum variation found within one crystal is approximately 0.4% Fo) in both lithologies.

ii) Clinopyroxene is of similar composition in both lithologies, in spite of differences in texture and mode. There is a suggestion in

Table 6.1 Selected mineral compositions from gabbro and troctolite, unit 9, Eastern Layered Series. Olivine and clinopyroxene analysed using combined wavelength- and energy-dispersive spectrometry techniques, plagioclase by energy-dispersive spectrometry only. All analyses made using an accelerating potential of 15kV and a probe current of 30 nanoamps. 100 second counts made on peak and 40 second counts on background.

PLAGIOCLASE

GABBRO 206Y/43

TROCTOLITE
206Z/50

CLINOPYROXENE

GABBRO 206Y/24

TROCTOLITE 206Z/32a/b

OLIVINE

GABBRO 206Y/6

TROCTOLITE
206Z/12

Wt%	<u>PLAGIOCLASE</u>		<u>CLINOPYROXENE</u>		<u>CLINOPYROXENE</u>		<u>CLINOPYROXENE</u>		<u>OLIVINE</u>		<u>OLIVINE</u>	
	<u>CORE</u>	<u>RIM</u>	<u>CORE</u>	<u>RIM</u>	<u>CORE</u>	<u>RIM</u>	<u>POIKILITIC</u>	<u>POIKILITIC</u>	<u>CORE</u>	<u>RIM</u>	<u>CORE</u>	<u>RIM</u>
SiO ₂	47.82	46.39	47.03	47.08	52.62	52.12	52.44	52.23	40.44	40.97	41.10	40.95
TiO ₂	-	-	-	-	0.45	0.57	0.72	0.67	-	-	-	-
Al ₂ O ₃	32.77	33.55	33.09	33.41	2.66	3.17	3.07	3.12	-	-	-	-
Cr ₂ O ₃	-	-	-	-	0.61	1.07	0.98	1.12	0.03	0.00	0.00	0.00
FeO	0.59	0.43	0.57	0.41	4.73	4.68	4.46	4.48	15.25	14.91	14.92	14.61
MnO	-	-	-	-	0.11	0.11	0.10	0.09	0.24	0.24	0.20	0.18
MgO	-	-	-	-	17.02	16.56	16.24	16.22	45.73	45.84	46.67	46.49
NiO	-	-	-	-	0.02	0.00	0.05	0.10	0.21	0.19	0.16	0.19
CaO	17.54	18.49	18.16	18.04	22.42	22.46	23.24	22.79	0.10	0.00	0.18	0.00
Na ₂ O	1.82	1.32	1.80	1.49	0.36	0.48	0.33	0.00	-	-	-	-
K ₂ O	0.10	0.00	0.00	0.00	-	-	-	-	-	-	-	-
TOTAL	100.64	100.18	100.65	100.43	101.00	101.22	101.63	100.82	101.9	102.15	103.23	102.42
Atoms												
Si ⁴⁺	2.190	2.138	2.159	2.160	1.912	1.893	1.897	1.901	0.997	1.005	0.998	1.000
Ti ⁴⁺	-	-	-	-	0.012	0.016	0.019	0.018	-	-	-	-
Al ³⁺	1.769	1.823	1.791	1.807	0.114	0.136	0.131	0.134	-	-	-	-
Cr ³⁺	-	-	-	-	0.018	0.031	0.028	0.032	0.000	0.001	0.000	0.000
Fe ²⁺	0.023	0.017	0.022	0.016	0.144	0.142	0.135	0.136	0.314	0.306	0.303	0.299
Mn ²⁺	-	-	-	-	0.003	0.003	0.003	0.003	0.005	0.005	0.004	0.004
Mg ²⁺	-	-	-	-	0.922	0.876	0.879	0.880	1.680	1.675	1.689	1.693
Ni ²⁺	-	-	-	-	0.001	0.000	0.002	0.003	0.004	0.004	0.003	0.004
Ca ²⁺	0.861	0.913	0.894	0.887	0.873	0.874	0.901	0.889	0.003	0.000	0.005	0.000
Na ⁺	0.162	0.118	0.160	0.132	0.025	0.032	0.023	0.000	-	-	-	-
K ⁺	0.006	0.000	0.000	0.000	-	-	-	-	-	-	-	-
O ²⁻	8.000	8.000	8.000	8.000	6.000	6.000	6.000	6.000	4.000	4.000	4.000	4.000
An/En/Fo*	84.2	88.6	84.8	87.0	86.5	86.3	86.7	86.6	84.3	84.6	84.8	85.0

* An = Ca/Ca+Na
En = Mg/Mg+Fe
Fo = Mg/Mg+Fe

	OLIVINE (FO) 100Mg/Mg+Fe		CLINOPYROXENE (EN) 100Mg/Mg+Fe	PLAGIOCLASE (AN) 100Ca/Ca+Na
GABBRO (C)	84.3 (6)		86.6 (6)	85.1 (34)
GABBRO (R)	84.5 (3)		86.2 (4)	88.0 (2)
TROCTOLITE (C)	84.8 (8)			84.8 (18)
TROCTOLITE (R)	84.9 (4)	POIKILITIC	86.6 (11)	87.0 (1)

TABLE 6.2

Table 6.2 Mean (number of analyses in brackets) mineral compositions in gabbro and troctolite from unit 9. Random spots chosen for analysis in poikilitic clinopyroxene.

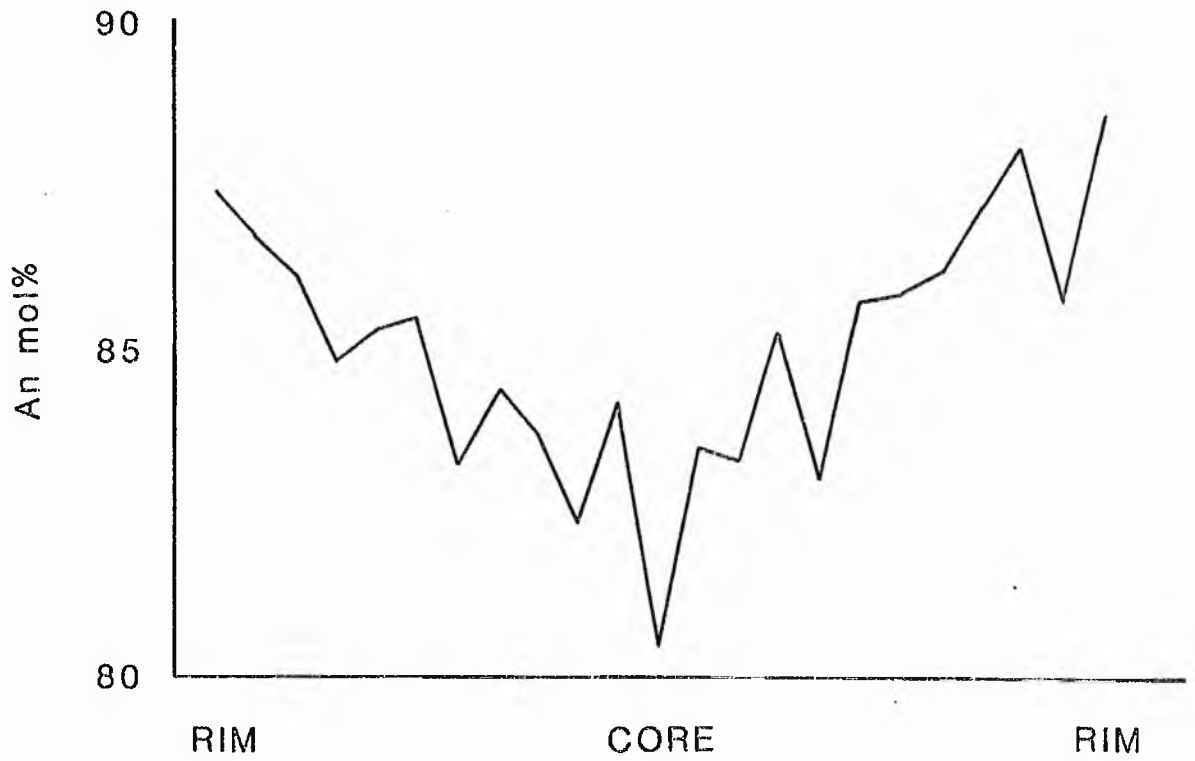


Figure 6.2 Microprobe traverse across a plagioclase grain (1 mm across) from the gabbro, 23 analyses.

some crystals of very slight zoning to more Fe-rich values at the rim (maximum variation in one crystal is approximately 1.4% En).

iii) Plagioclase is variable in composition internally (see fig 6.2) and is generally reverse zoned. Mean core compositions are similar in both lithologies (see table 6.1 and 6.2).

6.2.2 Discussion.

The geometry of, and abrupt density increase across the undulatory contacts in both the Harris Bay and Unit 9 exposures are similar to structures produced by the spontaneous deformation of the interface between two fluids with a reverse density gradient (eg Ramberg, 1967; Anketell et al, 1970; Whitehead & Luther, 1975; Marsh, 1979). Similar structures in other layered and bedded rocks, of both igneous and sedimentary origin, have been interpreted in the same way (eg Allen, 1970; Collinson & Thompson, 1982; Thy & Wilson, 1980; Lee, 1981; Parsons & Butterfield, 1981). The structures are most reminiscent of situations where the viscosities of both fluids are almost equal (see Allen, 1970; Anketell et al, 1970) and thus both the Harris Bay and the unit 9 sets of structures are considered to have formed by the deformation of crystal mushes.

Accepting deformation under the influence of gravity as the process producing the Unit 9 undulatory contact, it is evident that the cross-cutting olivine laminae and olivine-plagioclase layers must have formed within the crystal mush. However the sinusoidal form of the cross-cutting layers indicates that the formation of these layers and laminae occurred before, during and after the deformation that produced the undulatory contact itself. Layers which have formed within the crystal pile are known elsewhere in the Rum intrusion (Dunham, 1965; Donaldson, 1982), however this is the first time that layers texturally identical to "normal" cumulate layers have been shown to have formed within the crystal mush on the intrusion floor.

The cross-cutting laminae are parallel to the feldspar lamination except at the margins of structures. Feldspar lamination is generally interpreted as a depositional feature whether the crystals are considered to have settled or not (compare Brothers, 1964 and McBirney & Noyes, 1979). Experiments on loading and diapirism clearly indicate, however, that the deformation is pervasive throughout the whole structure (Ramberg, 1967; Anketell et al, 1970; Berner et al, 1972; Allen, 1977) and thus it is concluded that the feldspar lamination must also have been produced during and after the deformation, within the crystal pile.

The observations further imply that minerals which form late within crystal mushes need not have poikilitic, ophitic, replacement or interstitial relationships with other phases, as proposed by some petrologists (eg Jackson, 1961; McCallum et al, 1980). Granular-textured layers and laminae formed within crystal mushes may be a common feature of layered intrusions. Evidence for the postcumulus formation of layers has been noted in other intrusions, though these examples are not associated with symmetrical deformation structures, the evidence is set out below.

6.2.3 Kiglapait Intrusion - Lower Zone - Hare Point dunitic horizon.

On the Hare Point peninsula, South Aulatsivik Island, (Appendix 4, fig 2) there is a zone of strong modal lamination consisting of interlayered dunite, melatroctolite, leucotroctolite and anorthosite. In places the laminae have been displaced by a series of faults. Adjacent to the fault planes the laminae are slightly bent in the inferred direction of movement on the faults. The fault planes themselves are filled with apparently normally textured dunite or melatroctolite. The dunite and melatroctolite sheets pass upwards into conformable dunite and melatroctolite layers, similar to many other dunite and melatroctolite layers in the sequence which do not have extensions down fault planes (see plate 6.11).

Plate 6.11 Melatroctolite occupying faults in strongly modally laminated troctolites, Hare Point, Lower Zone, Kiglapait Intrusion. Note that the thick, central sheet extends upwards into a conformable metatroctolite layer.

Plate 6.12 Concentration of poikilitic clinopyroxene along a fault plane in allivalite, Central Series, Rum.



The rock occupying the fault planes is necessarily later than the faulted rocks themselves, thus the most reasonable interpretation of the conformable sections of these sheets is that they too postdate the formation of the faulted rocks. This may be true also of similar, wholly conformable, dunite and melatroctolite layers both here and at other places in the intrusion.

Comparable structures have been noted in the Central Series of the Rum intrusion but in these cases the sheets occupying the fault planes are rich in poikilitic clinopyroxene (see plate 6.12).

6.2.4 Beinn Buie gabbro intrusion, Centre 1 caldera, Mull.

The Beinn Buie intrusion outcrops as an arcuate mass on the south western margin of the centre 1 caldera (Skelhorn et al, 1969) and was either emplaced at the caldera margin (Lobjoit, 1959) or has been cut by later faulting (Skelhorn et al, 1969). Lithologies present include peridotite, allivalite, eucrite and gabbro which are both cryptically and rhythmically layered (Lobjoit, 1959). The rhythmic layering dips away from the convex margin of the body moderately to steeply (Skelhorn et al, 1969).

Plate 6.13 Irregular, anastomosing layers of clinopyroxene oikocrysts,
Beinn Buie gabbro, Mull.

Plate 6.14 Extremely regular layers of clinopyroxene oikocrysts, unit
9, Eastern Layered Series, Rum.



Three localities have been identified in the intrusion where layers considered are to postdate the rocks in which they are set.

i) Poikilitic layers.

At grid reference N592275 clinopyroxene oikocrysts become a prominent feature of the layered rocks. Stratigraphically upwards these pass into a zone in which the oikocrysts are formed into laminae, 0.5-2 cm thick (1-4 crystal diameters). The laminae are irregularly spaced and anastomosing (plate 6.13).

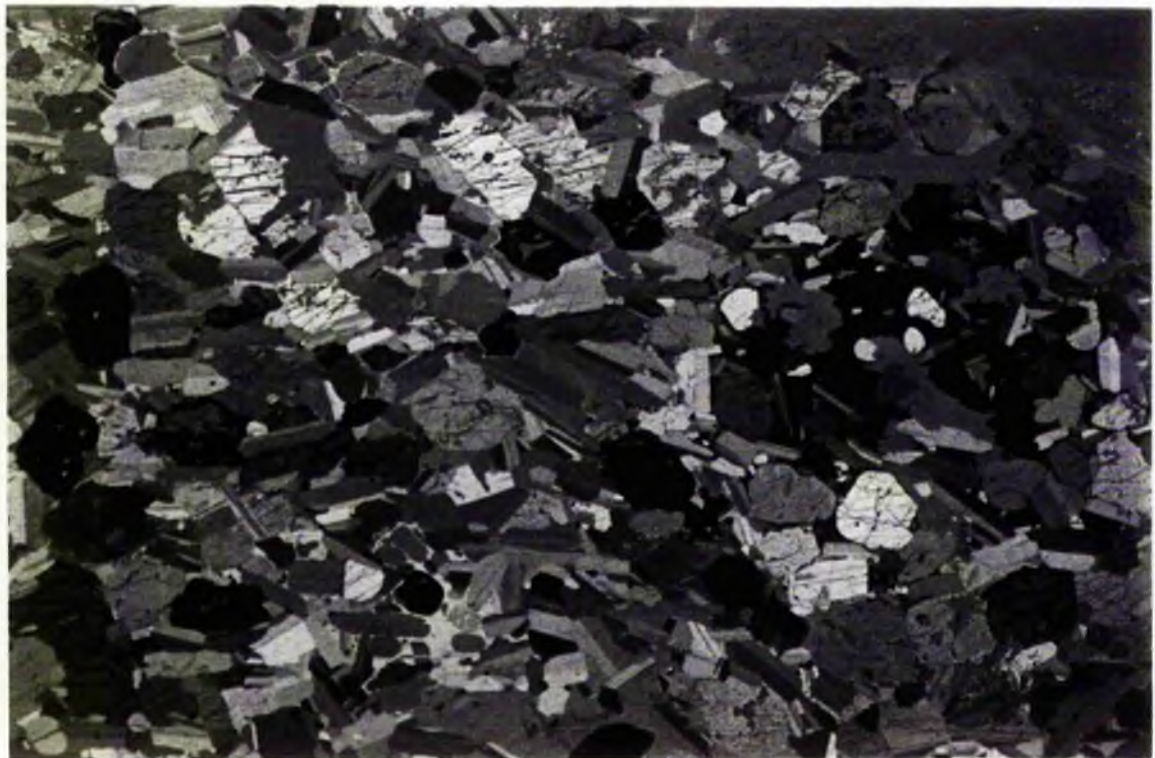
Laminae composed of poikilitic clinopyroxene have also been noted in the Rum intrusion. In Unit 9, several hundred metres south of the outcrops described earlier, there is an outcrop where spherical ophitic clinopyroxenes form extremely regular laminae 0.5-1 cm thick and up to 4cm apart (plate 6.14), separated by "normally"- textured allivalite, though it may contain sporadic clinopyroxene oikocrysts.

Notable textural features of these rocks, and others containing scattered oikocrysts, include:-

- a) Chadacryst centres are more widely separated than crystal centres in the surrounding rocks.
- b) Chadacrysts are typically smaller than crystals in the surrounding rocks.
- c) Chadacrysts are randomly orientated, or poorly laminated, while surrounding rocks are well laminated, that lamination generally

Plate 6.15 Clinopyroxene oikocrysts enclosing plagioclase and olivine, unit 9, Eastern Layered Series, Rum. Note difference in grain size and plagioclase orientation between the enclosed phases and those outside the oikocrysts. (x7, partially crossed polars)

Plate 6.16 Clinopyroxene oikocryst in gabbro, Belhelvie intrusion, Aberdeenshire, showing unlaminated and finer-grained plagioclase chadacrysts as compared with the coarser feldspar wrapped around the oikocryst. (x4.7, partially crossed polars)



being wrapped around the oikocryst (plates 6.15 & 6.16).

Oikocrysts are generally held to have crystallised within the crystal mush after or during the growth of the enclosed crystals (eg Jackson, 1961; McCallum et al, 1980;), though the possibility exists that they may grow at the mush/magma interface (Wager & Brown, 1968; Brooks & Nielsen, 1978). The occurrence of regular layering defined by concentrations of oikocrysts confirms that layer-forming mechanisms can operate within the crystal mush as suggested in chapter 4 and section 6.2.

ii) Isomodal leucogabbro layers.

At grid reference N584287 two isomodal, leucocratic gabbro layers are exposed. Both have sharply defined upper and lower contacts. The upper layer however, has two offshoots of similar leucogabbro (plate 6.17), and with the development of each offshoot the layer itself decreases in thickness by an amount similar to the thickness of that offshoot.

The offshoots from the main layer cannot have formed by any depositional mechanism and are interpreted as intrusive; therefore the most reasonable explanation of the main layer is that it too is intrusive.

iii) Cross-cutting poikilitic and granular sheets.

Plate 6.17 Two isomodal leucogabbro layers set in gabbro, Beinn Buie, Mull. The upper layer has two modally similar offshoots which penetrate into the surrounding gabbro, each of which diminishes the thickness of the layer.

Plate 6.18 Cross-cutting relationships of poikilitic and granular sheets, Beinn Buie, Mull. A diffuse banding, defined by the concentration of poikilitic clinopyroxene can be picked out running from top left to bottom right of the picture. These are cut by thinner sheets of poikilitic clinopyroxene, running bottom left to top right, which are cut by the anorthositic gabbro sheets in the centre.



The third locality shows the development of three sheet-like features, with cross-cutting relationships allowing their age relationships to be discerned. The oldest is a diffuse banding picked out by variations in the concentration of poikilitic pyroxene, this banding is cut by two sheets composed of pyroxene oikocrysts. These sheets are in turn cut by two anorthositic gabbro sheets (plate 6.18), about 10 cm thick, composed of randomly orientated plagioclase and poikilitic pyroxene. The anorthositic gabbro is uniformly medium-grained and poikilitic crystals at its margins with the enclosing rock include granular crystals from both.

The field relations indicate two generations of poikilitic textured sheet formation and the later formation of the anorthositic gabbro sheets which can only be interpreted as being post-cumulus by their cross-cutting relationships.

6.2.5 Hypersthene gabbro, Centre 2, Ardnamurchan.

This intrusion is the oldest of the ring-shaped intrusions of centre 2 (Gribble *et al.*, 1976) and is either a ring dyke (Richey & Thomas, 1930) or the remnants of a circular mass cut by later intrusions (Wells, 1954). It is layered in places, the layers consisting of variable proportions of olivine, augite, hypersthene, magnetite and plagioclase (Wells, 1954). Layering is particularly

Plate 6.19 Three coarse-grained protrusions of peridotite into gabbro
(Hypersthene gabbro, centre 2, Ardnamurchan).

Plate 6.20 Irregular, undulatory upper surface of peridotite layer
overlain by gabbro (Hypersthene gabbro, centre 2, Ardnamurchan).



well developed on the coast between Sanna Bay and Sanna Point at grid reference N441700 (Gribble et al, 1976) and some olivine-rich layers exhibit structural features, described below, which are more consistent with a postcumulus rather than a cumulus origin.

The layering dips at around 20° to the south. The most prominent layers are isomodal peridotite layers, 1-30 cm thick. Several have undulatory upper contacts, the undulations taking the form of 10-30 cm wavelength, low-amplitude, irregular, pointed or rounded waves (fig 6.3c; plate 6.20). These features have been noted previously by Skelhorn and Elwell (1971) and ascribed to loading, in spite of the density gradients being presently stable (dense peridotite underlying gabbro). One particularly thick layer has three finger-shaped, coarser grained, protuberances extending from its upper surface which cut through the lamination in the overlying rocks (fig 6.3d; plate 6.19). As this layer is traced eastward, along strike, it passes under a hornfelsed basic xenolith, where it encloses two thin enclaves of hypersthene gabbro (fig 6.3b), and then splits into several thinner layers which eventually thin out (fig 6.3a).

These relationships, while not inexplicable in terms of accumulation on the floor of the chamber, are more simply attributed to intrusion into a crystal mush of either peridotite magma, or magma from which olivine then crystallised.

6.2.6 Discussion.

The above observations demonstrate clearly that layers with textures identical to those in rocks interpreted as cumulates can form within crystal mushes, and that layers with ophitic textures are likely to have done so. The mode of formation of the layers in the Rum, Kiglapait, Beinn Buie and Ardnamurchan intrusions, which can be considered cumulates in the sense that they are unlikely to represent liquid compositions, is discussed in this section.

Nucleation and growth within the mush may lead to the development of the tangential relationship of plagioclase to granular olivine and ophitic pyroxene crystals by crystallisation in a mush with a high porosity, followed by compaction, in a manner similar to the formation of deformed laminae around concretions in clastic sediments (Raiswell, 1970; Potter *et al.*, 1980). Alternatively, forceful shouldering aside of feldspar grains by growing crystals may have taken place (cf the concept of "force of crystallisation", Becke, 1903). Though now generally rejected by metamorphic petrologists (Spry, 1969), shouldering aside has been shown to occur in experiments in aqueous systems in which growing copper sulphate crystals push aside sand laminae (Schuiling and Wensink, 1962). The observation that chadacrysts are often randomly orientated suggests that compaction about oikocrysts is likely to have occurred. Schuiling and Wensink suggested (1962) that the development of inclusion-rich and inclusion-free crystals was related to the rate of crystal growth and the same may be true in

Figure 6.3 Schematic sketches of field relations of isomodal peridotite layers, hypersthene gabbro, centre 2. Stippled ornament represents peridotite, dashed ornament represents gabbro which has a weakly-developed lamination and layering and the v ornament is a part of basalt xenolith. Diagram shows (a) bifurcation (b) enclaves of gabbro (c) uneven upper contact and (d) fingers of pegmatitic peridotite. Scale bars equivalent to 10cm.

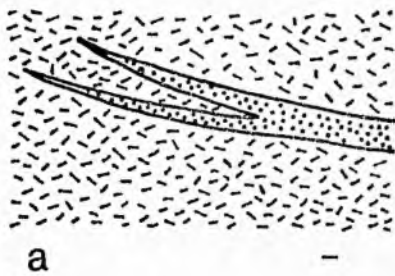
Figure 6.4 Suggested mechanism of cumulate-like layer formation by fractionation from transitory sills. Arrows marked L indicate direction of liquid movement and those marked W indicate direction of movement of the bounding surfaces.

(a) Injection of liquid into fracture from the surrounding crystal mush or laterally.

(b) Crystallisation of, for example, olivine.

(c) Removal of residual liquid from the "sill".

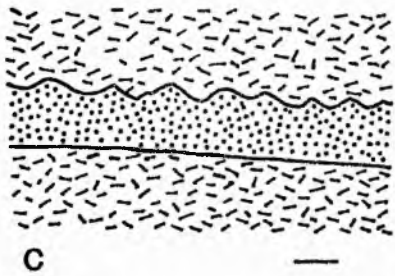
(d) New cumulate-like layer.



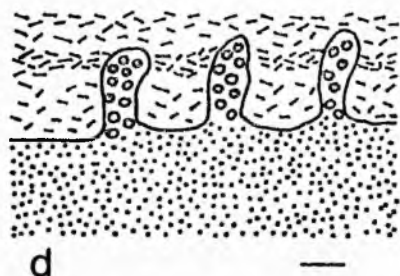
a



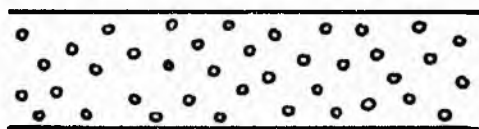
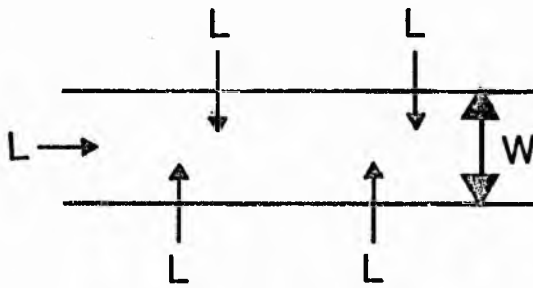
b



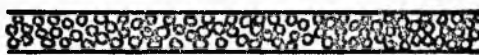
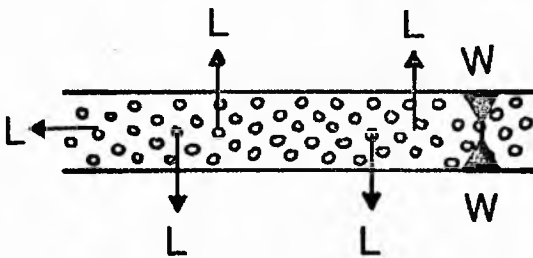
c



d



CRYSTALLISATION



NEW LAYER

plutonic rocks. Specific experiments to test these ideas, in both aqueous and silicate systems are needed.

Though the textural relations are understandable, the mechanism of formation of the Rum unit 9 olivine laminae and thicker layers elsewhere remains enigmatic. They cannot represent liquids injected into the crystal mush since the liquidus temperatures would be excessively high. However, precipitation of new minerals often occurs in thin stratiform sheets in clastic sediments undergoing compaction and diagenesis (eg Curtis et al, 1975). By analogy, the transport of components to growing crystals within cumulate mushes may occur by a combination of diffusion and advection (Berner, 1980). Possible advective flows include upward movement of interstitial fluid expelled by compaction (see section 6; chapter 7; Irvine, 1980b; Donaldson, 1982), convection wholly within the mush driven by either thermal or compositional gradients (Hess, 1972), double-diffusive convection within the mush (Irvine, 1980b; Donaldson, 1982) or convective flow occurring between the porous mush and the contemporary magma (Chapter 7; cf Lapwood, 1948).

Several of the observations suggest, however, that the layers are derived from intrusive bodies which form within the crystal mush, most notably the Beinn Buie and Ardnamurchan examples; the same is true of harrisite in the Rum intrusion, some of which apparently crystallised within the crystal mush (Donaldson, 1982). These rocks are unlikely to have been liquid compositions, they must be solute-enriched fractions (and in this sense are analogous to cumulates). Two alternative explanations may account for this.

Liquid may continually flow through the crystallisation zone providing a supply of fresh components and a sink for rejected components and the latent heat of crystallisation (Donaldson, 1982).

An alternative explanation is suggested by N.L. Bowen (1919) in a paper on banding in the Duluth gabbro; he proposes that warping of the partially crystalline mass and differences in the rigidity of this mass caused "compaction of crystals locally and the formation of lenticular pools of residual liquid". However, this mechanism must produce bands with the composition of the residual liquid, thus I suggest that the segregated liquid may partially crystallise, then the liquid residual from this crystallisation may be reabsorbed by the crystal mush (see figure 6.4). Such a mechanism may also produce veins which are residual fractions of the intruding liquid. Most intrusions, however, show no evidence of the folding necessary for Bowen's mechanism of interstitial liquid segregation. It has been demonstrated, however, that pressure pulses travelling through a fluid-filled medium can lead to transitory sill formation (Shaw, 1980).

6.3 Asymmetrical deformation structures.

6.3.1 Flame structures.

In clastic sediments pointed protrusions of mud, known as flame structures, often occur between bulbous sandstone load casts. Geometrically similar structures have been noted in cumulates. In the Rum intrusion they occur at junctions between feldspathic and mafic rhythmic layers and are particularly common at the bases of normally graded layers (plates 6.22 & 6.23). In cross-section they are pointed and overturned, often in the direction of dip. Where several such structures are present in one outcrop they are generally all overturned in the same direction (plates 6.21 - 6.23), though examples have been found where they face in opposite directions. In three dimensions they are crested rather than pointed, though the length of the structures along these crests is indeterminate. Internally, laminae tend to follow the outline of the structures (plate 6.22). With increasing distance into the underlying cumulates the folds in the deformed laminae flatten out. The structures do not 'penetrate' far into the overlying rock, however, in the sense that succeeding layer boundaries, or internal boundaries in the case of graded/paired layers, are often straight (see plate 6.21).

Plate 6.21 Flame structures penetrating the base of a paired layer containing an anorthosite block, Central Series, Rum.

Plate 6.22 Flame structures penetrating the base of a thick graded layer, Central Series, Rum. Note deformation in lamination underneath the structures.



6.3.2 Cumulate "dykes".

Larger scale flame and dyke-like protrusions of allivalite into peridotite have also been noted on Rum. Particularly spectacular examples occur at the base of the size-graded fragmental layer described in section 3.3.4. These structures take the form of sinuous, tapering protrusions of allivalite into peridotite. Occasionally these protrusions spread laterally at some height (plate 6.24). Lamination in the allivalite is drawn upwards into the structures. Between them layers in the allivalite are attenuated by bulbous masses of peridotite (plate 6.24).

6.3.3 Folded layers.

Folds are perhaps the most common kind of deformation structure in layered igneous rocks. Most previous workers have stressed the role of down-slope slumping in discussing the origin of folded structures (eg Brown, 1956; Hess, 1960; Wager and Brown, 1968; Wadsworth, 1973; Parsons and Butterfield, 1981), though the association of folding with fragments impacting on the top of the crystal mush has been recognised by Thompson and Patrick (1968) and Irvine 1974; 1980c).

Plate 6.23 Flame structures penetrating the base of a graded layer,
Central Series, Rum.

Plate 6.24 Cumulate "dyke" in fragmental peridotite, Central Series,
Rum. Note deformed feldspathic layers adjacent to the structure.



In the course of this study folded layers have been noted in the Kiglapait intrusion (though they are extremely rare), the Kolotulik troctolite in the Tigalak intrusion, the gabbro of the Beinn Buie intrusion and the Rum intrusion. Particularly well-exposed examples of folded cumulates occur in the leucocratic portion of unit 14 in the Eastern Layered Series of the Rum intrusion, on the south-east ridge of Askival at grid reference N13927952.

The structures occur wholly within the leucocratic portion of unit 14 and are bounded above and below by undeformed allivalite. The folds consist of large-scale, sharp-crested anticlines of allivalite and broad synclines, the cores of which are composed of peridotite. The hinges of the anticlines are overturned down dip. Superimposed on the large structures are many smaller amplitude folds which are either regular and sinusoidal in form, or are geometrically similar to the large-scale folds, with sharp-crested anticlines overturned down dip. The base and top of the folded region are gradational into the undeformed layers; there is no evidence for the existence of any zone, or plane, of dislocation.

Plate 6.25 Folded layers, unit 14, Eastern Layered Series, Rum. The anticlines are predominantly allivalite whereas the cores of the synclines are filled with peridotite. The hinges of the folds are overturned down dip. Small parasitic folds are developed on the large-scale folds.



6.3.4 Discussion.

The flame structures are similar to the structures found in sediments (eg Lowe, 1975; Collinson and Thompson, 1982) and in experiments designed to reproduce the sedimentary structures (eg Anketell et al, 1970) by loading of a denser fluid into a lighter one, with the addition of a lateral shear, and are thus given a similar interpretation.

The dyke-like structures have evidently formed by injection of allivalite into peridotite and thus imply that liquefaction or fluidisation of allivalite mush took place (cf Lowe, 1975).

Further evidence for liquefaction of crystal mushes comes from the folded layers in unit 14, Rum. The lack of down-dip thickening of the folded unit, together with the absence of a basal or an upper dislocation plane, indicates that significant downslope movement did not take place (see Dzulynski & Walton, 1965). The form of the folds is reminiscent of convolute lamination, especially common in muddy, fine-grained sands and silts (Leeder, 1982) and which form when sediment is either deposited in a "quick" condition or is partially or wholly liquefied some time after deposition (Kuenen, 1953; Lowe, 1975; Allen, 1977). A similar interpretation is inferred for the unit 14 structures from their morphology and from the relative densities of the lithologies forming the cores of the synclines and anticlines. Thus, these structures are held to record liquefaction of the magmatic sediment. Liquefaction occurs when a

grain-supported sediment is transformed into a temporarily fluid-supported one (Terzaghi, 1947; Lowe, 1975). Pre-conditions for liquefaction are more likely to exist in cumulate mushes than clastic sediments since the density difference between grains and fluid is smaller than in water-lain sediments and since sub-volcanic magma chambers are probably seismically active. Liquefaction in sediments is often associated with consolidation and fluid-escape (Lowe, 1975) though there is no direct evidence for this in the Rum structures. The possibility ought not to be discounted, however, and further evidence for migrating interstitial liquid is described below and in chapter 7.

6.4 Finger structures in the Rum intrusion - evidence for plagioclase resorption by migrating interstitial liquid.

6.4.1 Description.

The intra-unit (allivalite overlying peridotite) junctions within cyclic units in the Central and Eastern Layered Series' and above minor peridotites within the feldspathic portions of cyclic units on Rum are characterised by protrusions of peridotite into allivalite. These structures were first described by Brown (1956) who compared them to the "fingers of an outstretched hand" and christened them "upward-growing pyroxene structures". Since they do not necessarily contain pyroxene, and have not formed by pyroxene

Plate 6.26 Vertically aligned finger structures cutting dipping layered and laminated allivalite, Central Series, Rum. On the right of the photograph fingers coalesce and the allivalite is embayed by massive peridotite.

Plate 6.27 Oblique section through finger structures showing their circular cross-section, Central Series, Rum.



growing upwards (see below) it has been proposed that they be called "finger structures" on account of their geometry (see Robins, 1982; Young, 1983).

The structures generally take the form of parallel-sided or tapering protrusions of peridotite into allivalite (plates 6.26 - 6.31). The tops of fingers are conical or hemispherical in shape. They are generally straight, though rare branching forms occur, or one thick finger may be topped with several smaller fingers. They are circular in cross-section (plate 6.27) and range from about 2 cm in diameter and height to 20 cm diameter and 1 m in height. Contacts with the allivalite are invariably sharp.

Fingers are generally oriented orthogonally to the general orientation of the peridotite/allivalite contact and/or to the planar structures in the allivalite. In some dipping exposures however, they are sub-vertical. In the field they appear to cut through layering, laminae and lamination without any associated deflection of the planar structures. Fingers cut through folded layers in allivalite. On encountering more mafic layers in the allivalite fingers sometimes widen, but have never been noted to narrow. Fingers may coalesce and allivalite is then embayed by massive peridotite. Thin (1m) allivalites are sometimes totally breached by peridotite embayments (plate 6.32). In other outcrops the fingered base of allivalite cuts out the whole of the feldspathic portion of the unit; in one example (East face of Minishal, grid reference N13528002) two isolated enclaves of allivalite sit in massive peridotite several metres along strike

Plate 6.28 Irregular fingers and embayments cutting layered and laminated allivalite, Eastern Layered Series, Rum.

Plate 6.29 Extremely regular fingers at the base of a folded allivalite, Unit 14, Eastern Layered Series, Rum. The resistant band immediately below the fingered contact is a late-stage vein.



Plate 6.30 Large finger structures cutting layered and laminated allivalite, Eastern Layered Series, Rum.

Plate 6.31 Finger structure which increases its horizontal dimensions when it encounters a relatively mafic layer, Central Series, Rum.



from the allivalite layer with fingers at their bases. In other localities (back wall of Coire Dubh, grid reference N13857976) enclaves of layered allivalite sit in massive peridotite. The dip and strike of the layering in these enclaves is conformable with the regional dip and strike. Their tops are planar and conformable with the layering. Chrome-spinel layers are present on the tops of these enclaves which continue into the peridotite on either side. Their bases are fingered by peridotite.

The rock filling most fingers has textures typical of "normal" peridotite. Olivine is euhedral to subhedral and equant to elongate. Elongate olivines tend to be aligned parallel to the margins of the structure (plate 6.34, Brown, 1956; A. Butcher pers. comm.). Clinopyroxene, plagioclase and occasionally amphibole and rarely biotite are present as poikilitic or interstitial phases. The largest fingers examined, from exposures on the east face of Minishal, are particularly rich in amphibole. Spinel occurs as inclusions in olivine or interstitially between olivine crystals. Opaques and chlorite are present as alteration products of amphibole.

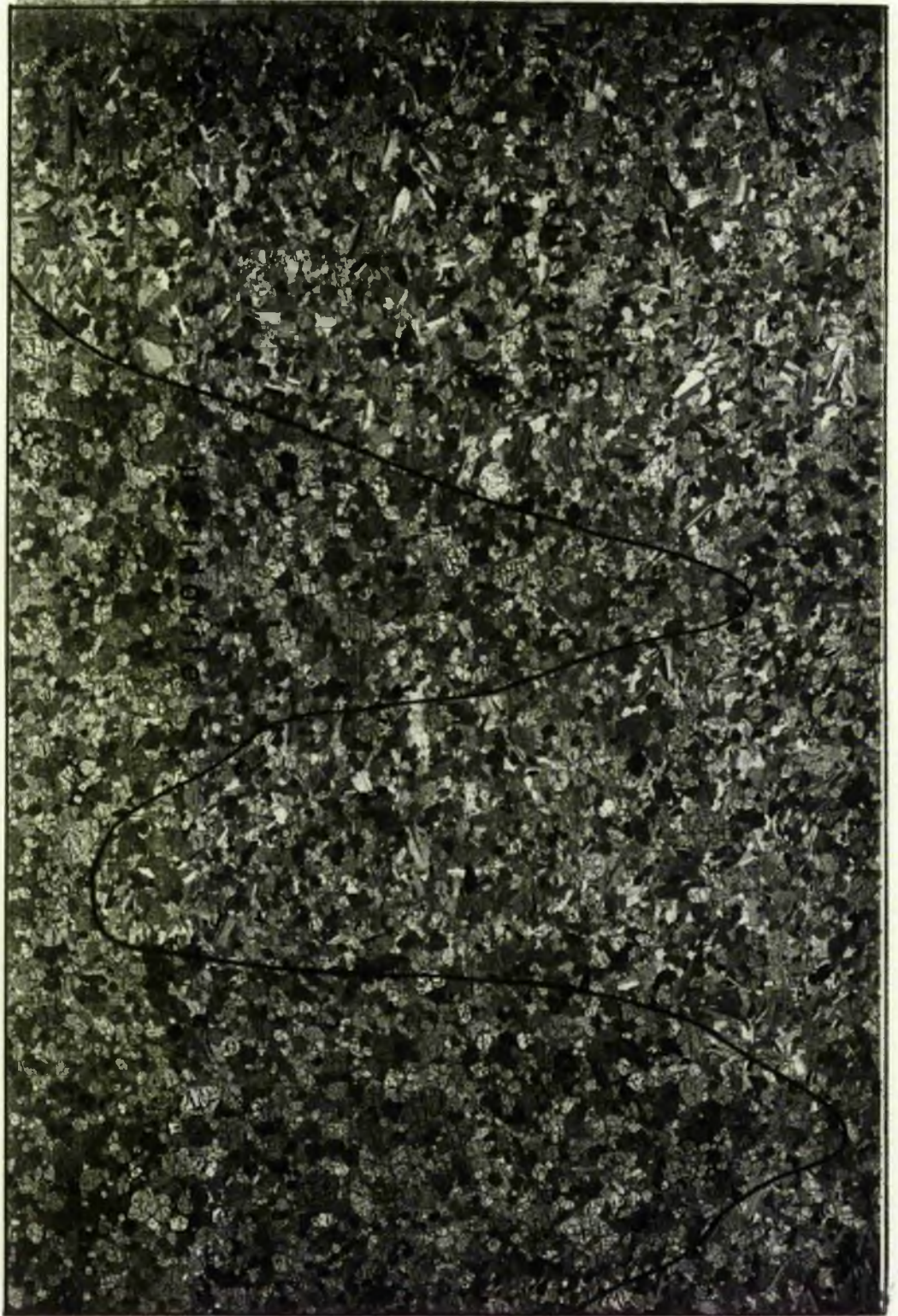
Textures in allivalites adjacent to finger structures are likewise typical of allivalites as a whole. However, upward deflections of the feldspar lamination at the margins of finger structures have been noted in examples from the Eastern Layered Series (Brown, 1956; A. Butcher pers. comm.).

Plate 6.32 Allivalite layer breached by peridotite, Central Series, Rum. One relatively narrow finger extends right through the allivalite in addition to the large breach in the centre-right of the photograph.

Plate 6.33 Large amphibole-rich fingers on the East face of Minishal Central Series, Rum. As this outcrop is traced to the right (North), the allivalite thins and is cut out by peridotite.



Plate 6.34 Photomicrograph of a section through a finger structure from the Central Series, Rum. A very weakly-developed preferred orientation of the olivine crystals can be discerned at the margins of the structure.. (x3, partially crossed polars)



6.4.2 Origin of the finger structures.

The possibility that the finger structures were formed by simple loading between two crystal mushes (see Wager & Brown, 1968, fig 153, p 270), whose relative densities were modified by the presence of differing proportions of interstitial liquid (cf Lee, 1981) is discounted by a) the lack of deformation of layering structures in allivalites on a scale necessary to allow the injection of peridotite and b) the prohibitively high proportion of liquid needed to be added to an olivine mush such that its density becomes less than that of one containing a high proportion of feldspar (fig 6.6). The spatial relationships and the observation that finger structures cut folded allivalite dictates that the finger structures formed within the crystal pile by replacement of allivalite by peridotite on a volume-for-volume basis. The rare deflection of feldspar lamination at the margins of some structures suggests that this replacement process was, at least in part, mechanical and took place while significant amounts of interstitial silicate liquid were present (perhaps more than 40%). The enrichment of some fingers in poikilitic phases does not necessarily represent enrichment of the local liquid in, for example, clinopyroxene components, but may be a reflection of differences in the porosities of different environments during the finger-forming process. Thus the fingers are held to record the replacement of plagioclase by olivine, an interpretation supported by the widening of some fingers when a less feldspathic lithology is encountered. Replacement is not, however, confined to the fingers; several

Figure 6.5 Schematic summary of field relations of finger structures in the Rum pluton. Stippled ornament represents peridotite, dashed ornament represents allivalite and the spacing and orientation of the dashes represents lamination and layering in allivalite. The diagram shows

- (a) Fingers cutting lamination and layering in allivalite.
- (b) Coalescing of fingers and embaying of allivalite by peridotite.
- (c) Fingers cutting folded allivalite.
- (d) Allivalite layers breached by peridotite.
- (e) Cutting out of allivalite by peridotite and residual enclaves of allivalite in peridotite.
- (f) Enclaves of allivalite with fingered bases and topped by chrome-spinel layers sitting in peridotite. Note that the chrome-spinel layers extend into the peridotite on either side of the allivalite.

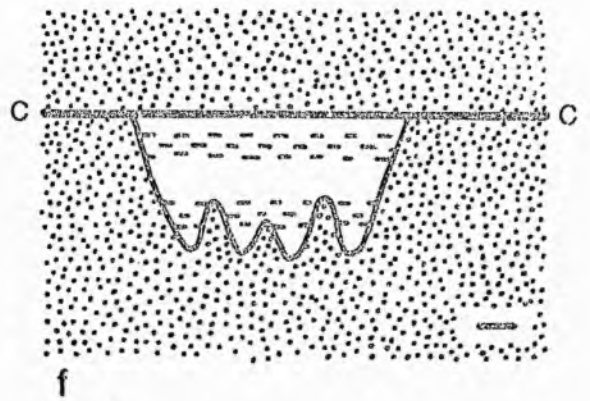
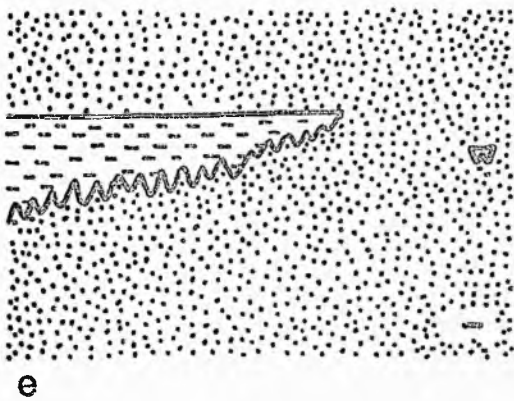
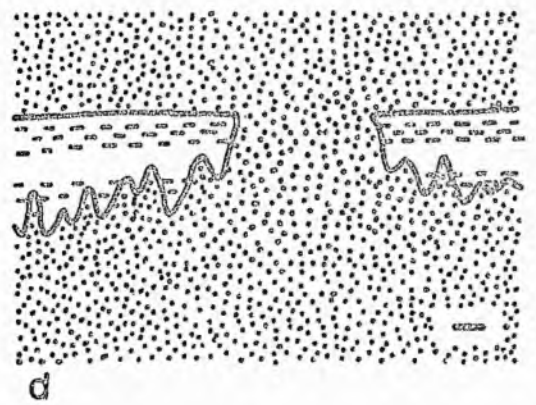
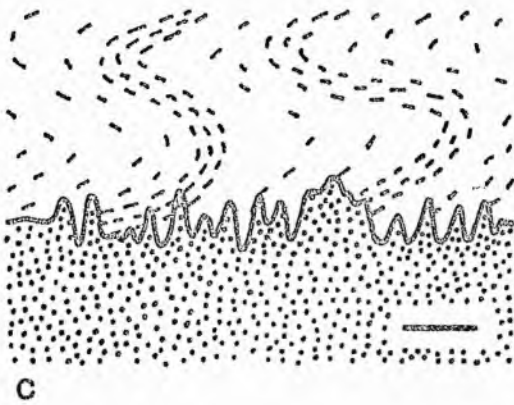
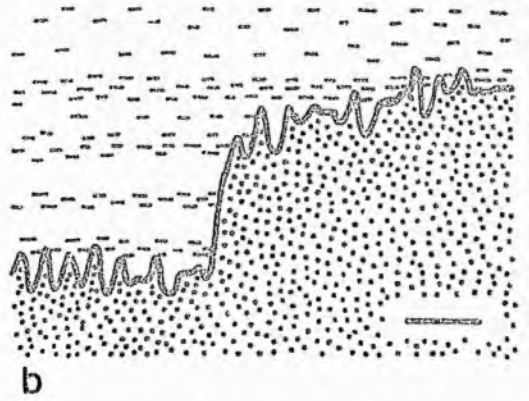
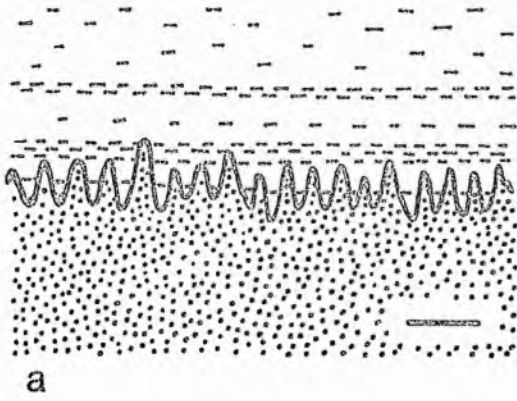
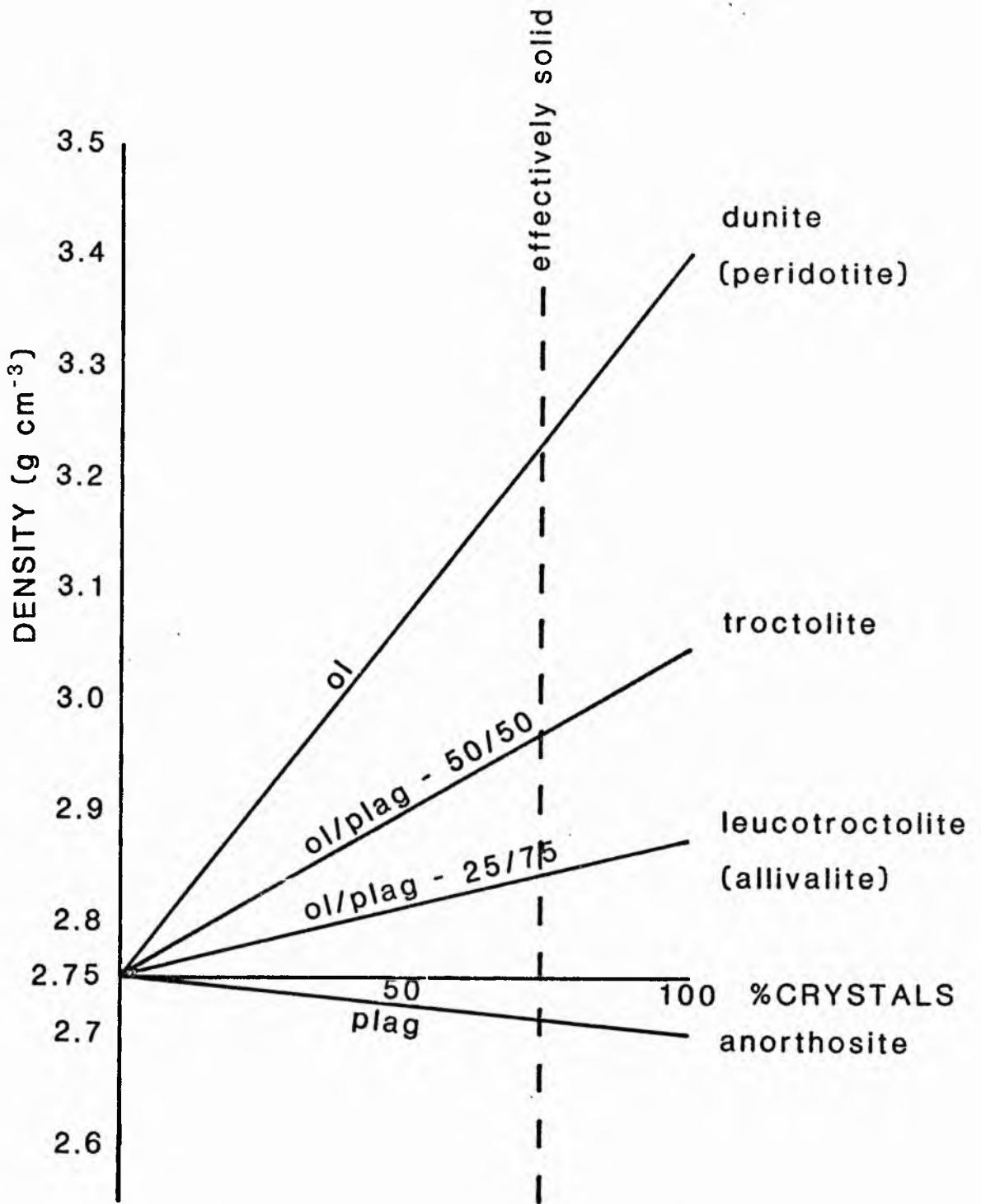


Figure 6.6 Relationship of bulk density to crystal content for Rum crystal mushes. Calculated on the basis of a liquid density of 2.75 g cm^{-3} , olivine density of 3.4 g cm^{-3} and plagioclase density of 2.7 g cm^{-3} . The dashed line shows the concentration of crystals at which the porous medium effectively becomes solid (see Chps 3 & 5 and Marsh, 1981). The diagram illustrates the very wide differences in crystal content necessary for a peridotite mush (olivine + liquid) to be less dense than an allivalite one (olivine + plagioclase + liquid). Even larger differences are necessary to invoke C.A. Lee's mechanism for the formation of undulatory upper contacts of chromitite layers in the Bushveld intrusion (Lee, 1981).



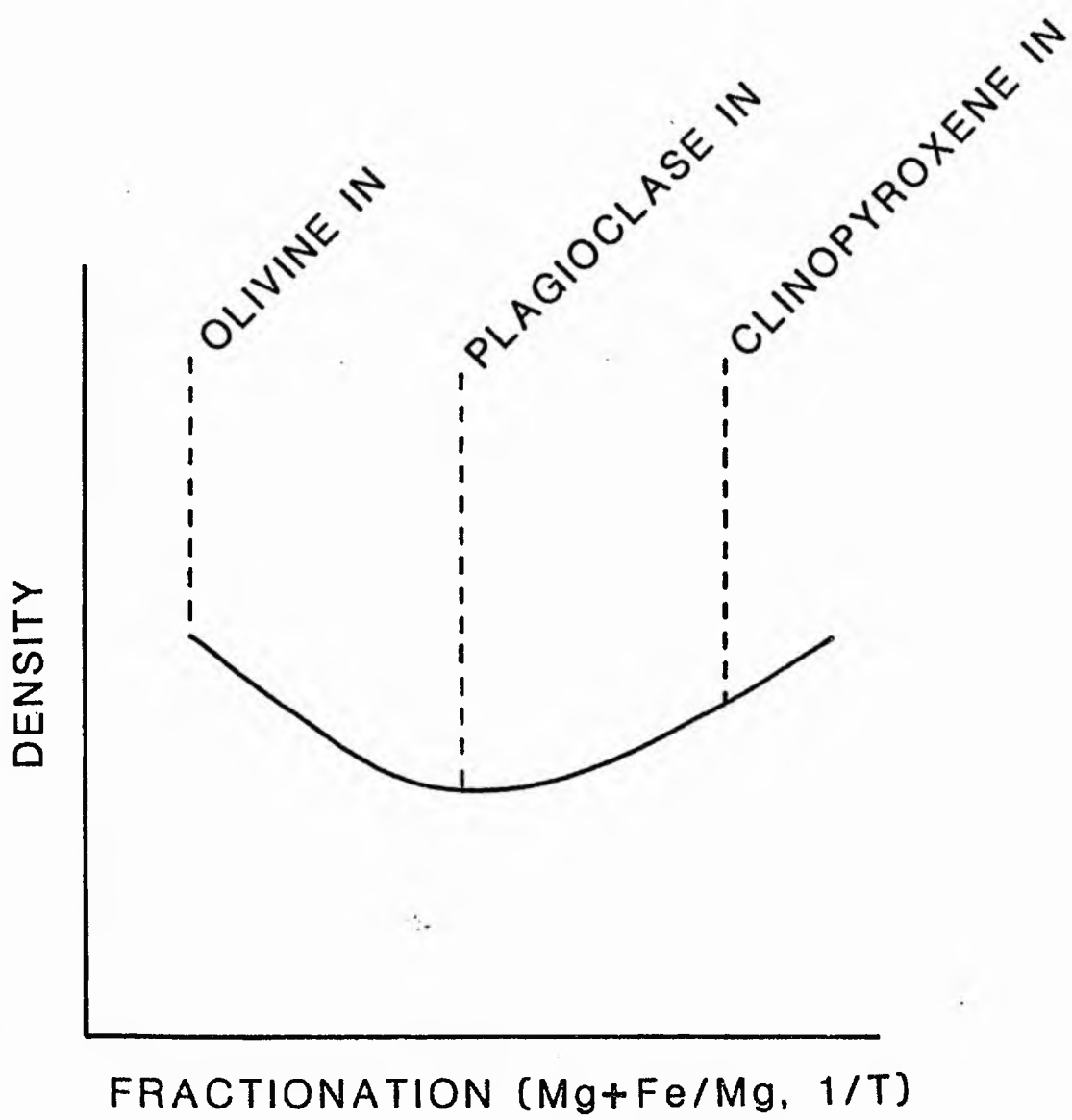
features of the outcrops indicate that replacement operated on a large scale in the Rum pluton. The coalescing of fingers into embayments, breaching and cutting out of allivalite layers by peridotite fingers and the enclaves of allivalite in the Coire Dubh exposures topped by chromite layers suggest that replacement has operated on a massive scale, and the possibility exists that large portions of Rum stratigraphy have been obliterated in this fashion.

6.4.3 A possible cause of finger formation.

It is proposed that the finger structures formed by infiltration into the permeable allivalite mush of a liquid which resorbed feldspar, or possibly feldspar and olivine and crystallised olivine in their place.

The vertical orientation of fingers in some dipping sequences is consistent with a density control on finger formation. A possible mechanism is suggested by the recognition of a density minimum in the MORB liquid line of descent (Stolper & Walker, 1980; Sparks et al., 1980). Liquids parental to the peridotites are now considered to have been picritic and those parental to the allivalites to have been basaltic (Huppert & Sparks, 1980). Liquid trapped within olivine cumulates must initially have become less dense on fractionation of olivine and that trapped in allivalites must initially become more dense on fractionation (see fig 6.7). Thus it is possible that liquid present in the olivine cumulates was

Figure 6.7 Form of density versus fractionation curve for MORB-like liquids. Liquids parental to olivine cumulates become less dense on fractionation, whereas those parental to troctolitic and gabbroic cumulates become more dense on fractionation. Thus it is possible for liquids saturated only in olivine to be less dense than those on the olivine - plagioclase or olivine - plagioclase - clinopyroxene cotectics.



initially, or became, less dense than that in the feldspar-rich cumulates. Gravitational instability would then drive relatively hot liquid upwards into mush with which it would not be in equilibrium. Assuming strictly isothermal conditions this would result in resorption of both feldspar and olivine until all the feldspar was consumed, or, if cooling of the relatively hot liquid occurred, feldspar alone would be resorbed and would be accompanied by crystallisation of olivine (see Bowen, 1928; McBirney, 1979). In either case resorption of feldspar would be accompanied by, or succeeded by, crystallisation of olivine.

Viscous drag at the margins of the structures can account for the rare deflection of feldspar lamination. The olivine alignment may be a product of physical 'plastering' to the sides of the growing finger, or crystallisation in the physico-chemical gradients which must have existed there (cf discussion on the development of igneous lamination in McBirney & Noyes, 1979). The margins of the structures can then be viewed as either former plagioclase saturation surfaces or the margins of regions where plagioclase was wholly resorbed (since plagioclase must ultimately appear on the cotectic it would then have either extended the remains of partially resorbed crystals or formed poikilitic crystals).

There is some supporting evidence from other sources for this interpretation of fingers as instabilities between two liquids in a porous medium. Situations where a relatively dense magmatic liquid must have overlain a less dense liquid have been recorded previously by Walker and Skelhorn (1966) and Weibe (1974). In both cases pipe,

or finger-like, protrusions of the light fluid penetrated the denser one. In addition, Saffman and Taylor (1958) have shown experimentally that when a liquid is accelerated into a more viscous liquid in a porous medium fingers of the less viscous liquid form in the more viscous liquid. This is precisely the situation envisaged in the formation of the Rum structures.

This hypothesis necessarily dictates that interstitial liquid fractionates less quickly than the contemporary magma, or that interstitial liquids of different compositions can be incorporated into cumulate piles at essentially the same time. This latter possibility is preferred and it is suggested in chapter 8 that peridotite and allivalite may have been the lateral equivalents of one another during the crystallisation of individual cyclic units. There is also some semi-empirical evidence for the contemporaneity of intercumulus liquids of different compositions from a study by Hermes and Cornell (1981) on glasses in cumulate nodules erupted from Vesuvius.

6.4.4 Replacement structures in other intrusions.

Similar finger-like embayments of allivalite by underlying peridotite have been noted by this author in the Beinn Buie intrusion and Robins has described (1982) similar features in the Lille Kufjord intrusion, northern Norway. Replacement bodies have been noted in the Skaegaard and Duke Island intrusions by Irvine

(1980b) and in the Bushveld intrusion by Cameron and Desborough (1964). These bodies have all been recognised by their extreme discordance to the layered rocks. The possibility that regular up- (or down-) stratigraphy replacement or reaction has occurred in other intrusions or other parts of, for example, the Rum intrusion, where evidence in the form fingering may be on a different scale (either very much smaller or with a smaller amplitude to wavelength ratio), or even absent (planar contacts), ought to be considered. Replacement processes may be especially important in replenished plutons.

6.5 Implications of dynamic interstitial liquids.

The recognition that layers and replacement bodies with textures identical to those of "normal" cumulates can form within the crystal pile on the floors of layered intrusions has important implications for the interpretation of the stratigraphy of layered intrusions. Crystals cannot be interpreted as having cumulus (in the sense of Wager et al., 1960) status on the basis of texture alone, or even on the combined bases of texture and layering. Many apparent variations in cryptic layering may only represent post-cumulus crystallisation of granular-textured bodies. Identification of cumulus minerals is probably best done on the basis of texture, phase relations and the presence of the mineral in layers considered to have formed at the mush/magma interface (eg normally graded layers). Attention should be concentrated on

analyses of crystals from such layers when attempting to trace the evolution of magma compositions through cryptic layering rather than on analyses from unlayered rock (cf Morse, 1979a).

The recognition that migrating interstitial liquid has played a large part in the formation of many of these structures has further implications. Recent interpretations of trace-element and isotope profiles through layered intrusions (eg Grant & Molling, 1981; Gray & Goode, 1982; Palacz, 1984) rely for the most part on whole-rock and mineral-separate analyses. These methods cannot distinguish between the cumulus and post-cumulus contributions to any particular mineral and often interpret conditions in the contemporary magma from variations in compositions of post-cumulus phases (eg strontium isotope variations in olivine cumulates must be almost entirely due to variations in the compositions of the poikilitic and interstitial phases, plagioclase and clinopyroxene).

The mechanism of finger formation outlined above is essentially one of compositional convection. Compositional convection may also occur in crystal mushes where the course of fractionation leads to progressively lighter residual liquid composition (Hess, 1972). Thermal effects will be stabilising if heat is removed through the base of the crystal pile, but the combination of thermal and compositional diffusive fluxes, or more than one diffusing component, may lead to double-diffusive convection in the porous medium (see Nield, 1968). Even in situations which are apparently stably-stratifying during slow crystallisation, metastable crystallisation of one or more phases due to suppression of

nucleation of new phases (for which there is ample evidence in many cumulates in the form of widely spaced oikocrysts or poikilitic crystals with metastable growth forms eg Donaldson et al., 1973) may lead to unstable density gradients. The possibility that migrating interstitial liquid is able to interact with, and be replaced by contemporary magma is discussed in the next chapter.

6.6 Conclusions.

- 1) Cumulates undergo spontaneous deformation of varying degrees of complexity.
- 2) Rocks with adcumulate textures are found in such deformation structures and therefore cannot have completed their solidification at the mush/magma interface as proposed by some petrologists (eg Wager et al., 1960; Jackson, 1961; Wager, 1963).
- 3) Crystals with granular textures can form within the mush on their own, in laminae, layers and replacement bodies.
- 4) The stratigraphies of some layered intrusions have been partially erased by postcumulus processes. Taking points 3 and 4 together it is clear that more care must be taken in interpreting magma evolution from "cumulus" mineral compositions.
- 5) Fluid flow occurs within crystal mushes and thus contributes to the overall differentiation of the pluton.

7 MUSH/MAGMA INTERACTION - EVIDENCE FROM THE RUM PLUTON.

7.1 Introduction.

Up till now the cumulus and postcumulus stages of the formation of cumulate rocks have been treated essentially separately, that is with no interaction between crystal mush and contemporary magma. This chapter describes structures defined by and associated with chrome-spinel layers in the Eastern Layered Series of the Rum intrusion which indicate that interaction between the two environments did take place. The nature of the interaction and its chemical consequences are examined in detail.

7.2 Chromite layers - previous hypotheses.

Chromite often occurs concentrated in layers of great areal extent in ultrabasic/gabbroic plutons, (Irvine, 1975). Interpretations placed on the origin of these layers range from local physical sorting of crystals to abrupt changes in some intensive parameter during an intrusion's cooling history. Several recent interpretations hinge on Irvine's proposition (1975,1977) that mixing of two liquids fractionating along the olivine-chromite cotectic in the system Forsterite - Diopside - Anorthite - Quartz - Picrochromite will push the resultant liquid composition into the

chromite primary phase field. The more- and less-fractionated liquids have been ascribed to mixing of magma in the chamber with acid liquid derived by melting of roof rock, (Irvine, 1975), mixing of parental and evolved magmas during chamber replenishment (Murck & Campbell, 1982), and double-diffusive mixing in a stratified magma chamber (Irvine, 1981).

7.3 Chromite in the Rum intrusion.

7.3.1 Stratigraphic setting and previous research.

The ultrabasic portions of the Rum intrusion consist of structurally complex, cyclic peridotite-allivalite or peridotite layered units with associated breccia zones. The major cycles have been interpreted as cumulates formed in a replenished magma chamber, (Brown, 1956; Wadsworth, 1961; Dunham and Wadsworth, 1978). In the Eastern Layered Series these replenishments are reflected in abrupt transitions from allivalite (plagioclase - olivine - clinopyroxene - chrome-spinel cumulates) to peridotite (olivine - chrome-spinel cumulates).

The presence of chrome-spinel layers was noted by Harker (1908). Subsequently Brown (1956) highlighted their occurrence at the contacts of allivalite with overlying peridotite and Wadsworth (1961) noted their presence within and between peridotitic and harrisitic cumulates. Both Brown and Wadsworth ascribed the layers to preferential settling of chromite grains.

The first detailed work on the chemistry of Rum chrome-spinels was carried out by Henderson and Suddaby (1971) who proposed that chrome-spinel layers at the bases of cyclic units were a consequence of the position of chromite on the liquidus of the Rum parent magma, early-formed chromite being concentrated by settling into layers. They also recognised that post-cumulus reaction of chromite with olivine, plagioclase and intercumulus liquid had taken place to give a more aluminous, and larger volume of, chrome spinel. This work was extended by Henderson (1975) and Henderson and Wood (1981) who recognised two post-cumulus reaction trends, an Fe-enrichment trend and an Al-enrichment trend, the position of any particular spinel on either trend being determined by the modal composition of the enclosing cumulates and the amount of trapped intercumulus liquid. Henderson and Wood sampled chrome-spinel layers from within the unit 7 peridotite.

As an alternative origin for chrome-spinel layers at the base of cyclic units, Huppert and Sparks (1980) proposed that picritic liquid newly emplaced in the magma chamber, hybridised with a little evolved liquid already present in the chamber, was able to melt the

allivalite floor with chrome-spinel formed as a product of the reaction of floor melt and hybrid liquid.

7.3.2 Structures associated with, or defined by chrome spinel concentrations.

Structural complexities associated with chrome-spinel layers in the Eastern Layered Series are well-exposed at the contacts of units 11 and 12, the "type" example of Brown (1956), on the northern and eastern flanks of Hallival, and units 7 and 8 on the true right flank of Coire Dubh. Sketches of structural features are presented in figure 7.1 and features considered pertinent to the genesis of chrome-spinel layers described below.

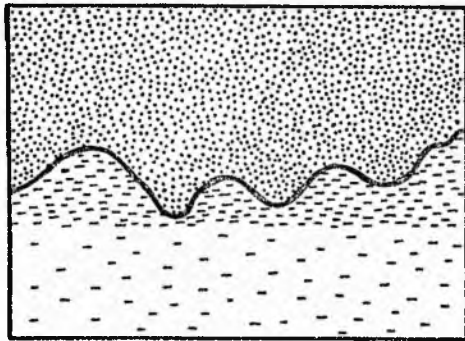
1). Peridotite may cut across the layering and feldspar lamination in allivalite, without associated deformation of either. This occurs on all scales from thin section to outcrop. The form of these transgressions ranges from regular undulations (fig 7.1a, plate 7.1), through larger irregular embayment structures (fig 7.1b) to horizontally extensive embayments, up to 1m deep and several metres across, which may be analogous to the pothole structures of the Bushveld complex (fig 7.1c, plate 7.2). These embayments often increase in their horizontal dimension where different textural or modal varieties of allivalite are encountered (fig 7.1b,c). Where an olivine lamination is developed at an undulatory contact it is invariably oriented parallel to that contact (plate 7.3).

Figure 7.1 Schematic diagrams of small-scale structures associated with chrome-spinel layers at unit junctions. Peridotite indicated by stippled ornament and chrome-spinel layers by heavy black line and shading (fig 7.1d). The dashed ornament indicates the orientation of the feldspar lamination and its density is proportional to the modal proportion of feldspar. Vertical and horizontal scales are equal.

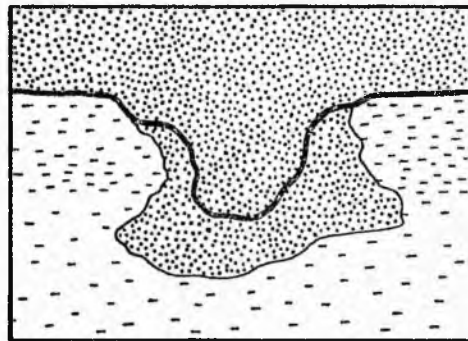
(a) Undulatory contact between peridotite and allivalite with intervening chrome-spinel layer. In three dimensions these structures take the form of circular depressions in the allivalite. The lamination in the allivalite is cut by the undulatory contact. Note also that the lower ratio contact of the top allivalite layer is unaffected by the irregularities at its upper contact. Horizontal dimension 30cm.

(b) Embayment structure with transgressive chrome-spinel layer. These structures are roughly equidimensional in plan. The structure illustrated increases in its horizontal dimension where a less feldspathic variety of allivalite is encountered by peridotite. Horizontal dimension 30cm.

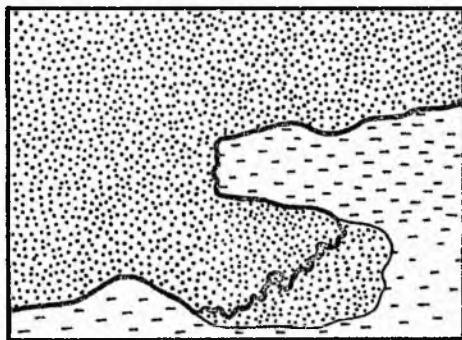
(c) Margin of horizontally extensive embayment structure illustrating the development of a chrome-spinel layer on the underside of a protrusion of allivalite into peridotite and the transgressive nature of some chrome-spinel layers. Only the two-dimensional form of these structures can be seen. Horizontal dimension 50cm.



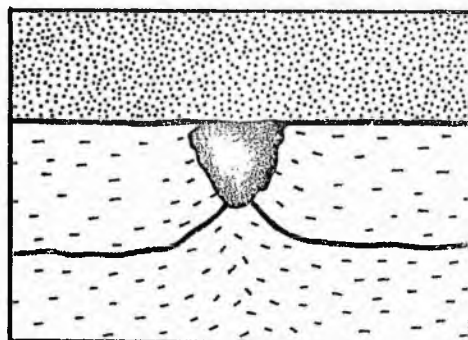
a



b



c

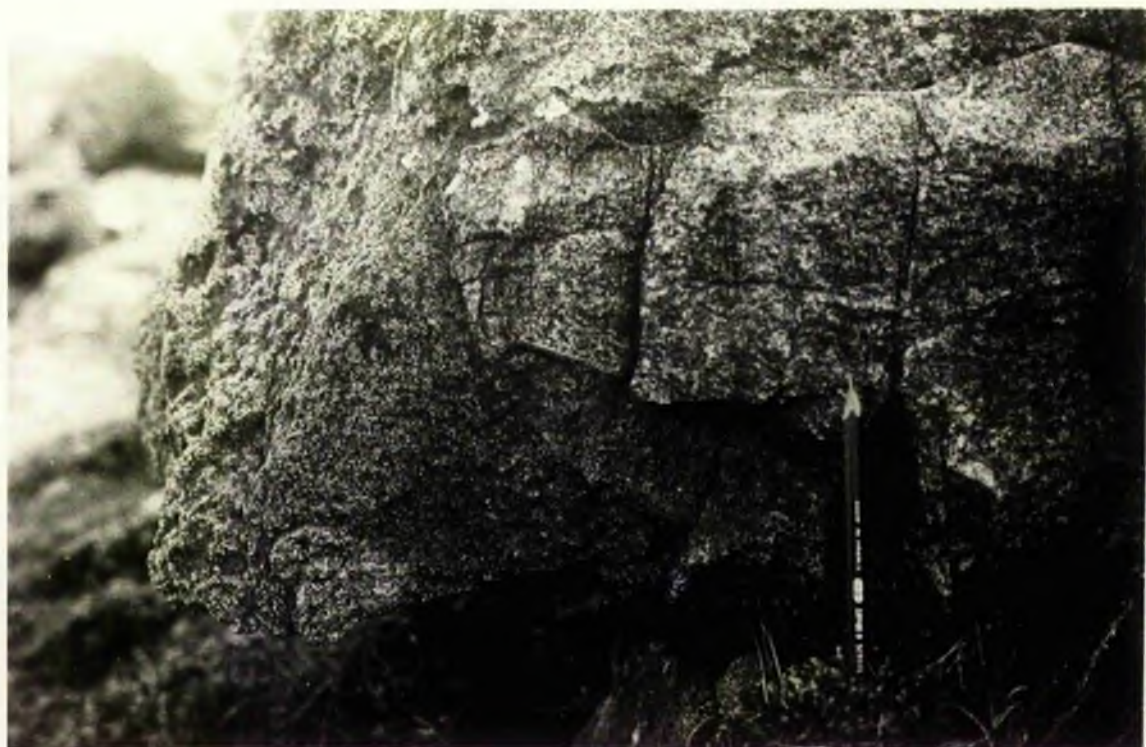


d

(d) Cone structure in unit 7 allivalite. Three chrome-spinel layers are developed at this locality, though only two are illustrated, one within each silicate lithology and one at their junction. That at the junction forms a number of cone structures, and in at least one case the underlying chrome-spinel layer is deflected upwards with the feldspar lamination into the cone. Horizontal dimension 8cm.

Plate 7.1 Undulatory transgression of peridotite across allivalite, their contact is marked by a chrome-spinel layer. Junction of units 11 and 12, Hallival, Eastern Layered Series, Rum.

Plate 7.2 Margin of horizontally extensive embayment structure at the contact between units 11 and 12, Hallival, Eastern Layered Series, Rum.



2). Chrome-spinel layers may line the margins of these embayments in allivalite (plate 7.3), or may locally transgress into peridotite (fig 7.1b,c). They have not been noted transgressing into allivalite.

3). Within embayment structures chrome-spinel layers may be developed on the underside of allivalite "overhangs" (fig 7.1c, plate 7.2). Where this is observed the layer is often thicker on the top surface of the allivalite protrusion.

4). Extreme concentrations of chrome-spinel are developed in small (1-3cm. in diameter and depth), irregularly shaped, downward-pointing cone structures which may have peridotite cores. Sections cut perpendicular to the plane of the layering indicate that these cones are developed at culminations in the lamination in the underlying allivalite (fig 7.1d, plate 7.4). Below these cone structures the feldspar is generally randomly or vertically oriented.

7.3.3 Petrography.

Chrome-spinel occurs in a variety of textural and silicate environments. Within layers at unit junctions spinels are small (average 0.2mm in diameter) and range from euhedral through sub-spherical to complex amoeboid shapes. On the scale of a thin section individual layers show large variations in thickness and may even be locally absent. Chain texture is poorly developed.

Plate 7.3 Photomicrograph of a section through the chrome-spinel-lined margin of an embayment structure showing truncation of the feldspar lamination in the allivalite by laminated peridotite. (x7, partially crossed polars)



Plate 7.4 Photomicrograph of section through a cone structure illustrating orientation of feldspar lamination. (x7.5, partially crossed polars)



Textural evidence for post-cumulus reaction is common in the form of chrome-spinel grains located within embayments in olivine crystals. Rare silicate inclusions can be identified in transmitted light, some are in optical continuity with the enclosing silicate phase, indicating a cylindrical embayment in the spinel, whereas others are discrete silicate phases. Optical examination with transmitted light reveals the presence of brown amphibole, pyroxene, olivine and plagioclase. Similar, though larger, inclusions are to be found within cumulus olivine crystals in the overlying peridotites. Poikilitic phases in the cones are much larger than in the adjacent chrome-spinel layers.

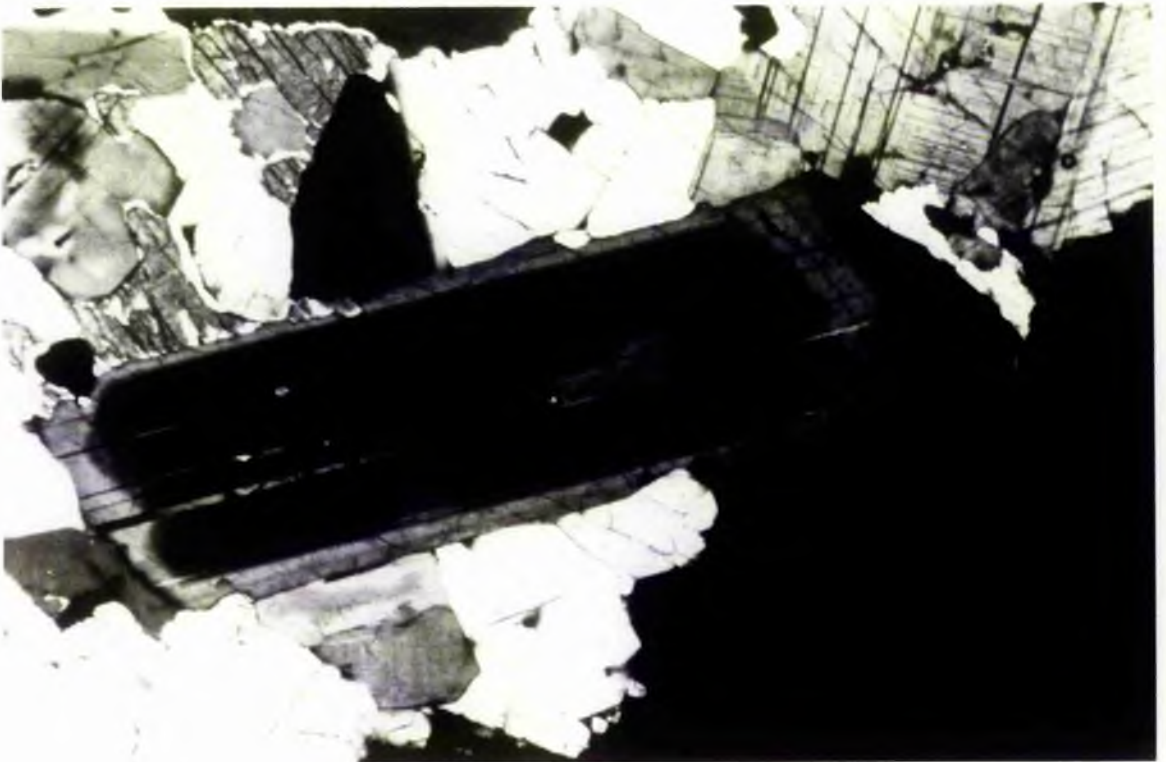
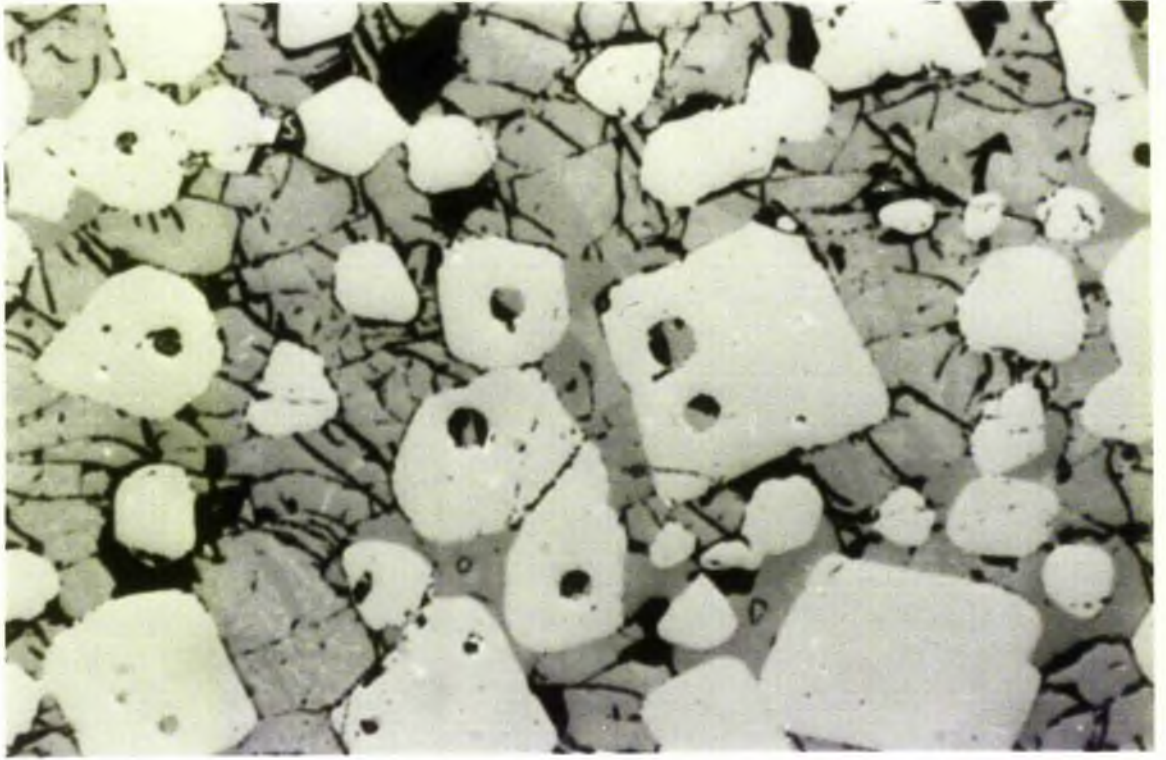
Examination under reflected light reveals patchy development within the cone structures of granular textures with 120° triple junctions between chrome-spinel grains. Exsolved ilmenite platelets are common in the 7/8 boundary samples though rare in the 11/12 boundary samples. It further reveals that the inclusions noted above are abundant and that some are occupied partially or wholly by sulphide; sulphide is more abundant as interstitial blebs within chrome-spinel layers or silicate cumulate. These inclusions are small (10-100microns), spherical and most commonly situated singly and centrally within their host (plate 7.5). Some spinels contain more than one inclusion and a very few contain a large number, up to eighteen having been counted in one grain. Spinel within the cone structures are especially rich in inclusions, whereas inclusions are very rare within disseminated spinels in allivalite. The compositions of a number of inclusions within chrome-spinel have been determined by electron microprobe using standard

Plate 7.5 Silicate and sulphide inclusions within chrome-spinels.

Sample from layer at unit 7/8 junction. (x116, reflected light)

Plate 7.6 Reverse zoned and embayed plagioclase crystal from unit 7

allivalite. (x58, crossed polars)



wavelength-dispersive spectrometry techniques. The small size of these inclusions renders it difficult to obtain analyses of pure phases, nonetheless enstatite, pargasitic hornblende, mica (a titanian natronphlogopite, slightly deficient in divalent cations), olivine, plagioclase, augite and chalcopyrite have been positively identified. Representative analyses of the selected phases are presented in table 7.1.

The underlying allivalites exhibit a range in the amount of poikilitic material and the extent of feldspar zoning. The poikilitic mineral is commonly olivine, a textural relationship peculiar to the top of the allivalite portions of units (Harker, 1908). Complex zoning patterns within cumulus plagioclase of unit 11 have been noted previously (Henderson and Suddaby, 1971), and are common within the unit 7 allivalite. Optical examination reveals two principal styles of zoning. In the more common type feldspars have a uniform core composition and a normally zoned rim (c.f. Brown, 1956). In the other type a small, sodic core is mantled by a more calcic zone which is in turn mantled by a normally zoned rim; this calcic zone is often embayed (plate 7.6, fig 7.2). In both types zoning outwards to the rim may be discontinuous or continuous. More rarely the reverse-zoned type shows two discontinuous reversals followed by normal zoning to the rim. The compositional changes have been measured by electron microprobe using standard wavelength dispersive spectrometry methods. One or more points were selected in each optically defined zone. Percentage anorthite values of the zones in three typical crystals are presented in figure 7.2. Patchy zoning and fine-scale,

Table 7.1 Selected analyses of silicate inclusions within chrome-spinels at the unit 7/8 boundary. All analyses made using an accelerating potential of 20 kV and a probe current (as measured in a Faraday cage) of 30 nanoamps, 4×10 second counts made on peak and 2×10 second counts on background.

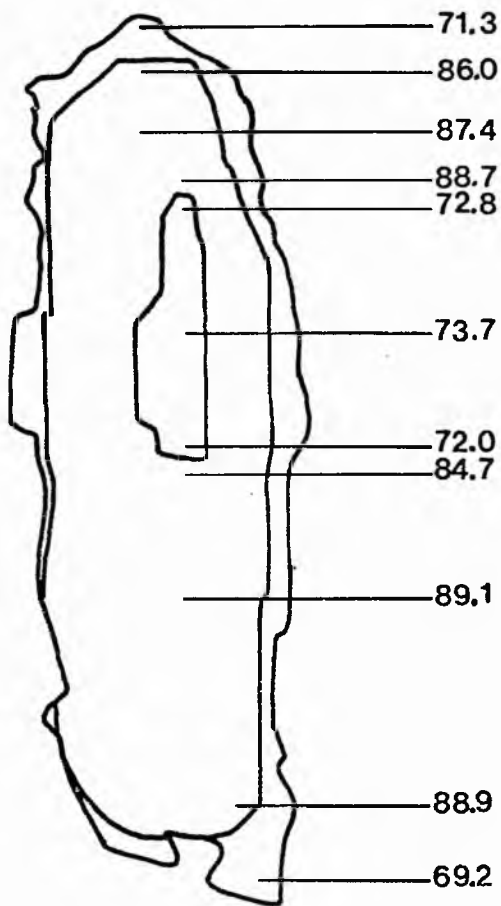
Wt%	plaq_106A/14	pl_106A/17	ppx_106A/4	ppx_106A/5	ppx_116/10	amph_104B/5	amph_106A/10	amph_116/15	mica_106A/6	mica_106A/7	mica_106/6
SiO2	46.87	41.38	54.40	56.02	54.67	41.46	43.42	44.50	38.95	38.63	38.67
TiO2	0.09	0.03	0.31	0.18	0.10	2.66	3.49	2.48	8.17	7.69	4.57
Al2O3	33.36	0.61	3.23	1.31	2.16	13.96	12.00	10.99	15.14	15.73	16.39
Cr2O3	-	0.51	1.06	0.91	2.76	0.00	0.00	2.46	-	-	-
Fe2O3	-	-	1.24	0.78	0.69	0.91	0.78	0.61	-	-	-
FeO	0.90	6.68	5.98	6.33	5.44	5.14	4.44	3.44	3.30	2.98	2.83
MnO	-	0.12	0.22	0.22	0.18	0.07	0.09	0.10	0.04	0.00	0.00
MgO	0.14	49.48	32.05	33.63	32.43	15.60	17.18	16.71	21.31	21.49	22.47
CaO	16.40	0.16	0.98	0.29	0.72	11.26	9.95	9.75	0.12	0.22	0.02
Na2O	2.07	0.11	0.16	0.06	0.24	3.70	3.79	4.99	6.74	6.95	4.54
K2O	0.04	-	-	-	-	0.05	0.06	0.00	0.61	0.42	3.23
F2O	-	-	-	-	-	0.12	0.07	0.00	0.02	0.11	0.08
TOTAL	99.87	99.08	99.63	99.73	99.39	94.93	95.27	96.03	94.40	94.22	92.80

Atoms	Si4+	Ti4+	Al3+	Cr3+	Fe3+	Fe2+	Mn2+	Mg2+	Ca2+	Na2+	K+	F-	O2-
Si4+	2.162	1.008	1.900	1.948	1.914	6.111	6.440	5.403	5.361	5.467			
Ti4+	0.003	0.001	0.008	0.005	0.295	0.382	0.270	0.852	0.803	0.486			
Al3+	1.814	0.018	0.133	0.054	2.425	2.058	1.875	2.475	2.573	2.731			
Cr3+	-	0.010	0.029	0.025	0.076	0.000	0.281	-	-	-			
Fe3+	-	-	0.033	0.020	0.100	0.086	0.066	-	-	-			
Fe2+	0.035	0.136	0.175	0.184	0.159	0.541	0.417	0.383	0.346	0.335			
Mn2+	-	0.002	0.007	0.006	0.005	0.011	0.012	0.005	0.000	0.000			
Mg2+	0.010	1.797	1.669	1.743	1.692	3.428	3.605	4.407	4.446	4.735			
Ca2+	0.811	0.004	0.037	0.011	1.778	1.551	1.512	0.018	0.033	0.003			
Na2+	0.185	0.005	0.011	0.004	1.057	1.069	1.400	1.813	1.870	1.224			
K+	0.002	-	-	-	0.009	0.011	0.000	0.108	0.074	0.582			
F-	-	-	-	-	0.039	0.023	0.000	0.006	0.034	0.025			
O2-	8.000	4.000	6.000	6.000	6.000	23.000	23.000	22.000	22.000	22.000			

Figure 7.2 Sketches of three feldspar crystals from the unit 7 allivalite showing optically defined zones and An mol % values determined by electron microprobe.

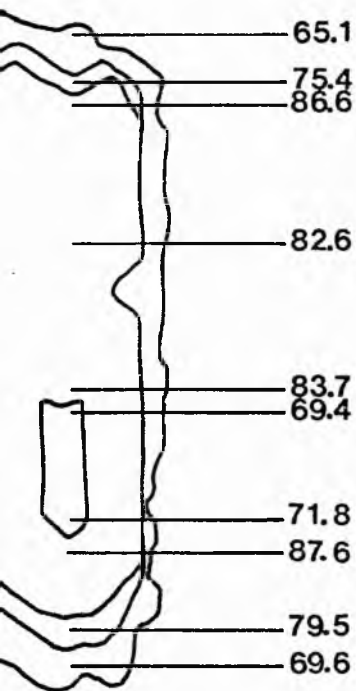
103/2

An%



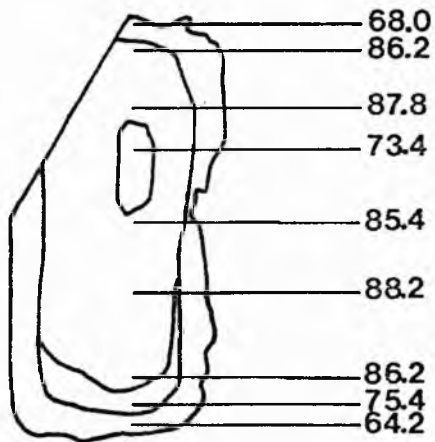
106A/1

An%



104B/3

An%



1mm



oscillatory zoning are found in some crystals. Complex zoning has been traced downwards to a depth of 2m in the unit 7 allivalite.

7.3.4 Origin of chrome-spinel layers at unit junctions.

The structures and textures described above constrain explanations of chrome-spinel layers at unit junctions. Truncation of lamination in allivalites and the presence of irregularly-shaped embayments within allivalites (fig 7.1a-c) indicates removal of allivalite cumulate before chrome-spinel accumulation and not slumping or loading within a crystal mush. Removal of allivalite could take place by either resorption or mechanical erosion. The lack of fragments of allivalite or of cumulus feldspar crystals within peridotite suggests that resorption, perhaps aided by mechanical loosening, was the dominant erosive process and thus, in part, confirms the predictions of Huppert and Sparks (1980). The transgressive nature of some chrome-spinel layers (figs 7.1b & 7.1c) suggests that either limited replacement of allivalite by peridotite has taken place after chromite crystallisation (see Chp 6 for a description of replacement structures elsewhere in the intrusion), or that some olivine accumulation occurred before chromitite formation. The presence of chrome-spinel layers on the underside of protrusions of allivalite (fig 7.1c) indicates conclusively that crystal settling was not important in the formation of such layers. Thus chromite must have crystallised in situ on an uneven floor of allivalite, with the possibility of minor olivine accumulation in

irregularities on that floor.

An alternative to previous models of chromite concentration is suggested by the cone structures at the unit 7/8 boundary. Their ubiquitous occurrence at culminations in the allivalite lamination cannot be fortuitous and rules out an origin by slumping, loading or auto-intrusion. Similar upward deflections of a pre-existing lamination have been recorded in the Bushveld complex and ascribed to fluid escape, (Lee, 1981), the analogy being with water-escape structures in clastic sediments (see Lowe, 1975, for review). If this interpretation is correct, then thick chrome-spinel accumulations are coincident with paths of relatively rapid fluid escape from the permeable crystal mush.

Petrographic descriptions by Brown (1956), Henderson and Suddaby (1971), Dunham and Wadsworth (1978) and Maaloe (1978) indicate that chrome-spinel is present, if somewhat sporadically, throughout the Eastern Layered Series. Thus magmas parental to peridotite must have been in equilibrium with olivine and chrome-spinel and those interstitial in allivalite in equilibrium with olivine, plagioclase, clinopyroxene and chrome-spinel. These relations can be illustrated in the system Forsterite - Diopside - Anorthite - Picrochromite - Quartz, eg path 1 in Irvine (1977, figs 51 - 54) models the evolution of a Rum cyclic unit. It is thus apparent that mixing of interstitial liquid from allivalite (in equilibrium with Fo, An, Di and Pc) with overlying picritic liquid (in equilibrium with Fo and Pc) must precipitate chromite alone due to the curvature of the cotectic fractionation path away from the

microchromite apex of the phase diagram (see also Irvine, 1981). Chromium concentrations must have been kept high in the neighbourhood of growing spinels by vigorous magma convection (Huppert and Sparks, 1980).

The discrete inclusions within the spinels may be interpreted as further evidence for the presence of a relatively evolved liquid. Their occurrence within olivine as well as spinel, and their morphological similarity to sulphide (immiscible liquid) inclusions suggests that they crystallised from liquid trapped within growing crystals, and are not products of reaction of spinel with trapped or supernatant liquid. Morphologically similar silicate inclusions in Muskox chromite grains have also been interpreted as crystallised droplets of trapped liquid (Irvine, 1975; 1981). Their compositions and similarity to interstitial phases present throughout the intrusion suggest that this liquid was residual and was relatively hydrous, siliceous and alkali-rich by comparison with the intrusion's parental picritic magma. They are not considered to represent an immiscible phase themselves but droplets of residual liquid from the underlying cumulates which may not have been readily miscible with the supernatant magma. Any liquid/liquid interface which may have existed would have been a convenient site for heterogeneous nucleation of chrome-spinel.

7.4 Discussion.

The upward expulsion of liquid from a cumulate pile is not a new concept. Previous studies have emphasised the role of compaction in driving fluid upwards (eg Irvine 1980b, Donaldson 1982). However compaction must be less effective in feldspar cumulates due to the small or even negative density contrast of feldspar with interstitial liquid. Consideration of the likely density contrast between dense picritic supernatant liquid and less dense interstitial liquid in the allivalite suggests that the driving force for fluid expulsion may have been convective overturn. The envisaged process is analogous to that described by Musgrave and Reeburgh (1982) in which a convective flow was set up between cold (dense), winter, bottom water in an Alaskan lake and warm (less dense) pore water in the lake-bottom sediments. A similar fluid flow was invoked by Morse (1981a) to explain apparently anomalous Rb and K concentrations in Kiglapait cumulates, in this case the driving force was assumed to be the density increase associated with iron enrichment. Dispersed sulphides in the footwall anorthosite of the Merensky reef in the Bushveld intrusion are considered to represent the downward percolation of a sulphide-rich fluid (Vermaak, 1976). Evidence for the migration of relatively hot, basic liquid into the allivalite mush may be provided by the common reversed zoning (fig 7.2, plate 7.6), irregular core shapes of allivalite feldspars and common poikilitic form of olivine towards the top of allivalites. Elsewhere in the Rum intrusion the process offers an alternative explanation of the cryptic reversal that

exists at the top of unit 10 (Dunham & Wadsworth, 1978) by the metasomatising action of the downward filtering liquid, and offers a source of high-temperature components for adcumulus growth.

The proposed explanation of chromitite formation has only been applied to chrome-spinel layers at allivalite/peridotite contacts. It is clear, however, that the mechanism could account for the formation of any chromite layer where the appropriate conditions of relatively slow silicate sedimentation and mixing of expressed and overlying liquids occurs which are far enough apart on the fractionation path to allow crystallisation of a significant amount of chromite. Thus all three chrome-spinel layers at the 7/8 junction may have formed in this way, perhaps during minor replenishment and mixing before the major replenishment which gave rise to the unit 8 peridotite. It is abundantly clear, however, that not all chrome-spinel layers in the Rum intrusion could have originated in this way, particularly problematical are the chromitites intimately associated with harrisite layers in the Western Layered Series.

The mechanism will be applicable to other intrusions where similar situations have arisen. In the Bushveld intrusion for example, the mechanism offers an alternative explanation of the chromitite which underlies the Merensky Reef (Vermaak, 1976), by mixing of expelled interstitial liquid and the mixed magma which gave rise to the Merensky Reef irrespective of its mechanism of formation (compare Campbell *et al*, 1983 and Irvine *et al*, 1983).

7.5 Applications of mixing mechanism to other phase-boundary geometries.

The process of mixing at the mush-magma interface described above may also be responsible or partially responsible for a number of layer types and compositions, whether the driving force is convection or episodic compaction. The type of layer produced will be sensitive to the geometry of the phase boundary or boundaries along which the liquids are fractionating. Situations can be envisaged in which the resultant (mixed) liquid is superheated (mixing across thermal valley or along concave-up liquidus surfaces), supercooled (mixing across thermal divide or along convex-up liquidus surface) or is displaced out of the stability field of one or more phases. For example, situations can be envisaged in which interstitial liquid in an olivine cumulate mixes with less, or more, fractionated supernatant magma; both of which are in equilibrium with olivine alone. The resultant mixed liquid will be supercooled due to the convex up form of the liquidus surface in the olivine primary phase field in the system Forsterite - Diopside - Anorthite. This supercooled liquid may crystallise olivine with distinctive textures, perhaps skeletal, and offers another explanation for some harrisitic cumulates.

7.6 Conclusions

- 1) Chrome-spinel layers in the Eastern Layered Series of the Rum intrusion have formed by crystallisation from mixed interstitial and supernatant magma. The mechanism is applicable to other intrusions and other phase boundaries in which case different types of layers may be formed.
- 2) Resorption of allivalite by replenishing picritic magma occurred on Rum, thus erasing parts of the stratigraphy (see also Chp 6).
- 3) Relatively primitive magma penetrated downwards into permeable crystal mush in the Rum intrusion. Reaction of those cumulates with this magma may have given rise to reversals in cryptic profiles. This magma may also have provided components for adcumulus growth.

8 LITHOSTRATIGRAPHY AND DIACHRONISM IN THE RUM INTRUSION.

8.1 Introduction.

The preceding chapters have primarily been concerned with processes, as interpreted from structures. Different structures and layering styles are often characteristic of different portions of layered plutons (for example lenticular, ultramafic layers are characteristic of the dunitic horizon in the Lower Zone of the Kiglapait intrusion, App 4; Morse, 1969), thus different processes were probably important in the formation of the different rocks. Conventionally, these processes have been assumed to operate separately in time but not in space, ie homogeneity of depositional conditions at any one time has been assumed (Wager & Deer, 1939; Brown, 1956). Thus correlation from one portion of a layered intrusion to another on the basis of lithostratigraphy has been assumed to be equivalent to a time-stratigraphic correlation (see fig 8.1a).

The presence of finger structures (chp 6) suggests that allivalite and peridotite may have formed simultaneously in the Rum intrusion and this is consistent with several recent investigations in volcanology, fluid dynamics and the mapping of layered intrusions which point to the existence of zoning, or stratification, within magma bodies (chp 2). Thus the possibility exists that different

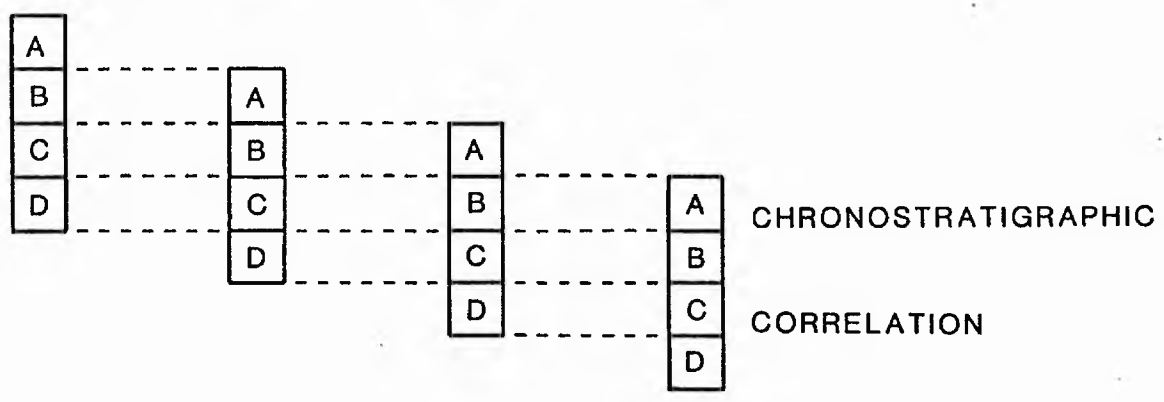
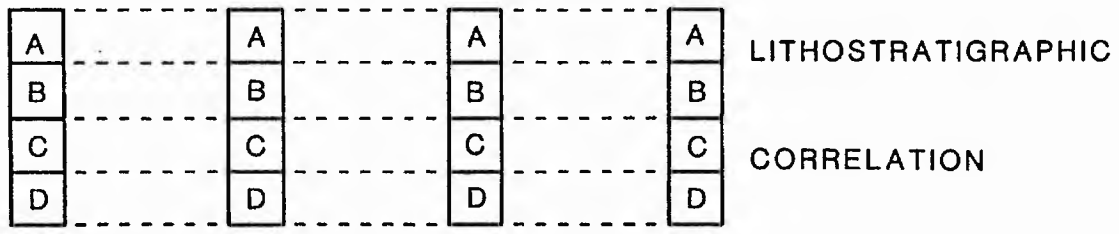


Figure 8.1 Correlation schemes of four hypothetical, diachronous rock units; A, B, C and D, on the basis of their lithology and on the basis of isochronous horizons.

environments of deposition existed within evolving basic plutons, separated in space but not in time. If crystallisation were to proceed contemporaneously in two or more zones in a magma chamber, driven, perhaps, by heat transfer from one liquid layer to an overlying liquid layer (see Huppert & Sparks, 1980) and ultimately to a hydrothermal cooling system, then the system can be compared to zones of bathymetrically defined environments of deposition in sedimentary basins, as in seaward facies changes off a river delta. Progradation and regression of these facies boundaries, controlled by the vertical movement of the liquid/liquid interfaces, must then lead to the formation of diachronous lithologic units; thus chronostratigraphic correlation schemes are not necessarily equivalent to lithostratigraphic ones (see fig 8.1). Recognition that such a situation applied during formation of a pile of rocks depends on the identification of time planes within the sequence under study (Conybeare, 1979).

8.2 Application of the concept to a hypothetical magma chamber.

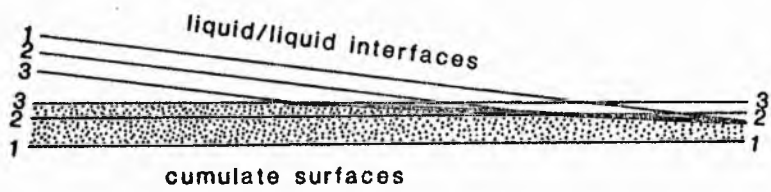
The following discussion refers to figure 8.2. Imagine a magma chamber zoned with respect to liquid composition (see Sparks et al, 1980; Huppert & Sparks, 1980) and crystallising two contrasted rock types on a gently dipping floor (fig 8.2a) at equal rates. Time horizons will then continue to be orientated parallel to that floor but the lithological boundary will be a diachronous one. If the liquid/liquid interface were to remain at a constant position in

Figure 8.2

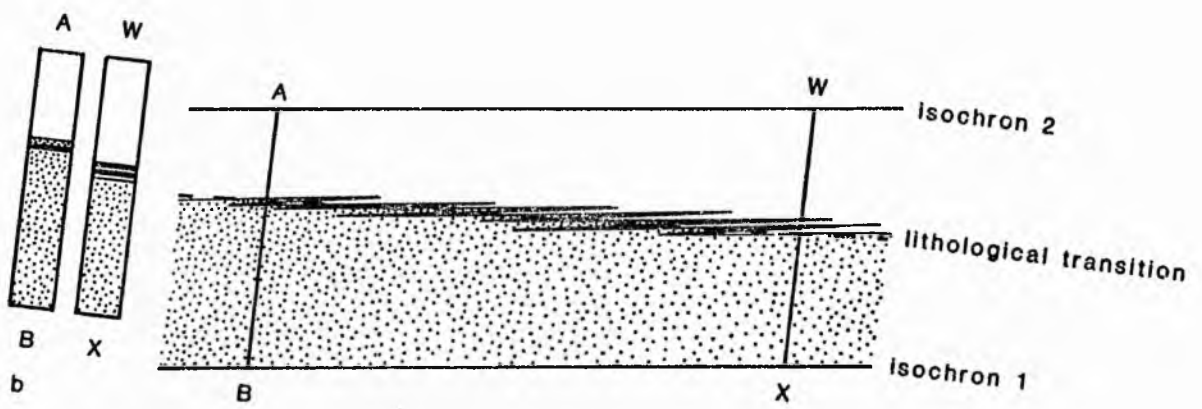
(a) Accumulation of a hypothetical cumulate slab on a gently dipping floor. Numbers 1, 2 and 3 refer to successive times. Horizontal lines are positions in space of a liquid/liquid (picrite/basalt) interface at equivalent times to the cumulate surfaces. As the slab accumulates the liquid/liquid interfaces migrate down-dip for reasons discussed in the text and this results in a dipping lithological transition being preserved in the rock record, which must dip more gently than the accumulation surfaces do. The net result of this is that the upper rock layer thins down-dip whereas the lower one thickens down-dip.

(b) An enlarged portion of figure 8.2a showing interleaving of lithologies due to minor transgressions and regressions of the liquid/liquid interface. Cross-sections AB and WX illustrate the variations in stratigraphy produced during equivalent times.

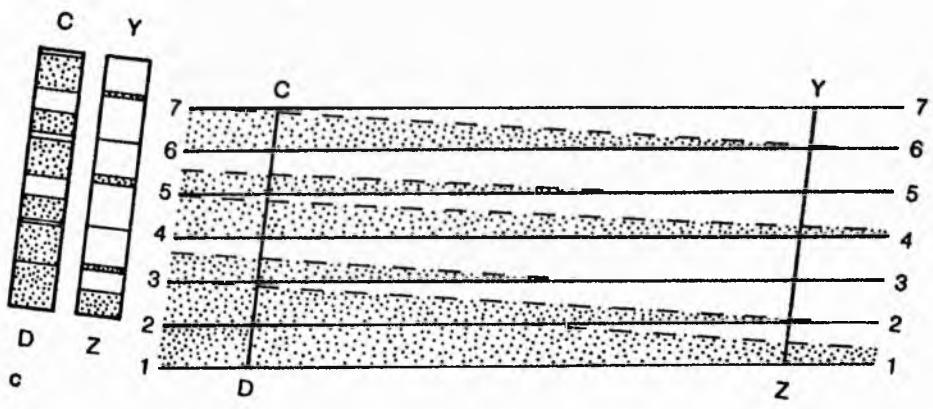
(c) Seven rock units, each built up as in the (a) and (b), but repeated by elevation of the liquid/liquid interface by replenishment, stoping, changes in chamber geometry etc. The upper portion of each unit thins down-dip and the lower thickens. The cross-sections CD and YZ illustrate differences in stratigraphy that can be produced by such a scheme during the same time interval.



a



b



c

space, then the transition between the two lithologies would necessarily develop horizontally. It is more likely, however, that the interface will migrate down dip as mass is transferred by diffusion into the upper liquid (Huppert & Sparks, 1980) and as the total volume changes due to crystallisation. In this case the lithological boundary will also dip, but at a lesser angle than the isochronous surfaces (fig 8.2a). It might be expected, however, that the migration of the liquid/liquid interface down-dip will not be steady, but that minor reversals or accelerations of its progress may be brought about by minor replenishments, stoping, dyke/sill emplacement, eruption etc. In those cases the lithologies will interleave as indicated on figure 8.2b. Such a scheme also predicts that the proportion of one rock type to the other within the unit and the nature and number of interleavings will vary from one part of the unit to another (fig 8.2b). Major, relatively abrupt replenishments or major movements of the interface caused by other processes will move the liquid/liquid interfaces rapidly up dip and repetition of the cycle will lead to the development of repetitive stratigraphy (see fig 8.2c).

Such a scheme predicts the interleaving of rock types at lithologic transitions within cyclic units, but abrupt transitions between cyclic units, thinning of the upper lithology down dip and the development of chronostratigraphic horizons parallel to unit contacts.

8.3 Lateral facies variations in the Rum pluton.

Several features of the Eastern Layered Series of the Rum intrusion suggest that different depositional environments may have existed contemporaneously:-

- i) The hypothetical parents of the peridotite and allivalite portions of each cyclic unit are considered to have been picritic and basaltic respectively. The fluid dynamics of replenishment of a basaltic chamber at geologically reasonable input rates predicts the development of chamber stratification (Huppert & Sparks, 1980; Campbell *et al.*, 1983).
- ii) intra-unit peridotite/allivalite contacts are fingered (chp 6) which may indicate the contemporaneous existence of two liquids of different compositions.
- iii) cyclic units in the Eastern Layered Series dip concentrically towards the centre of the intrusion (Brown, 1956) and thus it is possible that any replenishment may not have covered the whole floor (cf Huppert & Sparks, 1980).

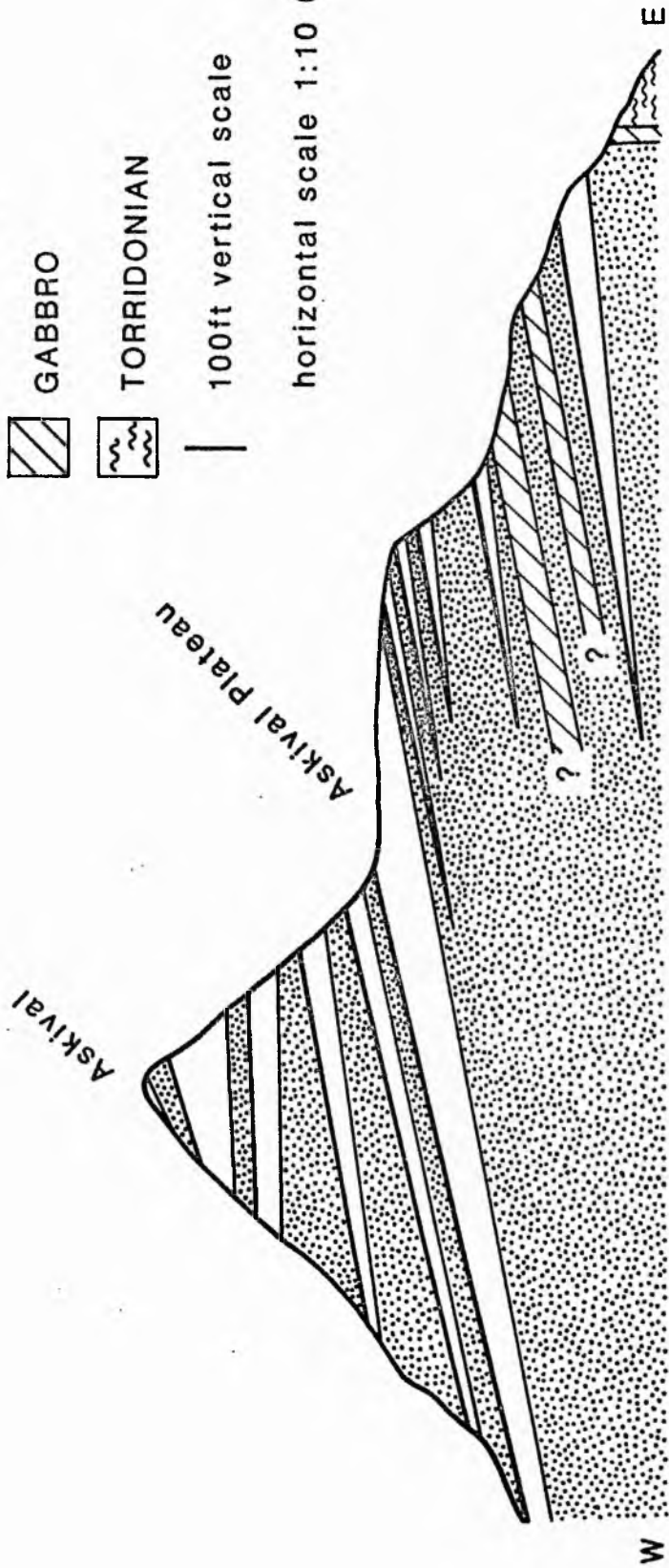
Several other features of the stratigraphy and structure of the Eastern Layered Series are consistent with an origin by the mechanism outlined above. Normally graded layers and other forms of rhythmic layering are generally developed parallel to unit junctions. Unit junctions are abrupt whereas inter-unit transitions from peridotite to allivalite are gradational through a zone where the two lithologies interleave (Brown, 1956). Allivalites are

Figure 8.3 East - West cross-section of the Eastern Layered Series of the Rum intrusion from the Bealach nan Oir (grid ref N13867952) to the country rocks (grid ref 14117953) drawn from Emeleus (1980). Note thinning of allivalite and thickening of peridotite down-dip and the gentler dips of the intra-unit contacts (indicated by thin lines) as compared with the inter-unit contacts (indicated by the thick lines). The exact relationship of the gabbro sheets to the layered series is presently under investigation by J. Faithfull. Askival Plateau Gabbro omitted for clarity.

- ALLIVALITE
- ▒ PERIDOTITE
- ▨ GABBRO
- ▤ TORRIDONIAN

100ft vertical scale

horizontal scale 1:10 000



laterally impersistent and there is a tendency for allivalites to thin, and peridotites to thicken, down dip (see Emeleus, 1980 and fig 8.3). Lithologic transitions within units tend to dip less steeply than unit contacts (see fig 8.3).

8.4 Discussion.

Similar schemes have been proposed by Irvine (1981) and Irvine et al (1983) to explain the formation of chromitite layers in the Muskox and platinoid-bearing layers in the Stillwater and Bushveld intrusions, respectively. These schemes depend on the formation of cyclic units at "accretion fronts" and predict angular discordance between chronostratigraphic horizons (the trace of rhythmic layering) and cyclic unit junctions and the development of cryptic variation laterally along individual layers, for which there is, as yet, no evidence (McCarthy & Cawthorn, 1983). Ultimately the testing of both models will depend on detailed investigations of lithologic, textural and cryptic variation in three dimensions which has not yet been attempted. It is plain, however, that simple interpretations of one-dimensional cryptic profiles through layered sequences (eg Palacz, 1984; Elthon et al, in press) where the magma body was likely to be compositionally and thermally stratified are open to reinterpretation in terms of relative movement of the magma body and the depositional surface and not simply fractionation versus replenishment.

8.5 Conclusions

1) Stratigraphic sequences in layered intrusions can be interpreted in terms of migration of different environments of deposition where there is evidence for zoning of the magma body.

9 IMPLICATIONS FOR THE INTERPRETATION OF LAYERED IGNEOUS ROCKS.

The conclusions set out in the previous eight chapters have been reached from observations on a very small number of plutons. There is however, a large body of information in the literature on layered plutons which can be used to determine whether many of the processes described in this thesis may have operated in other plutons. Information collected from the literature has been used to construct table 9.1 which shows that; (i) solid transport, of crystals and rock fragments, is widespread, (ii) structural evidence for a mush zone is widespread, (iii) advection of interstitial liquid is probably ubiquitous and (iv) many magma bodies were probably compositionally zoned, thus lateral variations in cumulus assemblages and compositions must be common features of basic plutons.

As pointed out in chapter 1, one of the principal aims of this study is to place constraints on the mechanisms of differentiation of major basic magma bodies. In this respect some small-scale structures indicate that crystal transport and sorting are common features in major basic magma bodies, though they do not indicate whether those crystals and liquid eventually separate by settling or convection. In a sense this question is unimportant, since the net result, differentiation of the magma, is the same in both cases.

Table 9.1 (following pages) Summary of principle features, layer types and evidence for liquid stratification, solid transport, mush zones and advection of interstitial liquid in a number of layered intrusions selected from a survey of the following sources; American Journal of Science, 1960 -; Journal of Petrology vol. 1 -; Contributions to Mineralogy and Petrology, vol. 1 -; Earth and Planetary Science Letters, vol 1 -; Mineralogical Magazine, 1960 -; Journal of Geology, 1960 -; Journal of the Geological Society of London, 1969 -; Scottish Journal of Geology, vol. 1 -; American Mineralogist, 1960 -; Chemical Geology, vol. 1 -; Geological Magazine, 1960 -; Bulletin of the Geological Society of America, 1960 -; Mineralium Deposita, vol. 1 -; Economic Geology, 1960 -; Canadian Journal of Earth Sciences, vol. 1 -; Wager & Brown, 1968; and the references in the text. The table is not comprehensive, in particular layered granites and references to layering, without any further description, have been omitted. Descriptions of layer types refer to lamination, types of rhythmic layering and other types of layering in that order. Liquid stratification is considered likely after any replenishment (Chp 2, Sparks et al, 1980; Campbell et al, 1983), as indicated by modal or cryptic regressions. Interpretations of small-scale structures either follow the named author or interpretations of similar structures described in this thesis.

NAME, age, location	Geometry, layering dips	Parent magma, lithologies	Layer types	Evidence for liquid stratification
BAY OF ISLANDS Ordovician W Newfoundland, Canada	Deformed - originally cylindrical (see fig 2.1)	picrite-basalt, ultramafic - mafic cumulates	modally-graded, nodal, textural, grain-size rhythmic, comb, intercumulus, cryptic	lateral cryptic variation, discordance of rhythmic, cryptic and phase layering
BAYS OF MAINE 7 Maine, USA	synformal	basalt, olivine gabbro, gabbro, quartz gabbro, diorite	planar lamination rhythmic	
BUSHVELD Precambrian South Africa	four-lobed, oval synform dips generally 10-15°	ultramafic and anorthositic norite, orthopyroxenite peridotite, chromitite, anorthosite	planar lamination, nodal lamination, nodal, textural, graded rhythmic, phase, cyclic	regressions, unconformities, paraconformities
CARR BOYD Precambrian West Australia	lobate, 75 km ² , moderate centripetal dips	3 distinct parent magmas - basaltic, dunite, troctolite, norite, bronzitite, gabbro, anorthosite	cyclic	regressions
COLDWELL 7 Canada	indotaxinatu dips generally 75-90°	undersaturated basic magma, alkaline gabbro, nepheline syenite	wispy, rhythmic graded	
CULLIN Tertiary Skye, Scotland	8 circular, 8 km in diameter, 5000 m thick, dips generally 30° inwards	high Ca basalt/ gicrite, peridotite, allivalite, eucrite, gabbro	planar lamination, nodal lamination, nodal, textural, graded rhythmic, phase, cyclic cryptic	regressions
DUKE ISLAND Cretaceous Alaska, USA	deformed	ultramafic ultramafic and gabbroic cumulates	nodal lamination, nodal, size-graded, fragmental rhythmic, phase	
DULUTH Precambrian Minnesota, USA	arcuate lopolith, 10000 km ² dips 25-30°	tholeiite, peridotite, troctolite, anorthosite, gabbro, diorite	planar lamination, rhythmic, phase	regressions
EASTERN LIZARD Cornwall, England	vertical dips deformed	peridotite, gabbro	planar lamination, graded and isomodal rhythmic	
EWARARA Precambrian Central Australia	200 m thick - remnant of much larger body	bronzitite, pyroxenites	vertical layers	
FISKENAESSET Precambrian Southwest Greenland	deformed sheet, 500 m thick	dunite, peridotite, anorthosite, gabbro, chromitite	planar lamination, nodal lamination, isomodal and graded rhythmic	
FONGEN-HYLLINGEN "Caledonian" Norway	elongate saucer shaped, 160 km ² up to 6200 m thick	tholeiitic basalt dunite, troctolite, gabbro, syenite	planar lamination nodal lamination, isomodal and graded rhythmic, cyclic, phase	regressions
FREETOWN 7 Sierra Leone	Funnel-shaped, 6000 m thick dips average 30°	basalt, gabbro, troctolite anorthosite	planar lamination, rhythmic, cyclic, phase	regressions
GARDINER Tertiary East Greenland	circular, 6 km in diameter dips steep, inwards	nephelinite/nepheline -hawaiite dunites, clinopyroxene dunites, olivine pyroxenites	planar lamination, rhythmic, phase	
GREAT 'DYKE' Precambrian Zimbabwe	linear, 480 km x 8 km (made up of 4 smaller complexes) synclinal in cross- section	picrite dunite, harzburgite, websterite, bronzitite, gabbro, chromitite	planar lamination, cyclic, phase	regressions
GRONNEDAL-IKA Precambrian South Greenland	8 km x 6 km, dips up to 80°	nepheline-syenite/ carbonatite syenite, foyisite	planar lamination, carbonatite	
HEYTASCH Precambrian Labrador, Canada	arcuate trough, 200 km ² dips 20°-70° on one limb, 5°-20° on the other	troctolite, anorthosite, leucotroctolite, gabbro	planar lamination, nodal lamination, isomodal and graded rhythmic, comb, phase	replenished
ILIMAUSSAQ Precambrian South Greenland	Elongate ring, 15 x 9 km x 3 km thick Dips up to 60°	Feldspathoidal syenite kekortokite, naujaite, sodalite foysisite, lujverite	planar lamination, isomodal and graded rhythmic, macro- rhythmic, phase	
IMILIK Tertiary East Greenland	see fig 2.1		planar lamination modally- and size- graded rhythmic, phase	
INGDNISH Cape Breton Island, Canada	Synform, 1 km across	intermediate and basaltic diorite and gabbro	planar lamination, rhythmic	flows of basic liquid in intermediate host
JIMBERLANA Precambrian Western Australia	180 x 2.5 km 7 canoe-shaped bodies joined by dykes dips from flat to vertical	basalt olivine, bronzite, plagioclase, augite, hypersthene cumulates	planar lamination, rhythmic, cyclic phase	regressions
KAERVEN Tertiary East Greenland	ring-shaped, 8 km x 1 km wide, 500 m thick average dip 20°	tholeiitic basalt gabbro	planar lamination, nodal lamination, rhythmic	regressions
KALKA Precambrian Central Australia	deformed 5000 m thick	basalt pyroxenite, norite gabbro, anorthosite	planar lamination, nodal lamination, isomodal and graded rhythmic cyclic, phase, intercumulus	regressions

Evidence for transport of solid material	Evidence for a mush zone	Evidence for movement of interstitial fluid	References
gabbro blocks			Cesay & Kerson, 1982
normally graded layers erosion structures	erosion structures		Bickford, 1963
autoliths, normally graded layers, erosion structures	load structures, fluid-escape structures, erosion structures, folds, flame structures	fluid-escape structures, replacement bodies	Wager & Brown, 1968; Wadsworth, 1973; Vermaak, 1976; Lee & Sharpe 1980; Lee, 1981 Irvine <i>et al.</i> , 1983 Purvis <i>et al.</i> , 1972
graded layers, erosion structures xenolith rich zones	erosion structures		Mitchell & Platt, 1982
autoliths, graded layers, erosion structures	erosion structures folds		Wager & Brown, 1968; Hutchison & Sevan, 1977
size-graded fragmental layers, autoliths, erosion structures	folds, erosion structures, deflections under blocks	replacement bodies	Irvine, 1974
autoliths	"flow" structures around blocks folds, "swirly" foliation		Wager & Brown, 1968; Walbran & Mony, 1980 Kirby, 1978
erosion structures, graded layers, troughs containing xenocrysts	erosion structures		Goode, 1977b Myers, 1976
autoliths and xenoliths, erosion structures, troughs, graded layers	erosion structures, load structures, folds, layering deflected under blocks		Wilson <i>et al.</i> , 1981
		pegmatitic gabbro segregations	Wells & Bowles, 1981 Nielsen, 1981
		chromitite layers at the base of cyclic units	Wilson, 1982
			Wager & Brown, 1968
graded layers troughs, erosion surfaces	erosion surfaces, folds, layers deflected around megacrysts		Berg, 1980
autoliths	layers deflected around blocks	possible filter-pressed residual liquid	Wager & Brown, 1968
size-graded layering			Brown & Farmer, 1971
	deformed inclusions of diorite in gabbro, injection structures	filter pressing of adamellite residue	Wiebe, 1974
possibly porphyritic			McClay & Campbell, 1976; Campbell, 1978
breccias			Wager & Brown, 1968
erosion structures	erosion structures, load structures		Goode, 1976 & 1977a

KANGERDLUGSSUAQ Tertiary East Greenland	Saucer-shaped 33 km diameter Dips 40-50°	alkaline syenite nordmarkite, pulsakite, foyasite	planar lamination	
KAPALAGULU Precambrian Iceland	deformed 15 x 2 km	tholeiitic basalt peridotite, gabbro	planar lamination, isomodal and graded rhythmic, cyclic, phase	regressions
KAP EDVARD HOLM Tertiary East Greenland	saucer-shaped, 20 x 12 km x 7500+ m thick dip average 20°	basalt gabbro	planar lamination, modal lamination, rhythmic	regression
KLOKKEN Precambrian South Greenland	elliptical, 3 x 2.5 km 600+ m thick concentric dips 30-50°	syenite syennite	planar lamination, modal lamination, reversely graded and normally graded rhythmic, textural	
KUNGNAT Precambrian South Greenland	elliptical, 40 x 20 km 1800+ m thick dips 20-60°	syenite syenite	planar lamination, isomodal and graded rhythmic, phase	
LILLE KUFJORD "Caledonian" North Norway	1400 m thick	subalkaline basalt peridotite, troctolite, gabbro	planar lamination isomodal and graded rhythmic, cyclic phase	regressions
LILLOISE Tertiary East Greenland	"Egg-shaped" outcrop 10 x 5 km	alkali basalt olivine-augite- chromite and olivine-augite- plagioclase-chromite cumulates	rhythmic phase	
MESSINA Precambrian South Africa	deformed	quartz tholeiite ultramafic gabbro, anorthosite	graded rhythmic, poikilitic clinopyroxene layers, modal (7macro) rhythmic	
MOUNT JOHNSON Cretaceous Quebec, Canada	oval, 680 x 550 m vertical dips	olivine essexite, essexite, hornblende pulsakite	planar lamination, isomodal and graded rhythmic phase	
MUSKOKA Precambrian Canada	120 km long (not all exposed) dyke-funnel-shaped (see fig 2.1) dips 25-30° inwards	silica-saturated tholeiite ultramafic and gabbroic cumulates	cyclic, phase	regressions
NAUSAHI Precambrian India	deformed	ultramafic	modal lamination, modally- and size- graded rhythmic	
NORTH CAPE Mesozoic New Zealand	deformed	serpentinite, gabbro	planar lamination, modally- and size-graded rhythmic	
NUNARSSUIT Precambrian South Greenland	20 x 25 km, (layered zone much smaller)	syenite syenite	planar lamination, graded rhythmic layers	
PANTON SILL Precambrian Western Australia	elliptical, 10 x 3 km 1500 m thick	dunite, harzburgite, gabbro, anorthosite, chromite	modal lamination, modally graded, macro-rhythmic	
ROGNSUND "Caledonian" Norway	deformed sheet, 1000 m thick	olivine basalt/ picrite peridotite, pyroxenite, gabbro	planar lamination, rhythmic, comb	regressions
SALT LICK CREEK Precambrian Western Australia	circular, 3.3 km in diameter dips 30°	peridotite, olivine, sucritite	modal lamination, rhythmic, macro- rhythmic, cyclic, phase	regression
SKAERGAARD Tertiary East Greenland	elliptical, 12 x 8 km (see fig 2.1) dips 0-25°	tholeiitic basalt gabbro, diorite	planar lamination, modal lamination, isomodal, graded, rhythmic, macro- rhythmic, micro-rhythmic, comb, colloform, banding, phase	
STILLWATER Precambrian Montana, USA	40 x 8 km deformed	ultramafic/anorthositic ultramafic and gabbroic cumulates	planar lamination modal lamination isomodal and graded rhythmic, "inch-scale", cyclic, phase	regressions
TIGALAK Precambrian	Sheet-like 10 x 6 km	troctolite norite, ferrodorite	planar lamination, isomodal and graded rhythmic	regression
VESTURHORN Tertiary Iceland		Basic and acid	planar lamination thick (5 m) size- graded layers, rhythmic	regressions

xenoliths				Wager & Brown, 1968
erosion structures graded layers	erosion structures folds			Wedoworth <u>et al.</u> , 1982
autoliths of gabbro and anorthosite				Wager & Brown, 1968
erosion structures, channel structures, spalled sheets	load structures, erosion structures, flame structures	pegmatitic flame structures		Parsons, 1979; Parsons & Butterfield, 1981
xenolithic horizons, erosion structures, troughs, graded layers	erosion structures			Wager & Brown, 1968
graded layers, xenoliths	finger structures	finger structures		Robins, 1982
	disruption by later intrusion while in plastic state			Brown, 1973; Matthews, 1976
				Barton <u>et al.</u> , 1979
xenoliths, erosion structures, troughs, graded layers	erosion structures			Philpotts, 1968
		evidence for metasomatism		Wager & Brown, 1968; Irvine, 1980b
autoliths, erosion structures	erosion structures, folds, load structures			Mukherjee & Haldar, 1975
channel structures	folds, channel structures	mafic "schlieren" and feldspathic gabbro segregations		Bennet, 1976
xenoliths erosion structures, channels, graded layers, "lag" breccias	folds, erosion structures, load structures			Parsons & Butterfield, 1981
		silicate inclusions in chromite (cf Chp 7)		Hemlyn, 1980
				Robins, 1973
				Wilkinson <u>et al.</u> , 1975
autoliths, erosion structures, troughs, graded layers, imbricated blocks, lateral variation in layers	erosion structures, folds, deformation under blocks	replacement bodies		Wager & Brown, 1968; Irvine, 1980 a,b,c 1982; McBirney & Noyes, 1979
graded layers, erosion structures	folds, deformation structures, flame structures, erosion structures	replacement bodies, plagioclase segregations		Hees, 1960; Jackson, 1961; Wager & Brown, 1968; McCallum <u>et al.</u> , 1980; Irvine <u>et al.</u> , 1983
erosion structures, trough bands	xenoliths, erosion structures	folds, erosion structures		Wiebe, 1980
size-graded layers, erosion structures	erosion structures			Roobol, 1972

More importantly the evidence from small-scale structures constrains the reliance that petrologists can place on mineral compositions as indicators of magmatic differentiation and intrusion stratigraphy as a record of magmatic processes. Minerals with "cumulus" textures have been shown to form within the crystal mush, by replacement and displacement of the host crystal mush; thus distinguishing those which did grow in equilibrium with the contemporary magma is a major problem. It is in this respect that the conclusions on the origin of normally graded layers in chapters 3 and 4 are perhaps most important, since these layers must have formed in contact, and therefore in equilibrium, with the contemporary magma.

It is clear that plutonic textures are poorly known in three dimensions, and the interpretations of such textures are based primarily on intuition. The variations in composition of individual plutonic minerals are even less well known in three dimensions, yet these are the principal data base on which complex petrogenetic schemes are based. . The wealth of evidence, especially on Rum, for the presence of dynamic interstitial liquids, capable of reacting with the crystalline permeable medium through which they pass, and capable of precipitating new minerals texturally indistinguishable from those through which the liquid is moving, raises a number of important questions and points to future work, essential if the study of layered intrusions is to develop on a sound basis:

(i) To what extent do minerals have their compositions altered by reaction and is it possible to find a window through such reaction (by analysing immobile trace-element contents on an ion probe perhaps), in both the postcumulus and subsolidus stages of the cooling process.

(ii) What are the factors which dictate whether a mineral crystallising in a porous medium assumes a poikilitic or a granular (inclusion-free) texture? (Schuiling & Wensinck, 1962, have suggested the rate of crystallisation may be an important factor - further analogue experiments would probably be fruitful).

(iii) What are the porosities and permeabilities of crystal mushes and at what rates can liquid flush through them?

(iv) What is the nature of the transition from mush to magma? - some structural evidence suggests it is rather abrupt and that a floor exists, at least at times, but a more accurate model is required before studies on convection, for example, can progress.

It is in the nature of this thesis that much of the work on particular structures, fingers for example, has had to be of a fairly preliminary nature. It is clear however, that such features are of extreme importance, as they offer a wealth of possible

information on the physical processes operating in cooling plutons.

APPENDIX 1 - TERMINOLOGY.

A terminology for layered igneous rocks has been in use, with modifications, since first defined by Wager et al in 1960. Recently this terminology has been the subject of both criticism (eg McBirney & Noyes, 1979) and major restatement and redefinition (Irvine, 1982). Certain of the observations, conclusions and speculations in this thesis indicate that several of Irvine's definitions are inadequate. This appendix gives new definitions of these terms (mostly textural) as used throughout this thesis. For the remainder Irvine's terminology has been adopted.

It was a fundamental aim of Wager et al to identify those crystals which had "separated from the magma", these were named cumulus crystals. As originally defined they need not have settled and they could occur in a variety of textural types (eg cresc- and heteradcumulates). Crystals identified as having "cumulus" status are generally interpreted as recording the evolution of the parent magma body (eg Dunham & Wadsworth, 1978; Morse, 1979a; Wilson, 1982; Loney & Himmelberg, 1983). Therefore, I have chosen to define a cumulus crystal as any crystal which is shown or inferred to have grown in contact with the contemporary magma in the chamber (though the crystal need not retain its original composition). Thus cumulus crystals can have settled, floated, grown in situ, grown in a previously existing porous medium, be euhedral, subhedral, anhedral, skeletal, poikilitic, ophitic etc.

Using this definition as a starting point, the following definitions have been formulated;-

CONTEMPORARY MAGMA. The magma occupying the main portion of the chamber at any point in time. It need not be isocompositional, isothermal or isobaric.

CUMULUS PHASE. CUMULUS CRYSTAL. CUMULUS MATERIAL. Those crystals or portions of crystals which have formed by extracting components from the contemporary magma alone. They may occur in a variety of textures and shapes but are most commonly euhedral to anhedral.

CUMULUS PROCESSES. Those processes which act to separate cumulus material from the contemporary magma by physically separating the crystals from the liquid (eg crystal settling), the liquid from the crystals (eg compositional convection) or by diffusion.

CUMULUS STAGE. The stage during the formation of the rock (cumulate) in which the cumulus crystals are in contact with the contemporary magma alone.

CUMULUS COMPOSITION. The composition of a cumulus crystal during the cumulus stage; not necessarily equivalent to the final composition a cumulus crystal in a cumulate rock.

CUMULATE. A rock partially or wholly formed of cumulus material.

POSTCUMULUS STAGE. The stage during the formation of a cumulate after the contemporary magma has stopped supplying all the components for the growth of phases and including sub-solidus recrystallisation, exsolution and reaction.

POSTCUMULUS PHASE, POSTCUMULUS CRYSTAL, POSTCUMULUS MATERIAL. Those crystals, or portions of crystals which form within a cumulate during the postcumulus stage.

POSTCUMULUS PROCESSES. Those processes operating during the postcumulus stage to fractionate the components which make up the postcumulus material or to physically mobilise cumulus and/or postcumulus material.

The definition and distinctions between "ortho" and "ad" cumulates are more difficult to define. The original definitions were both textural and genetic, it being believed that the one texture could have only one genesis. However there exists the possibility (Chps 6 & 9) that rocks which would have been called adcumulates by Wager et al can be formed in one of several ways, at the mush magma interface, within the mush, or by sub-solidus recrystallisation. Two possibilities present themselves; one in which adcumulates are defined on the basis of their texture alone and one in which they are defined on the basis of their genesis alone (ie rocks fully crystallised during the cumulus stage). Both have apparently been adopted in recent literature (compare Irvine, 1980b and Morse, 1980a pp 239 - 241). Since the textural definition

is more widely applicable I have chosen to use it here, thus;-

ADCUMULATE. A cumulate rock formed entirely of unzoned cumulus phases, ie an apparently "isothermal" rock.

ORTHOCUMULATE. A cumulate rock in which the cumulus phases show appreciable zoning or in which postcumulus phases are obvious, ie a "polythermal" rock.

The terms "cresc" and "heterad" cumulate have been abandoned since the rocks they were designed to describe may have more than one mode of origin.

APPENDIX 2 - DESCRIPTIONS OF THE RUM AND KIGLAPAIT INTRUSIONS.

Brief descriptions of the lithologies, stratigraphy and structure of the Rum and Kiglapait intrusions are appended here for the assistance and information of readers.

The Rum layered intrusion.

The major intrusive rocks on Rum make up one of the seven Tertiary central complexes which outcrop on the west coast of Scotland and where emplacement accompanied a period of late Cretaceous-Tertiary volcanism associated with the opening of the N. Atlantic (Harris, 1983; Emeleus, 1983). The plutonic rocks on Rum are dominated by a large body of layered ultrabasic rocks and associated gabbroic intrusions (Harker, 1908) which form a four-lobed outcrop oriented N-S and E-W. Many of the rocks are regarded as type examples of igneous cumulates (Wager *et al.*, 1960) and the island was the first place where the concept of the open-system magma chamber was clearly formulated (Brown, 1956).

The layered rocks have been divided by other workers into three structural series. The Eastern Layered Series forms the eastern lobe of the complex and was partially described by Brown (1956). It is built up of a number of layered, cyclic units which are of peridotite at their base and allivalite at their tops. Frequently a thin (2-5 mm) layer of chromitite separates successive cyclic units.

The western lobe is occupied by the Western Layered Series which is made up of rhythmically-layered, cyclic units of eucrite, feldspathic peridotite and peridotite (Wadsworth, 1961). This is the type locality for the rock harrisite (Harker, 1908) which is less common elsewhere on the island. The relative ages and structural relationship between the Eastern and Western Layered Series are unclear.

The central portion of the complex is occupied by the recently defined Central Series which extends into the northern and southern lobes (and possibly includes the Ruinsival Series of Wadsworth, 1961) and is separated from the Eastern and Western Layered Series by lines of igneous breccias and zones of disruption (McLurg, 1982; J. Volker pers comm 1983). The Central Series is structurally very complex but peridotite/allivaitite cycles can be recognised.

The Rum pluton is generally believed to be the solidified remnants of a replenished magma chamber; each cyclic unit representing one replenishment (Brown, 1956; Dunham & Wadsworth, 1978; Huppert & Sparks, 1980; Palacz, 1984; of Chapter 8). The parent magma was formerly believed to be basaltic (Brown 1956; Wadsworth, 1961; Wager and Brown 1968; Dunham & Wadsworth, 1978) though it is now thought to have been more basic than basalt and was probably picritic (see Gibb, 1976; Donaldson, 1976; Huppert and Sparks, 1980; Emeleus, 1983 and Emeleus written comm 1983).

Kiglapait Intrusion

The Kiglapait intrusion is one of many layered plutons found associated with the Precambrian Nain anorthosite. It has an egg-shaped outcrop, measuring approximately 60 x 40 km, and is most likely conical in form, with a maximum thickness of 9.6 km (Morse 1969, 1979a). Stratigraphically and structurally simple, it has been divided into Inner, Outer and Upper Border Zones and a layered series, which is subdivided into a Lower Zone of troctolites, and an Upper Zone, of gabbros and syenites, defined by the presence of "cumulus" clinopyroxene (Morse 1969). The Upper Zone is further subdivided based on the presence of index minerals, magnetite, apatite etc. Cryptic and petrographic variations in the Upper Border Zone are a mirror image of those from the upper part of the layered series, to which it is considered to be time-stratigraphically equivalent. Whole-rock chemistry, mineral compositions and petrographic variations suggest the steady, single-stage fractionation of a troctolitic parent along a strong iron-enrichment trend to late-stage, Mg-free ferrosyenite (Morse, 1969; 1979a; 1979b; 1981b). Small-scale structures are extremely rare, as is obvious layering, most of the intrusion being made up of so-called average rock.

APPENDIX 3 - MISCELLANEOUS STRUCTURES.

A number of structures have been identified which have either not been investigated in much detail or do not fit easily into the layout of the text but which are nevertheless worth recording. Photographs, brief descriptions and tentative interpretations are appended here.

Plate A3.1 Vertically orientated olivine crystals in anorthositic gabbro, Loch a' Chroisg intrusion, Mull. Vertical orientation of olivine on this scale is a very rare phenomenon, even on the Rum intrusion, and extremely so in such a feldspathic rock. The outcrop may be interpreted as direct evidence for the in situ crystallisation of olivine crystal with the dimensions of those commonly believed to have settled, though reorientation during fluid-escape from a crystal mush (see Irvine, 1980b) cannot be ruled out.

Plate A3.2 Stellate, skeletal olivines lying in the plane of the layering in allivalites, Coire nan Grunnd, Eastern Layered Series, Rum. Possibly a unique occurrence of skeletal olivine in such a feldspathic cumulate in the Rum pluton. The texture may be evidence for crystallisation in situ of crystals lying in the plane of the layering, though they may have settled into this orientation.



Plate A3.3 Plan view of concentric circular structure defined by lamination and of olivine-rich laminae in allivalite. The structures may be analogous to "swirl" structures described by Parsons (1979) from the Klokken intrusion.

Plate A3.4 Cross-section of circular structure illustrated in Plate A3.3. This view reveals that the structures have the form of a series of stacked, concave-up, circular dishes. The structures are reminiscent of coil structures in lavas described by Peck (1966) and possibly record the impingement of turbulent eddies into the chamber floor. If this interpretation is correct then it is perhaps surprising that the structures are not more common, unless the floor is "protected" from such eddies by the presence of a stagnant boundary layer (cf Chps 2,3,4).



Plate A3.5 Branching, poikilitic plagioclase crystals in peridotite, fallen block, Eastern Layered Series, Rum. The texture is probably analogous to the poikilo-macro-spherulitic textures reported by Donaldson et al (1973) from the Central Series. In this case, however, the texture probably records unidirectional crystallisation within the crystal mush under supersaturated conditions.

Plate A3.6 Vertical banding defined by poikilitic plagioclase in feldspathic peridotite Eastern Layered Series, Rum. The presence of vertical banding in otherwise horizontally layered rock is unusual and may be evidence for feldspar crystallisation from a convecting interstitial liquid.



Plate A3.7 Tabular olivine crystals draped over a vertically orientated olivine, Western Layered Series, Rum. The texture can be interpreted as being due to settling or growth of olivine crystals over the vertical crystal; compaction around the vertical crystal; or perhaps to later growth of the vertical crystal pushing aside the overlying crystal mush (cf Chp 6).

Plate A3.8 Inclusions of peridotite in allivalite which have cross-sections similar to those of aerofoils. Similar shaped inclusions of anorthosite can also be found. The inclusions generally all have their rounded ends pointing in the same direction in any one outcrop. The structures may represent reworking of either former layers or blocks of crystal mush during flow of the enclosing crystal mush.



APPENDIX 4 - SUBMITTED FOR INCLUSION IN THE 1981 FIELD REPORT.

NAIN ANORTHOSITE PROJECT.

Two new breccias in the Kiglapait layered intrusion.

Introduction.

In the course of work undertaken on layering styles in the Kiglapait intrusion, Young (this report), two breccia zones were discovered. One situated on the north shore of Slambang Bay has predominantly xenolithic clasts in a troctolite matrix while the other is of autolithic material in a predominantly dunitic matrix (see fig. 1). Previous to this only one other brecciated zone was known in the intrusion, situated to the west of Caplin Bay at the 15 PCS level and investigated by Morse, (1969). Xenoliths were also virtually unknown in the intrusion, see Morse et al (this report).

Slambang Bay Breccia.

A lens of xenolithic and some presumably autolithic fragments set in a troctolite matrix was mapped on the north shore of Slambang Bay (see fig. 1) at around 9 PCS. The lens is conformable with the regional layering. At its maximum it reaches 50m in thickness. To the northeast the lens thins and lithic fragments become less abundant until "normal" Lower Zone troctolite is encountered within 200m. To the southwest the lens thins slightly until outcrop disappears underwater and does not occur along strike on the other side of the small bay. Neither the base nor the top of the lens is sharply

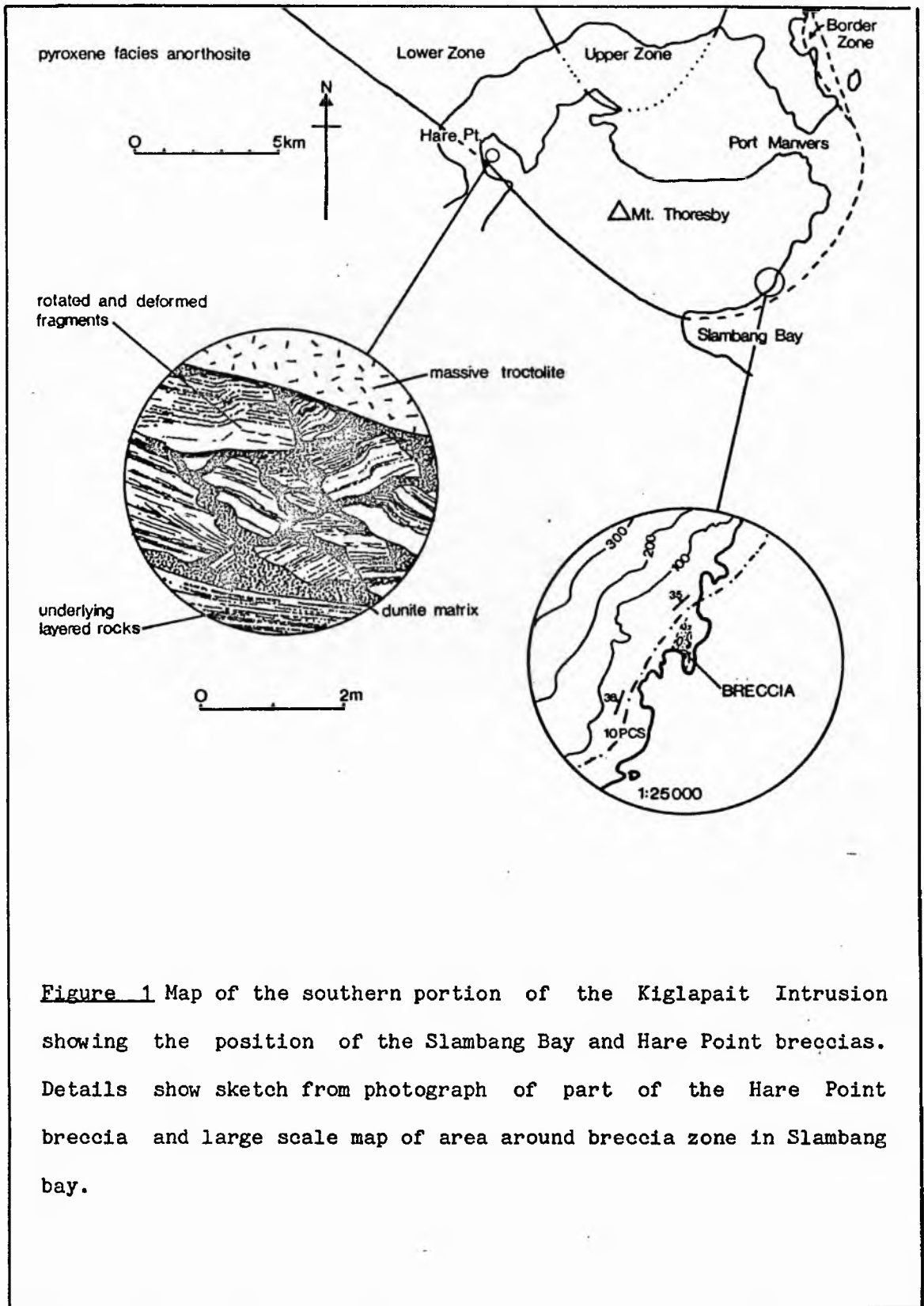


Figure 1 Map of the southern portion of the Kiglapait Intrusion showing the position of the Slambang Bay and Hare Point breccias. Details show sketch from photograph of part of the Hare Point breccia and large scale map of area around breccia zone in Slambang bay.

defined but rather the fragments become less abundant and eventually become absent.

Fragments range in size from a few centimetres in diameter to one which is 4m x 0.5m. Elongate fragments tend to lie in the plane of the regional layering, though there are notable exceptions. The matrix is of unlayered, though occasionally laminated, troctolite. There is a tendency for this lamination to be parallel or sub-parallel to the regional layering.

Lithologies represented include metasediments (gneisses and calc-silicates), pyroxene granulite, anorthosite (one fragment of which is found associated with granophyric material) and layered and unlayered troctolite and gabbro. The metasedimentary fragments are surrounded by a 1-2cm rind of pyroxene (and perhaps a little amphibole and/or oxide). Fragments appear generally angular except for the smaller of the metasedimentary xenoliths which are more rounded.

Hare Point Breccia.

This breccia lies at the stratigraphic top of the finely layered rocks of the dunitic horizon at Hare Point (approx. 15 PCS). It occupies a zone approximately 4m long by 3m thick and set between the finely layered rocks of the dunitic horizon and unconformably overlying massive troctolite. The fragments are of broken and deformed troctolite, similar to that immediately underlying the breccia. Several of the fragments appear to fit

together in a jigsaw-like fashion. The margins of the fragments are generally sharp. There is one small (20cm x 8cm) xenolith of pyroxene anorthosite. The matrix is of dunite with a few small feldspathic segregations. The underlying layered rocks have been plastically deformed in places. Minor dislocations are also common. Deformed zones are however separated from one another above and below by undeformed layered rocks.

Discussion.

The Hare Point breccia outcrops on the opposite side of Port Manvers Run from, and along strike from a breccia which outcrops to the west of Caplin Bay described and illustrated in Morse (1969 plate 22). The similarity of style both of brecciation and deformation in the underlying cumulates in both breccias suggests that they may be correlatable across Port Manvers Run. Suggestions about the mode of formation of this style of breccia have been made by Morse (1969). Whether they represent the remnants of a once much larger breccia zone or not, their presence indicates significant disturbance of the cumulate pile in this zone followed by a distinctive change in the conditions under which crystals accumulated. This deformation may have been related to movement along the large fault to their immediate southwest.

The conformable nature and preferred orientation of the fragments in the Slambang Bay breccia suggest that it is neither an intrusion breccia nor a fault scarp deposit, unlike some of the breccias of the Rhum intrusion, (Wadsworth, 1961, Donaldson, 1975). It

cannot be an autobreccia since most of the material is foreign to the intrusion. The restriction of xeno and autoliths fragments to such a small area makes it unlikely that they accumulated randomly from the overlying, circulating magma. In the Skaergaard intrusion it is common to find large numbers of foundered blocks in restricted horizons in the layered series, McBirney and Noyes, (1979). These authors suggest that breccias of this type in the Skaergaard intrusion were deposited from vertical density currents. A similar process operating in the Kiglapait intrusion can account for all of the field observations.

The similarities of the lithologies within the Slambang Bay breccia to those in the Snyder Group, Berg FR 1975, Docka FR 1980, is noteworthy and may indicate that this group bounded a greater part of the intrusion than is indicated by the present exposure level. The presence of all of these breccias indicates significant departures from the closed system conditions proposed elsewhere, (Morse 1969, 1979). The question of possible assimilation of foreign material and contamination of the Kiglapait magma has been addressed elsewhere, Morse et al (this report).

Observations on layering styles in the Kiglapait Intrusion.

Introduction.

The Kiglapait Intrusion records the strong fractionation of a high- alumina, high-FeO, low- K basaltic magma under essentially closed system conditions. Lithologies range from early troctolite to late Mg-free ferrosyenite, Morse (1979). The intrusion is layered on a number of scales and in a number of styles described by Morse (1969). Until recently, most layering in igneous rocks was generally regarded as being due to the mechanical separation of solid phases from magma and their accumulation on the floor of the chamber, sorting processes of several types producing the observed spectrum of layering types. It was recognised, however, that in the dense iron-rich magmas of the Kiglapait and Skaergaard Intrusions plagioclase was less dense than the fluid it was supposed to have settled out of, Morse (FR 1973), Bottinga and Weill, (1970). This fact formed the basis of Campbell's (1978) attack on cumulus theory and has led recent authors, eg. McBirney and Noyes (1979), to attempt reinterpretations of layered rocks in terms of in situ crystallisation. Morse writing about the Kiglapait Intrusion (1979) opted for a compromise solution by proposing that mafic minerals may have settled and that feldspars crystallised in place and were then retained on the floor of the intrusion by the rheologic changes in the fluid accompanying plagioclase precipitation. Irvine has recently (1980) suggested a means whereby plagioclase may be transported and laid down by density currents even in conditions where it has a negative density contrast with the liquid.

As Morse (1979) has pointed out, however, most hypotheses of layer formation are too unspecific to allow any clear-cut testing. In particular, little is known of the variation within individual layers along strike and down dip, ie in the second and third dimensions. For example, if graded layers are the result of current deposition then this should presumably be mirrored in structural changes as any layer is traced both laterally and distally. Similarly, structural changes in other styles of layering may place constraints on their origin.

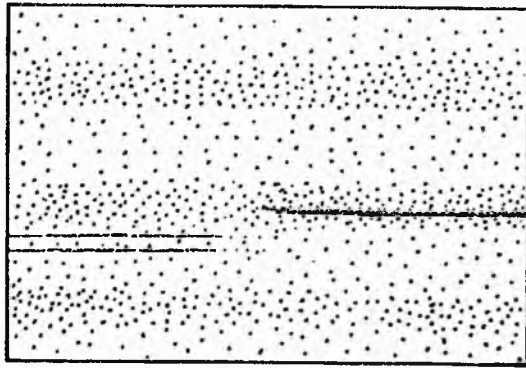
Such an approach has been used by Parsons and Butterfield (1981) to compare and contrast the modes of formation of layers in two chemically similar syenite intrusions, the Klokken and Nunarssuit Intrusions in south Greenland. This report describes a number of different layering styles and their associated structures in the Kiglapait Intrusion and draws some preliminary conclusions.

Macrorhythmic layers.

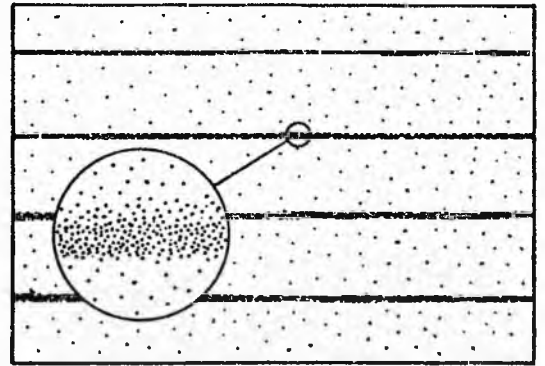
A distinctive style of layering was recognised which closely resembles the macrorhythmic layering described by Irvine (1980) from the Skaergaard Intrusion. The layering is defined by alternations of leucocratic and melanocratic rocks between 0.5m and 5m thick. The cumulus mineralogy of each appearing identical, only the plagioclase/mafic ratio varying. The contacts between layers are generally gradational over distances between 10cm and 20cm, though they can be sharp. Layers of this type are invariably conformable

Figures 2 - 6 Stylised sketches of layering styles and their associated structures:-

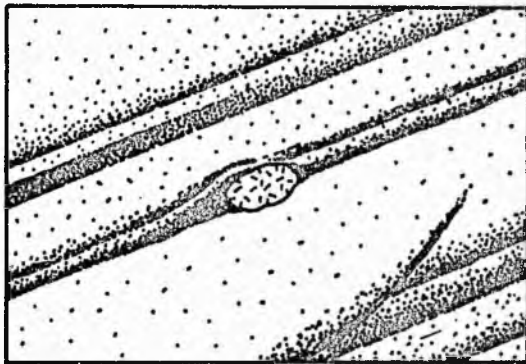
- 2) Macrorhythmic layering, strike or dip section; note superposition of other layer types.
- 3) Normally graded layering, dip section; note crosscutting relationships and relationship of layering to autolith fragment.
- 4) Lenticular layering, strike and dip sections; note differences in dip and strike sections, lens attenuations and occasional cross-cutting relationships.
- 5) Fine scale layering (i), strike or dip section.
- 6) Fine scale layering (ii), strike section; note thick ultramafic layers changing along strike from conformable to crosscutting relationship, deformation of layers and relationship of layering to autolith fragments.



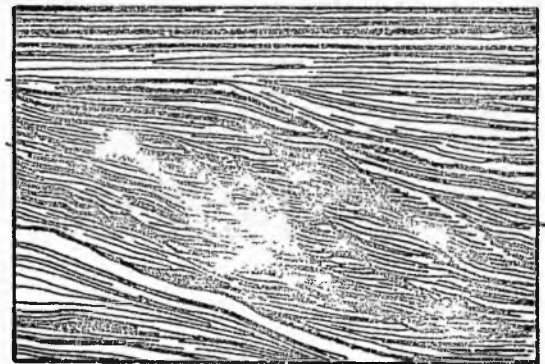
2 0 2m



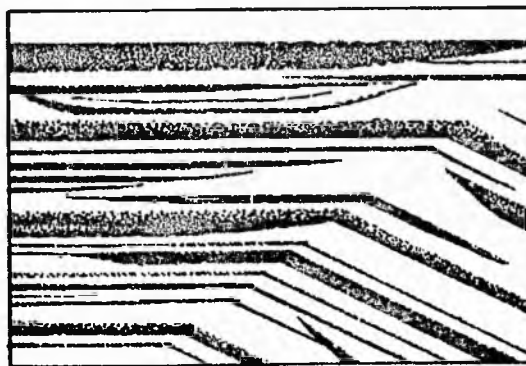
5 0 60cm



3 0 1m



6 0 1m



4 0 3m

with one another. Other styles of layering may be developed within a macrorhythmically layered sequence but these generally seem to have little effect on the overall sequence. (see fig. 2). Macrorhythmic layers are laterally extensive and in some places can be traced by eye for several hundred metres. Outcrop was nowhere good enough to indicate whether these layers are as laterally extensive as the Skaergaard examples, which extend over areas of up to 4km, Irvine (1980b). The best examples of layers of this type seen in the portions of the intrusion examined are to be found on the upper slopes of Mt. Thoresby overlooking Slambang Bay (at around 35 PCS) and in the Kiglapait Mountains, east of Sally Brook, in the upper part of the Lower Zone and the lower part of the Upper Zone (at around 70-90 PCS).

Normally graded layers.

These are layers which grade from a mafic base to a feldspathic top, both of which have sharp contacts. Such layers are the "gravity stratified layers" of Wager and Brown (1968) or "graded layers" of Morse (1979). They tend to occur in groups in the intrusion, Morse (1979). Layers of this type range from 5cm to 1m thick. The mafic portion can represent anything from 20% to 80% of this amount. No individual layer could be traced for more than 70m along strike. However groups of individual layers may be traced for much longer distances (100s m). Many graded layers cannot be followed due to smearing and shearing of individual layers together. Several graded layers were seen to contain autolithic fragments. In such cases the top of the layer may be draped across the top of the

autolith, or more rarely the fragment may protrude into the overlying layers. In all cases there is slight asymmetry of the structure when viewed in dip sections (see fig. 3). Graded layers may be seen to rest unconformably on one another especially when viewed in dip sections. In several places graded layers were traced passing down dip into a pair of sharply defined mafic and leucocratic layers (see fig. 3).

Lenticular layers.

This is something of a misnomer since all layers appear to be lenses (apart from the major phase layers like the Main Ore Band), however some ultramafic layers show a much more extreme development of a lenticular geometry. Layers of this type are best exposed on the north shore of Slambang Bay (see fig. 4), though well developed examples can be found elsewhere in the intrusion (eg. in the Lower Zone at 65 PCS to the south of the Kiglapait Mountains). A block diagram of the salient features is shown as fig. 4. The following points are of particular importance. Layers of this geometry were invariably seen as ultramafic lenses set in a more leucocratic matrix. Lenses have generally convex lower boundaries and have concave or straight upper ones. They vary from a few centimetres to approximately one metre in thickness and range in length from a few metres to approximately 30m. Their bases are generally sharp but tops may be sharp or gradational. In strike sections lenses appear generally symmetrical. In dip sections lenses appear to attenuate more sharply up dip. In dip sections lens attenuations are numerous enough to suggest that lenses are not

extremely elongate down dip. Cross-cutting relationships between layers of this type are rare, but more common in dip sections. The thickness of any particular ultramafic or leucocratic layer is not directly related to the thickness of the leucocratic or ultramafic layer immediately below.

Fine scale layering.

The vertical dimension of this layering type is measured in millimetres or centimetres rather than decimetres or metres. Two distinctive types were recognised:

(i) One is characterised by 1-2cm of mafic material in otherwise "normal" troctolite. In the Lower Zone such layers are olivine concentrations while in the Upper Zone they may be pyroxene or pyroxene and oxide concentrations. Commonly they have a slightly sharper base than top, (see fig. 5). These layers commonly occur in groups, though isolated examples exist, and they are remarkably persistent along strike (one such layer in the Lower Zone was traced for over 200m before being lost due to lack of exposure). Where these layers occur in groups they are parallel. No layer of this type was seen to cut any other layer. When traced along strike groups of layers tend to become less clearly defined as a group (though retain a constant thickness and separation) until they became indistinguishable from the surrounding normal rock.

(ii) The other type of fine scale layer recognised was much more variable in character. Such layers range in thickness from 2mm (one crystal) to 8cm. They generally have sharp upper and lower boundaries, though grading may occur. There is no obvious relationship between the thickness or character of successive layers. Individual layers may be extremely short, 20cm, or remain remarkably constant for distances of up to 50m along strike. Zones of layering of this type may however be very persistent along strike (up to 1km Morse, 1969). Bifurcations and truncations of one layer by another are common. Deformation is common and has apparently led to the formation of "new" layers in some cases (see fig. 6). Where autolithic fragments are present layers may exhibit asymmetry of structure around them (see fig. 6).

Discussion.

Layering in the Kiglapait intrusion has recently been discussed generally level by Morse (1979), who suggests that co-operative settling of mafic phases and plagioclase feldspar together with oscillatory nucleation about a cotectic boundary can account for all the field and laboratory observations. It seems reasonable to suggest, however, that under specific conditions a specific style of layering is produced. Thus Irvine has argued (1980) that graded layering may be produced in any mafic or ultramafic intrusion by deposition from a crystal-laden density current. Other authors, for example McBirney and Noyes (1979), have suggested quite different layering mechanisms in investigations on, for example, the

Skaergaard Intrusion. The most fundamental distinction to be made is between layers produced by deposition and those produced by in situ crystallisation. Most authors agree that erosion may take place by current scour and lead to truncation of one layer by another. Unusual and assymetric accumulations of material around obstacles may be other indications of current activity. Three of the layer types described above show truncation and/or accumulations around obstacles, namely normally graded, lenticular and one type of fine scale layer. The other layers, macrorhythmic and 2cm mafic bands, show neither of these structures and their most remarkable feature is their parallelism. Note also that these layer types are identical when viewed in strike or dip section, unlike the other styles described, (see figs. 2 - 6). If both processes occur, then it seems that the most likely candidates for an in situ origin are the 2cm mafic bands and the macrorhythmic layers (a similar conclusion has been reached by Irvine, 1980b, in his discussion of macrorhythmic layering in the Skaergaard intrusion). Layer types showing unconformable relationships with one another are the most likely candidates for mass transport processes. Another intriguing possibility suggested by the deformed layers at Hare Point is that some layering may be produced by reworking and segregation of cumulus grains within the crystal mush. The recognition of large scale oscillations of mafic content in the field (macrorhythmic layers) may explain the rarity of samples of apparently average rock with the cotectic ratio (see Morse 1969).

REFERENCES.

- Ahern JL, Turcotte DL, Oxburgh ER (1981) On the upward migration of an intrusion. *J Geol* 89: 421-432
- Allen JRL (1970) *Physical processes of sedimentation*. George Allen & Unwin, London.
- Allen JRL (1971) Mixing at turbidity current heads, and its geological implications. *J Sed Petrol* 41: 97-113
- Allen JRL (1977) The possible mechanics of convolute lamination in graded sand beds. *J Geol Soc London* 134: 19-31
- Anketell JM, Cegla J, Dzulyński S (1970) On the deformational structures in systems with reversed density gradients. *Annals Geol Soc Poland* XL: 3-29
- Barker DS (1983) *Igneous rocks*. Prentice-Hall, New Jersey.
- Bartlett RW (1969) Magma convection, temperature distribution, and differentiation. *Am J Sci* 267: 1067-1082
- Barton JM Jr., Fripp REP, Horrocks P, McLean N (1979) The geology, age, and tectonic setting of the Messina layered intrusion, Limpopo mobile belt, Southern Africa. *Am J Sci* 279: 1108-1134
- Becke F (1903) Über Mineralbestand und Struktur der Kristallinen Schiefer. *Rendus ix Cong Geol Intern Vienne*: 553-570
- Becker GF (1897a) Some queries on rock differentiation. *Am J Sci* 3: 21-40
- Becker GF (1897b) Fractional crystallization of rocks. *Am J Sci* 4: 257-261
- Bell BR (1983) Significance of ferrodioritic liquids in magma mixing processes. *Nature* 306: 323-326
- Bennet MC (1976) The ultramafic-mafic complex at North Cape, northernmost New Zealand. *Geol Mag* 113: 61-76
- Berg JH (1975) In: Morse SA (ed), *Main Anorthosite Project, Labrador*:

- Field Report 1974, University of Massachusetts.
- Berg JH (1980) Snowflake troctolite in the Hettasch intrusion, Labrador: Evidence for magma-mixing and supercooling in a plutonic environment. *Contrib Mineral Petrol* 72: 339-351
- Berg JH, Pencak MS (1980) Troctolitic rocks in the Nain complex. In: Morse SA (ed), Nain Anorthosite Project, Labrador: Field Report 1980, University of Massachusetts Contribution 38, 58-63
- Berner H, Ramberg H, Stephansson O, (1972) Diapirism in theory and experiment. *Tectonophysics* 15: 197-218
- Berner RA (1980) Early diagenesis. A theoretical approach. Princeton University Press, Princeton.
- Berkebile CA, Dowty E (1982) Nucleation in laboratory charges of basaltic composition. *Am Mineral* 67: 886-899
- Bickford ME (1963) Petrology and structure of layered gabbro Pleasant Bay, Maine. *J Geol* 71: 215-237
- Bottinga Y, Weill DH (1970) Densities of liquid silicate systems calculated from partial molar volumes of oxide components. *Am J Sci* 269: 169-182
- Bottinga Y, Weill DH (1972) The viscosity of magmatic silicate liquids: A model for calculation. *Am J Sci* 272: 438-475
- Bowen NL (1915) Crystallisation differentiation in silicate liquids *Am J Sci* 39: 175-191
- Bowen NL (1919) Crystallization-differentiation in magmas. *J Geol* 27: 393-340
- Bowen NL (1928) The evolution of the igneous rocks. Princeton University Press, Princeton.
- Brooks CK, Nielsen TFD (1978) Early stages in the differentiation of the Skaergaard magma as revealed by a closely related suite of dyke

- rocks. *Lithos* 11: 1-14
- Brothers RN (1964) Petrofabric analyses of Rhum and Skaergaard layered rocks. *J Petrol* 5: 255-274
- Brown GM (1956) The layered ultrabasic rocks of Rhum, Inner Hebrides. *Philos Trans R Soc London, Ser B* 240: 1-53
- Brown PE (1973) A layered plutonic complex of alkali basalt parentage: the Lilloise intrusion, east Greenland. *J Geol Soc London* 129: 405-418
- Brown PE, Farmer DG (1971) Size-graded layering in the Imilik gabbro, East Greenland. *Geol Mag* 108: 465-475
- Browning P, Smewing JD (1981) Processes in magma chambers beneath spreading axes: evidence from magmatic associations in the Oman ophiolite. *J Geol Soc London* 138: 279-280
- Cameron EN, Desborough GA (1964) Origin of certain magnetite-bearing pegmatites in the eastern part of the Bushveld Complex, South Africa. *Econ Geol* 59: 197-225
- Campbell IH (1978) Some problems with the cumulus theory. *Lithos* 11: 311-323
- Campbell IH, Naldrett AJ, Barnes SJ (1983) A model for the origin of the platinum-rich sulfide horizons in the Bushveld and Stillwater complexes. *J Petrol* 24: 133-165
- Campbell IH, Roeder PL, Dixon JM (1978) Crystal buoyancy in basaltic liquids and other experiments with a centrifuge furnace. *Contrib Mineral Petrol* 67: 369-377
- Carruthers JR (1976) Origins of convective temperature oscillations in crystal growth melts. *J Crystal Growth* 32: 13-26
- Casey JF, Karson JA (1982) Magma chamber profiles from the Bay of Islands ophiolite complex. *Nature* 292: 295-301

- Cathles LM (1977) An analysis of the cooling of intrusives by ground
-water convection which includes boiling. Econ Geol 72: 804-826
- Cawthorn RG (1982) An origin of small-scale fluctuations in ortho-
pyroxene compositions in the lower and critical zones of the Bushveld
Complex, South Africa. Chem Geol 36: 227-236
- Cawthorn RG, McCarthy TS (1980) Variations in Cr content of magmatic
from the upper zone of the Bushveld Complex - evidence for hetero-
geneity and convection currents in magma chambers. Earth Planet
Sci Lett 46: 335-343
- Chen CF, Turner JS (1980) Crystallization in a double-diffusive system.
J Geophys Res 85: 2573-2593
- Clark SP, Jr. (1966) Handbook of physical constants (revised ed). Mem
Geol Soc Am 97
- Collinson JD, Thompson DB (1982) Sedimentary Structures. George Allen
& Unwin, London
- Conybeare CEB (1979) Lithostratigraphic analysis of sedimentary basins.
Academic Press, London
- Curtis CD, Pearson MJ, Somogyi VA (1975) Mineralogy, chemistry and
origin of a concretionary siderite sheet (clay-ironstone band) in
the Westphalian of Yorkshire. Mineral Mag 40: 385-393
- Deer WA, Howie RA, Zussman J (1966) An introduction to the rock forming
minerals. Longman, London
- Docka JA (1980) Geology of the Snyder Bay area: part 1. In: Morse SA
(ed), Nain Anorthosite Project, Labrador: Field Report 1980,
University of Massachusetts Contribution 38, 15-22
- Donaldson CH (1975a) Ultrabasic breccias in layered intrusions -
the Rhum complex. J Geol 83: 33-45
- Donaldson CH (1975b) Calculated diffusion coefficients and the

- growth rate of olivine in a basalt magma. *Lithos* 8: 163-174
- Donaldson CH (1977) Petrology of anorthite-bearing gabbroic anorthosite dykes in northwest Skye. *J Petrol* 18: 595-620
- Donaldson CH (1982) Origin of some of the Rhum harrisites by segregation of intercumulus liquid. *Mineral Mag* 45: 201-209
- Donaldson CH, Drever HI, Johnstone R (1973) Crystallisation of poikilomacrospherulitic feldspar in a Rhum peridotite. *Nature Phys Sci* 243: 69-70
- Dunham AC (1965) A new type of banding in ultrabasic rocks from central Rhum, Inverness-shire, Scotland. *Am Mineral* 50: 1410-1420
- Dunham AC, Wadsworth WJ (1978) Cryptic variation in the Rhum layered intrusion. *Mineral Mag* 42: 347-356
- Dzulynski S, Walton EK (1965) Sedimentary features of flysch and greywackes. Elsevier, Amsterdam
- Elder JW (1968) Quantitative laboratory studies of dynamical models of igneous intrusions. In: Newall G, Rast N (eds), Mechanism of igneous intrusion. Gallery Press, Liverpool. pp 245-260
- Elder JW (1981) Geothermal systems. Academic Press, London
- Elsdon R (1969) The structure and intrusive mechanism of the Kap Edvard Holm layered gabbro complex, East Greenland. *Geol Mag* 106: 46-56
- Elthon D, Casey JF, Komor S Cryptic mineral chemistry variations in a detailed traverse through the cumulate ultramafic rocks of the North Arm Mountain massif of the Bay of Islands complex, Newfoundland. *J Geol Soc London in press*
- Emeleus CH (1980) Rhum: Solid geology map (1:20 000 scale). Nature Conservancy Council
- Emeleus CH (1983) Tertiary igneous activity. In: Craig GY (ed), *Geology*

- of Scotland pp 357-397. Scottish Academic Press, Edinburgh
- Fisk MR, Bence AE (1980) Experimental crystallisation of chrome spinel in FAMOUS basalt 527-1-1. *Earth Planet Sci Lett* 48: 111-123
- Foster TD (1968) Haline convection induced by the freezing of sea water. *J Geophys Res* 73: 1933-1938
- Gibb FGF (1968) Flow differentiation in the xenolithic ultrabasic dykes of the Cuillins and the Strathaird peninsula, Isle of Skye, Scotland. *J Petrol* 9: 411-443
- Gibb FGF (1976) Ultrabasic rocks of Rhum and Skye: the nature of the parent magma. *J Geol Soc London* 132: 209-222
- Goode ADT (1976) Sedimentary structures and magma current velocities in the Kalka layered intrusion, central Australia. *J Petrol* 17: 546-558
- Goode ADT (1977a) Intercumulus igneous layering in the Kalka layered intrusion, central Australia. *Geol Mag* 114: 215-218
- Goode ADT (1977b) Vertical igneous layering in the Ewarara layered intrusion, central Australia. *Geol Mag* 114: 365-374
- Grant NK, Molling PA (1981) A strontium isotope and trace element profile through the Partridge River troctolite, Duluth complex, Minnesota. *Contrib Mineral Petrol* 77: 296-305
- Gray CM, Goode ADT (1982) Strontium isotope resolution of magma dynamics in a layered intrusion. *Nature* 294: 155-157
- Gribble CD, Durrance EM, Walsh JN (1976) Ardnamurchan, a guide to geological excursions. Edinburgh Geological Society, Edinburgh
- Grout FF (1918) Two phase convective currents in magmas. *J Geol* 26: 481-499
- Grove TL, Baker MB (1983) Effects of melt density on magma mixing in calc-alkaline series lavas. *Nature* 305: 416-418

- Gruntfest IS (1963) Thermal feedback in liquid flow; plane shear at constant stress. *Trans Soc Rheol* 7: 195-207
- Hamlyn PR (1980) Equilibration history and phase chemistry of the Panton Sill, Western Australia. *Am J Sci* 280: 631-668
- Hardee HC (1983) Convective transport in crustal magma bodies. *J Volc Geotherm Res* 19: 45-72
- Harker A (1908) The geology of the Small Isles of Inverness-shire. *Mem Geol Surv Scotland*
- Harris AL (1983) The growth and structure of Scotland. In: Craig GY (ed) *Geology of Scotland*. Scottish Academic Press, Edinburgh pp1-22
- Henderson P (1975) Reaction trends shown by chrome-spinels of the Rhum layered intrusion. *Geochim Cosmochim Acta* 39: 1035-1044
- Henderson P, Suddaby P (1972) The nature and origin of the chrome-spinel of the Rhum layered intrusion. *Contrib Mineral Petrol* 33: 21-31
- Henderson P, Wood RJ (1981) Reaction relationships of chrome-spinels in igneous rocks - further evidence from the layered intrusions of Rhum and Mull, Inner Hebrides, Scotland. *Contrib Mineral Petrol* 78: 225-229
- Hermes OD, Cornell WC (1981) Quenched crystal mush and associated magma compositions as indicated by intercumulus glasses from Mt. Vesuvius, Italy. *J Volc Geotherm Res* 9: 133-149
- Hess GB (1972) Heat and mass transport during crystallization of the Stillwater igneous complex. *Mem Geol Soc Am* 132: 503-520
- Hess HH (1960) Stillwater igneous complex, Montana: a quantitative mineralogical study. *Mem Geol Soc Am* 80
- Hildreth W (1981) Gradients in silicic magma chambers: implications for lithospheric magmatism. *J Geophys Res* 86: 10153-10192
- Hoover JD (1978) Petrologic features of the Skaergaard marginal border

- group. Carnegie Inst Washington Yearb 77: 732-739
- Howard LN (1966) Convection at high Rayleigh numbers. In: Gortler H (ed), Proc 11th Int Congr Appl Mech. Springer, Berlin pp 1109-1145
- Hubbert MK (1937) Theory of scale models as applied to the study of geological structures. Bull Geol Soc Am 48: 1459-1520
- Huppert HH, Sparks RSJ (1980) The fluid dynamics of a basaltic magma chamber replenished by influx of hot, dense ultrabasic magma. Contrib Mineral Petrol 75: 279-289
- Huppert HE, Sparks RSJ, Turner JS (1982) Effects of volatiles on mixing in calc-alkaline magma systems. Nature 297:554-
- Huppert HE, Turner JS (1981) A laboratory model of a replenished magma chamber. Earth Planet Sci Lett 54: 144-152
- Huppert HE, Turner JS (1981) Double-diffusive convection. J Fluid Mech 106: 299-329
- Huppert HE, Turner JS, Sparks RSJ (1981) Replenished magma chambers: effects of compositional zonation and input rates. Earth Planet Sci Lett 57: 345-357
- Hurle DTJ (1972) Hydrodynamics, convection and crystal growth. J Crystal Growth 13/14: 39-43
- Hutchison R, Bevan JC (1977) The Cuillin layered igneous complex - evidence for multiple intrusion and former presence of a picritic liquid. Scott J Geol 13: 197-209
- Irvine TN (1970) Heat transfer during solidification of layered intrusions. I Sheets and sills. Can J Earth Sci 7: 1031-1061
- Irvine TN (1974) Petrology of the Duke Island ultramafic complex, southeastern Alaska. Mem Geol Soc Am 138
- Irvine TN (1975) Crystallisation sequences in the Muskox intrusion and other layered intrusions - II Origin of chromitite layers and similar

deposits of magmatic ores. Geochim Cosmochim Acta 39: 991-1020

- Irvine TN (1977) Chromite crystallisation in the join Mg_2SiO_4 - $CaMgSi_2O_6$ - $CaAl_2Si_2O_8$ - $MgCr_2O_4$ - SiO_2 Carnegie Inst Washington Yearb 76: 465-472
- Irvine TN (1978a) Density current structure and magmatic sedimentation. Carnegie Inst Washington Yearb 77: 717-725
- Irvine TN (1978b) Infiltration metasomatism, adcumulus growth and secondary differentiation in the Muskox Intrusion. Carnegie Inst Washington Yearb 77: 743-751
- Irvine TN (1980a) Magmatic density currents and cumulus processes. Am J Sci 280A: 1-58
- Irvine TN (1980b) Magmatic infiltration metasomatism, double-diffusive fractional crystallisation, and adcumulus growth in the Muskox intrusion and other layered intrusions. In: Hargraves RB (ed), Physics of Magmatic Processes. Princeton University Press, Princeton. pp325-384
- Irvine TN (1980c) Observations on layering in the Skaergaard intrusion. Carnegie Inst Washington Yearb 79: 257-269
- Irvine TN (1980d) Experimental modelling of convection in layered intrusions. Carnegie Inst Washington Yearb 79: 247-251
- Irvine TN (1980e) Convection and mixing in layered liquids. Carnegie Inst Washington Yearb 79: 251-256
- Irvine TN (1981) A liquid-density controlled model for chromitite formation in the Muskox intrusion. Carnegie Inst Washington Yearb 80: 317-324
- Irvine TN (1982) Terminology for layered intrusions. J Petrol 23: 127-162
- Irvine TN, Keith DW, Todd SG (1983) The J-M platinum-palladium reef of

the Stillwater complex, Montana: II Origin by double-diffusive convective magma mixing and implications for the Bushveld complex.

Econ Geol 78: 1287-1334

Irvine TN, Smith CH (1967) the ultramafic rocks of the Muskox intrusion

In: Wyllie PJ (ed) Ultramafic and related rocks. Wiley, New York.

pp 38-49

Irvine TN, Stoesser DB (1978) Structure of the Skaergaard trough bands.

Carnegie Inst Washington Yearb 77: 725-732

Jackson ED (1961) Primary textures and mineral association in the Ultra-

mafic Zone of the Stillwater Complex, Montana. U.S. Geol Surv Prof

Pap 358: 1-106

Jackson ED (1967) Ultramafic cumulates in the Stillwater, Great Dyke

and Bushveld intrusions. In: Wyllie PJ (ed), Ultramafic and related

rocks. John Wiley and Sons, New York. pp 20-38

Jaupart C, Brandeis G (1982) Igneous graded layering and Bingham

plastic flow. (abs) EOS 62: 1063

Karcz I (1968) Fluvial obstacle marks from the wadis of the Negev

(southern Israel). J Sed Petrol 38: 1000-1012

Kerr RC, Turner JS (1982) Layered convection and crystal layers in

multicomponent systems. Nature 298: 731-733

Kirby GA (1978) Layered gabbros in the Eastern Lizard, Cornwall,

and their significance. Geol Mag 115: 199-204

Krishnamurthi R (1970) On the transition to turbulent convection. Part 2

The transition to time-dependent flow. J Fluid Mech 42: 309-320

Kuenen PhH (1953) Graded bedding, with observations on Lower Palaeozoic

rocks of Britain. Verh K ned Akad Wet 20: 1-47

Lapwood ER (1948) Convection of a fluid in a porous medium. Proc

Cambridge Phil Soc 44: 508-521

- Lee CA (1981) Post-deposition structures in the Bushveld Complex mafic sequence. *J Geol Soc London* 138: 327-341
- Lee CA, Sharpe MR (1980) Further examples of silicate liquid immiscibility and spherical aggregation in the Bushveld Complex. *Earth Planet Sci Lett* 48: 131-147
- Leeder MR (1982) *Sedimentology process and product*. George Allen and Unwin, London
- Lobjoit WM (1959) On the form and mode of emplacement of the Ben Buie intrusion, Isle of Mull, Argyllshire. *Geol Mag* 96: 393-402
- Lofgren GE (1983) Effect of heterogeneous nucleation on basaltic textures: a dynamic crystallisation study. *J Petrol* 24: 229-255
- Loney RA, Himmelberg GK (1983) Structure and petrology of the La Perouse gabbro intrusion, Fairweather range, southeastern Alaska. *J Petrol* 24: 377-423
- Loomis TP (1983) Numerical simulations of crystallisation processes of plagioclase in complex melts: the origin of major and oscillatory zoning. *Contrib Mineral Petrol* 81: 219-229
- Lowe DR (1975) Water escape structures in coarse-grained sediments. *Sedimentology* 22: 157-204
- Lowe DR (1976) Subaqueous liquefied and fluidized sediment flows and their deposits. *Sedimentology* 23: 285-308
- Maaloe S (1976) The zoned plagioclase of the Skaergaard intrusion, East Greenland. *J Petrol* 17: 398-419
- Maaloe S (1978) The origin of rhythmic layering. *Mineral Mag* 42: 337-345
- Marsh BD (1979) Island arc development: observations, experiments and speculations. *J Geol* 87: 687-713
- Marsh BD (1981) On the crystallinity, probability of occurrence and rheology of magma and lava. *Contrib Mineral Petrol* 78: 85-98

- Marshall LA, Sparks RSJ (1984) Origin of some mixed-magma and net-veined ring intrusions. *J Geol Soc London* 141: 171-182
- Matthews DW (1976) Post-cumulus disruption of the Lilloise intrusion, East Greenland. *Geol Mag* 113: 287-296
- McBirney AR (1979) Effects of assimilation. In: Yoder HS Jr. (ed) *The evolution of the igneous rocks. 50th anniversary perspectives.* Princeton University Press, Princeton pp 307-338
- McBirney AR (1980) Mixing and unmixing of magmas. *J Volcanol Geotherm Res* 7: 357-371
- McBirney AR, Noyes RM (1979) Crystallisation and layering of the Skaergaard intrusion. *J Petrol* 20: 487-554
- McCallum IS, Raedeke LD, Mathez EA (1980) Investigations of the Stillwater Complex: Part I, Stratigraphy and structure of the banded zone. *Am J Sci* 280A: 59-87
- McCarthy TS, Cawthorn RG (1983) The geochemistry of vanadiferous magnetite in the Bushveld complex: Implications for crystallisation mechanisms in layered complexes. *Mineral Deposita* 18: 505-518
- McClay KR, Campbell IH (1976) The structure and shape of the Jimberlana intrusion, Western Australia, as indicated by an investigation of the bronzite complex. *Geol Mag* 113: 129-139
- McClurg JE (1982) Petrology and evolution of the northern part of the Rhum ultrabasic complex. Unpublished PhD thesis, University of Edinburgh
- Middleton GV (1966) Experimentation on density and turbidity currents 2: Uniform flow of density currents. *Can J Earth Sci* 3: 627-637
- Middleton GV, Hampton MA (1973) Sediment gravity flows: mechanics of flow and deposition. SEPM, Pacific Sec., Short Course Lecture Notes Turbidites and deep water sedimentation

Middleton GV, Southard JB (1978) Mechanics of sediment movement.

SEPM short course, no.3 Tulsa, Oklahoma

Mitchell RH, Platt RG (1982) Mineralogy and petrology of nepheline syenites from the Coldwell alkaline complex, Ontario, Canada.

J Petrol 23: 186-214

Morse SA (1969) The Kiglapait layered intrusion, Labrador. Geol Soc Am Mem 112

Morse SA (1973) The feldspar-magma density paradox. In: Morse SA (ed), Nain Anorthosite Project, Labrador: Field Report 1972. Univ Massachusetts Contribution. 11, 113-116

Morse SA (1979a) Kiglapait geochemistry I: Systematics, sampling and density. J Petrol 20: 555-590

Morse SA (1979b) Kiglapait geochemistry II: Petrography. J Petrol 20: 591-624

Morse SA (1980a) Basalts and phase diagrams. Springer-Verlag, New York

Morse SA (1980b) Introduction and overview. In: Morse SA (ed), The Nain Anorthosite Project, Labrador: Field Report 1980, University of Massachusetts Contribution 38, 1-10

Morse SA (1981a) Kiglapait geochemistry III: potassium and rubidium. Geochim Cosmochim Acta 45: 461-479

Morse SA (1981b) Kiglapait geochemistry IV: the major elements. Geochim Cosmochim Acta 45: 461-479

Morse SA (1982) Origin of strongly reversed rims on plagioclase in cumulates. (abs) EOS 63: 454

Morse SA, Lindsley DH, Williams JK (1980) Concerning intensive parameters in the Skaergaard intrusion. Am J Sci 280A: 159-170

Morse SA, Nolan K (1980) Strong reverse zoning in plagioclase of the Kiglapait intrusion. In: Morse SA (ed), Nain Anorthosite Project,

- Labrador: Field Report 1980, University of Massachusetts Contribution 28, 47-52
- Mukherjee S, Haldar D (1975) Sedimentary structures displayed by the ultramafic rocks of Nausahi, Keonjhar District, Orissa, India. Mineral Deposita 10: 109-119
- Murase T, McBirney AR (1973) Properties of some common igneous rocks and their melts at high temperatures. Bull Geol Soc Am 84: 3563-3592
- Murck BW, Campbell IH (1982) A model for the formation of chromite seams in the Stillwater complex. (abs) EOS 63: 455
- Musgrave DL, Reeburgh WS (1982) Density-driven interstitial water motion in sediments. Nature 299: 331-333
- Myers JS (1976) Channel deposits of peridotite, gabbro and chromitite from turbidity currents in the stratiform Fiskenaesset anorthosite complex, southwest Greenland. Lithos 9: 281-291
- Myers JS (1980) Structure of the coastal dyke swarm and associated plutonic intrusions of East Greenland. Earth Planet Sci Lett 46: 407-418
- Naslund HR (1971) Mineralogical variation in the upper part of the Skaer gaard intrusion, East Greenland. Carnegie Inst Washington Yearb 75: 640-644
- Naslund HR (1984) Petrology of the Upper Border Series of the Skaergaard intrusion. J Petrol 25: 185-212
- Naylor MA (1981) The origin of inverse grading in muddy debris flow deposits - a review. J Sed Petrol 50: 1111-1116
- Nelson SA, Carmichael ISA (1979) Partial molar volumes of oxide components in silicate liquids. Contrib Mineral Petrol 71: 117-124
- Nield DA (1960) Onset of thermohaline convection in a porous medium. Water Resources Research 4: 553-560

- Nielsen TFD (1981) The ultramafic cumulate series, Gardiner complex, East Greenland. Cumulates in a shallow level magma chamber of a nephelinitic volcano. *Contrib Mineral Petrol* 76: 60-72
- Norton D, Knight J (1977) Transport phenomena in hydrothermal systems: cooling plutons. *Am J Sci* 277: 937-981
- O'Hara MJ (1977) Geochemical evolution during fractional crystallisation of a periodically refilled magma chamber. *Nature* 266: 503-507
- O'Hara MJ, Mathews RE (1981) Geochemical evolution in an advancing periodically replenished, periodically tapped, continuously fractionated magma chamber. *J Geol Soc London* 138: 237-278
- Palacz ZA (1984) Isotopic and geochemical evidence for the evolution of a cyclic unit in the Rhum intrusion, north-west Scotland. *Nature* 307: 618-620
- Parmentier EM (1982) Hydrothermal cooling of a large gabbroic intrusion: interpretations based on ^{18}O depletion and contact metamorphism. (abs) *EOS* 63: 455
- Parsons I (1979) The Klokken gabbro-syenite complex, south Greenland: cryptic variation and origin of inversely graded layering. *J Petrol* 20: 653-694
- Parsons I, Butterfield AW (1981) Sedimentary features of the Nunarssuit and Klokken syenites, S. Greenland. *J Geol Soc London* 138: 289-306
- Peck DL (1966) Lava coils of some recent historic flows, Hawaii. *U.S. Geol Surv Prof Pap* 550-B: B148-B151
- Petraske AK, Hodge DS, Shaw R (1978) Mechanics of emplacement of basic intrusions. *Tectonophysics* 46: 41-64
- Philpotts AR (1968) Igneous structures and mechanics of emplacement of Mount Johnson, a Monteregean intrusion, Quebec. *Can J Earth Sci* 5: 1131-1137

- Purvis AC, Nesbitt RW, Hallberg JA (1972) The geology of part of the Carr Boyd rocks complex and its associated nickel mineralisation, Western Australia. *Econ Geol* 67: 1093-1113
- Raiswell (1971) The growth of Cambrian and Liassic concretions. *Sedimentology* 17: 147-171
- Ramberg H (1967) Gravity, deformation and the earth's crust. Academic Press, London
- Reading HG (ed) (1978) Sedimentary environments and facies. Blackwell, Oxford
- Richardson PD (1968) The generation of scour marks near obstacles. *J Sed Petrol* 38: 965-970
- Richey JE, Thomas HH (1930) The geology of Ardnamurchan, North-west Mull and Coll. Mem Geol Surv Scotland
- Robins B (1973) Crescumulate layering in a gabbroic body on Seiland, northern Norway. *Geol Mag* 109: 533-542
- Robins B (1982) Finger structures in the Lille Kufjord layered intrusion Finnmark, northern Norway *Contrib Mineral Petrol* 81: 290-295
- Rohsenow WM, Choi H (1961) Heat, mass, and momentum transfer. Prentice-Hall, New Jersey
- Roobol MJ (1972) Size-graded igneous layering in an Icelandic intrusion. *Geol Mag* 109: 393-404
- Roscoe R (1953) Suspensions. In: Hermans JJ (ed). Flow properties of disperse systems. North Holland Pub. Co., Amsterdam, pp 1-38
- Russell AD (1977) Ultrabasic breccias in the Rhum layered complex. Unpublished Hons. Thesis, Univ of St Andrews
- Saffman PG, Taylor GI (1958) The penetration of a fluid into a porous medium or Hele-Shaw cell containing a more viscous fluid. *Proc R Soc* 245A: 312

- Schuiling RD, Wensink H (1962) Porphyroblastic and poikiloblastic textures. The growth of large crystals in a solid medium. Neues Jahrbuch fuer mineralogie monatshefte 247-254
- Selig FA (1965) A theoretical prediction of salt dome patterns. Geophysics 30: 633-643
- Sharpe MR (1981) The chronology of magma influxes to the eastern compartment of the Bushveld Complex as exemplified by its marginal border groups. J Geol Soc London 138: 307-326
- Shaw HR (1965) Comments on viscosity, crystal settling and convection in granitic magmas. Am J Sci 263: 120-152
- Shaw HR (1969) The rheology of basalt in the melting range. J Petrol 10: 510-535
- Shaw HR (1980) The fracture mechanisms of magma transport from the mantle to the surface. In: Hargraves RB (ed), Physics of magmatic process, Princeton University Press, Princeton. pp 201-264
- Shaw HR, Wright TL, Peck DL, Okamura R (1968) The viscosity of basaltic magmas: and analysis of field measurements in Makaopuhi Lake, Hawaii. Am J Sci 266: 225-264
- Sigurdsson H, Sparks RSJ (1981) Petrology of rhyolitic and mixed magma ejecta from the 1875 eruption of Askja, Iceland. J Petrol 22: 41-84
- Simkin T (1967) Flow differentiation in the picritic sills of north Skye. In: Wyllie PJ (ed). Ultramafic and related rocks. John Wiley and Sons, New York, pp 64-69
- Skelhorn RR, Elwell RWD (1977) Central subsidence in the layered hypersthene gabbro of centre II, Ardnamurchan, Argyllshire. J Geol Soc London 127: 535-551
- Skelhorn RR, MacDougall JDS, Longland PJW (1969) The Tertiary igneous geology of the Isle of Mull. Geol Assoc Guide no. 20

- Smith TE (1975) Layered granitic rocks at Chebucto Head, Halifax County, Nova Scotia. Can J Earth Sci 12: 456-463
- Sparks RSJ, Huppert HH (1984) Density changes during the fractional crystallization of basaltic magmas: fluid dynamic implications. Contrib Mineral Petrol 85: 300-309
- Sparks RSJ, Huppert HE, Turner JS, Tait SR (1983) Fluid dynamic implications of density changes during crystallisation. (abs) IUGG XVIII General Assembly, Hamburg. IAVCEI Prog and Abs: 4
- Sparks RSJ, Mayer P, Sigurdsson H (1980) Density variations amongst mid-ocean ridge basalts: Implications for magma mixing and the scarcity of primitive lavas. Earth Planet Sci Lett 46: 429-430
- Sparks RSJ, Pinkerton H, MacDonald R (1977) The transport of xenoliths in magma. Earth Planet Sci Lett 35: 234-238
- Sparrow EM, Hussar RB, Goldstein RJ (1970) Observations and other characteristics of thermals. J Fluid Mech 41: 793-800
- Spry A (1969) Metamorphic textures. Pergamon Press Ltd, Oxford
- Stolper E, Walker D (1980) Melt density and the average composition of basalt. Contrib Mineral Petrol 74: 7-12
- Tait SR, Sparks RSJ, Huppert HE (1984) The role of compositional convection in the formation of adcumulate rocks. Lithos in press
- Taylor HP, Forester RW (1979) An oxygen and hydrogen isotope study of the Skaergaard intrusion and its country rocks: a description of a 55-M.Y. old fossil hydrothermal system. J Petrol 20: 355-419
- Terzaghi K (1947) Shear characteristics of quicksand and soft clay. Proc 7th Texas Conf Soil Mechanics and Foundation Engineering, 1-8.
- Thompson RN, Patrick DJ (1968) Folding and slumping in a layered gabbro. Geol J 6: 139-146
- Thy P, Esbensen KH (1982) Origin of fine-grained granular rocks in

- layered intrusions. Geol Mag 119: 405-412
- Thy P, Wilson JR (1980) Primary igneous load-cast deformation structures in the Fongen-Hyllingen layered basic intrusion, Trondheim Region, Norway. Geol Mag 117: 363-371
- Tritton DJ (1977) Physical fluid dynamics. Van Nostrand Reinhold, London.
- Turner JS (1980) A fluid-dynamical model of differentiation and layering in magma chambers. Nature 285: 213-215
- Turner JS, Gustafson LB (1978) The flow of hot saline solutions from vents in the sea floor - some implications for exhalative massive sulfide and other ore deposits. Econ Geol 73: 1082-1100
- Turner JS, Gustafson LB (1981) Fluid motions and compositional gradients produced by crystallisation or melting at vertical boundaries. J Volc Geotherm Res 11: 93-125
- Usselman TM, Hodge DS (1978) Thermal control of low-pressure fractionation processes. J Volc Geotherm Res 4: 265-281
- Vermaak CF (1976) The Merensky Reef - thoughts on its environment and genesis. Econ Geol 71: 1270-1298
- Wadsworth WJ (1961) The ultrabasic rocks of southwest Rhum. Philos Trans R Soc London, Ser B 244: 21-64
- Wadsworth WJ (1973) Magmatic sediments. Minerals Sci Eng 5: 25-35
- Wadsworth WJ, Dunham AC, Almohandis AA (1982) Cryptic variation in the Kapalagulu layered intrusion, western Tanzania. Mineral Mag 45: 227-236
- Wager LR (1963) The mechanism of adcumulus growth in the layered series of the Skaergaard intrusion. Spec Pap Min Soc Am 1: 1-9
- Wager LR, Brown GM (1968) Layered igneous rocks. Oliver & Boyd, Edinburgh.

- Wager LR, Brown GM, Wadsworth WJ (1960) Types of igneous cumulates.
J Petrol 1: 73-85
- Wager LR, Deer WA (1939) (re-issued 1962) The petrology of the
Skaergaard intrusion, Kangerdlugssuaq, East Greenland. Medd om
Gronland 105: 1-352
- Walker D, DeLong SE (1982) Soret separation of mid-ocean ridge
basalt magma. Contrib Mineral Petrol 79: 231-240
- Walker GPL, Skelhorn RR (1966) Some associations of acid and basic
igneous rocks. Earth Sci Reviews 2: 93-109
- Weiblen PW, Morey GB (1980) A summary of the stratigraphy, petrology,
and structure of the Duluth complex. Am J Sci 280A: 88-133
- Wells MK (1954) The structure and petrology of the hypersthene-
gabbro intrusion, Ardnamurchan, Argyllshire. Quart J Geol Soc
London 109: 367-398
- Wells MK, Bowles JFW (1981) The textures and genesis of metamorphic
pyroxene in the Freetown intrusion. Mineral Mag 44: 245-
- Welsh BJ, Gomatam J, Burgess AE (1983) Three-dimensional chemical
waves in the Belousov-Zhabotinski reaction. Nature 304: 611-614
- Whitehead JA, Luther DS (1975) Dynamics of laboratory diapir and
plume models. J Geophys Res 80: 705-717
- Wiebe RA (1974) Co-existing intermediate and basic magmas, Ingonish,
Cape Breton Island. J Geol 82: 74-87
- Wiebe RA (1980) Commingling of contrasted magmas in the plutonic
environment: examples from the Nain anorthositic complex.
J Geol 88: 197-209
- Wiebe RA (1980) Further study of the Tigalak layered intrusion.
In: Morse SA (ed), Nain Anorthosite Project, Labrador: Field
Report 1980. University of Massachusetts Contribution 38, 53-57

Wilkinson JFG, Duggan MB, Herbert HK, Kalocsai GIZ (1975) The Salt Lick Creek layered intrusion, East Kimberley region, Western Australia. Contrib Mineral Petrol 50: 1-23

Wilson JR, Esbensen KH, Thy P (1981) Igneous petrology of the synorogenic Fongen-Hyllingen layered basic complex, south-central Scandinavian Caledonides. J Petrol 22: 584-627

Wilson JR, Larsen SB (1982) Discordant layering relations in the Fongen-Hyllingen basic intrusion. Nature 299: 625-626

Young IM (1983) Resorption of plagioclase by migrating interstitial liquid in the Rhum intrusion N.W. Scotland. (abs) IUGG XVIII General Assembly Hamburg. IAVCEI Prog and Abs: 8

NOTATION AND DEFINITIONS.

Several of the terms used in this thesis will be unfamiliar to most igneous petrologists and thus their definitions are included in the following list of symbols.

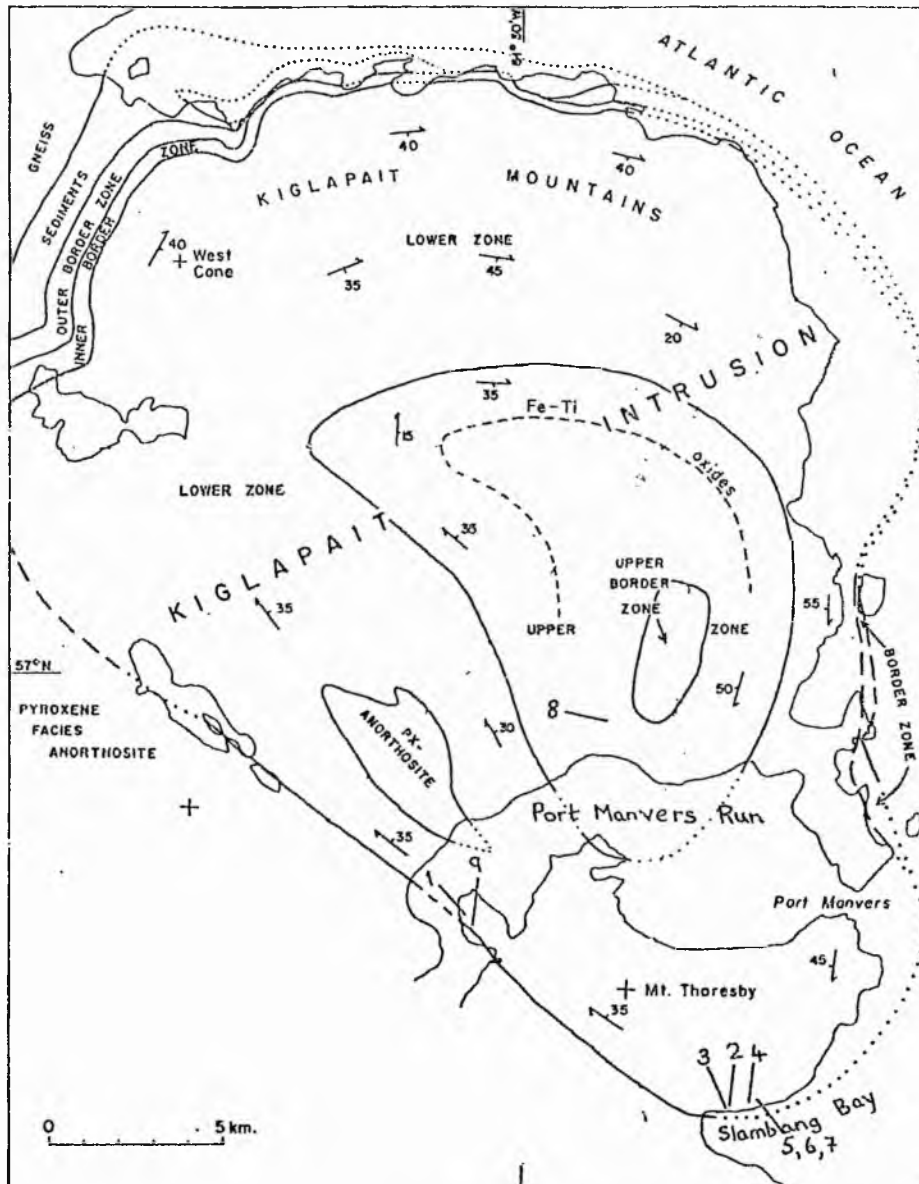
- a radius of fluid drop
- d characteristic length in the system being described
- g acceleration due to gravity
- h depth of fluid layer
- [#]
h diameter of circular source
- k thermal diffusivity
- t time
- v velocity of vertical density current
- z vertical co-ordinate
- distance through layer cross-section
- A area of cumulate drained by vertical density current
- C_L concentration of a potential phase in a magma
- C_S concentration of a postcumulus phase in a rock
- F_L residual porosity - amount of liquid trapped on closure of a rock
- Pr Prandtl number -- ratio of kinematic viscosity to thermal diffusivity
- R numerical constant used in Roscoe's equation to determine the viscosity of a suspension
- Ra Rayleigh number - dimensionless number describing whether a temperature-induced density gradient in a fluid will induce it to convect and if so, the form that convection will take

- Re Reynolds number - dimensionless measure of the relative importance of viscous and inertial forces in a fluid flow
- T temperature
- U velocity
- X proportion of solids in a suspension
- X_{An} mole fraction anorthite in plagioclase
- angle of spread the angle defined by the linear margins of a spreading density current
- flow separation separation of a boundary layer from a solid boundary at a point where the solid boundary begins to diverge from the direction of mean flow
- tortuosity the complexity of interconnected pores in a porous medium - inversely related to permeability
- vorticity a measure of rotation of a fluid
- von Karman vortex sheet - concentrated regions of high vorticity (rapidly rotating flow) forming rows in the wake of an obstacle
- α coefficient of thermal expansion
- ϵ ratio of two dynamic viscosities
- ρ fluid density (ML^{-3})
- μ dynamic viscosity ($ML^{-1}T^{-1}$) (commonly measured in poises by petrologists)
- ν kinematic viscosity (L^2T^{-1}) (dynamic viscosity divided by fluid density)

PLATE LOCALITIES.

The following is a list of the localities illustrated in the text. Localities in Scotland are given as six- or eight-figure grid references together with brief locality descriptions and those in the Kiglapait intrusion refer to the map facing page 191. Photographs of structures in the Tigalak intrusion were all taken on the largest of the small islands in the northwest corner of Kolotulik Bay (see recently published map of the intrusion in Wiebe RA, Wild T (1983) Fractional crystallization and magma mixing in the Tigalak intrusion, the Nain anorthosite complex, Labrador. Contrib Mineral Petrol 84:327 - 344.).

<u>Plate number</u>		<u>Locality information</u>
3.1	-	Rum 13477972 West side of Kinloch-Harris track.
3.2	-	Beinn Buie 578295 1km S of Coladoir River
3.3	-	Kiglapait 1
3.4-8	-	Rum 13627991 Low ridge 200m northwest of N. end of Long Loch.
3.9	-	Kiglapait 2
3.10-12	-	Tigalak
3.13	-	Kiglapait 3
3.14	-	Kiglapait 4
3.15	-	Rum 13527967 1km SW of An Dornabac
3.17-18	-	Tigalak
4.1	-	Kiglapait 5
4.2	-	Kiglapait 6
4.3	-	Kiglapait 7



Map of the Kiglapait layered intrusion showing plate localities. The observations on layering styles in Chapter 4 and Appendix 4 were made in the Lower Zone on the N shore of Slambang Bay, on the N shore of Port Manvers Run and on the southern slopes of the Kiglapait Mountains and in the Upper Zone on the N shore of Port Manvers Run.

- 4.4 - Kiglapait 8
- 6.1-2 - Rum 13417949 Coastal exposures on SE side of Harris Bay
- 6.3-8 - Rum 13967968 Unit 9, ELS, N flank of Hallival
- 6.11 - Kiglapait 9
- 6.12 - Rum 13507964 1km SW of An Dornabac
- 6.13 - Beinn Buie 592275 NW shoulder of Beinn Bheag
- 6.14 - Rum 13977968 Unit 9, ELS, N flank of Hallival
- 6.17 - Beinn Buie 584287 W bank of Abhainn Loch Fuaran
- 6.18 - Beinn Buie 580295 100m south of Coladoir River
- 6.19-20 - Ardnamurchan 441700 Coastal exposures between Sanna Bay and Sanna Point
- 6.21 - Rum 13627991 Low ridge 200m NW of N end of Long Loch
- 6.22 - Rum 13507964 1km SW of An Dornabac
- 6.23-24 - Rum 13627991 Low ridge 200m NW of N end of Long Loch
- 6.25 - Rum 13927952 Unit 14, ELS, SE ridge of Askival
- 6.26-27 - Rum 13627991 Low ridge 200m NW of N end of Long Loch
- 6.28 - Rum 140796 Unit 8, ELS, Coire nan Grunnd
- 6.29 - Rum 13947962 Unit 14, ELS, W flank of Hallival
- 6.30 - Rum 140795 Unit 8, ELS, Coire nan Grunnd
- 6.31-32 - Rum 13627991 Low ridge 200m NW of N end Long Loch
- 6.33 - Rum 13528002 Large crag, E face Minishal
- 7.1-2 - Rum 13947966 Unit 11/12 junction, ELS, N flank

- of Hallival
- A3.1 - Loch a' Chroisg 622244 Coastal exposure 1km E
of More Castle
- A3.2 - Rum 13987959 Unit 8, ELS, Coire nan Grundd
- A3.3-4 - Rum 14007960 Unit 7, ELS, Coire nan Grundd
- A3.5 - Rum 13947954 ELS, fallen block on NW ridge
of Hallival
- A3.6 - Rum 13947962 Unit 13, ELS, W flank of
Hallival near to Hallival-Askival col
- A3.7 - Rum 13427953 Harris Bay Series, SE corner of
Harris Bay
- A3.8 - Rum 13967958 ELS, fallen block at head of Coire nan
Grundd below Halival-Askival col